

University of Windsor

Scholarship at UWindor

Electronic Theses and Dissertations

Theses, Dissertations, and Major Papers

1-1-1988

Environmental isotope and geochemical study of landfill leachate migration

Jason Thomas Balsdon
University of Windsor

Follow this and additional works at: <https://scholar.uwindsor.ca/etd>

Recommended Citation

Balsdon, Jason Thomas, "Environmental isotope and geochemical study of landfill leachate migration" (1988). *Electronic Theses and Dissertations*. 7330.
<https://scholar.uwindsor.ca/etd/7330>

This online database contains the full-text of PhD dissertations and Masters' theses of University of Windsor students from 1954 forward. These documents are made available for personal study and research purposes only, in accordance with the Canadian Copyright Act and the Creative Commons license—CC BY-NC-ND (Attribution, Non-Commercial, No Derivative Works). Under this license, works must always be attributed to the copyright holder (original author), cannot be used for any commercial purposes, and may not be altered. Any other use would require the permission of the copyright holder. Students may inquire about withdrawing their dissertation and/or thesis from this database. For additional inquiries, please contact the repository administrator via email (scholarship@uwindsor.ca) or by telephone at 519-253-3000ext. 3208.

ENVIRONMENTAL ISOTOPE AND GEOCHEMICAL
STUDY OF LANDFILL LEACHATE MIGRATION

by

Jason Thomas Balsdon

A Thesis
submitted to the
Faculty of Graduate Studies and Research
through the Department of Geology
in Partial Fulfillment of the requirements
for the Degree of Master of Applied Science at
the University of Windsor

Windsor, Ontario, Canada

1988

LEPA

THSR

THESIS

1988

B357

DEPARTMENT OF GEOLOGY AND GEOCHEMICAL
ENGINEERING AND MINING

John Thomas Balaban

A Thesis
Submitted to the
Faculty of Graduate Studies and Research
in partial fulfillment of the requirements
for the degree of Master of Applied Science
The University of Windsor

ACA 9560

This thesis has been examined and approved by

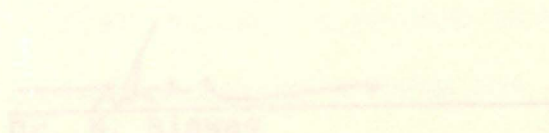
©

Jason Thomas Balsdon
All Rights Reserved

1988


Dr. M.G. Splash
Advisor

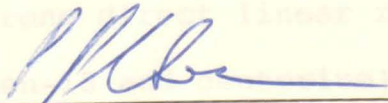

Dr. F.P. Hodac
Department Reader


Dr. K. Sigwas
Outside Department Reader

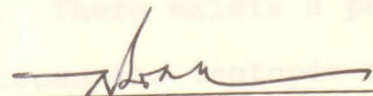
This thesis has been examined and approved by



Dr. M.G. Sklash
Advisor



Dr. P.P. Hudec
Department Reader



Dr. N. Biswas
Outside Department Reader

ABSTRACT

The Essex County Sanitary Landfill Site No. 2 is located west of Leamington in Essex County, Ontario. The landfill is on a groundwater recharge zone composed of glaciolacustrine and glaciofluvial sand and gravel.

Oxygen-18 and deuterium data from the site indicate enrichment within the contaminant plume boundaries of 0.5 to 1.0‰ for oxygen-18 and 10 to 20‰ for deuterium. Enrichment is mainly the result of organic decomposition within the contaminant plume. The oxygen-18 enrichment is a product of CO_2 , enriched in oxygen-18 relative to plume organics, equilibrating with the groundwater. Hydrogen sulphide production causes the hydrogen fractionation which enriches the groundwater in deuterium.

There is a strong direct linear relationship between the isotopic (oxygen-18 and deuterium) data and the following chemical parameters: chloride, sodium, potassium, and bicarbonate. There exists a poorer inverse linear relationship between the isotopic data and calcium and sulphate. Except for calcium and sulphate, ionic concentrations decrease away from the refuse cells. The strong direct linear relationships tend to suggest that dilution is the dominant contaminant attenuating process with adsorption, biochemical reactions, precipitation and

cation exchange probably having limited purification effects.

Isotopic tracers show promise in environments incompatible to the use of contaminant tracers. Chloride tracing of a landfill contaminant plume in a coastal environment or in an area of periodic road salting would indicate anomalous chloride concentrations. Isotopic tracers could determine the location of the landfill contaminant plume and identify the possible sources of the anomalous chloride concentrations.

ACKNOWLEDGEMENTS

Several people deserve special recognition since without them, this thesis would have been much more difficult to complete.

I wish to express my sincere gratitude to my advisor, Dr. Michael Sklash for sharing his expertise in hydrogeology in both the field and in the lab. His encouragement and good nature made the long hours more endurable.

Robert Hyde and Samuel Braithwate were invaluable in their field support and in helping to maintain my sanity during a very hot summer of intense field work. Thanks to Ingrid Churchill for her support in analysing my water samples.

I am very grateful for the moral support given by Wendy Upper, the gang at 264 Bridge Street, and my family, which provided that extra strength required to overcome the barriers.

1.1.1.1. Sensitivity Survey	44
1.1.1.2. Seismic Survey	49
1.1.2. Existing Monitoring Network	51
1.1.2.1. MW Water Well Records	52
1.1.2.2. Gartner Lee Wells	54
1.1.2.3. Surface Water Yodias	56
1.2. Piezometer Installation	56
1.2.1. Drilling Methods	58
1.2.1.1. Jet-drilling	58
1.2.1.2. Hollow Stem Augering	59
1.2.2. Piezometer Design	59
1.2.2.1. Bundle Piezometer	63

TABLE OF CONTENTS

	Page
ABSTRACT.....	iii
ACKNOWLEDGEMENTS.....	v
TABLE OF CONTENTS.....	vi
LIST OF FIGURES.....	viii
LIST OF TABLES.....	xi
LIST OF NOTATIONS.....	xii
1.0. INTRODUCTION.....	1
1.1. Objectives and Scope.....	1
1.2. Thesis Structure.....	2
2.0. STUDY AREA.....	4
2.1. Site Location.....	4
2.1.1. Site Operations.....	4
2.2. Physiography.....	8
2.3. Climate.....	9
2.4. Geology.....	9
2.4.1. Paleozoic Geology.....	9
2.4.2. Quaternary Geology.....	11
2.5. Surface Drainage.....	13
2.6. Hydrogeology.....	14
3.0. THEORETICAL CONSIDERATIONS.....	18
3.1. Environmental Isotopes.....	18
3.1.1. Oxygen-18 and Deuterium.....	18
3.1.2. Tritium.....	22
3.2. Environmental Isotopes as Tracers.....	24
3.3. Processes of Isotopic Enrichment.....	26
3.4. Groundwater Chemistry.....	30
3.4.1. Carbon Dioxide.....	30
3.4.2. Sulphate.....	32
3.4.3. Alkalinity.....	34
3.4.4. Chloride.....	35
3.4.5. Major Cations.....	36
3.5. Attenuation Processes.....	41
4.0. METHODS OF STUDY.....	44
4.1. Site Evaluation.....	44
4.1.1. Geophysical Techniques.....	44
4.1.1.1. Resistivity Survey.....	44
4.1.1.2. Seismic Survey.....	49
4.1.2. Existing Monitoring Network.....	51
4.1.2.1. MOE Water Well Records.....	52
4.1.2.2. Gartner Lee Wells.....	54
4.1.2.3. Surface Water Bodies.....	56
4.2. Piezometer Installation.....	56
4.2.1. Drilling Methods.....	56
4.2.1.1. Jet-drilling.....	56
4.2.1.2. Hollow Stem Augering.....	59
4.2.2. Piezometer Design.....	59
4.2.2.1. Bundle Piezometer.....	62

4.2.2.2.	Nest/Single Piezometer.....	63
4.2.2.3.	Minipiezometer.....	67
4.3.	Hydrogeological Analysis.....	68
4.3.1.	Field Work.....	68
4.3.1.1.	Soil Sampling.....	68
4.3.1.2.	Slug and Bail Tests.....	71
4.3.1.3.	Water Level Measurements...	73
4.3.1.4.	Water Sampling Procedure...	73
4.3.2.	Laboratory Analysis.....	74
4.3.2.1.	Grain Size Analysis.....	74
4.3.2.2.	Soil Identification.....	75
4.3.2.3.	Water Analysis.....	76
4.3.2.4.	Isotope Analysis.....	78
5.0.	RESULTS AND DISCUSSION.....	80
5.1.	Geophysical Analysis.....	80
5.1.1.	Resistivity Analysis.....	80
5.1.2.	Seismic Survey.....	90
5.2.	Surface Water Body Electrical Conductivity...	102
5.3.	Subsurface Geology.....	105
5.4.	Hydrogeological Analysis.....	110
5.4.1.	Soil Identification.....	110
5.4.2.	Hydraulic Conductivity.....	112
5.4.3.	Water Table Levels.....	119
5.5.	Hydrochemical and Isotopic Data.....	122
5.5.1.	Hydrochemical Analysis.....	122
5.5.1.1.	Carbon Dioxide.....	126
5.5.1.2.	Chloride.....	126
5.5.1.3.	Alkalinity.....	128
5.5.1.4.	Sulphate.....	131
5.5.1.5.	Major Cations.....	131
5.5.2.	Isotopic Analysis.....	137
5.5.3.	Chemical and Isotopic Relationships..	143
6.0.	CONCLUSIONS AND RECOMMENDATIONS.....	160
6.1.	Conclusions.....	160
6.2.	Recommendations.....	166
REFERENCES.....		168
APPENDIX I.....		174
APPENDIX II.....		194
VITA AUCTORIS.....		229
4.2.2.2.	Nest/Single Piezometer (after Sklar)	63
4.2.2.3.	Minipiezometer installation.....	67
4.3.1.1.	Soil Sampling.....	68
4.3.1.2.	Slug and Bail Tests.....	71
4.3.1.3.	Water Level Measurements...	73
4.3.1.4.	Water Sampling Procedure...	73
4.3.2.1.	Grain Size Analysis.....	74
4.3.2.2.	Soil Identification.....	75
4.3.2.3.	Water Analysis.....	76
4.3.2.4.	Isotope Analysis.....	78
5.1.1.	Resistivity Analysis.....	80
5.1.2.	Seismic Survey.....	90
5.4.1.	Soil Identification.....	110
5.4.2.	Hydraulic Conductivity.....	112
5.4.3.	Water Table Levels.....	119
5.5.1.1.	Carbon Dioxide.....	126
5.5.1.2.	Chloride.....	126
5.5.1.3.	Alkalinity.....	128
5.5.1.4.	Sulphate.....	131
5.5.1.5.	Major Cations.....	131
5.5.2.	Isotopic Analysis.....	137
5.5.3.	Chemical and Isotopic Relationships..	143

LIST OF FIGURES

Figure		Page
1	Study area location.	5
2	Local topography (after Surveys and Mapping Branch, 1970).	6
3	Study area, surrounding municipalities, and villages.	7
4	Surface soils (after Experimental Farm Service, 1947).	10
5	Quaternary geology (after Vagners, 1972).	12
6	Probable local groundwater flow directions.	15
7	Schematic of local hydrogeology.	16
8	Meteoric Water Line (after Craig, 1961a).	20
9	Tritium concentrations in precipitation from Ottawa and Simcoe, Ontario, Canada (after I.A.E.A., 1979).	23
10	$\delta^{18}\text{O}$ - δD relationships (after Fritz et al., 1976).	27
11	Wenner array for electrical resistivity surveys.	45
12	Location of resistivity survey sites.	48
13	Location of seismic survey sites.	50
14	Location of MOE wells and Gartner Lee piezometers.	53
15	Casing apparatus for jet-drilling method.	57
16	Location of bundle piezometers, single and nest piezometers, minipiezometers and piezometer profile traces.	60
17	Bundle piezometer installation.	64
18	Nest and single piezometer installation.	66
19	Stainless steel minipiezometer (after Sklash et al., 1985).	69
20	Polyethylene minipiezometer installation.	70
21a	Cluster analysis for apparent resistivity for sites at an 'a' spacing of 1 m.	82

21b	Cluster analysis for apparent resistivity for sites at an 'a' spacing of 3 m.	83
21c	Cluster analysis for apparent resistivity for sites at an 'a' spacing of 6 m.	84
21d	Cluster analysis for apparent resistivity for sites at an 'a' spacing of 9 m.	85
22	Apparent resistivity distribution (Ωm) for an 'a' spacing of 1 m.	88
23	Apparent resistivity distribution (Ωm) for an 'a' spacing of 3 m.	89
24	Apparent resistivity distribution (Ωm) for an 'a' spacing of 6 m.	91
25	Apparent resistivity distribution (Ωm) for an 'a' spacing of 9 m.	92
26	Cluster analysis for seismic primary velocities of layer 1 (V_{p1}).	96
27	Distribution of seismic primary velocities for layer 1 (V_{p1}).	97
28	Cluster analysis for seismic primary velocities of layer 2 (V_{p1}).	98
29	Distribution of seismic primary velocities for layer 2 (V_{p1}).	99
30	Cluster analysis for seismic primary velocities of layer 3 (V_{p1}).	100
31	Distribution of seismic primary velocities for layer 3 (V_{p1}).	101
32	Possible contaminant plume locations.	103
33	Electrical conductivity for surface water bodies.	104
34a	Subsurface profiles from A-A'.	106
34b	Subsurface profiles from B-B'.	107
34c	Subsurface profiles from C-C'.	108
34d	Subsurface profiles from D-D'.	109
35	Topography of the till surface.	111

36	Example plot of the slug and bail test.	115
37	Water table and groundwater flow directions for (a) October 31, 1987 and (b) for March 19, 1988.	121
38	Areal distribution of chloride.	123
39	Areal distribution of major ions.	124
40	Chloride-alkalinity relationship.	130
41	Calcium relationship with (a) sodium and (b) potassium.	133
42	Calcium-magnesium relationship.	135
43	Saturation indices of water samples.	136
44	Electrical conductivity-chloride relationship. ...	138
45	Areal distribution of (a) ^{18}O , (b) D, and (c) tritium.	139
46	$\delta^{18}\text{O}$ - δD relationship for groundwater samples.	141
47	Relationship between tritium and (a) $\delta^{18}\text{O}$ (b) and δD	144
48	Cluster analysis of chemical and isotopic data. ..	145
49	Relationship between chloride and (a) $\delta^{18}\text{O}$ and (b) δD	148
50	Relationship between sodium and (a) $\delta^{18}\text{O}$ (a) and (b) δD	150
51	Relationship between potassium and (a) $\delta^{18}\text{O}$ and (b) δD	151
52	Relationship between alkalinity and (a) $\delta^{18}\text{O}$ and (b) δD	152
53	Relationship between electrical conductivity and (a) $\delta^{18}\text{O}$ and (b) δD	153
54	Relationship between magnesium and (a) $\delta^{18}\text{O}$ and (b) δD	154
55	Relationship between calcium and (a) $\delta^{18}\text{O}$ and (b) δD	156
56	Relationship between sulphate and (a) $\delta^{18}\text{O}$ and (b) δD	157

LIST OF TABLES

Table	Page
1. Accuracy and precision of selected analytical methods (Rand <i>et al.</i> , 1975).	77
2. Apparent resistivities for 'a' spacings of 1 to 10 m.	81
3. Resistivity values (ρ_m) for surface and subsurface material.	86
4. Primary velocities (V_p) and depths to interfaces (z) for seismic sites.	93
5. Seismic velocities for surface and subsurface material.	95
6. Values for parameters used in till identification.	113
7. Time lag and hydraulic conductivities for the slug and bail tests.	116
8. Effective diameter and hydraulic conductivities using Hazen's formula.	117
9. Hydraulic conductivities from Hazen's formula and the slug and bail tests.	118
10. Water table levels for October 31, 1987 and March 19, 1988.	120
11. Chemical and isotopic concentrations of groundwater within the study area.	125
12. Subsurface indices of calcite (SI_{cal}) and dolomite (SI_{dol}), and partial pressures of carbon dioxide.	127
13. Slopes, y-intercepts, and correlation coefficients for the isotope-contaminant relationships.	146

LIST OF NOTATIONS

^{18}O	-oxygen-18
^{16}O	-oxygen-16
δ	-del or delta value
%	-part per mil
H or ^1H	-protium
D or ^2H	-deuterium
T or ^3H	-tritium
R	-isotopic ratio
C	-celcius
TU	-tritium units
$\sigma^{18}\text{O}$	-relative concentration of oxygen-18
σD	-relative concentration of deuterium
$p\text{CO}_2$	-partial pressure of carbon dioxide
aq	-aqueous
g	-gas
l	-liquid
atm	-atmospheric
ρ	-resistivity
ρ_a	-apparent resistivity
i	-incident angle
r	-refraction angle
K	-hydraulic conductivity

1.0. INTRODUCTION

Essex County Sanitary Landfill Site No. 2 is situated within an abandoned sand and gravel pit located in southwestern Ontario approximately 3 km west of the Town of Leamington. It obtains municipal wastes from the surrounding towns and townships.

Sand and gravel deposits north, south and east of the landfill are conducive to the migration of leachate from refuse cells in the landfill into the shallow unconfined aquifer. Contaminants in concentrations above background levels have been detected to the south and east of the landfill in piezometers, water supply wells and surface water bodies (Essop and Brown, 1980; Gartner Lee Associates Limited, 1986).

1.1. Objectives and Scope

The first of two primary objectives of this study is to determine the applicability of using environmental isotopes as natural tracers of contaminant migration from a sanitary landfill. The second primary objective is to determine the principal modes of contaminant attenuation within the study area using relationships developed between the isotopic and geochemical data.

The secondary objectives of the study are : (1) to define the location of the contaminant plume using geophysical surveys and electrical conductance testing of

surface water bodies, and (2) to sample and analyse groundwater to determine its geochemical characteristics.

The majority of monitoring sites consist of one single port piezometer. This permits only a limited examination of the contaminant plume throughout the study area.

Groundwater was sampled and analysed once for the isotopes and major ions. This precluded verification of anomalous responses and an examination of isotopic and geochemical concentration variations with time.

1.2. Thesis Structure

The objectives and scope of the study are presented with the introduction in the opening chapter. Chapter 2 describes the study area by identifying its geographic location, then examining the physiography, climate, geology, surface drainage and hydrogeology of the area.

Theoretical considerations are presented in Chapter 3. This chapter discusses the theory behind environmental isotopes, their uses as tracers, and the processes of isotopic enrichment. The groundwater chemistry common to sand and gravel glacial environments and landfills is also presented.

Chapter 4 examines the methods of study. It discusses the site evaluation prior to the design and installation of piezometers in a monitoring network and the hydrogeological analysis of the subsurface material and groundwater, both in the field and in the lab.

The results of the study are presented in Chapter 5. A discussion of the results demonstrates the associations between the isotopes and the chemical data. Conclusions of the study and recommendations for preventing further spreading of the contaminant plume and for further study, are discussed in Chapter 6.

The landfill is used and operated by five municipalities: the Town of Lexington and the Town of Andover, and the Townships of Warren, Gosfield North and Gosfield South. The waste is also received from the village of Plympton.

2.1.2. Site Operations

Landfilling operations began in 1970 at the northern section of the landfill and have recently moved to the western section. The site is a combination of an existing landfill for the Town of Lexington and the Township of Gosfield North, a mini-landfill, and undeveloped private lands. A closed landfill that was operated by H.J. Jones, Inc. lies directly to the east (Figure 2).

2.0. STUDY AREA

2.1. SITE LOCATION

Essex County Sanitary Landfill Site No. 2 is located in southwestern Ontario in the County of Essex (Figure 1). It is approximately 3 km west of Leamington in Lot 13, Concession II, of Gosfield South Township. The landfill is bounded by the Chesapeake and Ohio Railway to the south and County Road 31 (Mersea Townline Road) to the east (Figure 2). Agricultural land borders on the western perimeter, with Township Concession III to the north. Residential and commercial development is sporadic around the landfill with greatest concentrations along Highway #3, 1.5 km west in Ruthven and 3 km east in Leamington.

The landfill is used and operated by five municipalities: the towns of Leamington and Kingsville, and the townships of Mersea, Gosfield North and Gosfield South (Figure 3). Wastes are also received from the village of Wheatley.

2.1.1. Site Operations

Landfilling operations began in 1970 at the northern section of the landfill and have recently moved to the western section. The site is a combination of an existing landfill for the Town of Leamington and the Township of Gosfield South, a mined-out sand pit, and undeveloped private lands. A closed landfill that was operated by H.J. Heinz, lies directly to the east (Figure 2).

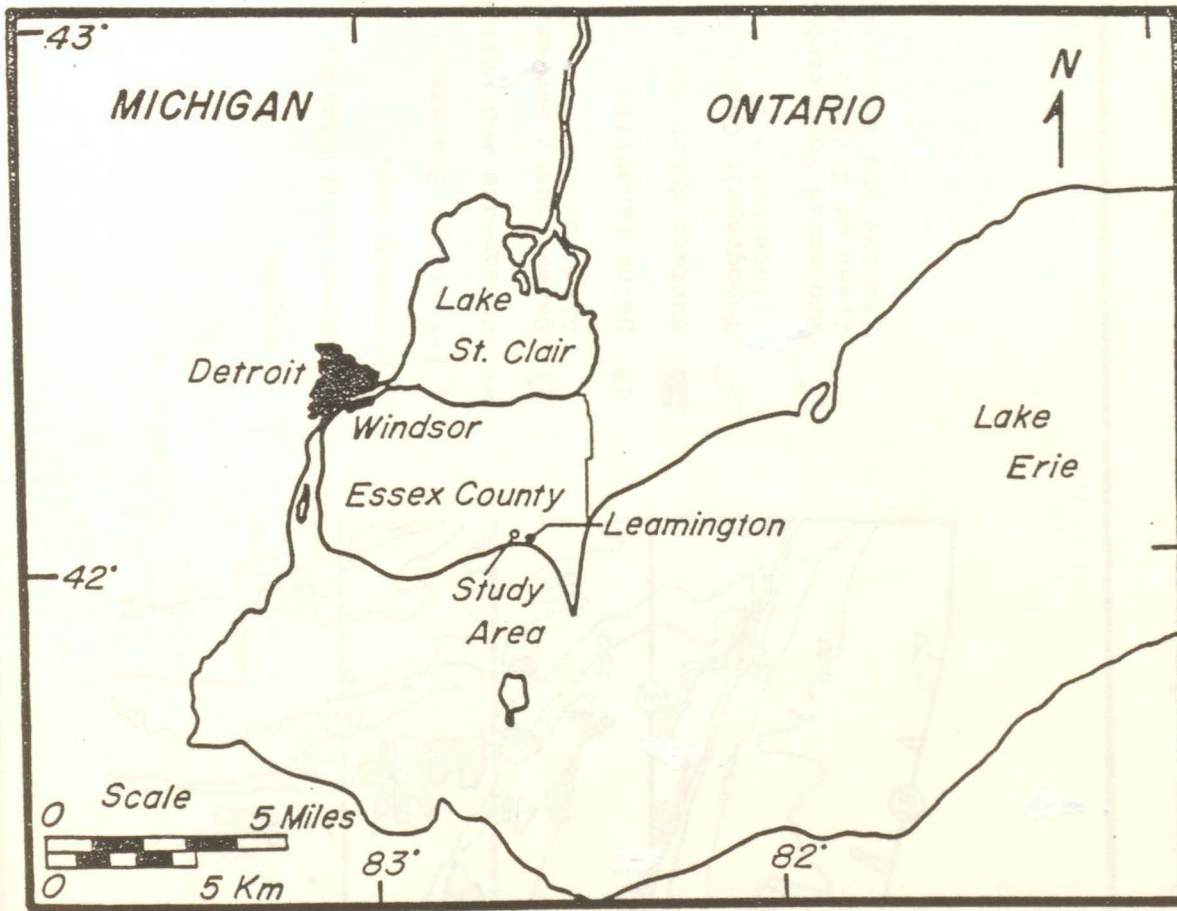


Figure 1. Study area location.

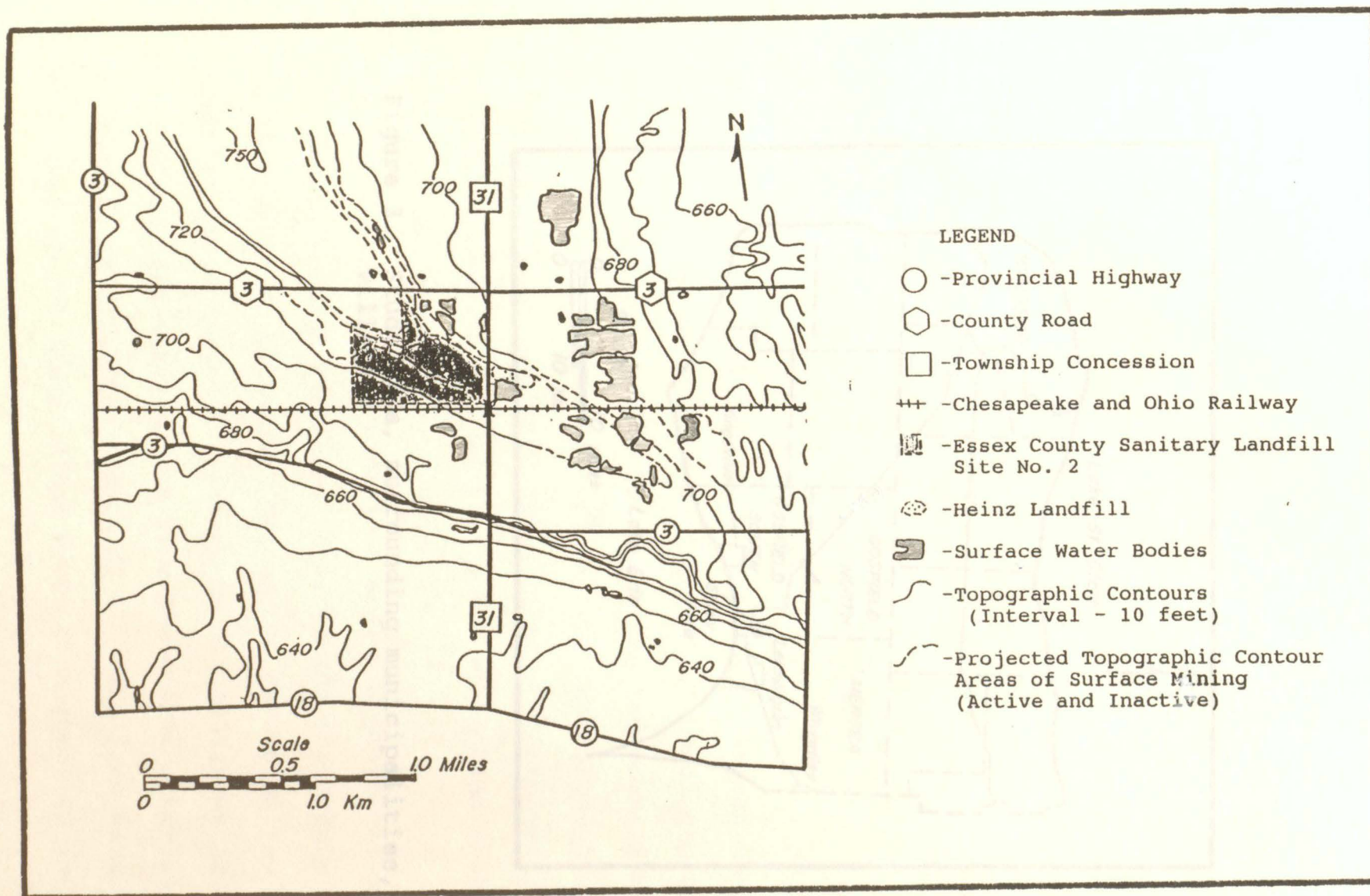


Figure 2. Local topography (after Surveys and Mapping Branch, 1970).

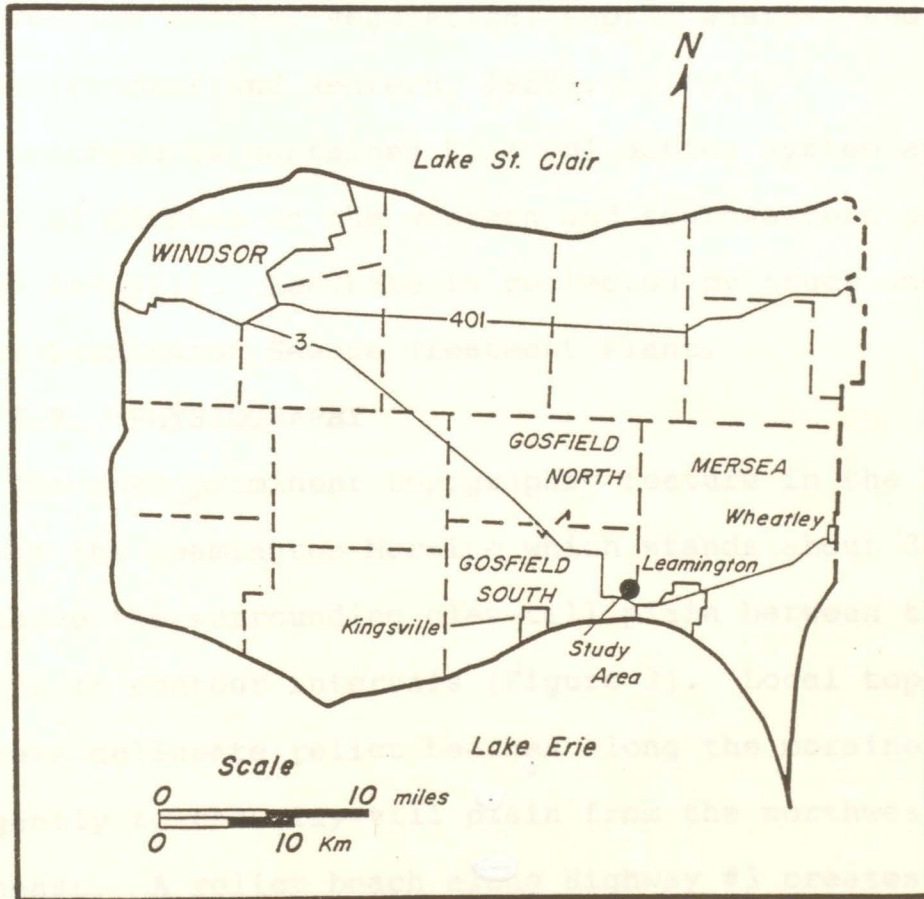


Figure 3. Study area, surrounding municipalities, and villages.

Landfill contents are mainly household wastes, processed and rejected vegetable wastes, canned products, construction debris, vegetation, septic wastes, and sewage sludge (Proctor and Redfern, 1985).

Leachate is contained by a collection system and a series of ditches on the western and southwestern perimeter of the landfill. Leachate is collected by truck and shipped to the Leamington Sewage Treatment Plant.

2.2. PHYSIOGRAPHY

The most prominent topographic feature in the study area is the Leamington Moraine which stands about 30 m (100 ft) above the surrounding clay-till plain between the 650 and 750 ft contour intervals (Figure 2). Local topographic contours delineate relict beaches along the moraine which dip gently to the clay-till plain from the northwest to the northeast. A relict beach along Highway #3 creates a steep embankment down to a lower till plain which dips south towards Lake Erie.

Intensive surface mining of sand and gravel along the Leamington Moraine continues to alter its topography and surface drainage patterns. Mining has ceased on the landfill property and to the north, but continues to the south and east. Clay borrow from the active mines is used as capping material for the landfill. The land west and southwest of the landfill and south of Highway #3 is agricultural.

Surface soils vary between loam and sandy loam, with depths averaging between 0.3 and 1 m (Figure 4). The Burford Loam follows the topographic high along the Leamington Moraine. The Fox Sandy Loam flanks the Leamington Moraine, closely paralleling the relict beaches.

2.3. Climate

Proximity to Lake Erie has a moderating affect on climate in the Leamington area (Sanderson, 1980). Winter temperatures average -4.1°C with approximately 185 days of frost per year. Frost penetration is minimal, reaching maximum depths of about 10 cm. The summer mean temperature is 22.2°C . Precipitation averages 815 mm a year in Leamington with most precipitation falling during the spring and summer months. Relative humidity is greatest at night with year-round averages between 80 to 90%. During the day, relative humidity increases with temperature, averaging 50 to 70% in the summer and 70 to 80% in the winter. Also, during the summer months, evapotranspiration exceeds precipitation resulting in a net soil moisture loss.

2.4. GEOLOGY

2.4.1. Paleozoic Geology

The bedrock below the landfill is a light tan microcrystalline and microsucrosic dolomite of the Lucas Formation which is part of the Middle Devonian Detroit River Group (Sanford, 1969). South of Highway #3, the bedrock is part of the Amherstburg Formation which is a grey to dark

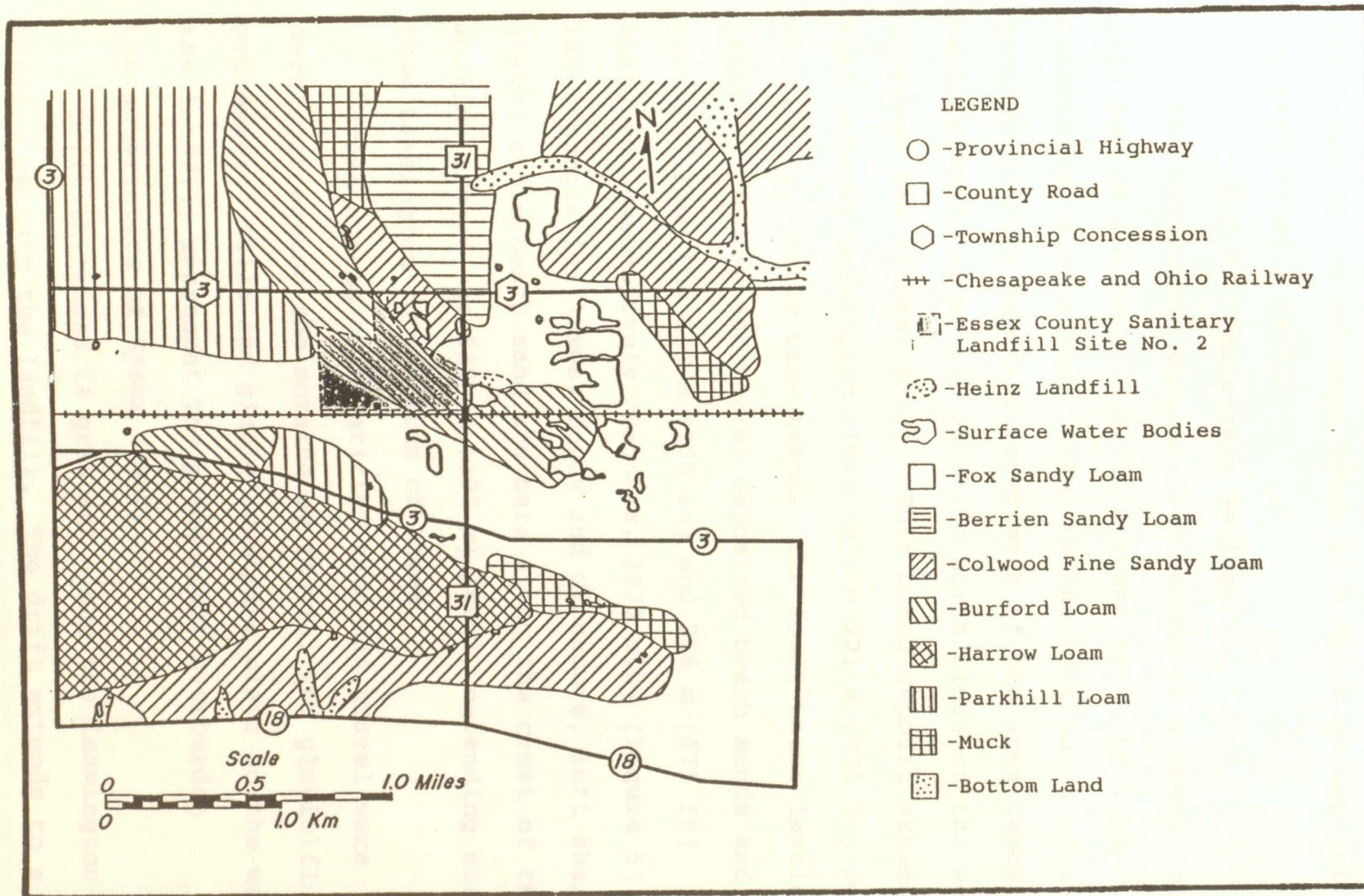


Figure 4. Surface soils (after Experimental Farm Service, 1947).

brown, crinoidal limestone. Bedrock does not outcrop near the landfill, it subcrops about 60 m below ground surface (Vagners *et al.*, 1973).

2.4.2. Quaternary Geology

The Leamington Moraine is composed of a heavy, compact till and is flanked by relict beaches from the late Wisconsinan glaciation. Prior to the Port Huron advance, proglacial Lake Arkona covered much of the area depositing beach gravels along the east and north sides of the moraine (Chapman and Putnam, 1973). This beach deposit extends as a spit towards Leamington close to the 221 m (725 ft) contour (Figure 2). After Lake Arkona, the lower water levels of Lakes Whittlesey and Warren deposited beach sands and gravels along the 213 m (700 ft) and 206 m (675 ft) contours, respectively (Vagners, 1972 a,b) (Figure 5). Two later proglacial lakes, Lundy and Grassmere, left shallow gravel storm beach sand and bars along the crest of the moraine around the 630 ft (192 m) level, extending northwest from Leamington to the Town of Essex.

Broad aprons of stratified sand and gravel were developed around the moraine by fluvial and glacialfluvial processes. Tills and glaciolacustrine clays to the west of the landfill represent the predominant overburden characteristics of Essex County.

Drift thickness is greatest along the Leamington Moraine beneath the landfill. The drift extends to a depth

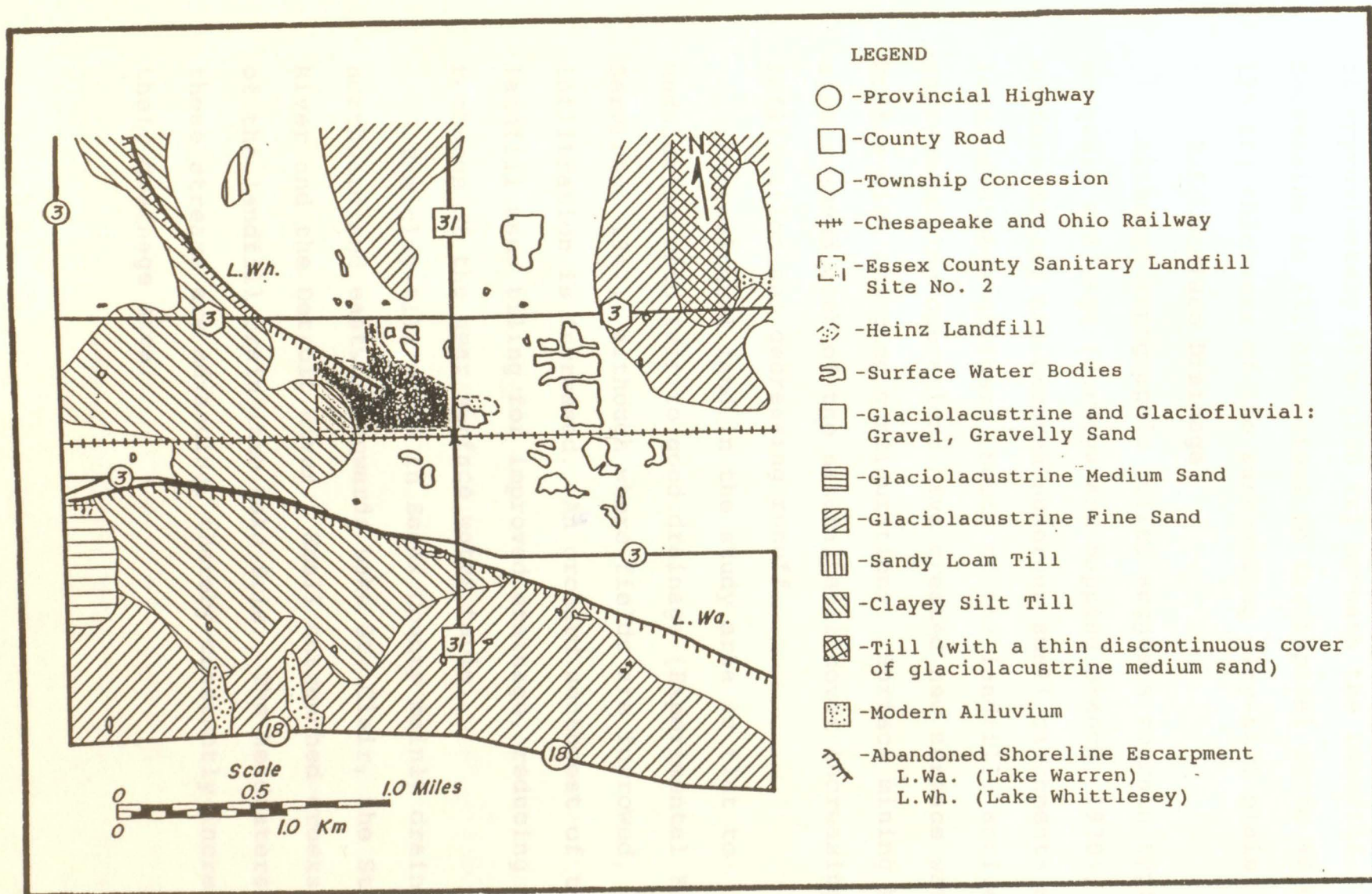


Figure 5. Quaternary geology (after Vagners, 1972).

of approximately 60 m (200 ft) beneath the landfill, decreasing in all directions to the typical 30 to 40 m (100-125 ft) thickness of the surrounding clay-till plain.

2.5 Surface Drainage

Although topographic relief suggests terrain typical of adequate drainage (Surveys and Mapping Branch, 1970), surface mining has created numerous small catchments and new local drainage divides. South of the landfill, active surface mining operations have created new surface water bodies with changing configurations. Surface mining has also removed much of the natural soil cover increasing infiltration and decreasing runoff.

Agricultural land in the study area is flat to undulating with fair to good drainage (Experimental Farm Services, 1947), although where fields are furrowed, infiltration is increased. An orchard southwest of the landfill uses tiling for improved drainage, reducing the recharge of the near surface water table.

The clay-till plain in Essex County mainly drains northward and eastward towards Lake St. Clair, the St. Clair River and the Detroit River. Small entrenched creeks south of the landfill drain into Lake Erie. The headwaters of these streams are advancing, thereby constantly increasing their drainage area.

2.6. Hydrogeology

As a topographic high, the Leamington Moraine is a local recharge zone with groundwater flow possibly radiating from southwest to northeast (Figure 6). Gartner Lee Associates Limited (1986) indicate a regional flow direction for the unconfined sand aquifer from west to east. Essop and Brown (1980) suggest that the regional groundwater flow is towards Lake Erie in the southeast.

Towards the south and east, the sand and gravel deposits thicken, developing a noticeable saturated zone. A till layer below the upper sand and gravel deposit separates a perched water table from a deeper, partly unconfined saturated zone in the study area (Figure 7) (Gartner Lee Associates Ltd., 1986) and in the immediate vicinity (MOE, 1984).

Some groundwater ion concentrations have been reported by Gillham *et al.* (1978) for an unconfined aquifer about 3 km northeast of the landfill. The area is in a similar geological setting as the landfill. The concentration ranges were less than 40 mg/L for chloride, below 20 mg/L for sodium, less than 10 mg/L for potassium, between 5 to 22 mg/L for magnesium and between 80 to 200 mg/L for calcium.

Below the unconfined aquifer, confined sandy gravel units supply variable quantities of groundwater (Essop and Brown, 1980). A deeper confined sand and gravel aquifer

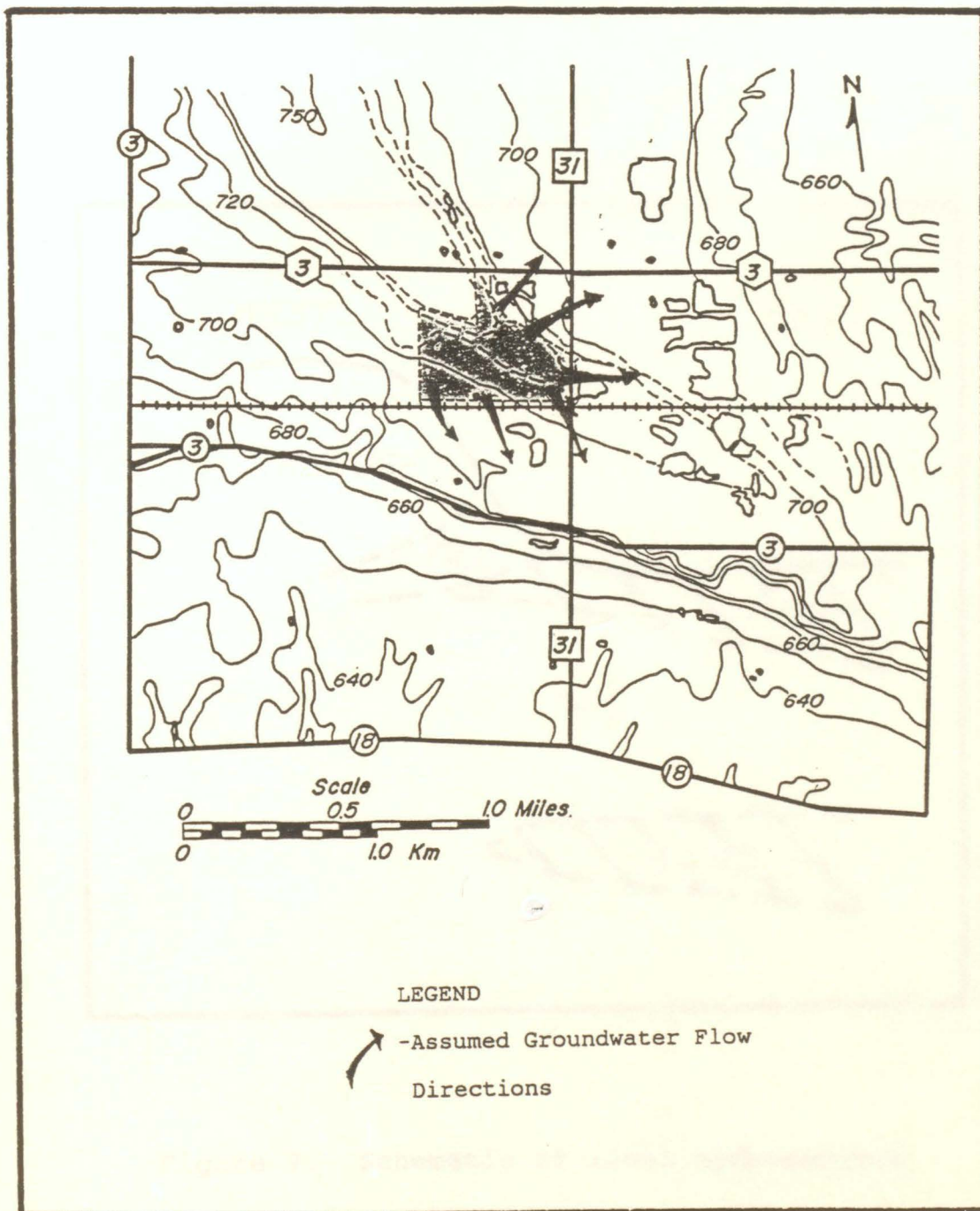


Figure 6. Probable local groundwater flow directions.

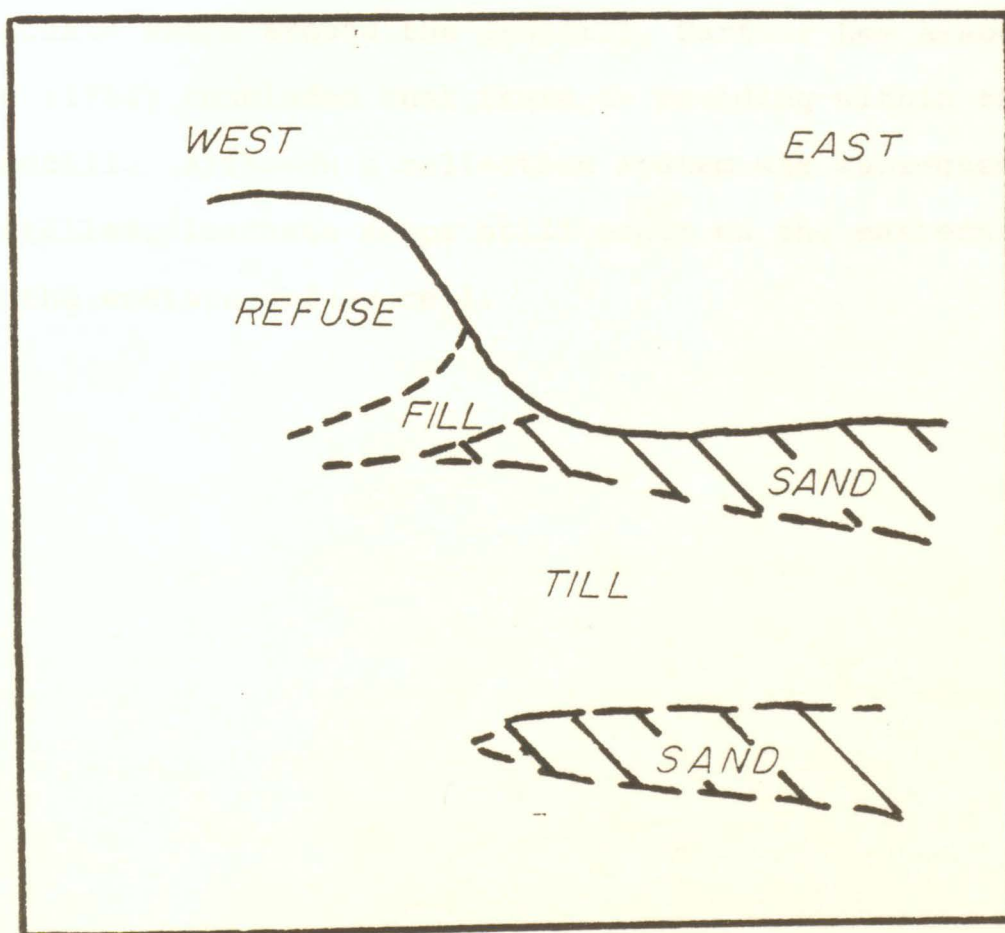


Figure 7. Schematic of local hydrogeology

consists of granular material and the upper few metres of the weathered and fractured bedrock (Essop and Brown, 1980).

Based on piezometric evidence and from the presence of leachate seeps around the landfill, Gartner Lee Associates Ltd (1986) concluded that there is mounding within the landfill. Although a collection system was subsequently installed, leachate seeps still occur on the eastern slopes of the western refuse cell.

3.0. THEORETICAL CONSIDERATIONS

3.1. Environmental Isotopes

Isotopes are atoms of an element which contain identical numbers of protons in their nuclei, but different numbers of neutrons (Hoefs, 1973). Environmental isotopes are naturally occurring isotopes (or those over which the hydrogeologist has no control) which can be used in solving hydrogeological problems.

This study involves the use of isotopes of oxygen and hydrogen. The oxygen atom has five isotopes, but only two are of practical interest, oxygen-16 (^{16}O) and oxygen-18 (^{18}O). The hydrogen atom has three isotopes: protium (H or ^1H), deuterium (D or ^2H) and tritium (T or ^3H). Isotopes of these two elements are constituent parts of some water molecules (eg. H_2^{16}O , H_2^{18}O , HDO, HTO).

3.1.1. Oxygen-18 and Deuterium

Since absolute abundances of the isotopes ^{18}O and D in the environment are very small compared to ^{16}O and ^1H , isotope ratios are used to report isotopic concentrations. These ratios compare the abundances of the heavy isotopes to those of the lighter:

$$R = \frac{^{18}\text{O}}{^{16}\text{O}} \quad R = \frac{\text{D}}{^1\text{H}} \quad (1)$$

A standard used in hydrogeology is SMOW (Standard Mean Ocean Water) (Craig, 1961b). Isotopic concentrations are

expressed as a relative difference between the isotopic ratio of an unknown water sample and a known standard (Craig, 1961b), as a "del" or "delta" value (^{18}O , D) given in parts per mil (‰):

$$\delta^{18}\text{O} \text{ or } \delta\text{D} = (R_{\text{sample}} - R_{\text{std}}) / R_{\text{std}} \times 10^3 \text{ (‰)} \quad (2)$$

If the del value is negative, then the water sample is depleted in the heavy isotope relative to the standard. If the del value is positive, then the water sample is enriched in the heavy isotope.

Bond energies in water molecules vary between atoms with the bonds in molecules with light isotopes being weaker than bonds in molecules with heavy isotopes. This difference in bond strength results in higher vapour pressures and a preference for the vapour phase for molecules containing the light isotopes (Saxena, 1987).

For meteoric water which has not been evaporated, the ^{18}O and D values are linearly related. A comparison of worldwide precipitation values indicates a relationship of:

$$\delta\text{D} = 8\delta^{18}\text{O} + 10 \quad (3)$$

This line is known as the Meteoric Water Line (MWL) (Craig, 1961a) (Figure 8). Local meteoric water lines may have slightly different slopes and intercepts. In southern

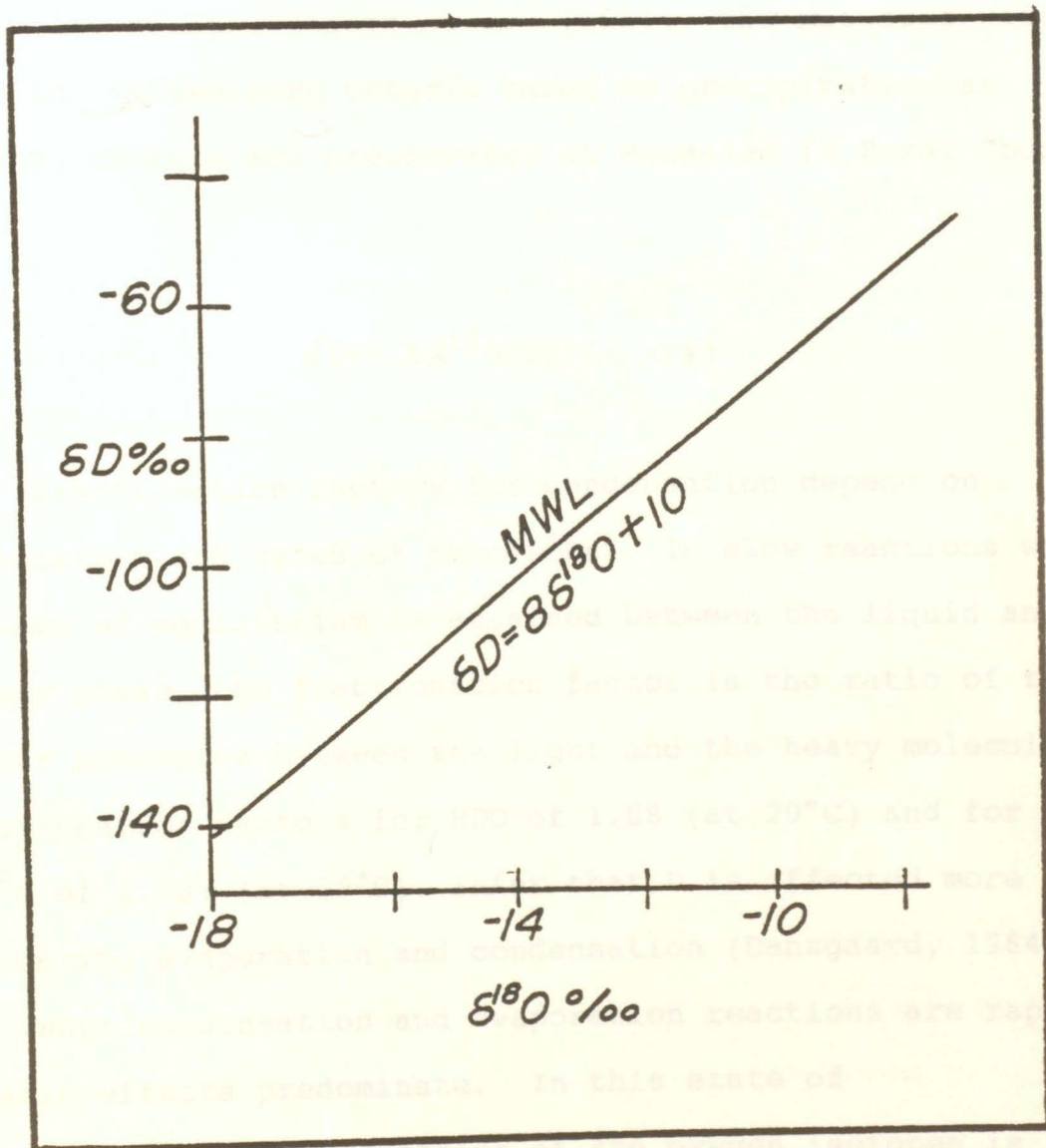


Figure 8. Meteoric Water Line (after Craig, 1961)

Ontario, the Great Lakes alter this relationship by causing moderate temperatures and a high relative humidity.

According to Desaulniers *et al.* (1981), the meteoric water line in southwestern Ontario based on precipitation at Simcoe, Ontario and groundwater at Woodslee in Essex County is:

$$\delta D = 7.5 \delta^{18}O + 12.6 \quad (4)$$

Fractionation factors for condensation depend on temperature and rates of reactions. In slow reactions where a state of equilibrium is attained between the liquid and vapour phase, the fractionation factor is the ratio of the vapour pressures between the light and the heavy molecules. Fractionation factors for HDO of 1.08 (at 20°C) and for H₂¹⁸O of 1.009 (at 20°C), infer that D is affected more than ¹⁸O during evaporation and condensation (Dansgaard, 1964).

When condensation and evaporation reactions are rapid, kinetic effects predominate. In this state of disequilibrium, fractionation of the oxygen isotopes is greater than that of the hydrogen isotopes. As a result, evaporation results in a slope of 4 to 6 for the $\delta D - \delta^{18}O$ relationship, depending on factors such as: humidity, temperature, water turbulence and wind speed component perpendicular to the water surface (Dansgaard, 1964). Enrichment of water in plants by evapotranspiration will

produce an even shallower slope (2.7 to 4.0) because of the boundary effect created by the plant's epidermal membrane. In this instance, kinetic effects are weighted higher than equilibrium fractionation of evaporation (Allison *et al.*, 1985).

3.1.2. Tritium

Tritium occurs both naturally and anthropogenically. Concentrations are given in tritium units (TU) where 1 TU is equivalent to 1 tritium atom in 10^{18} protium atoms. Ottawa has the longest continuous record of T in precipitation (Figure 9). In nature T is produced in very low concentrations (4 to 25 TU) by the bombardment of atmospheric nitrogen by cosmic rays creating carbon-14 and T (Fritz and Fontes, 1980). Man-made production of T began in the mid-1940's with the commencement of nuclear testing. Tritium is one of the fallout products which became noticeable in 1953 and peaked in North America in 1963, several magnitudes above natural levels. Stratospheric mixing during late winter and early spring creates seasonal fluctuations of T in precipitation (Fritz and Fontes, 1980).

Interpretation of T data is semi-quantitative. Tritium can be used to indicate if the water is new (post-1953) or old (pre-1953) with high T concentrations indicating areas of recent infiltration and high pollution potential. With a half-life of 12.34 years, old natural T will have decayed to < 5 TU while post-1953 values will be higher.

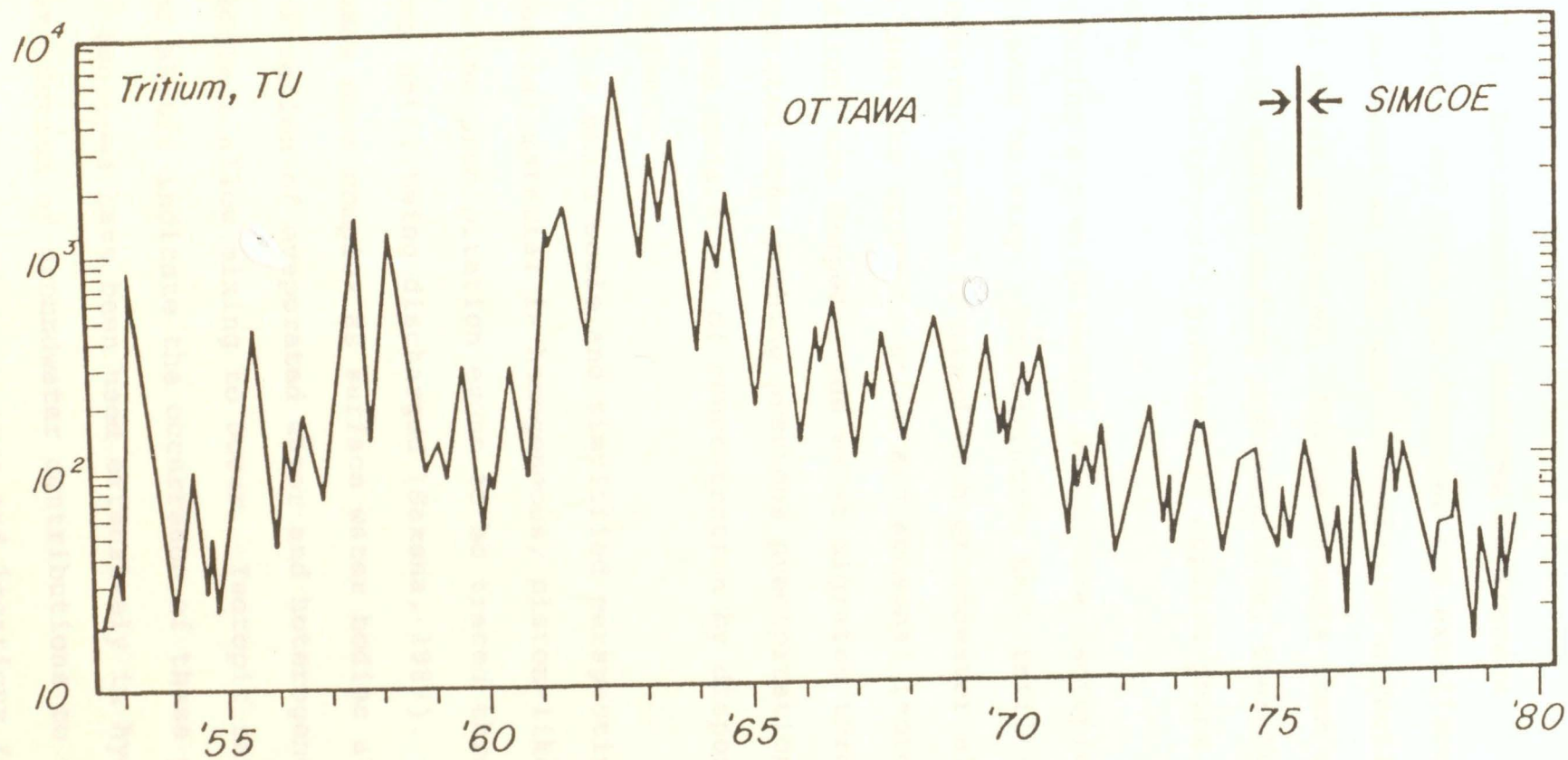


Figure 9. Tritium concentrations in precipitation from Ottawa and Simcoe, Ontario, Canada (after I.A.E.A., 1979).

3.2. Environmental Isotopes as Tracers

Oxygen and hydrogen isotopes are excellent tracers of water movement as they are incorporated directly into natural water molecules. Nature injects them into the hydrologic system during precipitation, thereby omitting the spatial and temporal problems of applied point source tracers.

During a precipitation event, the isotopic content of rain tends to vary. Precipitation that infiltrates into the groundwater system is mixed with groundwater already present such that the storm-to-storm and seasonal isotopic variations are damped. The water migrates through the unsaturated zone pushing previous precipitation events ahead with some moderation of concentration by dispersion and diffusion.

In a small scale and simplified perspective, if the geological material is homogeneous, piston-like flow will allow the precipitation event to be traced through the system until being discharged (Saxena, 1987). The scenario becomes more complex as surface water bodies allow infiltration of evaporated water and heterogeneities in the subsurface allow mixing to occur. Isotopic ratios of the water should indicate the occurrence of these processes.

Isotopes have been used extensively in hydrogeology for determination of groundwater contributions to stream flow (Sklash, 1983), recharge rates and locations for water

supply (Airey *et al.*, 1974), and properties of water supply aquifers (Fritz *et al.*, 1975). Recently, attempts have been made to use isotopic tracers to delineate the extent of contamination from sanitary landfills (Fritz *et al.*, 1976).

Fritz *et al.* (1976) and Baedecker and Back (1979) observed that landfill leachate may be isotopically different from the background groundwater. Various retardation processes attenuate migrating contaminant concentrations, thereby affecting the migration of contaminant tracers such as chloride (Fritz *et al.*, 1979), however the isotopic content of the leachate will change only by dilution. Recognition of the isotopically tagged leachate may therefore be useful in tracking leachate movement and in identifying dilution effects on contaminant attenuation.

Tritium can also be used as a tracer, however the presence or absence of T in groundwater reflects the actual water movement, not the migration or attenuation of dissolved constituents. Work by Van Duijvenbooden (1985) in the Netherlands has indicated the presence of higher T concentrations in leachate beneath and around a sanitary landfill, relative to background levels. This suggests the possibility of using T as a tracer of leachate movement. Similar work by Egboka *et al.* (1983) at Borden, Ontario also demonstrates the usefulness of T as a tracer of contaminant migration.

In clays, T and D show apparent retardation compared to protium, while chloride has been found to migrate at a faster rate than T (Stewart, 1967). Causes range from exchange with soil material or adsorbed water, to diffusion rate variations. Isotopic removal, however, is insignificant in migration through sand and gravel or in relation to analytical error (Stewart, 1980).

3.3. Processes of Isotopic Enrichment

Studies at landfills by Fritz *et al.* (1976) and Baedecker and Back (1979) have indicated the occurrence of enriched $\delta^{18}\text{O}$ and δD values in leachate. Fritz *et al.* (1976) detected both ^{18}O and D enrichment while Baedecker and Back (1979) identified only D enrichment. There are four possible processes of enrichment as suggested by Fritz *et al.* (1976). These processes are: evaporation, decomposition of organic matter, oxygen exchange between water and carbon dioxide, and recharge.

Evaporation results in a decreased slope in the $\delta\text{D}-\delta^{18}\text{O}$ relationship relative to precipitation. The predominance of kinetic fractionation results in the evaporated waters developing a $\delta\text{D}-\delta^{18}\text{O}$ relationship with a slope of 4 to 6 (Fritz and Fontes, 1980) (Figure 10).

There are two processes of enrichment by decomposition of organic matter: (1) decomposition of vegetation and (2) hydrogen sulphide exchange. As indicated by Allison *et al.* (1985), the epidermal effect of the leaves in living

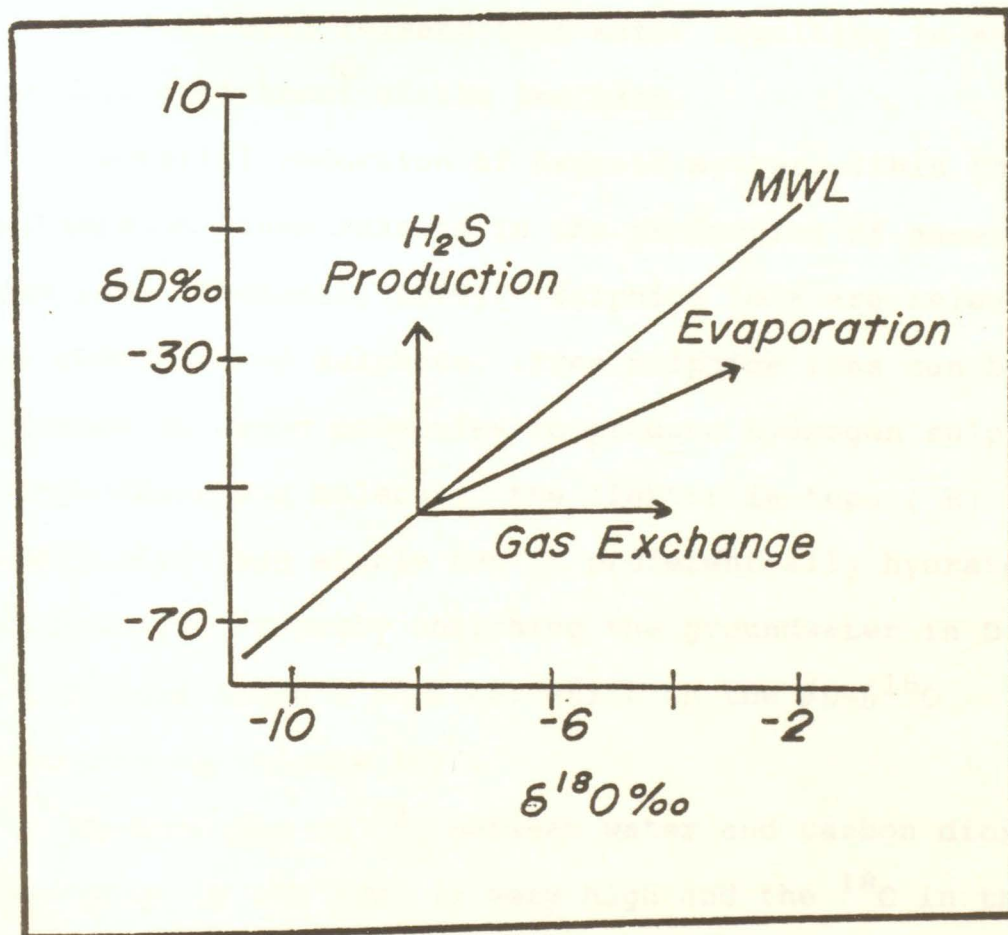


Figure 10. $\delta^{18}O$ - δD relationships (after Fritz et al., 1976).

vegetation causes kinetic fractionation during evapotranspiration, resulting in a $\delta D - \delta^{18}O$ relationship with a slope of 2.7 to 4. Decomposition of the vegetation within the landfill will release this water resulting in an isotopic enrichment of the leachate.

Bacterial reduction of organic matter within the contaminant plume results in the production of gases and free ions (Postgate, 1979). Sulphide ions are released by the reduction of sulphate. Free sulphide ions can become hydrated by water molecules to produce hydrogen sulphide. Within the water molecule, the lighter isotope (1H) is kinetically less stable and it preferentially hydrates the sulphide ion, thereby enriching the groundwater in D. This effect will cause a vertical shift in the $\delta D - \delta^{18}O$ relationship (Figure 10).

An exchange of ^{18}O between water and carbon dioxide will occur if the pCO_2 is very high and the ^{18}O in the water and in the CO_2 are not in equilibrium. Bacterial respiration within the contaminant plume produces CO_2 increasing the pCO_2 of the subsurface, thereby achieving the first requirement for the exchange. Bacterial reduction of sulphate results in fractionation of the ^{18}O , enriching the CO_2 relative to the decomposed organic matter. If the groundwater is newly recharged, the ^{18}O within the water and the CO_2 will not be in equilibrium, fulfilling the second requirement of the reaction. The large isotope

fractionation factor between CO_2 and water would cause a shift to enriched ^{18}O values in the leachate (Fritz et al., 1976) (Figure 10).

Examination of ^{18}O enrichment in sanitary landfill contaminant plumes by Basharmal (1985) shows a strong tendency for the greatest ^{18}O enrichment to occur in the centre of the contaminant plume where the greatest biological activity occurs. The reducing activity of the bacteria also causes ^{18}O enrichment within the residual sulphate ions. However, this enrichment process tends to continue only until the $\delta^{18}\text{O}$ of the sulphate is in equilibrium with the $\delta^{18}\text{O}$ of the groundwater (Basharmal, 1985). Prior to achieving this state of equilibrium, exchange of ^{18}O between the sulphate and the water would be very slow to negligible (Fritz and Fontes, 1980).

For the $\delta^{18}\text{O}$ in the CO_2 to be greater than in the water, the initial $\delta^{18}\text{O}$ in the reduced sulphate must be in equilibrium with, or greater than, the $\delta^{18}\text{O}$ of the groundwater. Since oxygen exchange between water and sulphate is extremely slow to nonexistent (Fritz and Fontes, 1980), the source of the sulphate is the deciding factor for the $\delta^{18}\text{O}$ of the CO_2 .

Recharge of water isotopically different from the groundwater can result in enrichment or depletion of the isotopic ratios. The final outcome is dependent on the magnitude of the differences in $\delta^{18}\text{O}$ and δD between the two

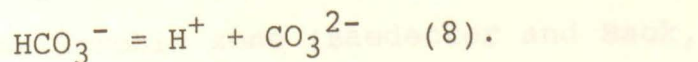
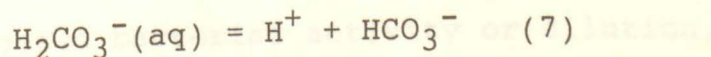
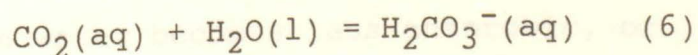
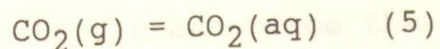
components and the volumes of the two components. Influx of foreign water with relatively depleted isotopic ratios may isotopically deplete the local groundwater, while an influx of foreign water with relatively enriched isotopic ratios may result in local groundwater enrichment.

3.4. Groundwater Chemistry

3.4.1. Carbon Dioxide

Carbon dioxide is an extremely important constituent in groundwater hydrochemistry. The partial pressure of carbon dioxide ($p\text{CO}_2$) in the atmosphere is $10^{-3.5}$ bars (at 25°C). Water in equilibrium with the atmosphere will have an equivalent $p\text{CO}_2$. In the subsurface, the $p\text{CO}_2$ is often higher owing to organic decomposition, microorganism respiration, and chemical reactions (Freeze and Cherry, 1979).

In a state of equilibrium, the concentration of dissolved carbon dioxide in water ($\text{CO}_2(\text{aq})$) equals the partial pressure of the carbon dioxide gas. If the $\text{CO}_2(\text{aq})$ is increased above equilibrium, CO_2 exsolution of the groundwater will occur until equilibrium is re-established. The reaction of $\text{CO}_2(\text{g})$ with groundwater is:



This reaction commences upon infiltration of precipitation into the root zone where organic decomposition increases the $p\text{CO}_2$ of the soil. The dissolution of CO_2 in water produces carbonic acid and bicarbonate thus increasing soil and water acidity.

Comparison of pH levels in sanitary landfills indicate a pH ranging between 6.5 and 7.5, even with elevated $p\text{CO}_2$ (Cherry, 1983). This pH level is controlled by one dominant chemical equilibrium reaction or by an interrelated set of reactions. The controlling ion is typically present in high concentrations or possesses the most rapid reaction rate (Hem, 1970).

In natural groundwater flow systems, it is usual for the redox potential to decrease along the flow path as $p\text{CO}_2(\text{aq})$ increases (Freeze and Cherry, 1979). Where surface mining has removed the soil zone, CO_2 production will be greatly reduced and an increased infiltration and mixing of water with $p\text{CO}_2(\text{atm})$ will deplete the $p\text{CO}_2(\text{aq})$.

Within a contaminant plume, bacteria reducing the organics produces CO_2 , increasing the $p\text{CO}_2$ of the groundwater. This reducing reaction occurs within the anaerobic zone. As the distance from the landfill increases, the groundwater becomes less anaerobic, or oxidized, from decreased bacterial activity or dilution, eventually forming an aerobic zone (Baedecker and Back,

1979; Fritz *et al.*, 1976). The area of mixing between the two zones is the 'transition' zone.

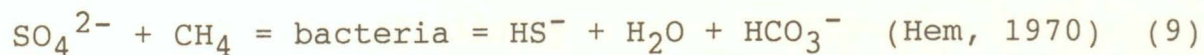
The elevated CO_2 values found within contaminant plumes create CO_2 and O_2 pressure gradients within the subsurface. These gradients may cause the diffusion of the CO_2 gas front ahead of the contaminant plume. An O_2 pressure gradient from O_2 depletion within the landfill could result in the migration of O_2 against the groundwater flow direction into the landfill, depleting the surrounding area in O_2 (Kunkle and Shade, 1976). A rapid influx of O_2 would create an environment detrimental to reducing-bacteria growth.

3.4.2. Sulphate

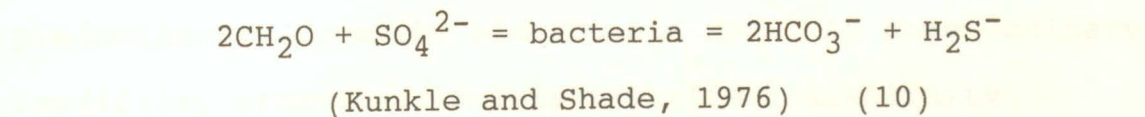
The sulphate anion acts as an oxidizing agent for the dissimilation, or breakdown, of organic matter. Reducing-bacteria use the oxygen bound in complex organic molecules, such as sulphate and nitrate complexes, instead of using the free oxygen in the groundwater (Postgate, 1979). It is the free oxygen in groundwater that inhibits bacterial growth. The absence of sulphate is a result of dissimilatory sulphate reduction by sulphate-reducing bacteria. The bacteria dissociate the sulphate ion into oxygen and sulphide. Only a small amount of the sulphide is assimilated by the organism with most escaping into the environment as sulphide ions or hydrating to produce hydrogen sulphide or hydrogen sulphite.

Concentrations of hydrogen sulphide have been detected at some sanitary landfills, for example: at Borden, North Bay, Woolwich and Gloucester (Basharmal, 1985), but not at the Army Creek landfill in Delaware (Baedecker and Back, 1979).

Sulphate reduction equations discussed by Hem (1970) and Kunkle and Shade (1976) indicate the production of bicarbonate with the reduction of sulphate.



or



The equation presented by Hem (1970) is typical in slightly alkaline environments while that of Kunkle and Shade (1976) is typical of slightly acidic environments. The bacteria require a pH environment close to neutral (Snoeyink and Jenkins, 1980). The ratio of the production of bicarbonate to the reduction of sulphate is 1:1 (Hem, 1970) or 1:2 (Kunkle and Shade, 1976). Hem (1970) also indicates that methane (CH_4) produced in landfills is reduced along with the sulphate.

The major metabolic oxidation occurs below a redox potential of -150 to -200 mV with bacterial growth occurring below -250 mV. Almost all redox reactions of importance in

groundwater are mediated by bacteria (Cherry, 1983). During sulphate reduction, the environment becomes alkaline unless compensating metabolic reactions forming acids are occurring or the sulphides are being trapped as insoluble heavy metal compounds in which case, little to no sulphide will be present in the groundwater (Postgate, 1979).

Sulphate reduction ceases when all the sulphate is reduced rather than when exhaustion of all organic matter occurs.

3.4.3. Alkalinity

Alkalinity in landfill contaminant plumes tends to be predominantly from the bicarbonate ion. At some sanitary landfills, organic-acid ions may affect alkalinity (Baedecker and Back, 1979), however, in carbonate environments, their contribution may be negligible. In natural waters with a pH less than 9, the concentration of carbonate is small compared to the concentration of bicarbonate (Stumm and Morgan, 1970).

In contaminant plumes, elevated bicarbonate concentrations can often be found with calcite and dolomite supersaturated groundwater since the elevated bicarbonate concentrations could be a result of increased calcite and dolomite dissolution. Another source of bicarbonate is associated with sulphate reduction. The amount of bicarbonate produced by sulphate reduction will depend on the pH environment which dictates the type of sulphate

reducing process. In the reducing state, elevated bicarbonate concentrations are associated with high levels of $p\text{CO}_2$.

The bicarbonate concentrations can be reduced by the bicarbonate hydrogenating with carbon dioxide to produce methane (Baedecker and Back, 1979). This process would also reduce the $p\text{CO}_2(\text{aq})$.

Although bicarbonate is usually the dominant ion in recharge zones (Freeze and Cherry, 1979), values lower than plume concentrations will indicate the presence of recently recharged water. Degassing at wells and during pumping can lower the bicarbonate alkalinity, therefore purging and sampling should be performed with the least agitation possible.

3.4.4. Chloride

Chloride is the contaminant most commonly used as a tracer for delineating the extent of subsurface contamination. Studies conducted at landfills in Michigan (Kunkle and Shade, 1976), Delaware (Baedecker and Back, 1979), Borden (MacFarlane et al., 1983) and North Bay and Woolwich (Basharmal, 1985) have used the chloride ion as a groundwater tracer. Chloride is considered to be a conservative tracer for three reasons: (1) chloride is believed not to form any important solute complexes with other ions or salts of low solubility (Hem, 1970), (2) chloride takes part in few vital biochemical processes and

(3) absorption to mineral faces is thought to be insignificant (Hem, 1970).

Chloride is a large anion so its migration can be retarded by the straining effect of the interstitial pores of clays and shales. The chloride negative charge can also result in repulsion from negatively charged mineral faces found in materials with high cation exchange potentials (Fritz *et al.*, 1976). The diffusion potential could cause chloride migration to be greater than that of the bulk water movement (Stewart, 1980). Therefore, slight differences in the percentage of clays in sands and gravels can have a great effect on chloride migration.

At the landfill at the Canadian Forces Base Borden, chloride concentrations were observed to be greatest towards the centre of the contaminant plume (MacFarlane *et al.*, 1983). Reduced concentrations away from the centre were a result of lateral and transverse hydrodynamic dispersion.

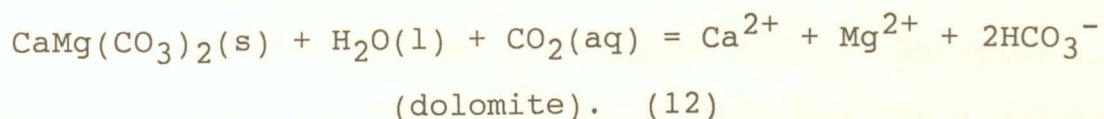
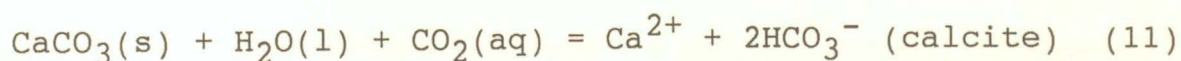
Chloride concentrations are known to become elevated with extensive use of road salt and fertilizers.

3.4.5. Major Cations

In solution, calcium can exist as a large free moving cation. The primary source of calcium is from the dissolution of calcite or dolomite abundantly distributed in the glacial material in southwestern Ontario (Freeze and Cherry, 1979). Calcium complexes with organics are usually in negligible proportions (Hem, 1970). In the case where

bicarbonate concentrations exceed 1000 mg/L, approximately 10% of calcium will complex as $\text{Ca}(\text{HCO}_3)_2$. Complexing with sulphate within contaminant plumes is often negligible owing to the reduction of sulphate to very low concentrations.

The dissolution of calcite and dolomite to release calcium is mainly dependent on water temperature and the $\text{pCO}_2(\text{aq})$. Calcite and dolomite solubility increases with decreasing temperature as a result of the increased solubility of CO_2 . The processes of dissolution (Snoeyink and Jenkins, 1980) are:



Calcite dissolution is a very rapid reaction producing calcium and bicarbonate. The dissolution of dolomite produces calcium, bicarbonate and magnesium. Unless other processes, such as cation exchange, modify the concentration of calcium or unless the bicarbonate concentration is modified, there should exist a relationship between high bicarbonate and high calcium concentrations.

Both reactions reduce the acidity of the groundwater. This buffering capacity is maintained as long as carbonates are available to dissolve. If there is not an acid forming

process to buffer this reaction, then an alkaline environment may be created.

Groundwater reacts towards saturation of calcite and dolomite. Undersaturation indicates that carbonates are being dissolved while supersaturation indicates that precipitation of calcite or dolomite is occurring. The degree of saturation is dependent on the geological terrain, temperature, $p\text{CO}_2$, cation exchange potential and the rate of reactions. Under $p\text{CO}_2(\text{atm})$, groundwater will become saturated in dolomite or calcite as it moves through the groundwater system. Most natural waters in contact with calcite or dolomite are close to saturated equilibrium or are supersaturated (Stumm and Morgan, 1970). Snoeyink and Jenkins (1980) indicates that it is possible for a solution only slightly supersaturated with respect to a solid phase to be stable indefinitely. Langmuir (1971) states that the theoretical solubilities of calcite and dolomite do not constitute real limits to the solubilities of these minerals in groundwater, so slight undersaturated or oversaturated levels could be identified from groundwater in equilibrium with the carbonate.

The Ca/Mg molal ratio may vary about unity. Low Ca/Mg molal ratios indicate the predominance of magnesium over calcium either by dissolution of dolomite, cation exchange, calcite precipitation, formation of calcium phosphate complexes with phosphorus from animal and human wastes

(Langmuir, 1971) or by addition of magnesium from leachate. A dolomitic source of magnesium requires the geological medium to be predominantly dolomite or the dolomite must react with the groundwater faster than the calcite. A 1:1 production ratio of calcium to magnesium during dolomite dissolution infers that when dolomite saturation is achieved, calcite saturation will also be reached, preventing further calcite dissolution.

Supersaturation of calcite will occur if the exsolution rate of CO_2 is greater than calcite precipitation (Langmuir, 1971). During exsolution of CO_2 , a preferential precipitation of calcite will deplete the groundwater in calcium. An incongruent dissolution of dolomite will re-equilibrate the calcium while creating groundwater supersaturation in magnesium.

Exsolution of the CO_2 through permeable sands (Cherry, 1983) and mixing with recharging water will decrease the pCO_2 resulting in supersaturation. Magnesium precipitates less readily than calcium in these conditions allowing dolomite supersaturation to be maintained with calcite undersaturation (Hem, 1970). A slight supersaturation of calcite and elevated bicarbonate concentrations can provide a buffer capacity against the CO_2 produced by bacterial reactions within the contaminant plume (Snoeyink and Jenkins, 1980)

As carbonate solubility is decreased, or supersaturation achieved, carbonate precipitation could result in a decrease in permeability of the geological material. Upon contact with atmospheric $p\text{CO}_2$ during discharge into surface water bodies, calcite and dolomite precipitation can result in a decrease in calcium and magnesium in solution accompanied by increased Ca/Mg molal ratios.

Studies by Canter et al. (1987) in mixtures of sand and clay saturated in calcium indicate that cation exchange is responsible for moderately attenuating the potassium, sodium and magnesium ions. Recent studies indicate that cation exchange processes in glaciofluvial sand and gravels may be partly responsible for temporal and spatial variability in groundwater chemistry (Reardon et al., 1983). At Woolwich, Borden and North Bay (Cherry, 1983), major ions such as potassium, sodium, magnesium and calcium showed decreased concentrations primarily due to cation exchange. For all of the ions except potassium, the change was small since the sands had a low cation exchange potential. A high cation exchange capacity can be developed in clayey sands as a result of oxides and organic matter forming coatings on the clay particles. This process is dependent on groundwater pH (Drever, 1982). Reducing-bacteria can also create a high cation exchange capacity since they are hydrophilic colloids

allowing the adsorption of cations in neutral to slightly acidic water (Canter *et al.*, 1987).

Elevated concentrations of cations within the contaminant plume may result from cation exchange between clays used for daily cover material and ammonium created in the leachate (Baedecker and Back, 1979).

Since the sodium and magnesium ions are smaller than calcium, they have an affinity for hydration and, once in solution, they often remain there achieving very high concentrations before precipitation (Hem, 1970). The mobility of an ion is affected by other solutes in the leachate and therefore the adsorption characteristics of a solute can vary between leachates.

Like calcium, magnesium predominates in ion form, but with bicarbonate and sulphate concentrations exceeding 1000 mg/L, complexes can form (Hem, 1970). Although magnesium adsorption tends to be greater than calcium, this is not a controlling factor of magnesium concentrations (Hem, 1970). The literature on contaminant migration indicates the existence of a calcium and magnesium hardness halo in contaminant plumes around sanitary landfills (Cherry, 1983).

3.5. Attenuation Processes

Attenuation is the process of decreasing contaminant concentrations during migration, much like a natural purification process. Attenuation can be a result of several reactions such as: dilution, adsorption, ion

exchange, precipitation, coprecipitation, or biochemical degradation (Freeze and Cherry, 1979).

Dilution of contaminants in the groundwater system can be a result of hydrodynamic dispersion and diffusion. The flow system lithology limits the effects of the dilution processes. Hydrodynamic dispersion predominates where groundwater velocities are high, such as in sands and gravels, while diffusion predominates where groundwater velocities are very slow, such as in silts and clays (Freeze and Cherry, 1979). An influx of less contaminated water can also be a dilution process.

Adsorption is not a dominant factor of inorganic attenuation in a sand and gravel environment. Slow groundwater velocities, high surface areas, and electrical fields typical of clays are preferred for adsorption (Drever, 1982). In contaminant plumes, it is difficult to determine the amount of adsorption occurring as the adsorptive characteristics of contaminants can vary from leachate to leachate (Canter *et al.*, 1987).

Ion exchange involves the exchange of ions of similar charge and accounts for observed temporal and spatial variabilities in groundwater (Reardon *et al.*, 1983). Inorganic contaminants commonly affected by this reaction are the cations calcium, sodium, potassium, and magnesium. The potential for cation exchange varies with pH and is a function of the ions at the exchange site (Drever, 1982).

Even if the cation exchange capacity is high, low permeability is often required for ion exchange to be a major attenuation process (Drever, 1982).

Contaminant precipitation and coprecipitation are the result of changing subsurface environments, such as: an increased contaminant influx, a drop in pCO_2 , a change in pH, a change in temperature, or a change in the compatibility of the contaminants. In the carbonate environment, precipitation of calcite and dolomite occur when the groundwater becomes supersaturated in calcite or dolomite.

Biochemical degradation involves biological activity, either acting as a catalyst for attenuation or by directly reducing the contaminant concentrations. An example would be sulphate-reducing bacteria. They are hydrophilic, thus act as adsorbers of cations (Canter et al., 1987). They also cause dissimilatory or assimilatory reduction of organics, such as sulphate, decreasing the organic concentrations (Postgate, 1979).

4.0. METHODS OF STUDY

4.1. Site Evaluation

4.1.1 Geophysical Techniques

4.1.1.1 Resistivity Survey

An electrical resistivity survey was conducted throughout the study area to determine the most likely route of contaminant migration and to indicate near surface horizontal and vertical lithological variations. A Soiltest R-50 Stratameter direct current electrical resistivity instrument was used for this survey.

The survey was conducted using the Wenner array. This array utilizes four electrodes equally separated by the desired 'a' spacing. The outer two electrodes are current electrodes and the inner two are potential receiving electrodes (Telford *et al.*, 1976). The 'a' spacing is increased as the electrodes are moved away from the stationary centre point of the array (Figure 11).

Operation of the resistivity array is based on Ohm's Law ($R=V/I$). Direct current is applied by an outside source, resistance to the current occurs in the subsurface, and voltage is the potential electrical current difference between two receiving electrodes. Current passing through a homogeneous subsurface in hemispherical patterns develops a depth of current penetration proportional to the distance between electrodes (Benson *et al.*, 1982).

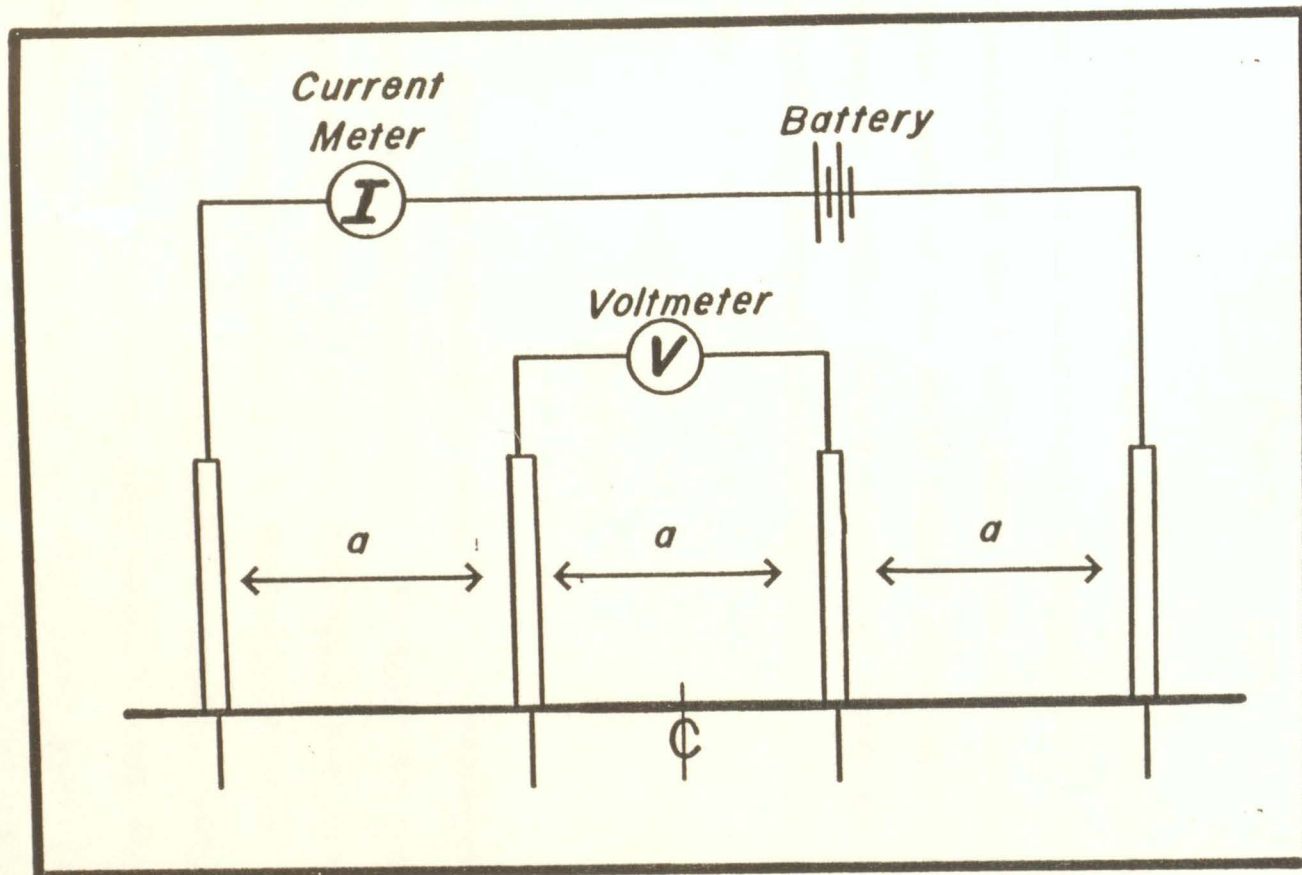


Figure 11. Wenner array for electrical resistivity surveys.

Resistivity (ρ) is the resistance (R) of a right angled cylinder of length 'L' and area 'A'.

$$\rho = RA/L \quad (13)$$

The resistance deals with ionic conductivity of the soil which depends on electrical resistance of the solid, resistance of the fluid phase, and the resistance due to the double layer of the solid liquid interface (Gilkeson and Cartwright, 1983). The fundamental equation for the Wenner resistivity method combines equation (13) with Ohm's Law to give:

$$\rho_a = 2 VA/I. \quad (14)$$

When the subsurface material is inhomogeneous, ' ρ_a ' is called apparent resistivity. The apparent resistivity is a weighted average of all the different resistivities present in the volume between the current electrodes.

Lithologies varying between gravel, sand, silt, clay and till over the study area, require that several 'a' spacings be used during the electrical profiling or traversing. This procedure may detect if material near the surface varies enough over the study area to mask similarities or differences at lower depths. A possibility of error with this survey method is that an increasing

electrode spacing could create lateral errors at vertical boundaries. A prime example evident in the study area would be the presence of gravel filled channel deposits within sand layers. In a study by Yazicigil and Sendlein (1982), the natural scatter created by large variations between lithological units masked the change in resistivity created by contamination.

The proportion of depth of current penetration to electrode spacing varies between each survey site. Depth of penetration is dependent on the lithology of the geological material, the degree of saturation and the ionic strength of the groundwater. A highly resistive surficial geological material will inhibit current flow, reducing penetration. Lower resistivity material at depth will conduct the current, also limiting the depth of penetration. Fluctuations of the water table and changes in ionic potential of the groundwater owing to chemical reactions can create spatial and temporal variations in current penetration.

Resistivity readings were made at 77 locations throughout the study area (Figure 12). Locations were chosen to cover all the possible lithological variations and to obtain enough background readings and readings within the contaminant plume such that a monitoring network could be designed. Locations were also chosen to avoid topographic highs and lows, overhead wires and steep embankments. Ten

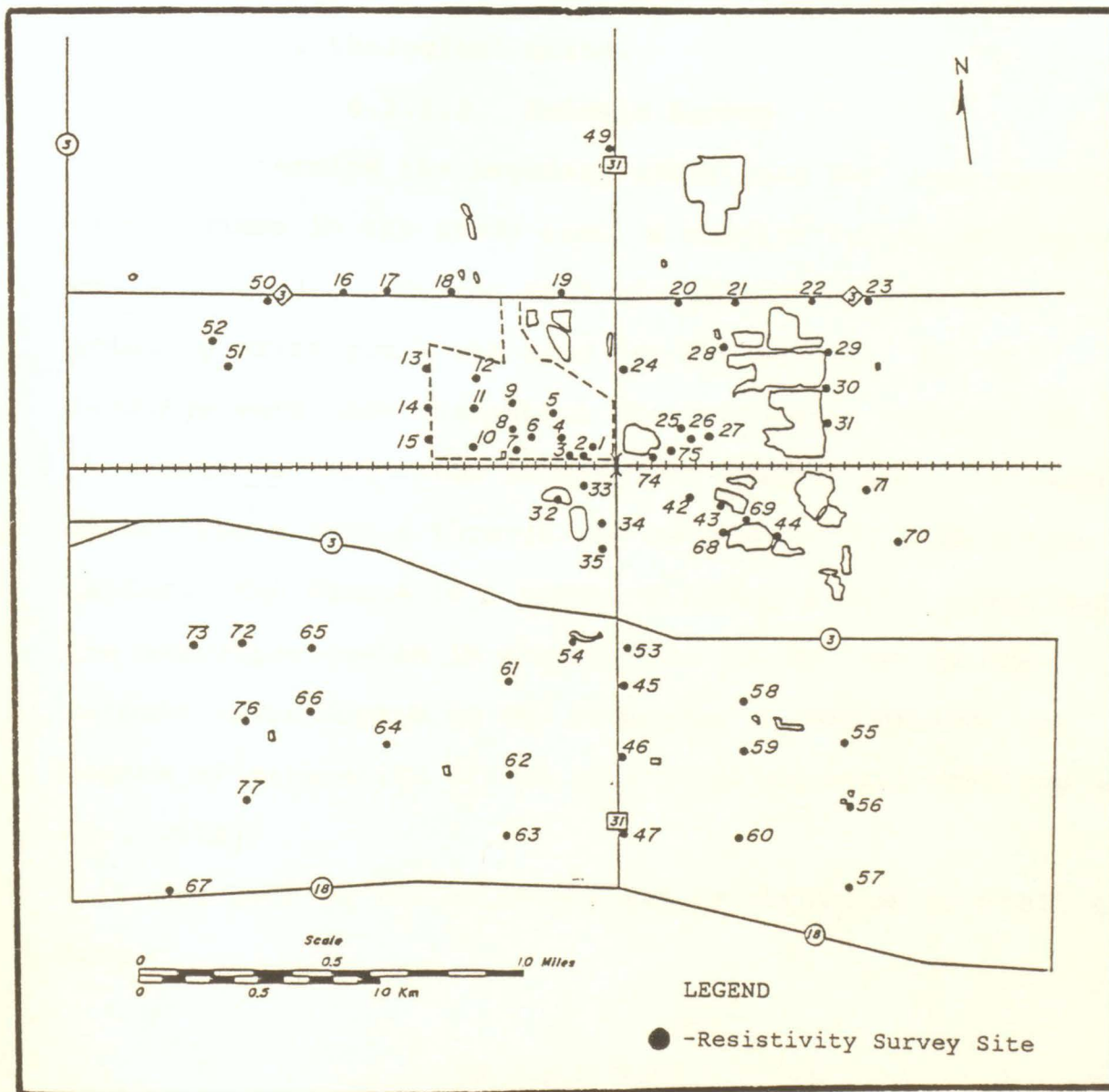


Figure 12. Location of resistivity survey sites.

locations were near existing wells to correlate readings with actual lithological units.

4.1.1.2. Seismic Survey

To determine the boundary conditions for near surface flow systems in the study area, a seismic refraction survey was conducted. A Hunttec FS-3 single-channel portable printing seismograph was used for the survey. Seismic readings were made throughout the study area (Figure 13).

Seismic refraction is based on propagation of seismic waves from a source through the subsurface to a detection device. The source is a hammer striking a metal plate and the detection device is a geophone. Velocities of the seismic waves depend on the hardness, consolidation, and degree of saturation of the geological material (Telford et al., 1976).

The path of the seismic waves is explained by Snell's Law:

$$\sin i / \sin r = V_1 / V_2. \quad (15)$$

The seismic waves pass through the first unit (V_1) hitting the interface at the angle of incidence (i) and leaving at the angle of refraction (r) into the second unit (V_2).

Refraction occurs when the seismic wave contacts the interface at a critical angle (i_c) resulting in a refraction

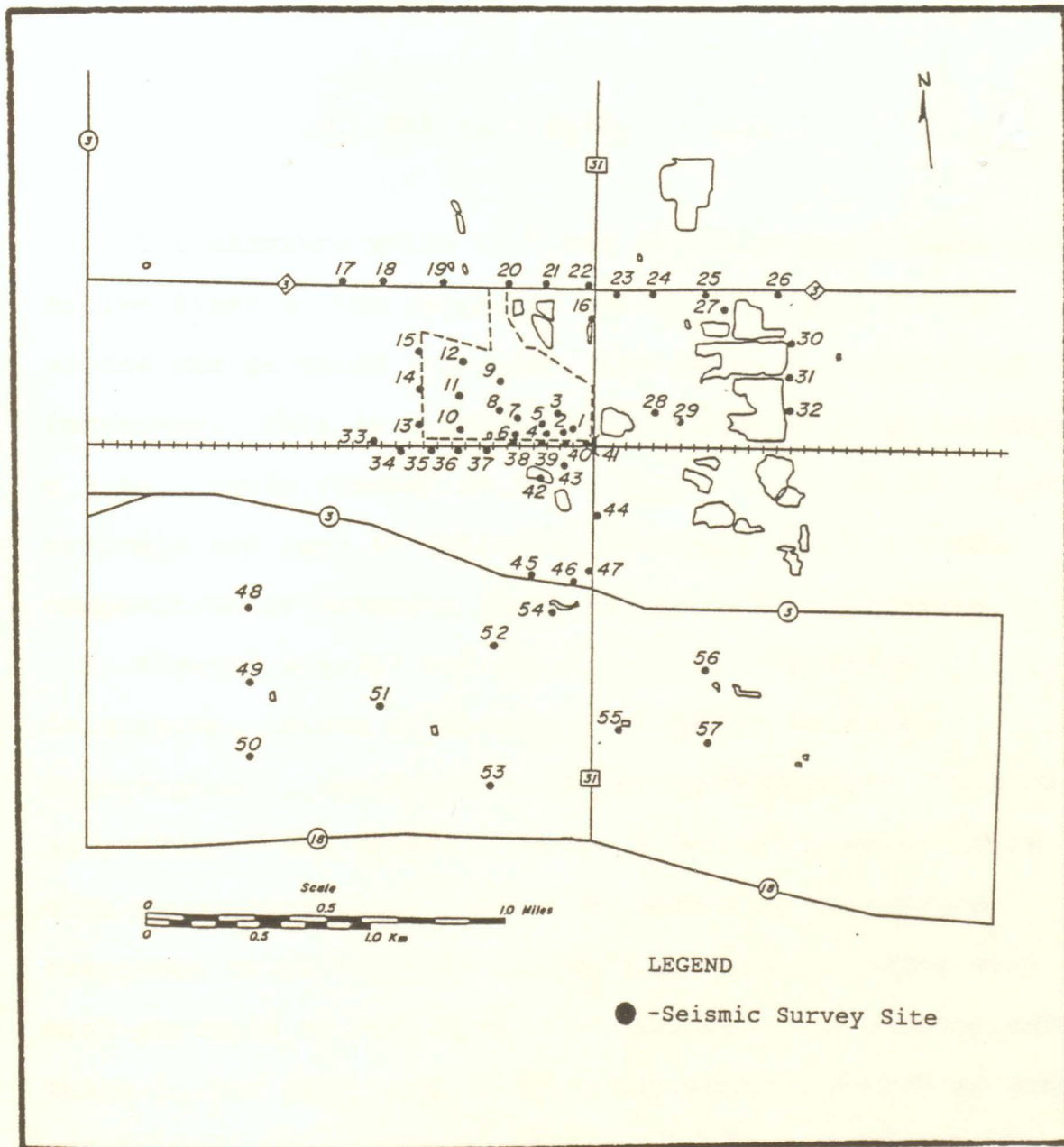


Figure 13. Location of seismic survey sites.

of 90 along the interface (Telford *et al.*, 1976). Snell's law is then refined to

$$\sin i_c = V_1/V_2. \quad (16)$$

The interpretation is based on the seismic waves which arrive first at the geophone. As the distance between source and geophone increases, the depth of penetration increases. This is a proportional increase of approximately a 3 to 1 ratio (Benson *et al.*, 1982). Plots of the first arrivals are used to determine interface depth and the composition of material above and below the interface.

Erratic results can occur because of dipping interfaces, lenses of sharply contrasting material, topographic irregularities, and background noise (Telford *et al.*, 1976). The presence of low velocity material below high velocity material will also result in misleading responses since arrivals of the high velocity layer will mask arrivals of the lower. For example, the perched water table in the study area will be represented simply as sand and gravel overlying a thick till deposit, ignoring the lower sand unit.

4.1.2. Existing Monitoring Network

Before establishing a groundwater monitoring network, an examination of existing sources of information is necessary to identify possible locations for the monitoring

wells and to identify important subsurface features. Three excellent sources of this type of information are Ontario Ministry of the Environment water well records (MOE, 1984), existing piezometers on the landfill site installed by Gartner Lee Associates Limited and characteristics of surface water bodies.

4.1.2.1. MOE Water Well Records

Water wells listed by the Ontario Ministry of the Environment are mainly private wells used for domestic and livestock consumption and for industrial and irrigation purposes (MOE, 1984). In the study area, water wells include both shallow wells into near surface confined and unconfined sand aquifers and deep wells into the confined sand and gravel aquifer immediately above the bedrock. Most of the water supplied is fresh with occasional mineral or sulphur waters from the deeper wells.

The water wells are scattered over the study area with the greatest density in residential areas and along roadways (Figure 14). Water wells immediately around the landfill are sparse owing to past intensive surface mining.

Well records identify the till as a blue clay often combined with silts, sands and gravels. Although depths to lithological contacts may not be exact, they provide an indication of what to expect. West of the landfill, there is clear indication of a sand layer, 1 to 30 m thick, confined between two till units. The description of this

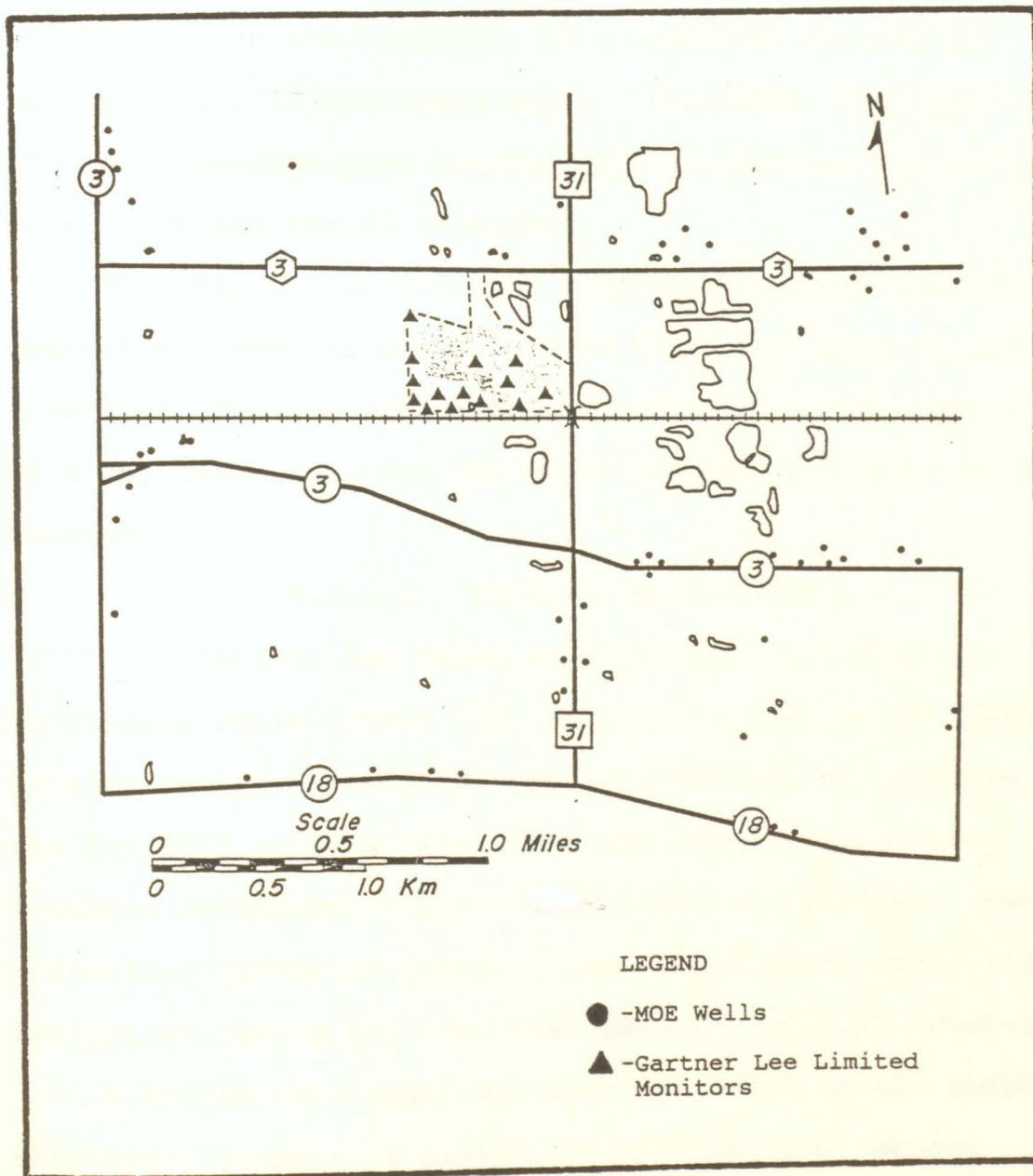


Figure 14. Location of MOE wells and Gartner Lee piezometers

confined aquifer varies from quicksand to a medium-fine sand. East of the landfill, this confined aquifer is reported only in scattered wells. Eastward, the till structure becomes more complex with increasing amounts of silt, sand and gravel streamers.

Evidence of the confined aquifer immediately above bedrock is found in wells located south and east of the landfill. The confined aquifer thickness ranges from 0 to 20 m and often includes the upper weathered surface of the bedrock.

4.1.2.2. Gartner Lee Piezometers

Gartner Lee Associates Limited installed 14 monitoring wells within the landfill boundaries in 1986 to develop an hydrogeological and geotechnical perspective of the landfill (Figure 14). This was done as part of a leachate management scheme to establish a toe-drain leachate collection system, a leachate collection pond, and a spray irrigation system for land treatment of landfill leachate.

A hollow stem auger was used for drilling the boreholes allowing placement of piezometers in the sand aquifer without the use of sandpacks or seals. Piezometers often extend into the till with caving sand supplying the required sand pack. The piezometers were slotted polyvinyl chloride (PVC) pipe covered with fibreglass cloth over the lower 0.5 m. Standpipes were also used and were constructed of PVC pipe with the bottom 2.4 m being slotted every 0.3 m.

The piezometers were used to measure the hydrostatic pressure, to obtain groundwater samples, and to measure in situ permeability. The standpipes were for measuring water table levels and for obtaining groundwater samples.

Borehole logs indicate a large variation in surface sand thicknesses within the landfill. Thin sand layers are often the result of excavation by earlier sand and gravel mining. Greater thicknesses occur in sand fill that had earlier been built up as a berm for waste confinement. Therefore, depths to the sand-till interface may not be truly indicative of original depths from surface. The borehole logs also indicate a 0.3 m confined sand layer within the till on the western edge of the landfill. This layer was not detected in the remaining boreholes, however its presence is consistent with MOE water well records which indicate that sand bodies do exist within the till.

Permeameter tests indicate a permeability of 2×10^{-2} cm/sec for the sand and a permeability of 10^{-6} cm/sec for the till. The porosity of the sand was determined to be about 35%.

Monitoring data of the water table levels indicate mounding within the landfill. This is substantiated by the presence of leachate springs on the surface of the landfill's western perimeter.

4.1.2.3. Surface Water Bodies

An electrical conductivity survey was conducted of all surface water bodies in the area to interface with the resistivity and seismic surveys. A YSI Model 32 conductance meter was used for obtaining temperature compensated readings.

4.2. Piezometer Installation

4.2.1. Drilling Methods

Formation material encountered during installation of the monitoring network was unconsolidated with a near surface water table. Both hollow stem augering and jet-drilling methods were employed for construction of boreholes.

4.2.1.1. Jet-Drilling

Jet-drilling was performed during the summer of 1987 as an inexpensive means of installing bundle piezometers. Owing to technical difficulties, jet-drilling was replaced by hollow stem augering after the installation of four bundle piezometers.

The jet-drilling method used an electric hammer to vibrate 1.5 m lengths of 5 cm ID metal casing into the unconsolidated subsurface material. Formation material was dislodged by the vibrations and a tapered bit attached to the leading pipe facilitated penetration (Figure 15). A removable adapter head allowed insertion of the water jetting apparatus and the removal of the dislodged formation

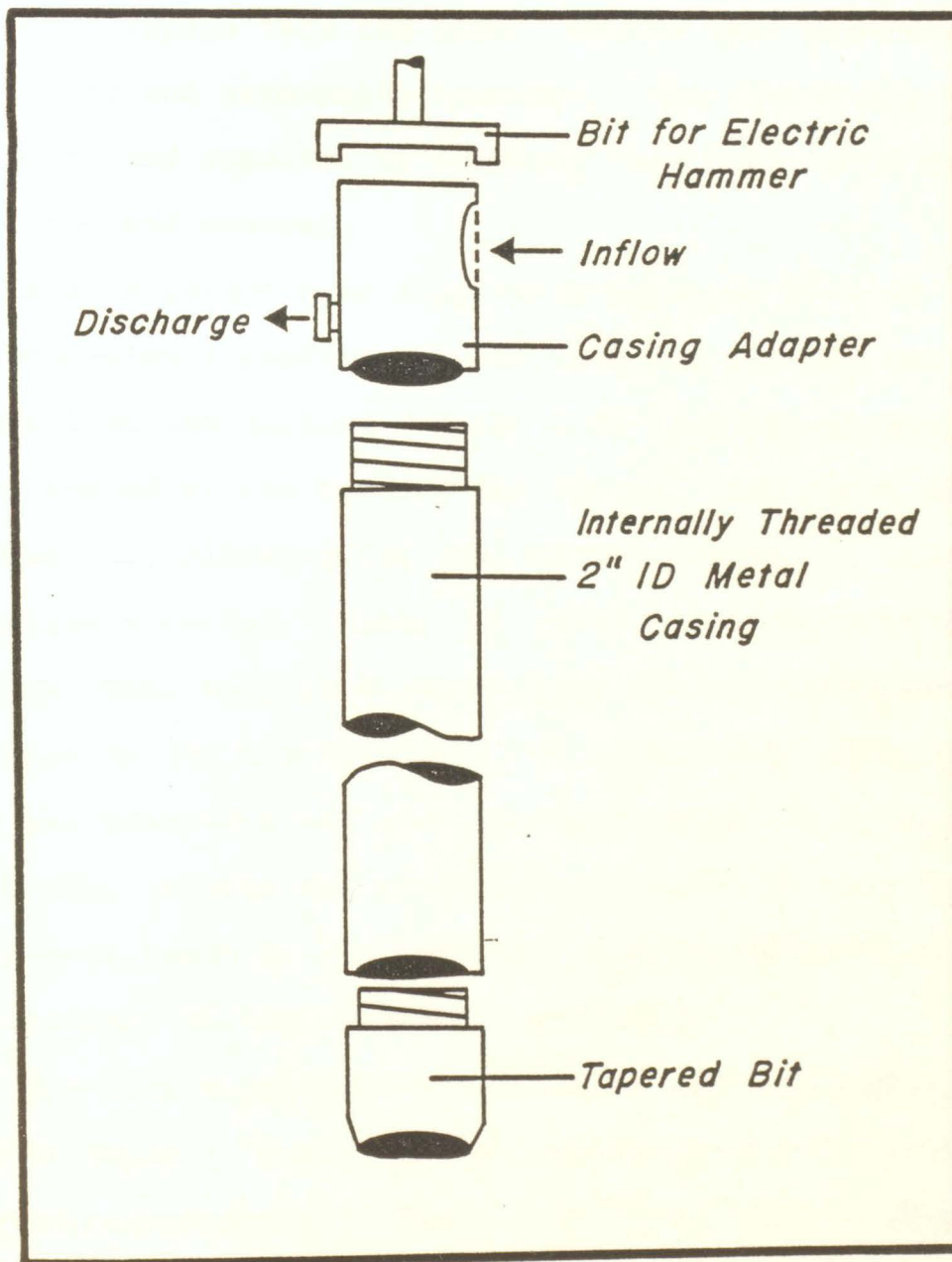


Figure 15. Casing apparatus for jet-drilling method.

material. A bit was developed for the electric hammer to prevent slippage from the pipe. Casing used was both internally and externally threaded. The internally threaded casing proved superior by creating less resistance during insertion and removal.

A 2 cm garden hose supplied a constant flow of water for loosening formation material and for lifting the material to the surface. Water flow from the garden hose was situated at the base of the casing, just above the tapered bit, allowing the full water velocity to dislodge formation material. Water for jetting was obtained from a surface water body in a nearby open pit and transported to the site in 190 L metal drums. A submersible pump connected to a gas generator was used to supply water at a rate of 3.0 L/min. Electrical conductivity values of this foreign water were taken so its presence could be detected and taken into account during piezometer sampling.

The bundle piezometer was placed into the casing to the desired depth. Removal of the casing permitted caving of unconsolidated material effectively creating a sand pack around the bundle piezometer.

A manual car jack of 3,600 kg capacity was used for casing removal. To prevent bending of the casing a tripod-jacking system was developed which would permit only vertical lift. This system was adequate up to a depth of

3 m. Friction created by casing below this depth made manual removal of the casing impossible.

4.2.1.2. Hollow Stem Augering

Drilling was by Dominion Soils Ltd. using a CME 750 four wheel drive power auger machine manufactured by Central Mining Equipment Limited. It operated a continuous flight hollow stem auger setup with an 82 mm inner diameter, 105 mm outer diameter auger.

A plug situated at the bottom of the auger prevented material from heaving up into the hollow stem. The plug could be removed for borehole sampling. A split spoon sampler was used for obtaining 'undisturbed' soil samples. Heaving of sand during removal of the plug was minimal and did not cause problems during drilling. As a result, foreign water was not required.

The hollow stem acted as a temporary casing for monitoring well placement. Upon withdrawal of the auger, unconsolidated material caved tightly around the piezometer creating a filter pack and minimizing the effect of a large borehole annulus which would have allowed vertical cross contamination.

4.2.2. Piezometer Design

The monitoring network for the landfill site required three varieties of piezometers to obtain depth and location specific hydrogeological and contaminant data (Figure 16). Within the landfill site, there are four bundle piezometers

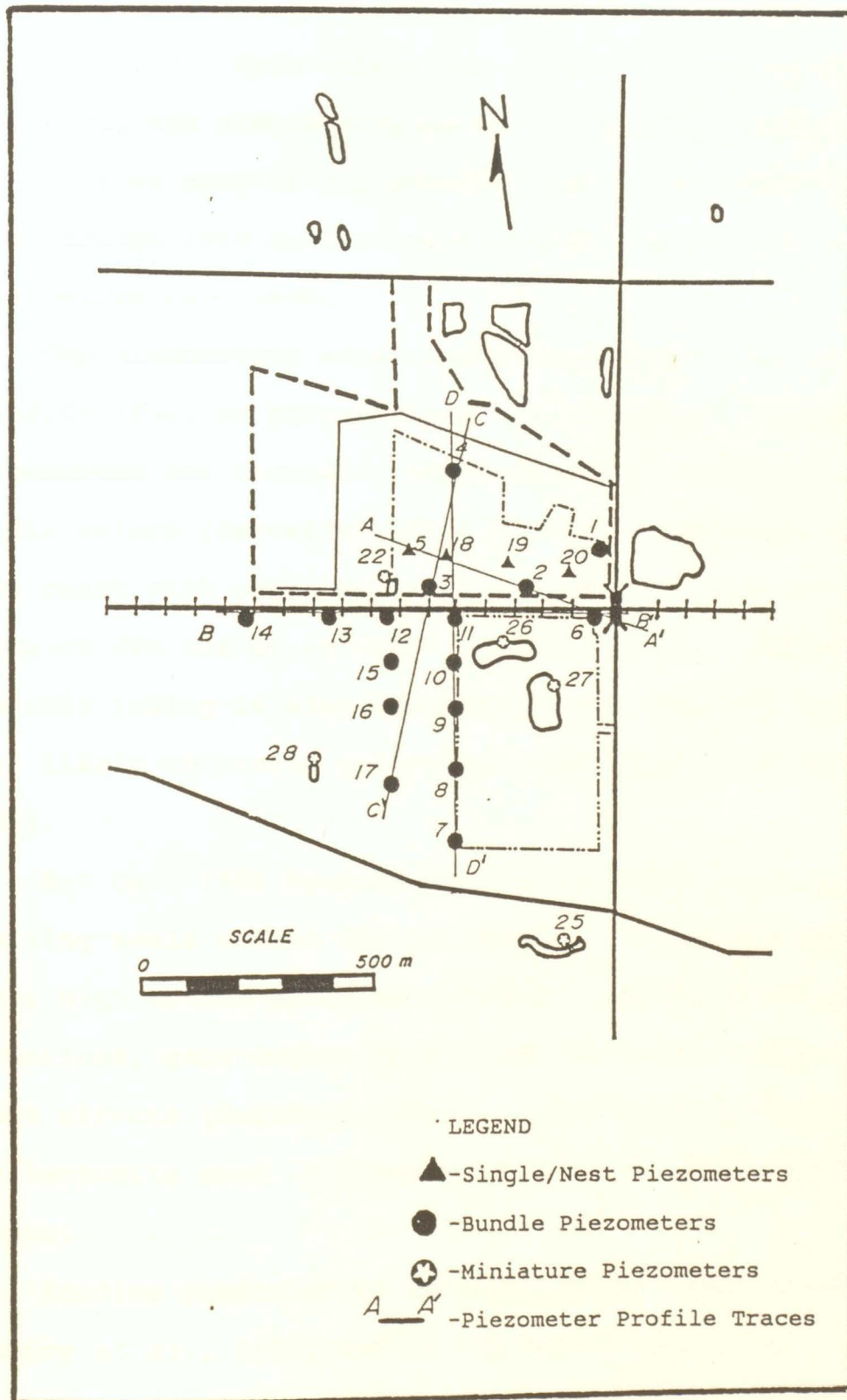


Figure 16. Location of bundle piezometers, single and nest piezometers, minipiezometers and piezometer profile traces.

for identification of vertical variations in head and contamination. Also within the landfill site and extending southward, are single piezometers as solitary monitoring points or as part of a piezometer nest. To permit sampling of discharge into surface water bodies, miniature piezometers were used.

The piezometers were constructed with either polyvinyl chloride (PVC) or polyethylene (PE) material. Rigid PVC is recommended for inorganic sampling and is resistant to acidic waters (Barcelona *et al.*, 1983). Polyvinyl chloride does react with organics found in landfill leachate, but organics are not of interest for this study. Polyethylene flexible tubing is also recommended and compared to PVC, is less likely to create analytical bias (Barcelona *et al.*, 1983).

M-I Gel, 100% Wyoming Bentonite powder was used for creating seals around the piezometers. Although bentonite has a high cation exchange potential, in the sand and gravel formations, groundwater velocities are high enough to limit these effects (Driscoll, 1986). Also, only in one case was the bentonite used in close proximity to the piezometer screen.

Studies performed at Canadian Forces Base Borden (Cherry *et al.*, 1983) and in the Netherlands (Van Duijvenbooden, 1985) indicate that contaminants typically migrate along the lower boundaries of unconfined aquifer

systems. It has been suggested that this type of flow is due to density differences, temperature gradients, recharge and subsurface heterogeneities. Therefore, in the study area, depth discrete monitoring wells were placed close to the sand-gravel and till interface. The bundles and piezometer nests were developed to obtain hydrogeological and chemical data above the interface.

The piezometers were developed by withdrawing 2 to 3 piezometer volumes of water by bailing and pumping. Development was necessary to remove particulates smeared to the borehole walls near the screen, thereby regaining formation permeability. The screen slots did not have the 'widening inward' design to decrease entrance velocities of the groundwater which would prevent turbidity and degassing resulting in changes in temperature, pH and chemical composition of the groundwater. However, use of a Marafi wrap filter cloth (Paul *et al.*, 1988) over the screen replaced the 'widening inward' design, reducing these effects to negligible proportions.

4.2.2.1. Bundle Piezometers

The bundle piezometers were installed using the jet-drilling method. They were positioned in a line running eastward from the eastern most refuse cell.

The central supporting piezometer consisted of 1.3 cm ID rigid schedule-80 PVC piping. The screen at the base of the PVC pipe was 20 cm in length. Slots 1.6 mm in width

were placed at 1 cm intervals. The screen was then double wrapped in Marafi 150 mesh PE geotextile and held in place by self locking non-biodegradable PE wire binders. The centre pipe screen was positioned at the sand-gravel and till interface (Figure 17).

Flexible PE tubing of 6.4 mm ID was secured around the PVC pipe by the wire binders. The screen slots and filter cloth were identical to the PVC pipe, but covered only the bottom 10 cm. These screens were placed at 60 cm intervals straight up the centre pipe.

Natural caving of the sands during removal of the metal casing provided the seal for the bundle in the saturated zone. Above this, natural fill was used up to the surface where a 5 cm ID PVC piezometer covering was placed. Surface material around the cap was sloped away from the piezometer to prevent ponding and recharge along the piezometer annulus.

4.2.2.2. Nest/Single Piezometers

Single piezometers were positioned where resistivity and surface water electrical conductivity values indicated a possible location for the contaminant plume. The network consists of three lines of piezometers (Figure 16). One profile runs east-west just south of the landfill's southern boundary and the other two lie perpendicular to the first. Several piezometers were situated off the profile lines for better plume delineation. Two piezometer nests, of two

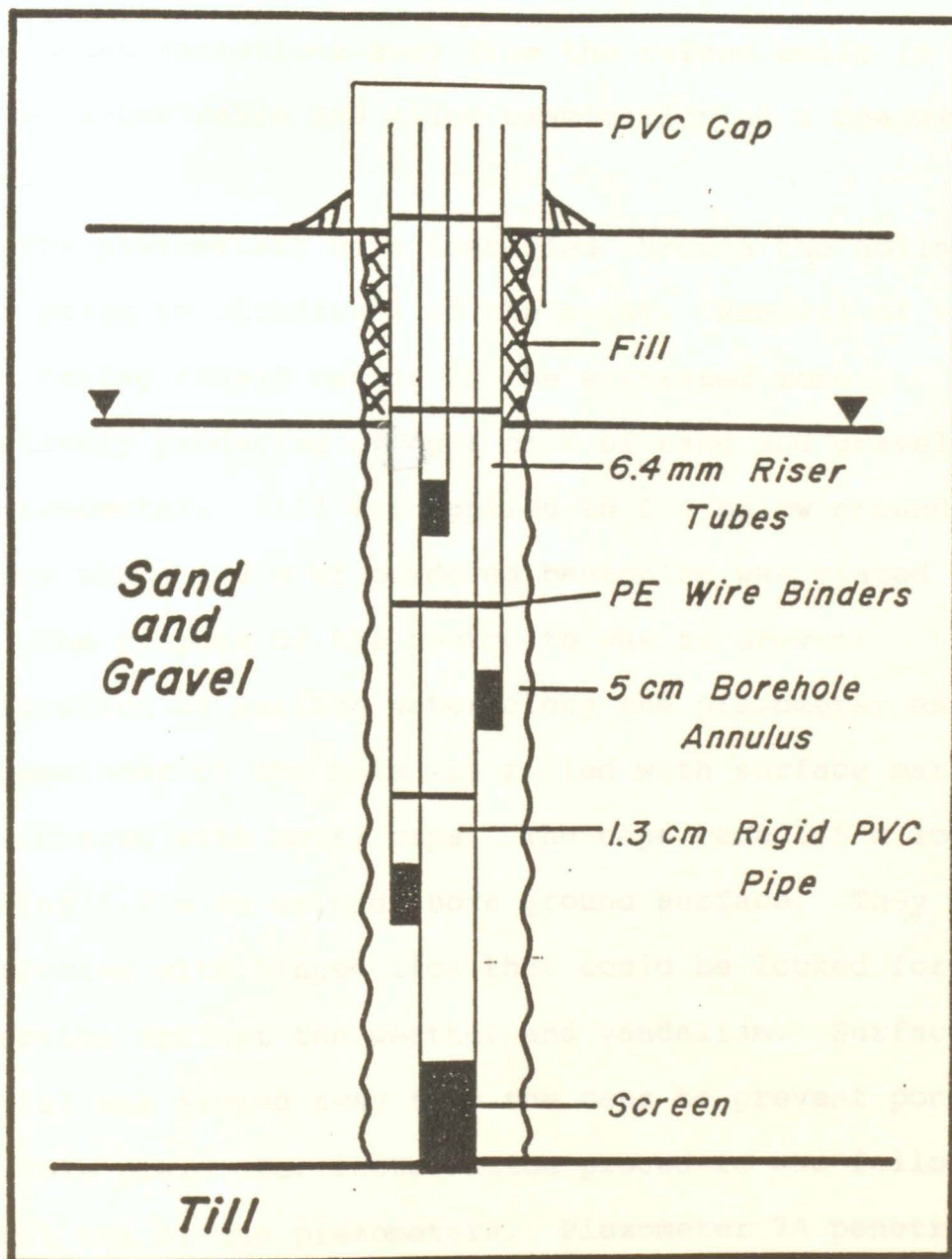


Figure 17. Bundle piezometer installation.

piezometers each, monitor vertical hydrogeological and contaminant variations away from the refuse cells in the perched water table and allow examination of a deeper water table.

The piezometers were installed through the hollow stem auger prior to withdrawal of the auger. Removal of the auger casing caused caving in the saturated zone, effectively producing a tight pack of sand and gravel around the piezometer. Fill was applied to 1 m below ground surface where 1/2 m of powdered bentonite was placed (Figure 18). The purpose of the bentonite was to prevent infiltration of surface water along the piezometer annulus. The remainder of the hole was filled with surface material then covered with metal caps. The caps were 1.5 m long allowing 1.0 m to extend above ground surface. They were constructed with hinged lids that could be locked for protection against the weather and vandalism. Surface material was sloped away from the caps to prevent ponding.

This piezometer installation procedure was followed for all but two of the piezometers. Piezometer 7A penetrated the perched water table confining layer. A 2 m section of the borehole, centred at the 10 cm thick confining layer, was filled with bentonite to effectively seal the confining layer and thereby preventing contamination of the lower aquifer by the upper aquifer. The second anomalous installation procedure was for Piezometer 14. At this

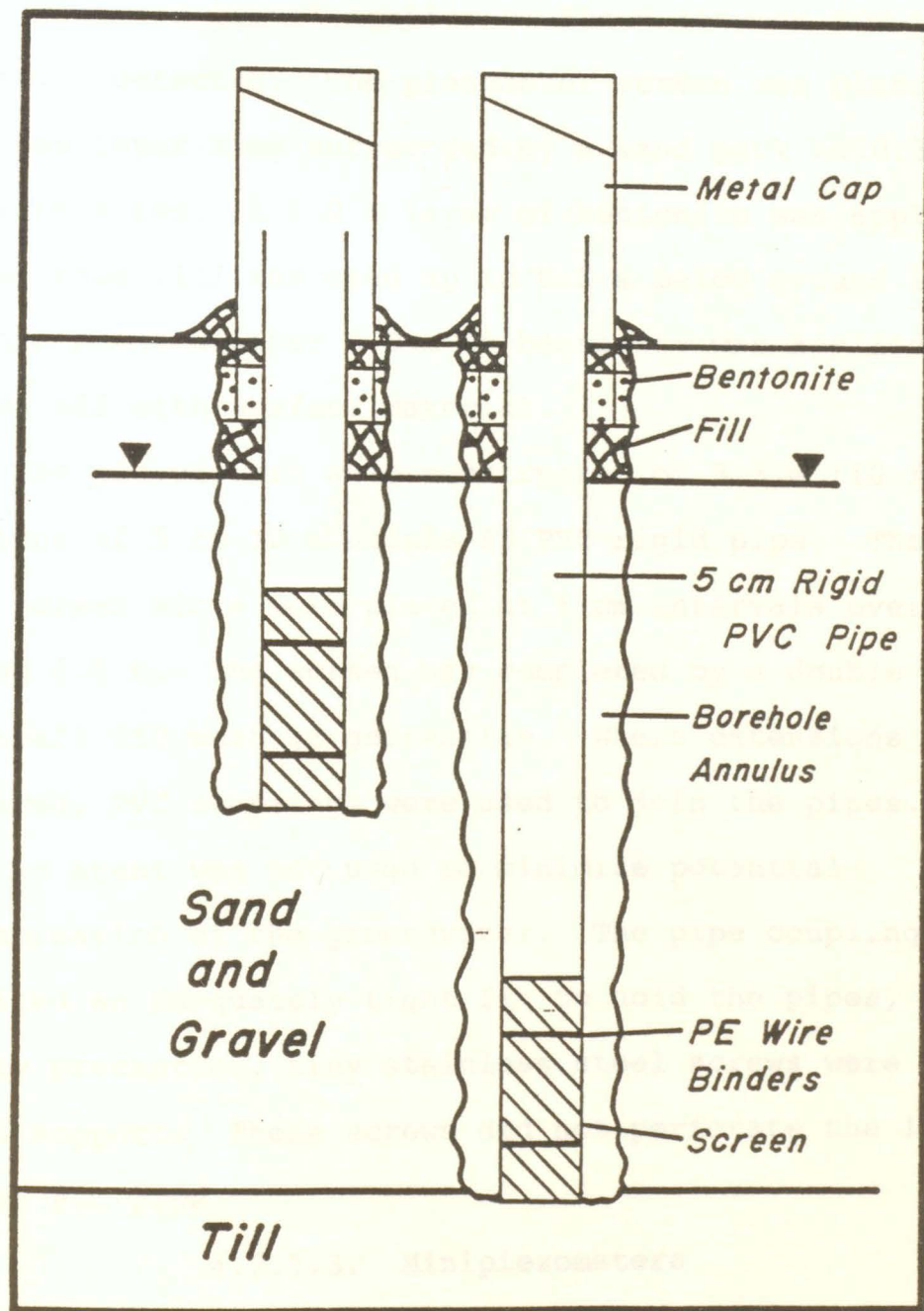


Figure 18. Nest and single piezometer installation.

location, a surface water table was not encountered, but a 10 cm sand and gravel aquifer confined between two till units was detected. The piezometer screen was placed at the confined layer then surrounded by a sand pack to 0.3 m above the screen top. A 1.0 m layer of bentonite was applied as a sealer then fill was used up to 0.8 m below ground level. At this point another 0.5 m of bentonite was applied then topped off with surface material.

The piezometers were constructed of 3.3 m (10 ft) sections of 5 cm ID schedule-80 PVC rigid pipe. The 3.2 mm wide screen slots were placed at 1 cm intervals over the bottom 0.5 m. The screen was completed by a double wrapping of Marafi 150 mesh PE geotextile. Where extensions were required, PVC couplings were used to join the pipes. A binding agent was not used to minimize potential contamination of the groundwater. The pipe couplings supplied an adequately tight fit to hold the pipes, but as a safety precaution, tiny stainless steel screws were used for added support. These screws did not perforate the interior of the PVC pipe.

4.2.2.3. Minipiezometers

Minipiezometers were used at four sites in the study area. One was at a leachate collection pond within the landfill site and the other three were at surface water bodies south of the landfill site. The minipiezometers allowed monitoring of discharging groundwater without the

effects of evaporation and dilution that would affect samples from the surface water body. After groundwater samples were obtained, the minipiezometers were removed.

The minipiezometer used at the leachate collection pond consisted of a thin-walled stainless steel casing that could be manually inserted into the pond sediments (Sklash *et al.*, 1985). A screen at the base of the minipiezometer prevented sediments from being collected during pumping (Figure 19). The system proved inadequate in the other three water bodies since suction created by the pump caused formation material and surface organics to plug the screen. A system similar to that designed by Lee (1978) was subsequently used.

Flexible PE tubing with 10 cm long screens at the end (Figure 20) were installed in the northern banks of the ponds. When suspended above water level, discharging groundwater would create a noticeable hydraulic head difference within the PE tubing. The indication of hydraulic head permitted the calculation of discharge velocity prior to collection of groundwater samples.

4.3. Hydrogeological Analysis

4.3.1. Field Work

4.3.1.1. Soil Sampling

Soil samples were obtained during drilling using a split spoon sampler. The split spoon was inserted through the hollow stem of the continuous flight auger and hammered into the subsurface material obtaining relatively

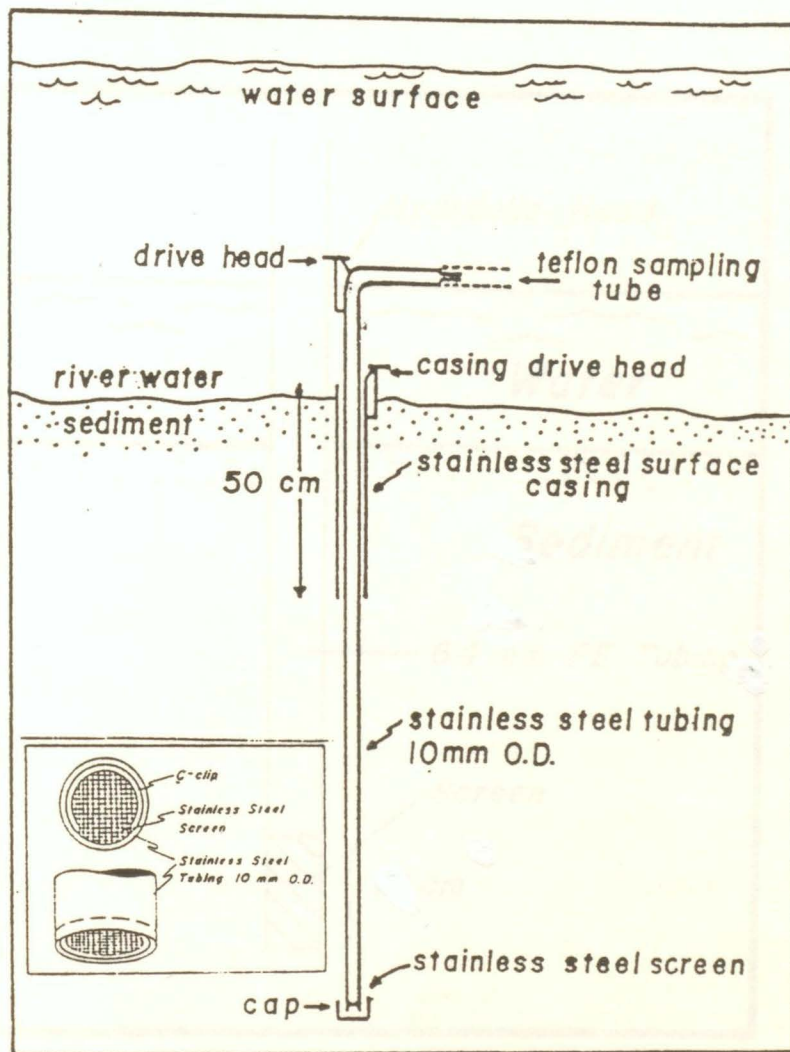


Figure 19. Stainless steel minipiezometer (after Sklash et al., 1985).

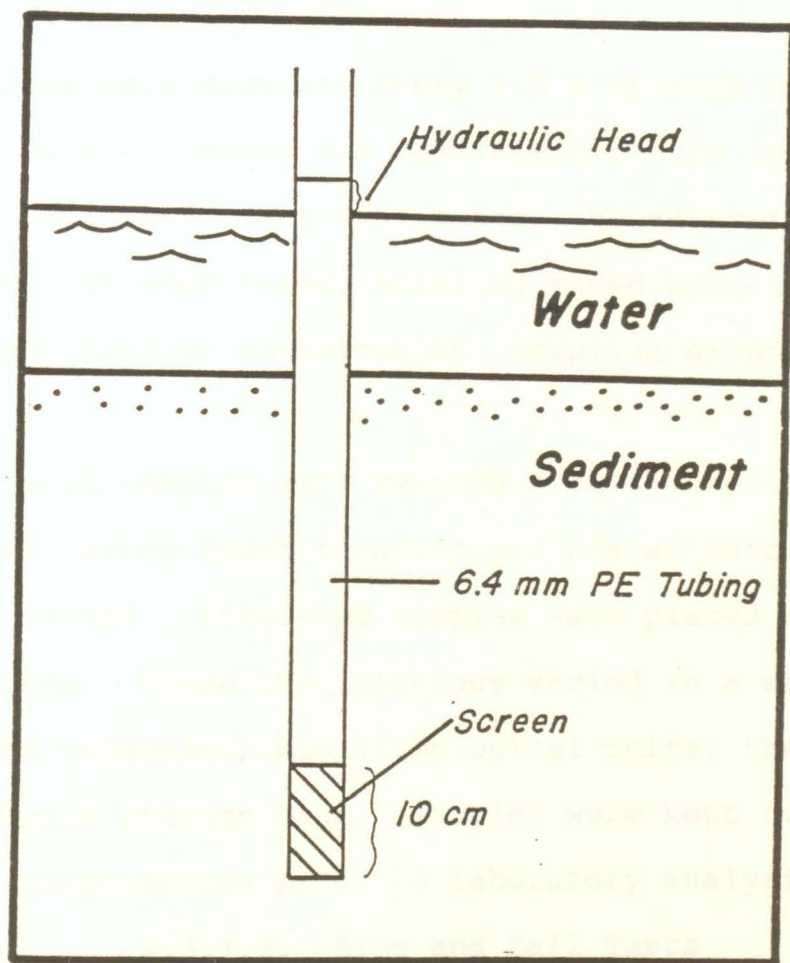


Figure 20. Polyethylene minipiezometer installation.

undisturbed samples. The samples lacked indications of structural features known to exist, such as fine laminations or cross bedding, but maintained the sharp lithological contacts.

Samples were obtained every 1.5 m through the unsaturated zone, which was equivalent to the length of one auger flight, then every 0.61 m once the saturated zone was contacted. In most cases, sampling ended once the till was penetrated, however occasionally, sampling extended into the till.

The soil samples were removed from the split spoon immediately after identification and placed into plastic bags and sealed. Saturated samples were placed into two storage bags. Where the lithology varied in a sample, the sample was segmented into lithological units, then placed into separate storage bags. Samples were kept cool at above freezing temperatures prior to laboratory analysis.

4.3.1.2. Slug and Bail Tests

Slug and bail tests using the Hvorslev method (Hvorslev, 1951) were performed in the 5 cm ID piezometers to determine the hydraulic conductivity (K) of the aquifer material. A solid aluminum slug, 3.8 cm in diameter and 50 cm in length was used to induce the head changes. Testing was successful on piezometers 2, 3, 4, 8, 13, 16 and 17. The inability to use the slug and bail tests on the remainder of the piezometers was a result of extremely rapid

response times or lack of enough hydraulic head within the piezometers for total emersion of the slug.

There are several sources of error that can affect the hydrostatic time lag. Drilling and installation plus addition and removal of water from the piezometers can alter the soil structure causing time lag variations owing to stress adjustments. In the medium grained sediments of the study area, the stress adjustment effects are likely negligible (Hvorslev, 1951). Movement of groundwater through the borehole annulus and the caved unconsolidated material can decrease the time lag of the recovery. Since calculated K values are based predominantly on the material closest to the intake point, the caved material and geotextile filter cloth may be controlling factors of K.

Volume changes of gas in the soil during testing cause a concave curvature in the initial time lag and a reduced line of equalization (Hvorslev, 1951). Addition of the slug increases pore water pressure around the piezometer decreasing the volume of gas bubbles in the soil. This permits excess outflow until pressures between the soil pores and the gas bubbles equilibriate. Recovery will be in steady state until pressure within the gas bubbles is greater than soil pore pressure allowing gas bubbles to reform reducing outflow from the piezometer. Recovery from bailing is similar except the effects are reversed.

4.3.1.3. Water Level Measurements

Water table levels were obtained from the bundle, single and nest piezometers using a measuring tape with an electrical contact at the end. The elevations of the piezometer were surveyed using the Gartner Lee piezometers as reference points.

4.3.1.4. Water Sampling Procedure

All piezometers were purged of 2 to 3 bore volumes of water by bailing prior to sampling. A portable Masterflex peristaltic sampling pump was used to purge the bundle piezometers while a PVC bailer was used to purge the 5 cm ID piezometers.

Groundwater samples for isotopic and chemical analyses were removed using the peristaltic pump and PE tubing. The samples were placed in 100 mL PE bottles which had previously been cleaned with triple distilled water and rinsed thoroughly with the sample water. Samples were immediately capped with as little entrapped air as possible, tagged, then stored in a cool environment until analysis. Filtering of the samples was performed in the laboratory. Preservatives were not added to the samples since either the analyses were performed within a 24 hour period or preservatives were not required (Rand *et al.*, 1975).

Electrical conductivity, temperature and pH were determined in the field prior to sampling. Sample water was passed through a polyethylene flow-through cell using the

peristaltic pump. Temperature and electrical conductivity readings were recorded using a YSI Model 32 conductivity meter once values became stable. The pH readings were made using a Corning portable pH meter. The pH measurements were taken after the electrical conductivity values had been obtained.

4.3.2. Laboratory Analysis

4.3.2.1. Grain Size Analysis

Combination grain size analyses as outlined by Lambe (1951) were performed on the soil core samples obtained from the study area. The combination analyses involved sieve size analyses and hydrometer analyses with the particle diameter of 200 mesh size as the dividing point between the two procedures.

During drying and sieving of formation material, the coarse particles required drying and sieving times of 60 hours and 20 minutes, respectively. Finer samples required extended drying times on the order of 72-96 hours and sieving times on the order of 30-60 minutes.

Gradation curves for coarser grained soils are often found to be useful, but curves for the finer-grained particles have limited applications (Lambe, 1951). It is common in a combined analysis to have an area of overlap around the 200 mesh grain size. This overlap is caused by the two procedures of the combined analysis being based on different definitions of particle diameter. The hydrometer

analysis indicates larger particle sizes than the sieve sizes. Particles in this overlap area are usually not plate shaped.

Soil permeability is related to the effective particle diameter. The particle diameter at 10% passing is assumed to be the sample's effective diameter. The permeability of the cohesionless soil is proportional to the square of the effective diameter. This relationship is known as Hazen's formula. Although it was initially intended for uniformly graded sands, it can be used as a rough estimate in the fine sand to gravel range (Freeze and Cherry, 1979).

4.3.2.2. Soil Identification

Soil samples which retained cohesion upon removal from the split spoons were typically the silts, clays and tills. These samples were analysed for several parameters to permit correlation throughout the subsurface. The parameters identified were bulk density, water content, porosity and saturation.

Two sections from each sample segment were identified, with the average of the two representing the value of that parameter for the soil sample. A total of 30 samples from the study area were identified.

Volumes of the cores were obtained using the paraffin and water displacement method given in McKeague (1978). Volume measurements were taken before measurements of bulk density, water content, porosity and saturation.

The bulk density is a dry weight bulk density. Water content (by weight), porosity and degree of saturation were obtained assuming a specific gravity for the core of 2.65 (McKeague, 1978).

4.3.2.3. Water Analysis

Water samples were analysed in the laboratory for chloride, sulphate, alkalinity, sodium, calcium, potassium, and magnesium. The chloride was analysed in the Department of Civil Engineering. The remainder of the samples were analysed in the Geochemistry Laboratory in the Department of Geology.

Most samples were filtered through Whatman 42 ashless filter paper with a retention of 2.5 μm , prior to analysis. Samples for the alkalinity analysis were not filtered. Tap water was also analysed and compared to analyses by the City of Windsor to check accuracies of the analytical methods. Accuracy and precision of the various analytical methods are given in Table 1.

Chloride was analysed using an Orion Ionalyzer Model 94-17 with a chloride electrode using Standard Methods for the Examination of Water and Waste Water (Rand *et al.*, 1975).

The turbidmetric method was used for sulphate determination (Rand *et al.*, 1975). Untreated samples and samples treated by addition of barium chloride to induce barium sulphate precipitation were prepared. They were then

METHOD	DETECTION LIMIT (ug/L)	TYPICAL SENS. (ug/L)	OPTIMUM WORKING RANGE (ug/L)	PRECISION	ACCURACY
AA-Mg	0.0003	0.003	0.1-0.4		
AA-Na	0.0003	0.003	0.15-0.6		
AA-K	0.003	0.01	0.5-2.0		
AA-Ca	0.0005	0.021	1-4		
EDTA titrimetric method (Ca)				1.9%	9.2%
Alkalinity Titration (as CaCO ₃)			10-500	±1 mg/L	±3 mg/L
Spectrophotometer Sulphate				2.2%	9.1%
Chloride				1.0%	

Table 1. Accuracy and precision of selected analytical methods (Rand et al., 1975).

placed in a SP6-300 Spectrophotometer where differences in the measured transmittance would be proportional to the concentration of the sulphate ion.

Alkalinity was determined by titration with end points determined by colour (Rand *et al.*, 1975). The alkalinity analyses were conducted within 24 hours of sampling and on unfiltered water samples. The analyses assumed an absence of other (weak) acids such as silicic, phosphoric and boric.

Sodium, calcium, potassium and magnesium were analysed using an atomic absorption spectrophotometer. Calcium concentrations were cross checked using an EDTA titrimetric method (Rand *et al.*, 1975).

4.3.2.4. Isotope Analysis

Isotopic analyses for ^{18}O and D were performed on a mass spectrometer at the Environmental Isotope Laboratory of the Department of Earth Sciences at the University of Waterloo. The ^{18}O determinations were made on CO_2 equilibrated with the water sample at 25 C (Hoefs, 1973). This method permits an analytical precision of $\pm 0.1\%$. Deuterium determination was from water evaporated to H_2 gas by being passed over hot metallic uranium for an analytical precision of $\pm 1.0\%$ (Edwards, personal communication).

There are two methods of analyzing T. "Direct" T counting and "enriched" T counting. Both methods are satisfactory for this study, however, owing to the high cost of the second method, "direct" T counting was used. Tritium

analyses were done by direct liquid scintillation counting on an Instagel-water cocktail (Egboka *et al.*, 1983). There is a maximum analytical precision of ± 8 to 10 TU with a detection limit of 15 TU. Samples with negative values or positive values less than 15 TU are considered to contain no detectable tritium.

5.0. RESULTS AND DISCUSSION

5.1. Geophysical Analysis

5.1.1. Resistivity Results

Correlation of apparent resistivity profiles with the Gartner Lee borehole logs indicates that the depth of current penetration is approximately 0.5-0.66 of the length of the 'a' spacing for the Wenner array. Examination of data from Ali (1984) indicates a depth of current penetration approximately equal to the 'a' spacing.

Sections of the study area were not surveyed because of inaccessibility, residential or commercial development and topography. Of the sites surveyed, 77 sites produced dependable results with the remainder showing too much irregularity for any discernable observations (Table 2). The irregularities may have been a result of buried cables or piping, or dry surficial material which would prevent an adequate subsurface current flow between electrodes. The 'a' spacings of 1, 3, 6 and 9 m were statistically clustered for groupings of similar apparent resistivities using the SAS (Statistical Analysis System, 1982) average linkage cluster analysis method (Figure 21a,b,c,d). The clustering succeeded in demonstrating that survey sites can be grouped into three lithological units of clayey loam, sand and gravel, and till by their apparent resistivities (Table 3). However, survey sites do not form similar groupings at the various 'a' spacings. This suggests that the subsurface is

SITE	a=1 (μm)	a=2 (μm)	a=3 (μm)	a=4 (μm)	a=5 (μm)	a=6 (μm)	a=7 (μm)	a=8 (μm)	a=9 (μm)	a=10 (μm)
1	400	364	109	168	131	107	83	80	70	71
2	163	238	270	254	226	201	164	150	117	131
3	314	349	286	173	110	98	69	59	70	55
4	174	172	131	95	67	61	59	78	58	65
5	289	139	74	62	42	43	43	44	45	46
6	94	46	24	21	23	27	30	29	31	39
7	41	44	56	52	47	44	41	43	43	45
8	226	77	27	21	22	25	27	30	34	37
9	48	19	16	19	19	21	24	27	29	33
10	32	21	27	30	33	34	37	38	40	41
11	77	122	130	113	100	59	49	44	36	37
12	51	37	30	26	23	21	21	21	22	20
13	17	25	28	30	35	41	45	50	54	58
14	15	18	21	22	22	26	29	31	28	30
15	29	30	32	33	33	33	33	34	33	36
16	134	85	71	61	57	57	54	54	54	57
17	353	351	290	177	117	147	78	69	65	68
18	329	103	82	53	67	66	65	62	59	61
19	95	76	75	66	62	58	59	53	58	59
20	68	44	32	28	26	21	20	17	19	20
21	88	134	181	211	239	244	230	230	214	202
22	95	104	96	87	71	70	61	60	58	57
23	122	125	126	108	98	84	79	79	77	73
24	109	82	63	55	52	49	48	49	58	59
26	137	220	213	149	112	78	79	75	68	70
27	68	106	245	238	214	162	133	126	110	115
28	174	330	419	342	240	114	85	76	72	70
29	116	94	155	158	148	175	155	108	61	18
30	83	125	95	93	92	76	79	75	70	83
31	117	163	150	131	73	58	28	18	19	31
32	108	192	233	277	310	324	350	357	366	353
33	55	39	36	37	44	53	57	65	72	83
34	165	81	47	39	45	56	64	70	76	83
35	151	93	80	89	96	106	113	130	141	153
36	48	52	49	48	47	51	55	57	64	69
43	108	93	90	89	85	82	79	76	78	75
44	113	69	62	63	92	67	70	71	69	72
45	96	88	87	97	100	99	99	101	111	90
46	56	26	23	21	18	18	14			
47	47	35	31	25	34	37	38	40		
48	77	42	32	32	32	35	38	40	40	47
49	423	410	270	190	125	88	70	58	50	49
50	33	33	29	27	28	32	32	33	34	32
51	219	216	229	243	267	279	295	264	266	248
52	253	112	54	46	52	54	57	65	74	88
53	33	39	41	46	48	49	50	56	56	55
54	43	43	54	61	60	55	64	69		
55	36	44	48	50	53	55	56	58	58	59
56	43	50	56	56	57	59	59	61	59	60
57	169	106	82	69	60	58	55	54	53	51
58	99	83	70	67	64	63	62	61	60	62
59	32	41	46	47	51	53	52	56	55	58
60	77	55	47	50	52	52	52	60	51	54
61	38	42	48	54	61	63	65	71	73	77
62	34	30	33	35	38	41	42	43	43	47
63	124	75	51	47	45	44	45	48	52	53
64	17	13	15	17	18	19	20	24	23	26
65	45	34	32	33	35	39	43	46	49	51
66	29	23	23	26	28	30	34	37	38	41
67	563	331	185	86	58	50	48	48	50	46
68	335	198	106	82	74	69	63	65	66	64
69	37	48	44	53	57	63	66	66	71	72
70	47	42	38	45	51	54	56	58	62	64
71	109	71	83	87	81	79	76	78	77	78
72	25	26	32	36	39	44	46	50	55	56
73	25	32	32	35	40	42	47	50	54	59
74	1050	373	65	38	43	43	46	57	56	61
75	39	38	39	41	42	45	49	54	58	61
76	30	27	28	32	33	36	39	38	38	37
77	46	60	60	56	56	57	58	58	62	63

Table 2. Apparent resistivities for 'a' spacings of 1 to 10 m.

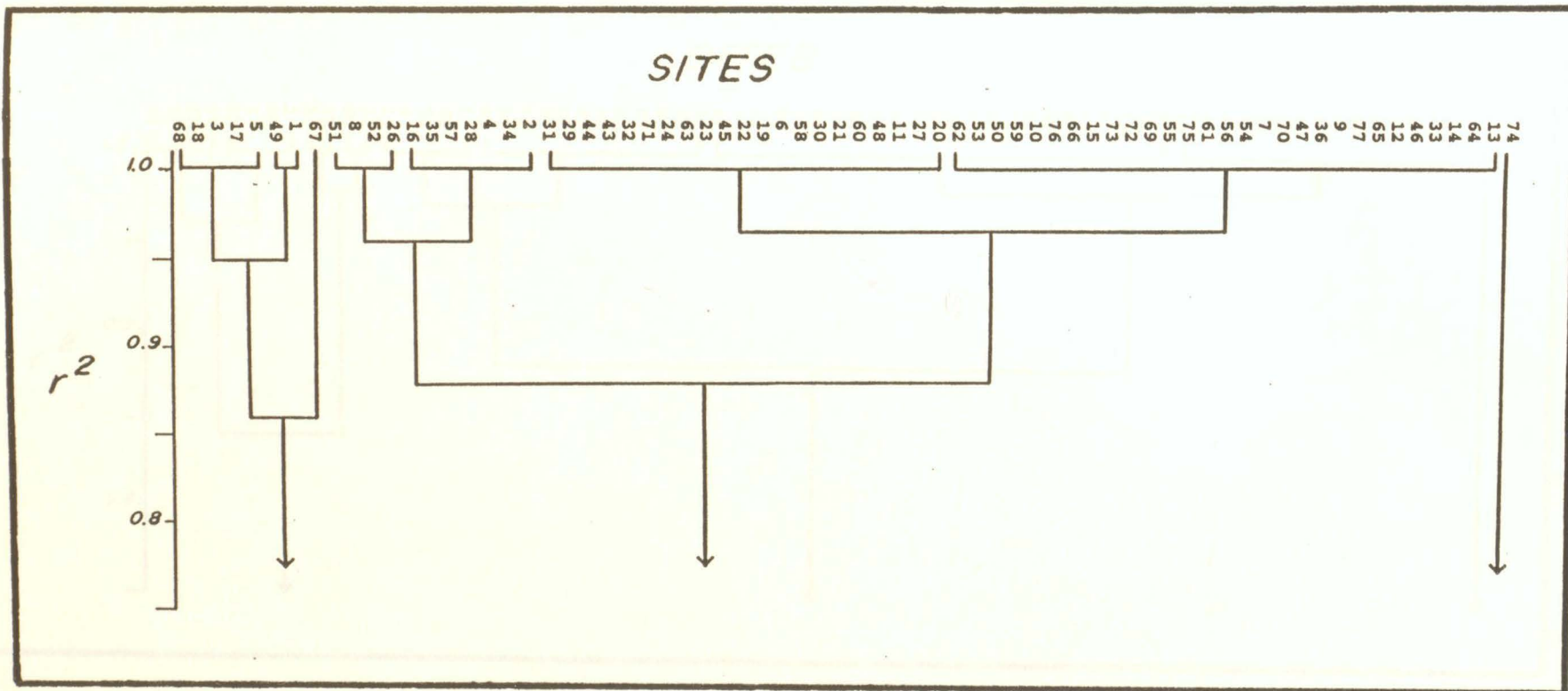


Figure 21a. Cluster analysis for apparent resistivity for sites at an 'a' spacing of 1 m

Figure 21b. Cluster analysis for apparent resistivity for sites at an 'a' spacing of 2 m

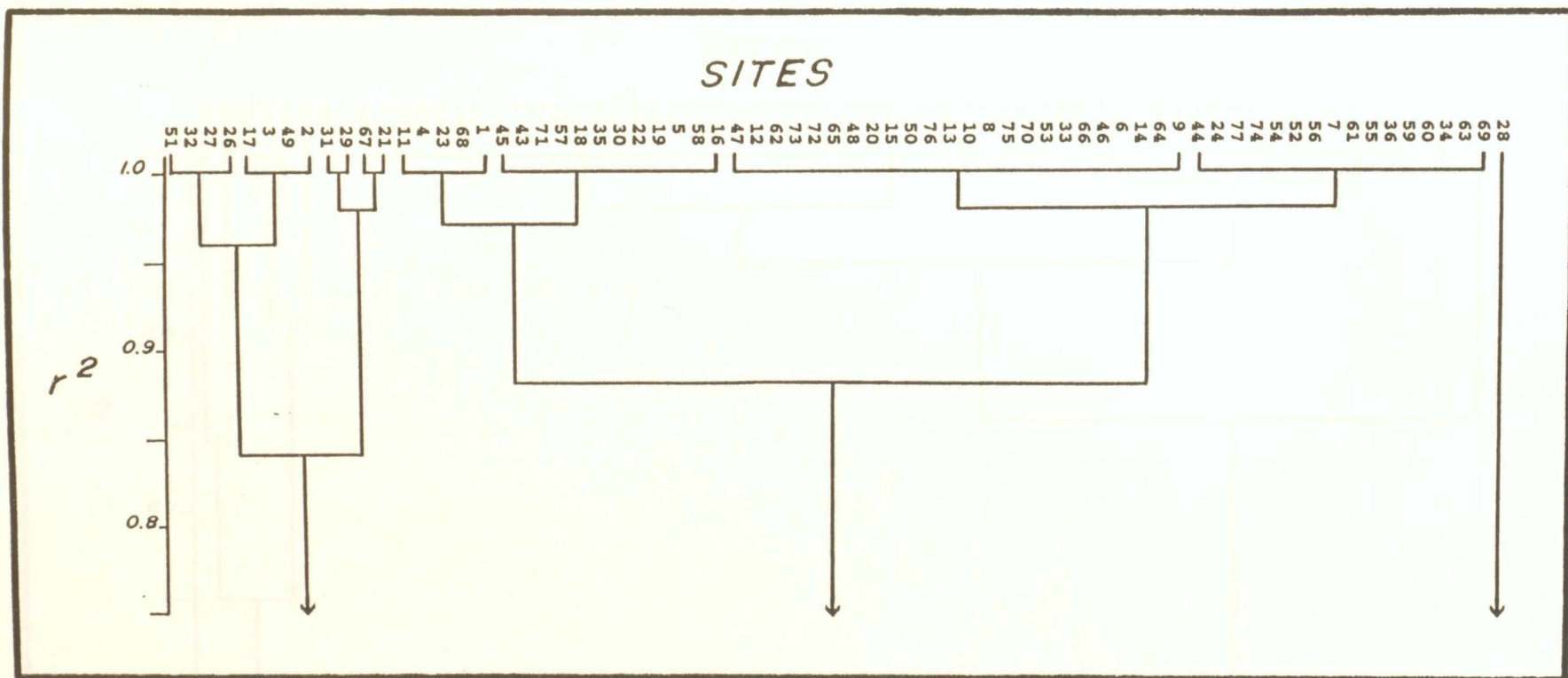


Figure 21b. Cluster analysis for apparent resistivity for sites at an 'a' spacing of 3 m.

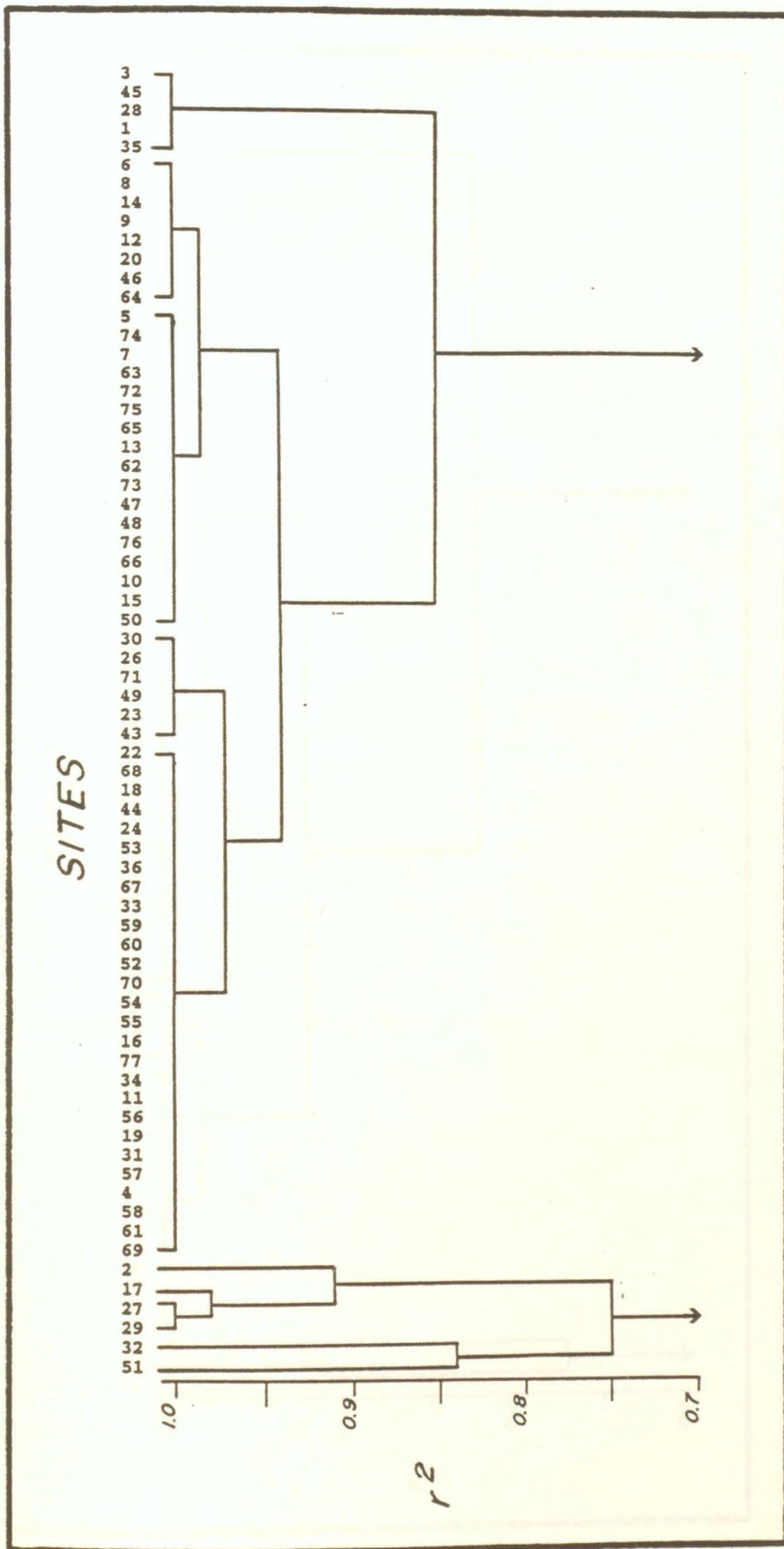


Figure 21c. Cluster analysis for apparent resistivity for sites at an 'a' spacing of 6 m.

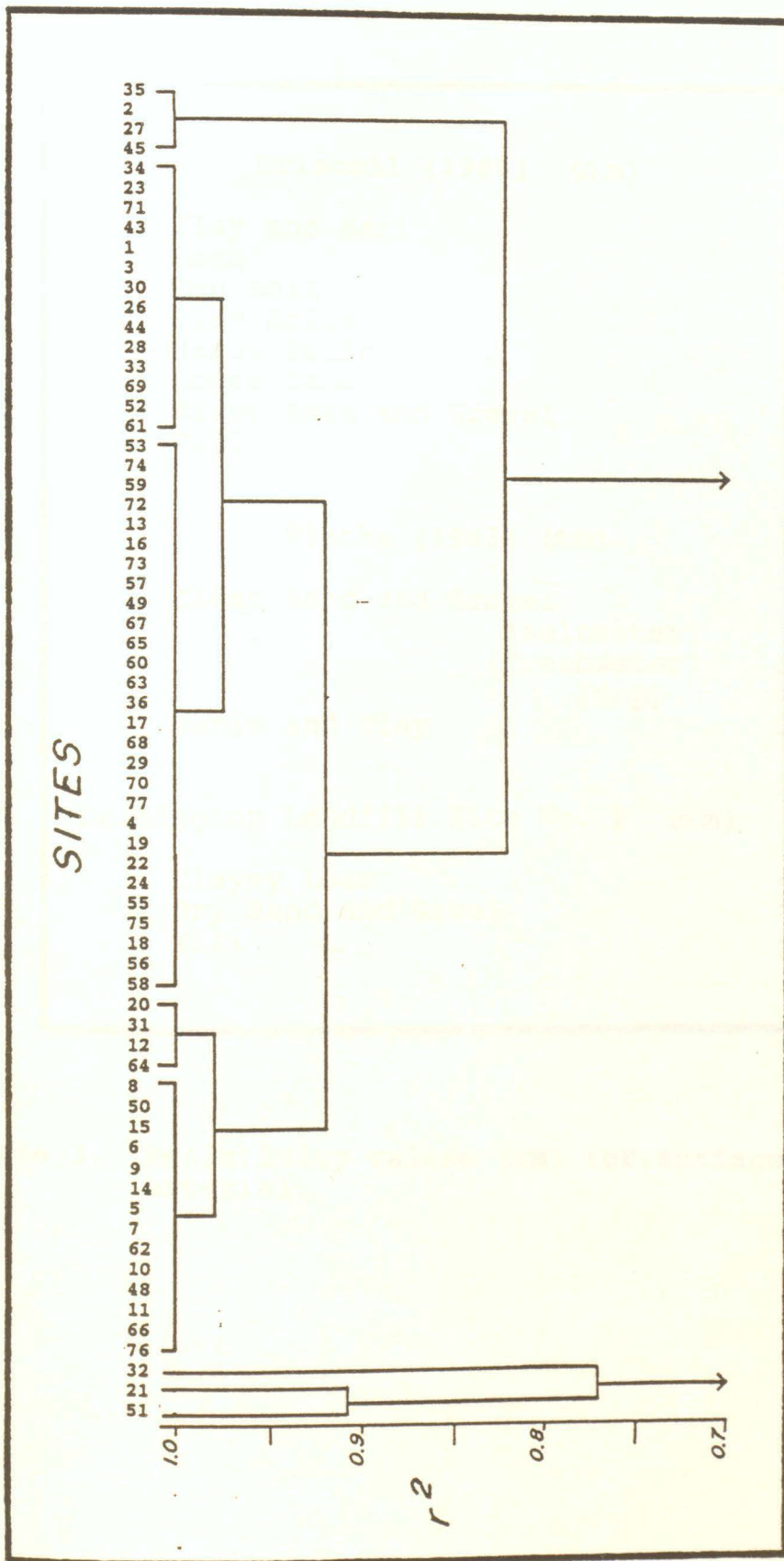


Figure 21d. Cluster analysis for apparent resistivity for sites at an 'a' spacing of 9 m.

Driscoll (1986) (Ωm)	
Clay and Marl	1-100
Loam	10-50
Top Soil	100
Clay Soils	100-500
Sandy Soils	500-2000
Loose Sand	1000-100,000
River Sand and Gravel	100-10,000
Till	10-5000
Flathe (1963) (Ωm)	
Clean Sand and Gravel	
(saltwater)	1-50
(freshwater)	50-2000
(dry)	>2000
Marls and Clay	2-50
Leamington Landfill Site No. 2 (Ωm)	
Clayey Loam	<50
Dry Sand and Gavel	>100
Till	<100

Table 3. Resistivity values (Ωm) for surface and subsurface material.

highly heterogeneous and that there does not exist a consistent group of anomalous values representative of subsurface contamination.

Apparent resistivity data for an 'a' spacing of 1 m tend to closely follow surficial deposits (Figure 4; Figure 22). Sites with apparent resistivities exceeding 100 Ω m are confined to mined out areas where surface soils have been removed. Clayey loam surface soils correspond to sites below 50 Ω m (Table 3). There is evidence of a near surface water table at sites located near position 'A'. Apparent resistivities less than 100 Ω m at this point may indicate the position of a contaminant plume from the abandoned Heinz landfill. This anomalous area was also evident in the resistivity survey conducted by Ali (1984) and suggests plume and groundwater movement towards the southeast.

At a depth of 1.5 to 2.0 m ('a'=3), the apparent resistivity contours tend to follow the subsurface lithology (Figure 5; Figure 23). Within the landfill at this depth, apparent resistivity values indicate contact with the water table. The suspected contaminant plume southeast of the Heinz landfill is still evident. Sites below 50 Ω m conform to the subsurface till except southeast and northeast of the landfill. Ali (1984) also detected low apparent resistivity values northeast of the landfill. In these areas, seismics and borehole logs suggest that the subsurface consists of saturated glaciofluvial and glaciolacustrine sands and

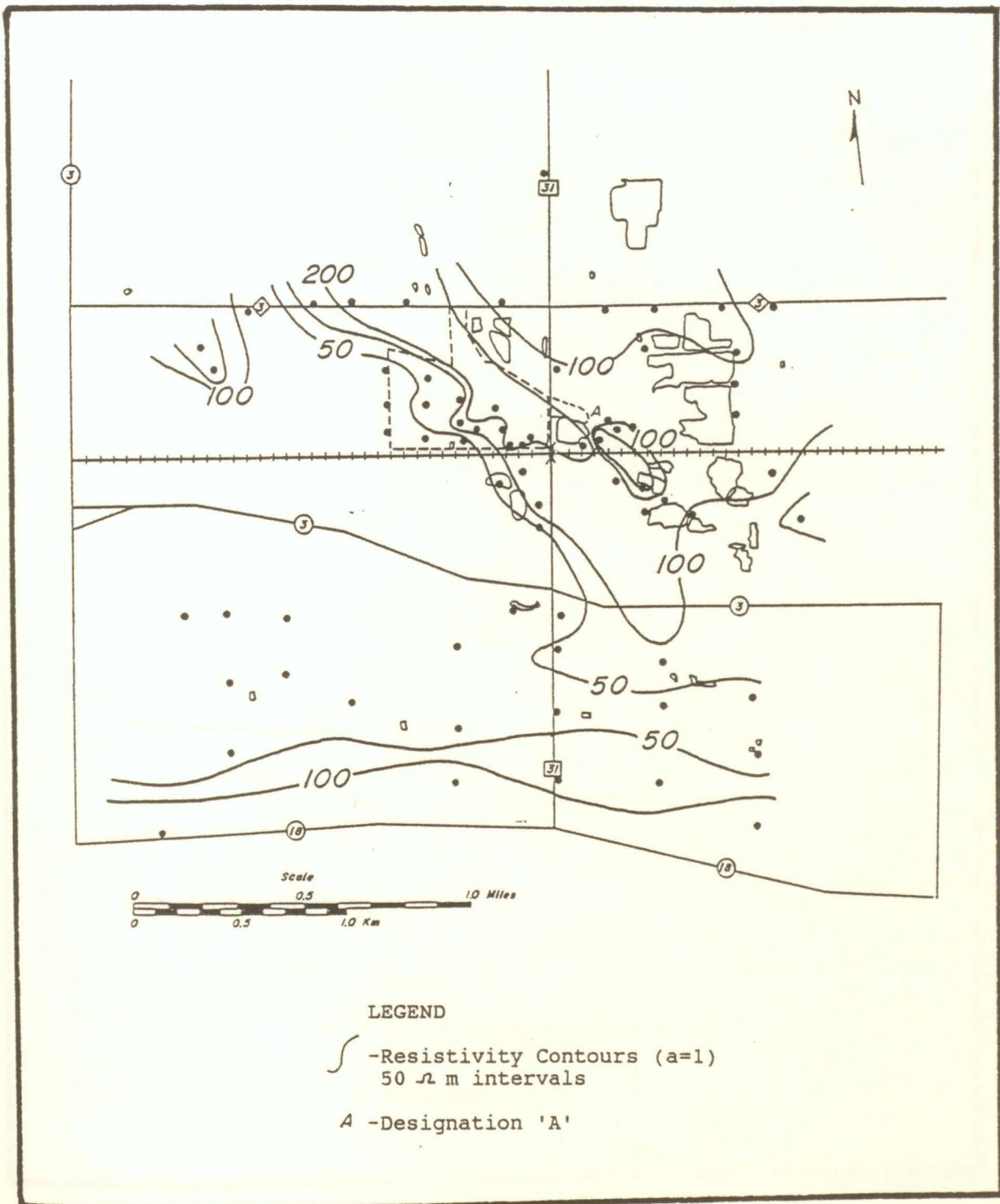


Figure 22. Apparent resistivity distribution (Ω m) for an 'a' spacing of 1 m

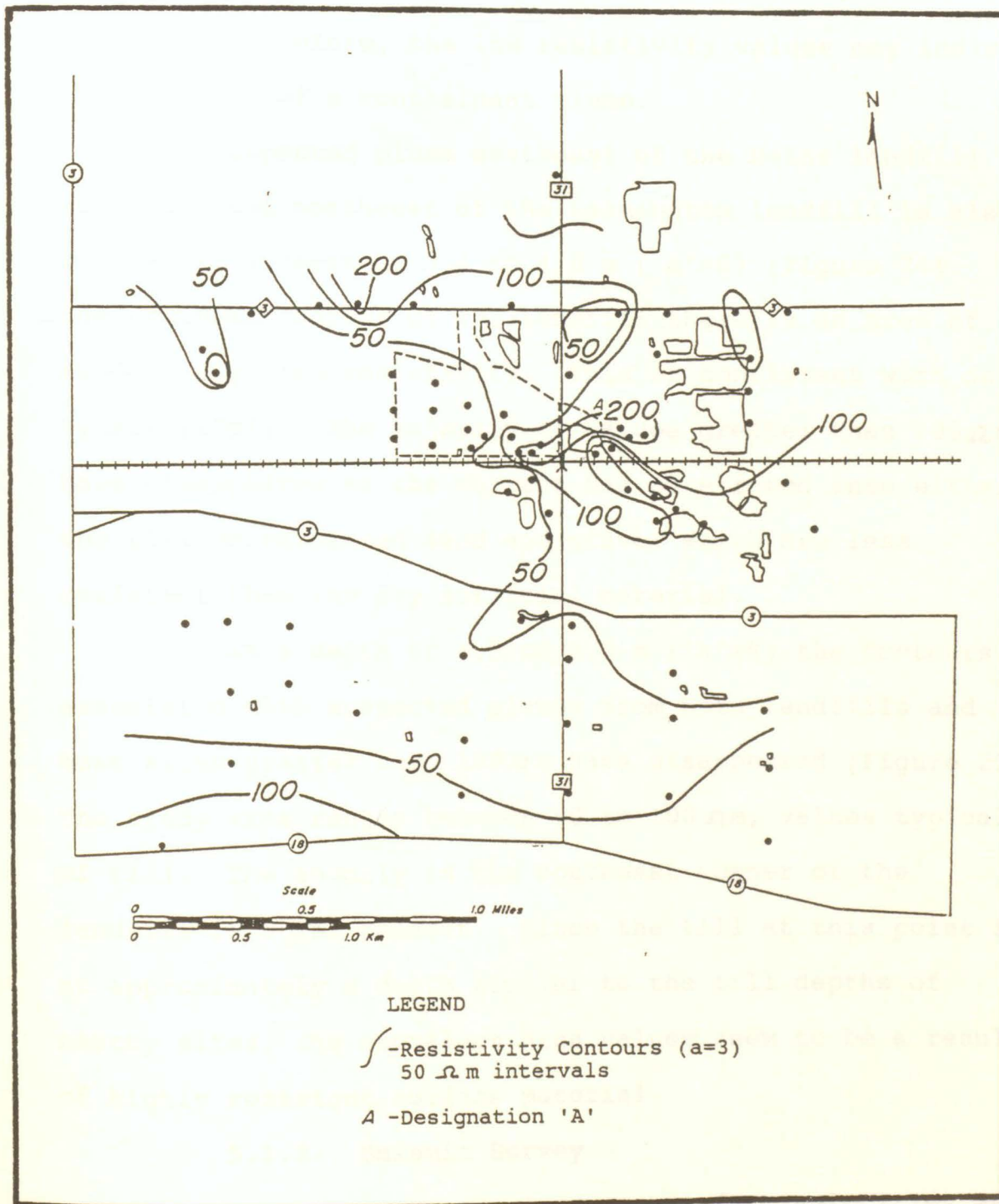


Figure 23. Apparent resistivity distribution (Ωm) for an 'a' spacing of 3 m.

gravels. Therefore, the low resistivity values may indicate the presence of a contaminant plume.

The suspected plume southeast of the Heinz landfill and southeast and northeast of the Leamington landfill is also evident at a depth of 3.4 to 4.0 m ('a'=6) (Figure 24). In the southeast corner of the landfill there is an area of anomalously high resistivity. This is consistent with data by Ali (1984). The majority of values greater than 100 Ω m have disappeared as the current has penetrated into either the till or saturated sand and gravel which are less resistant than the dry surficial material.

At a depth of 4.5 to 6.0 m ('a'=9) the contours associated with suspected plumes from both landfills and most sites greater than 100 Ω m have disappeared (Figure 25). The study area ranges between 50 to 100 Ω m, values typical of till. The anomaly in the southeast corner of the landfill is still present. Since the till at this point is at approximately a depth similar to the till depths of nearby sites, the anomalous high values seem to be a result of highly resistant surface material.

5.1.2. Seismic Survey

At most sites, three primary subsurface velocities were observed (Table 4). Each velocity set of the seismic data was statistically clustered using SAS (1982). The resulting groups of similar velocities were compared to known

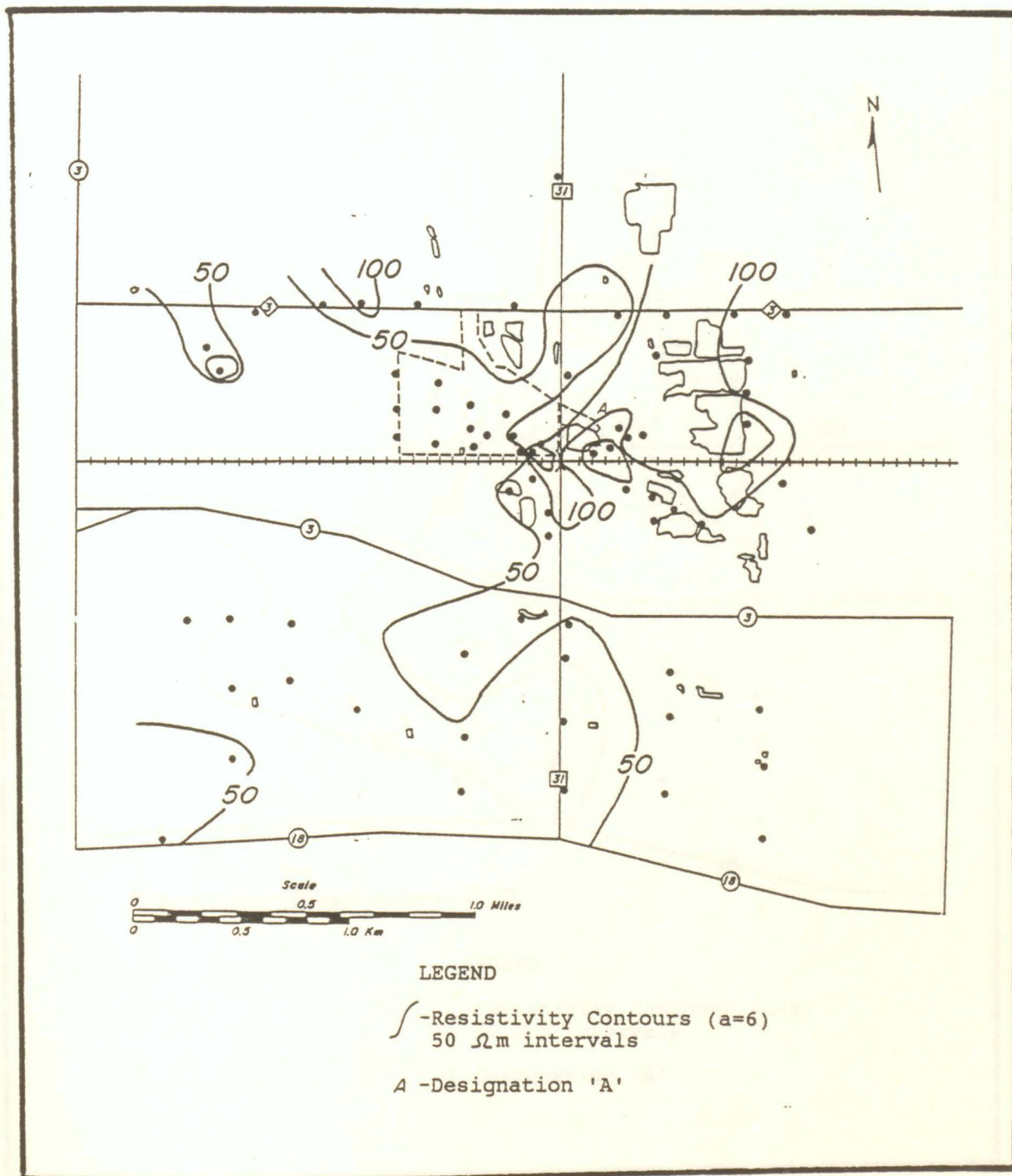


Figure 24. Apparent resistivity distribution (Ωm) for an 'a' spacing of 6 m.

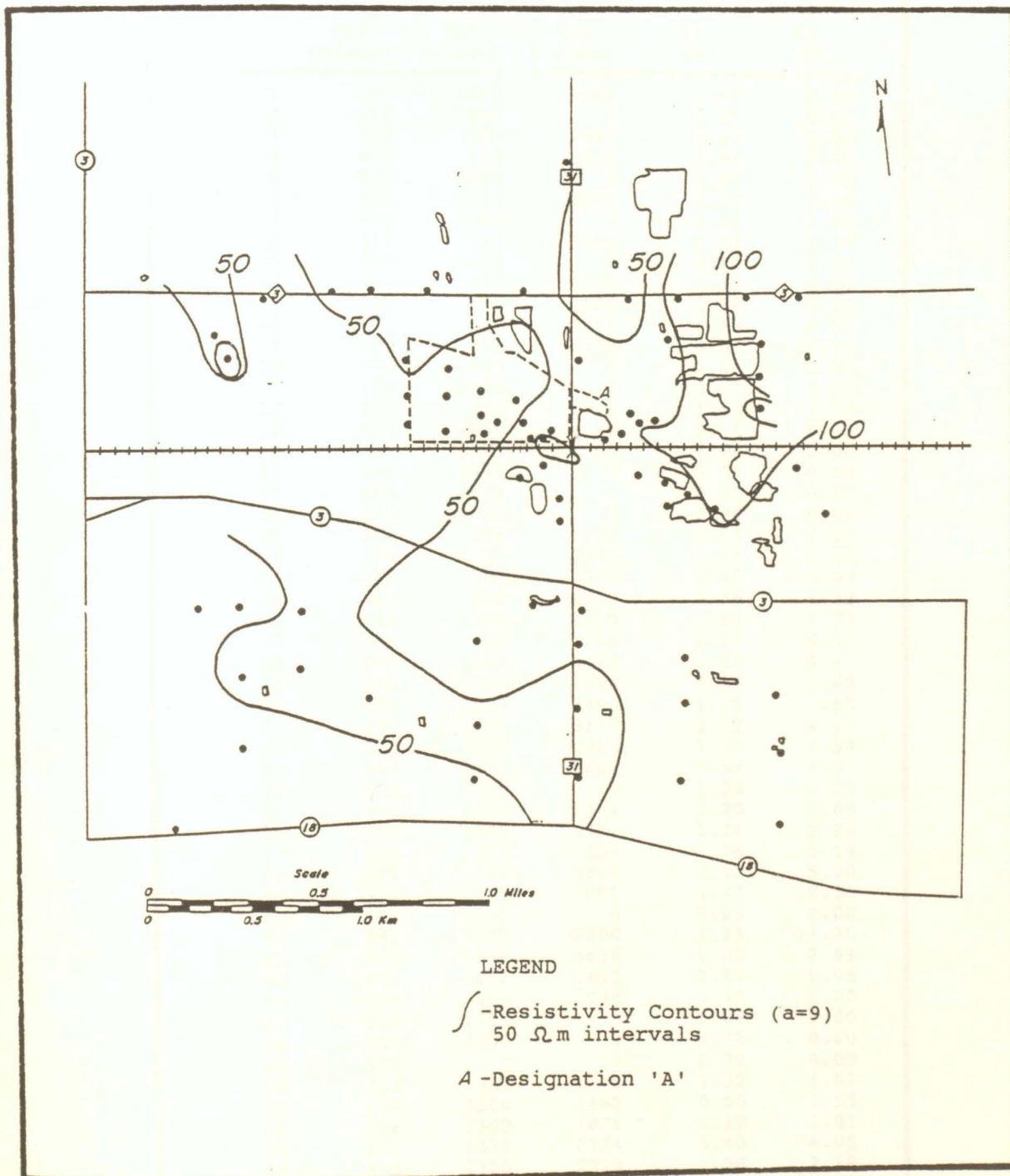


Figure 25. Apparent resistivity distribution (Ωm) for an 'a' spacing of 9 m.

SITE	PRIMARY			VELOCITIES	
	Vp1 (m/sec)	Vp2 (m/sec)	Vp3 (m/sec)	Z1 (m)	Z2 (m)
1	409	1667	2500	1.69	5.66
2	421	3666	0	2.22	0.00
3	333	783	1935	1.47	3.04
4	500	813	2000	1.59	5.94
5	516	1058	0	0.89	0.00
6	375	1500	2500	1.36	2.67
7	421	3666	0	2.22	0.00
8	273	714	1800	1.33	5.37
9	333	1600	0	0.85	0.00
10	389	875	2222	2.17	5.62
11	348	882	2286	1.99	3.21
12	350	692	2571	1.83	6.35
13	700	1375	2400	0.81	10.72
14	775	1739	0	2.60	0.00
15	766	1565	0	3.07	0.00
16	213	410	4705	1.62	2.03
17	600	2000	0	3.14	0.00
18	625	1600	0	2.04	0.00
19	500	1455	0	3.19	0.00
20	600	1818	0	2.54	0.00
21	466	1733	0	2.90	0.00
22	166	538	2632	0.96	2.86
23	209	727	3333	1.15	7.32
24	250	774	2500	1.45	8.89
25	387	888	3333	2.58	6.48
26	266	1250	4750	1.84	7.77
27	278	952	2389	2.03	0.66
28	263	1130	3428	1.62	3.46
29	225	700	3090	0.89	3.66
30	500	1529	2400	1.85	7.69
31	333	1000	3167	2.12	4.37
32	310	727	2923	1.11	3.54
33	400	1429	1852	0.62	6.05
34	400	1739	0	1.03	0.00
35	466	1538	2307	2.20	5.65
36	333	968	2571	1.24	2.99
37	357	871	2125	1.76	3.19
38	409	1333	3600	3.12	5.00
39	303	1571	3000	1.47	8.33
40	400	1135	0	0.85	0.00
41	381	930	2800	1.25	16.30
42	370	1000	3636	0.80	7.91
43	421	842	1412	0.49	5.05
44	478	612	938	2.30	0.00
45	542	1333	0	5.04	0.00
46	600	2000	0	4.72	0.00
47	484	0	0	0.00	0.00
48	364	1333	1765	1.32	4.01
49	318	1200	1667	0.66	2.53
50	286	1300	1875	1.10	1.81
51	625	1385	2174	1.40	4.05
52	400	1200	2222	1.38	2.19
53	385	857	1692	0.86	1.54
54	720	1333	3600	0.86	5.19
55	545	1125	2143	0.62	4.22
56	909	1500	0	2.29	0.00
57	545	1500	0	2.19	0.00

Table 4. Primary velocities (Vp) and depths to interfaces (z) for seismic sites.

subsurface material to determine the lithological characteristics of the velocity ranges (Table 5).

Primary velocities (V_{p1}) of the uppermost layer form three divisions at a Pearson correlation coefficient (r^2) of 0.85 (Figure 26). East of the landfill, in previously mined sand and gravel pits, material is predominantly a loose dry gravel (Figure 27). Abundant gravel is visible on the surface within this area. The highest velocities for this layer are west of the landfill in the clayey silt tills. Loose dry sand and gravel deposits cover the remaining area.

The second cluster analysis of primary velocities of the second layer separates the data into predominantly two groupings ($r^2=0.85$) of saturated compact till and saturated sand and gravel (Figure 28). The saturated sand and gravel velocities are centred around areas of thick deposits of sand and gravel (Figure 29). The compact till velocities occur where till is close to the surface, west of the landfill and south of Highway #3.

Primary velocities of the lowermost layer (V_{p3}) are representative of either bedrock (shale or limestone), or saturated compact till (Figure 30). Values indicating the till interface are predominantly below the area designated by the second layer velocities as saturated sand and gravel (Figure 31).

Although velocities for the various lithologies correlate very well with known deposits, the depths of

Driscoll (1986)

Gravel & Sand (wet)	- 457-915 m/sec
Sand (wet)	- 610-1830 m/sec
Clay	- 915-2740 m/sec
Water	- 1430-1680 m/sec
Shale	- 2740-4270 m/sec
Limestone	- 2130-6100 m/sec

Costa & Baker (1981)

Soil	- 240-460 m/sec
Loose Sand (dry)	- 240-600 m/sec
Loose Sand (wet)	- 460-1220 m/sec
Loose Gravel (wet)	- 460-915 m/sec
Loose Sand & Gravel (wet)	- 460-1220 m/sec
Clay	- 915-1525 m/sec
Water	- 1525 m/sec
Glacial Till (loose)	- 300-1500 m/sec
Glacial Till (compact)	- 1220-2135 m/sec
Shale (soft)	- 1220-2135 m/sec
Shale (hard)	- 1830-2740 m/sec

Essex County Sanitary Landfill Site No. 2

Loose Gravel (dry)	- 150-300 m/sec
Loose Sand & Gravel (dry)	- 300-450 m/sec
Loose Sand & Gravel (wet)	- 450-1000 m/sec
Fine Sand, Silt, Clay	- 450-650 m/sec
Glacial Till (loose)	- 700-950 m/sec
Glacial Till (compact)	- 1000-2000 m/sec
Bedrock	- >2000 m/sec

Table 5. Seismic velocities for surface and subsurface material.

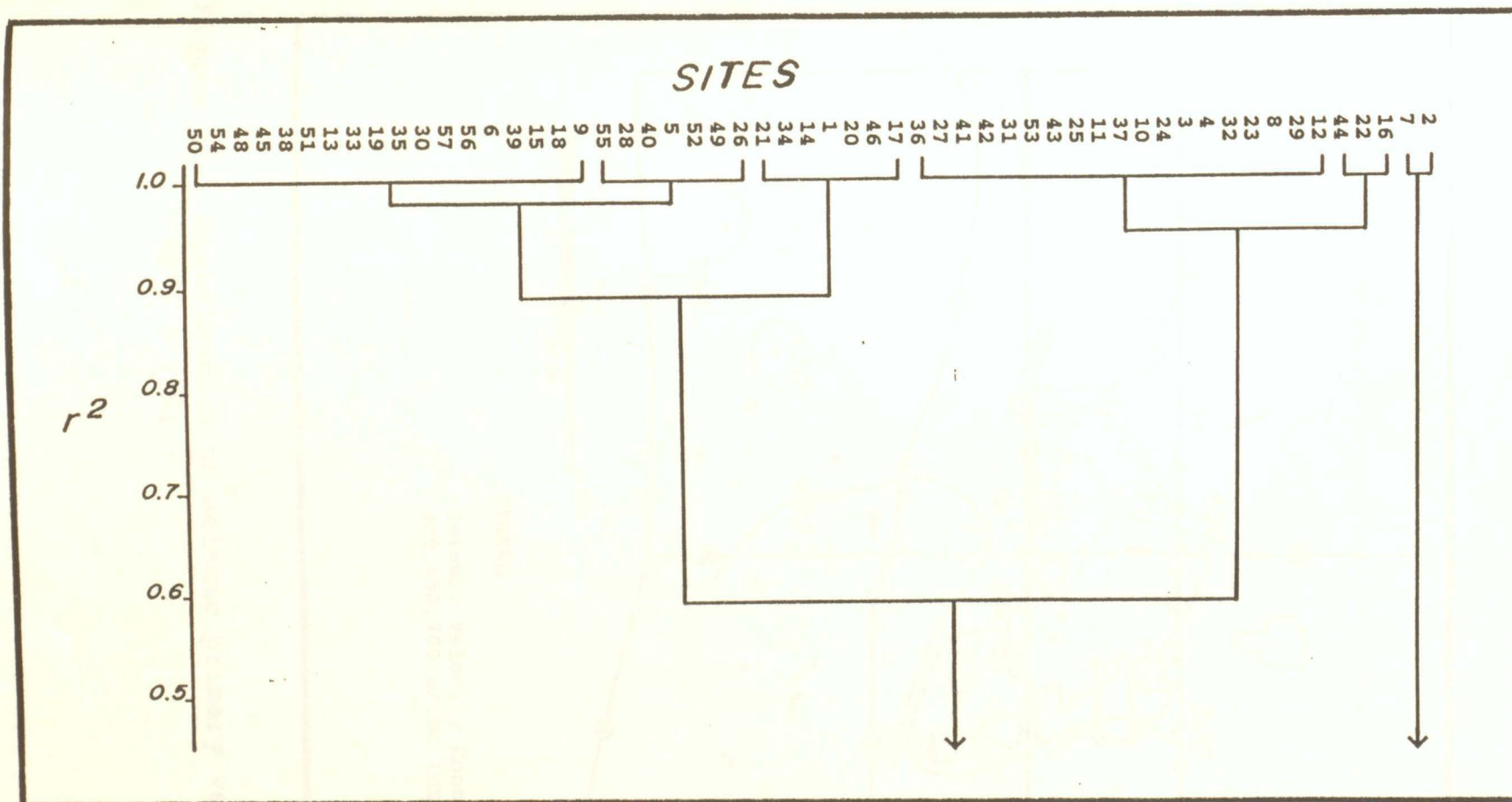


Figure 26. Cluster analysis for seismic primary velocities of layer 1 (V_{p1})

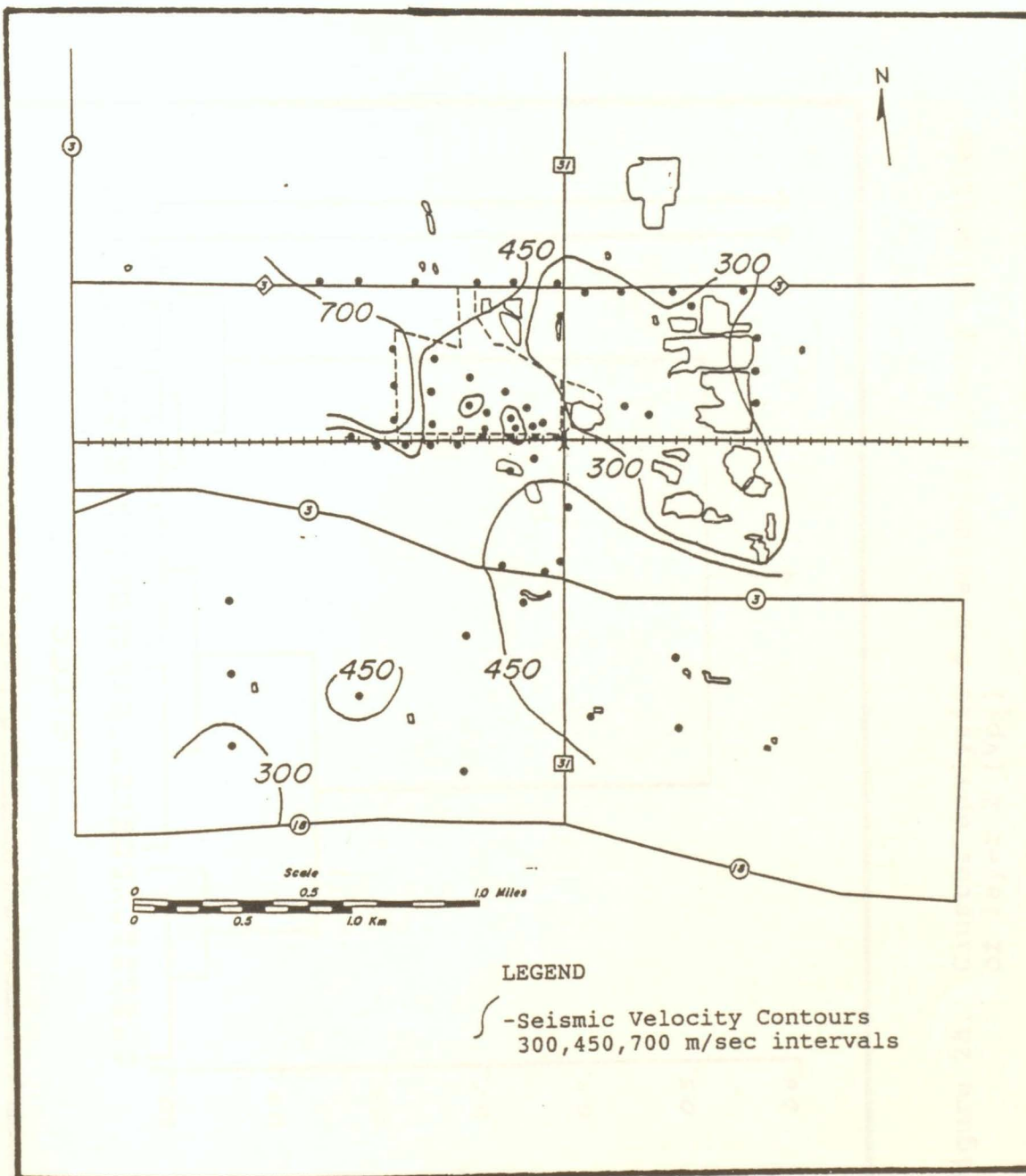


Figure 27. Distribution of seismic primary velocities for layer 1 (V_{p1}).

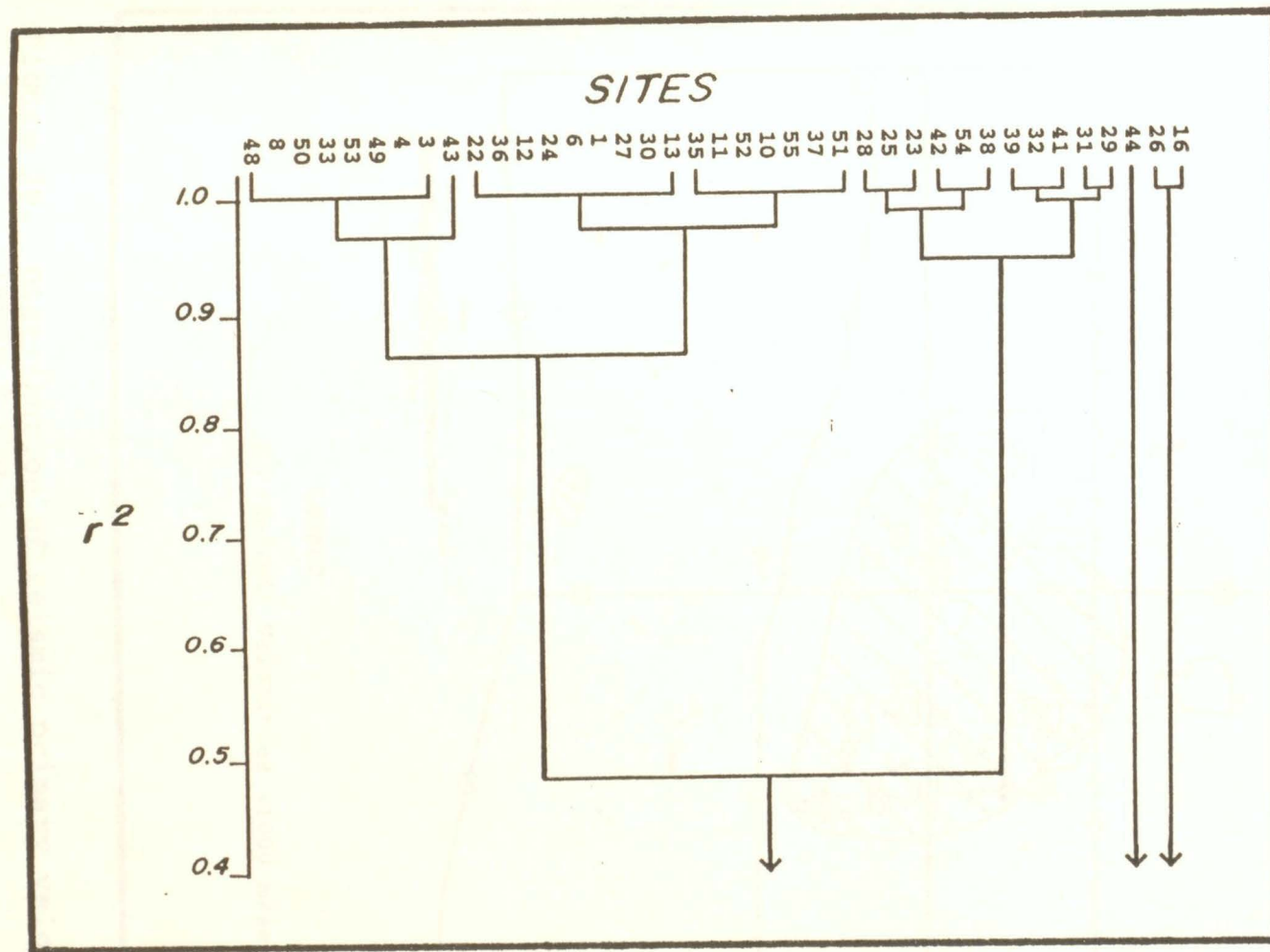


Figure 28. Cluster analysis for seismic primary velocities of layer 2 (V_{p1})

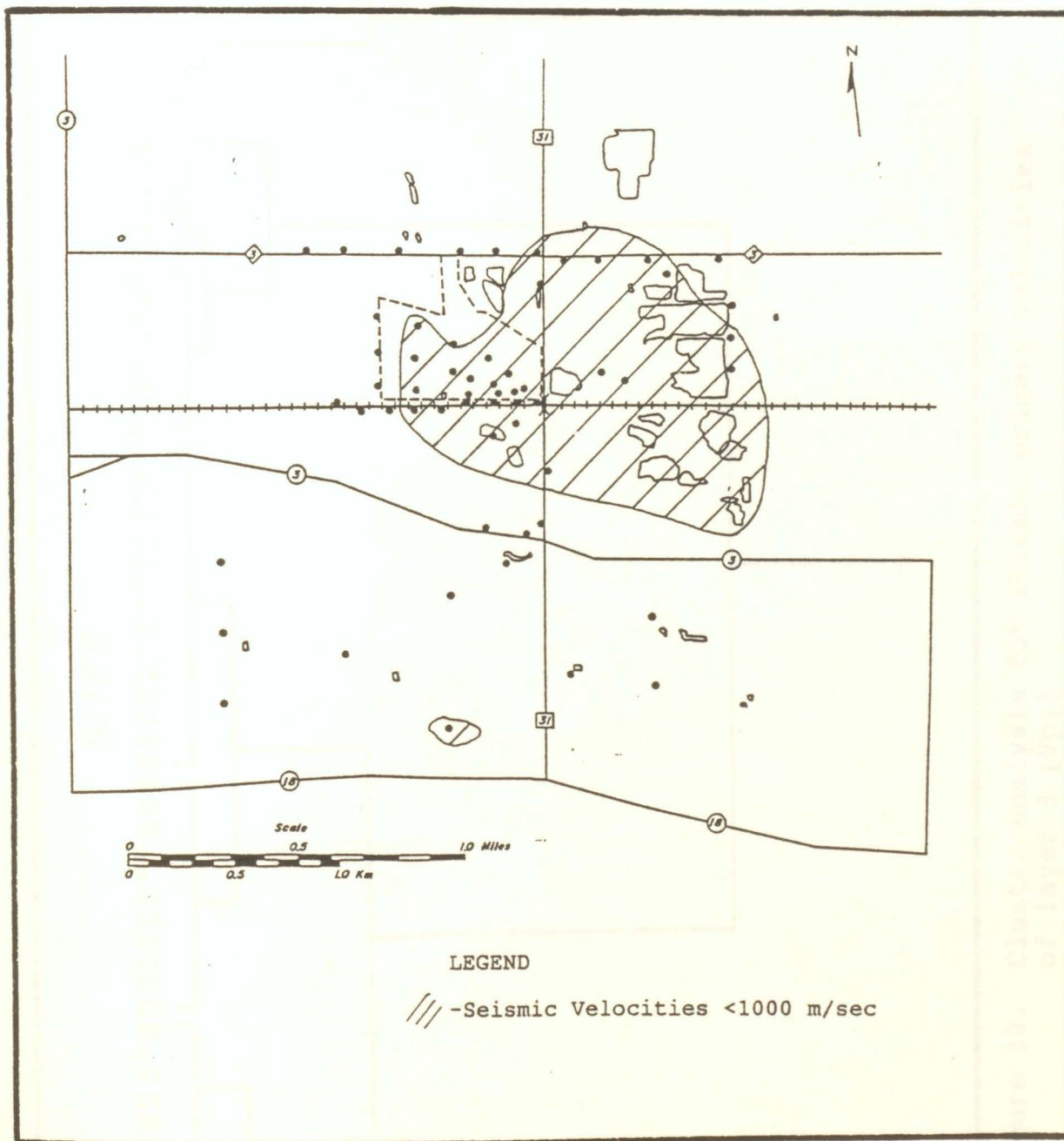


Figure 29. Distribution of seismic primary velocities for layer 2 (VP_1).

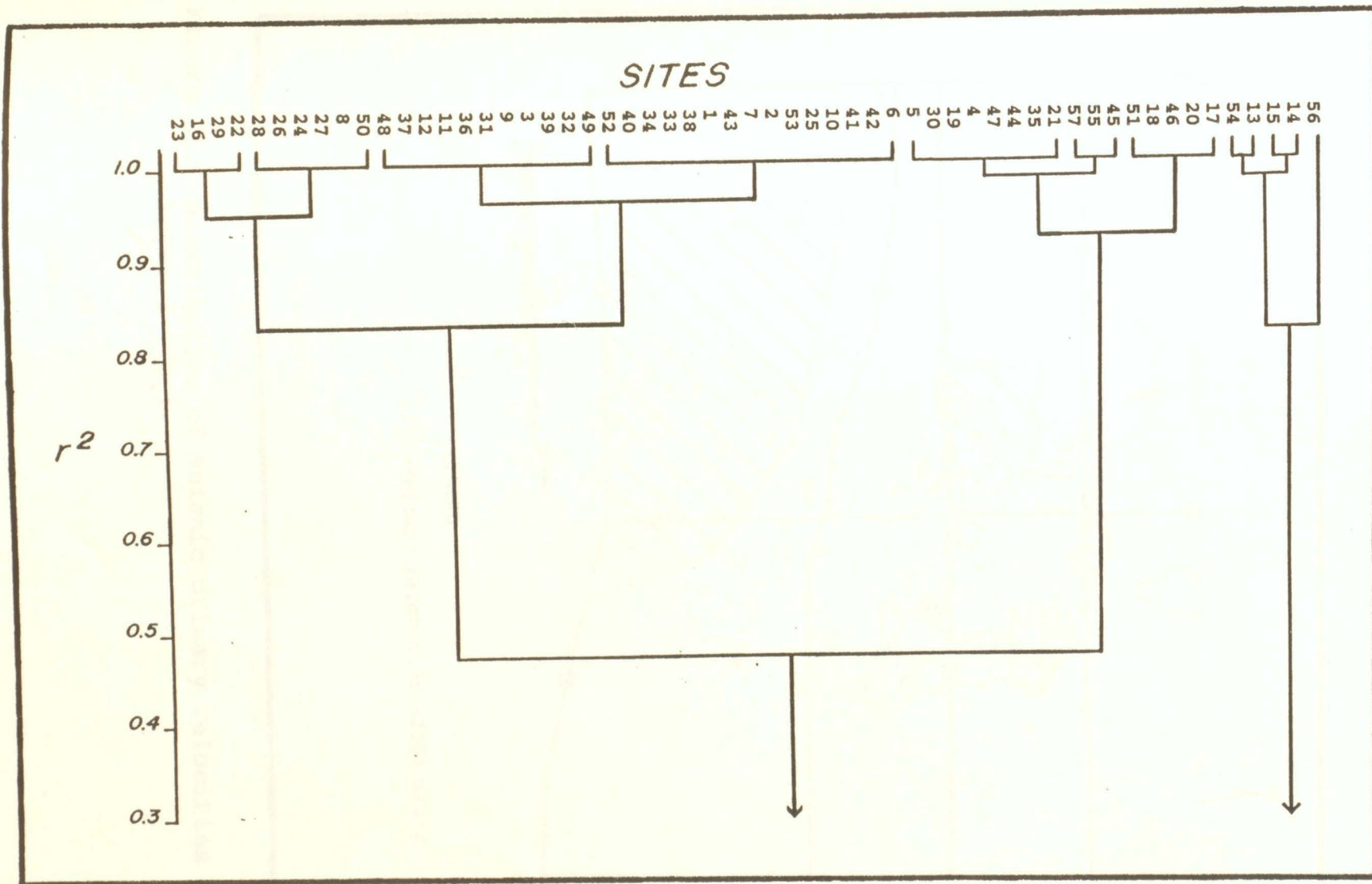


Figure 30. Cluster analysis for seismic primary velocities of layer 3 (V_{p1})

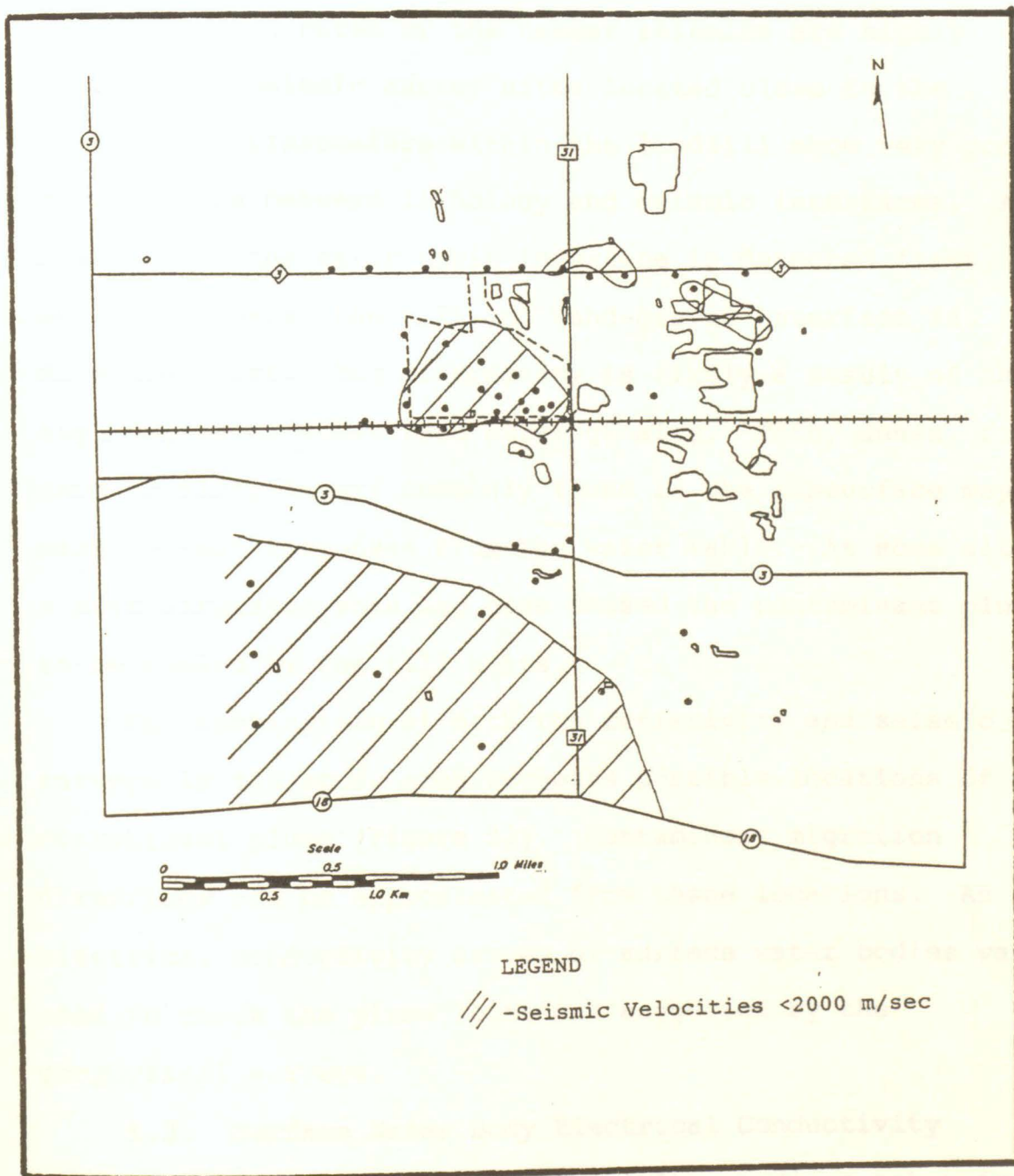


Figure 31. Distribution of seismic primary velocities for layer 3 (V_{p1}).

interfaces indicated by the hammer seismics are highly irregular. Seismic survey sites located close to the Gartner Lee piezometers within the landfill show very poor correlations between lithology and seismic interfaces. At some sites, the water table interface is detected first, while in others, the till and sand-gravel interface is detected first. The discrepancy is likely a result of the high degree of subsurface heterogeneity. Thin, dense, fine sand or silty layers commonly found in the subsurface may mask seismic responses from the water table. At some sites, a thin saturated zone may have caused the contaminant plume to be masked by the till units.

The combination of both the resistivity and seismic surveys in the study area suggests possible locations of the contaminant plume (Figure 32). Contaminant migration directions can be approximated from these locations. An electrical conductivity survey of surface water bodies was used to check the plume locations suggested by the geophysical surveys.

5.2. Surface Water Body Electrical Conductivity

Background electrical conductivity readings taken from surface water bodies range from the low 200 $\mu\text{S}/\text{cm}$ range to the mid 400 $\mu\text{S}/\text{cm}$ range (Figure 33). The highest observed electrical conductivity was 9389 $\mu\text{S}/\text{cm}$ at the leachate collection ditch at the landfill's southern boundary. Values decreased towards the south and east suggesting that

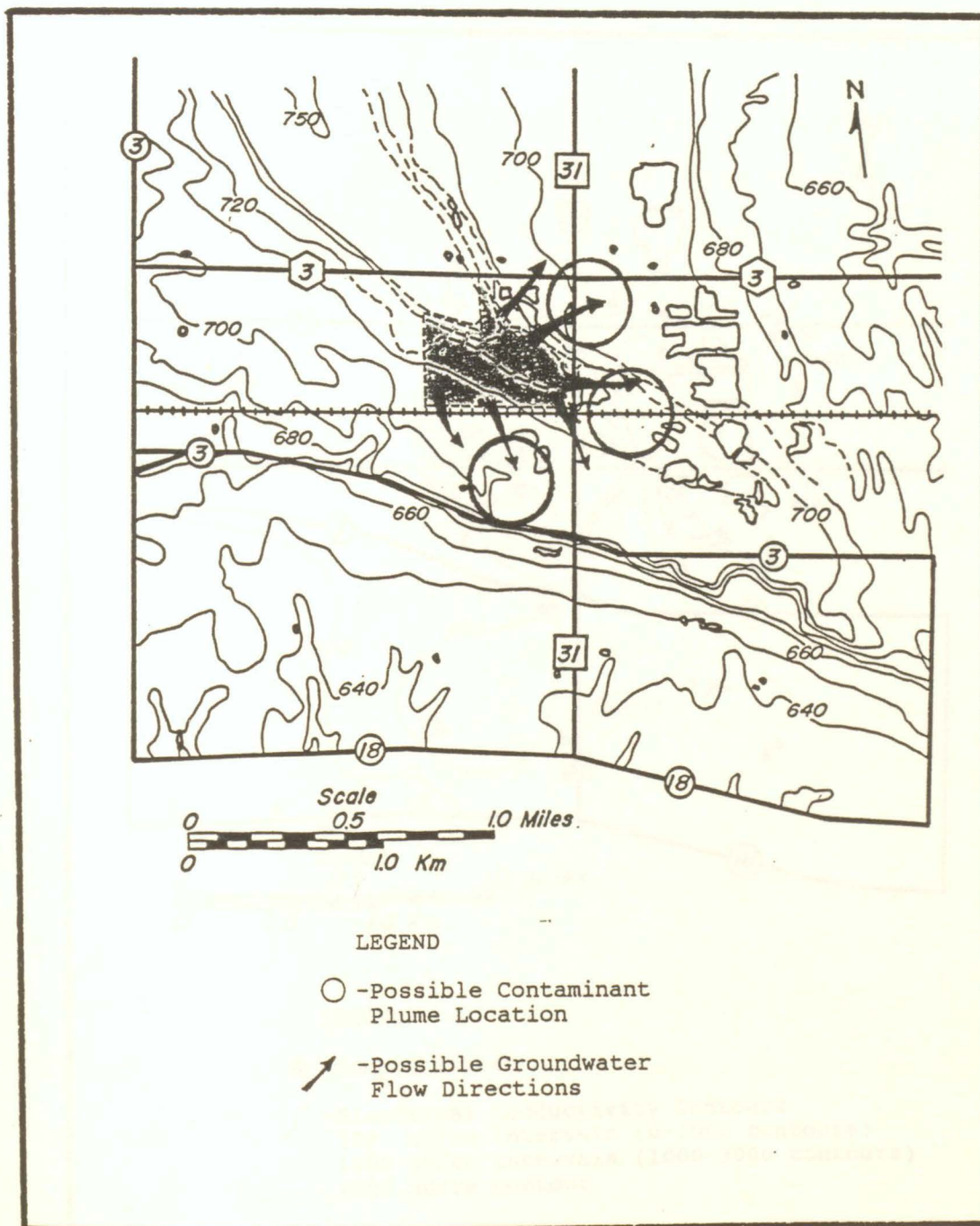


Figure 32. Possible contaminant plume locations.

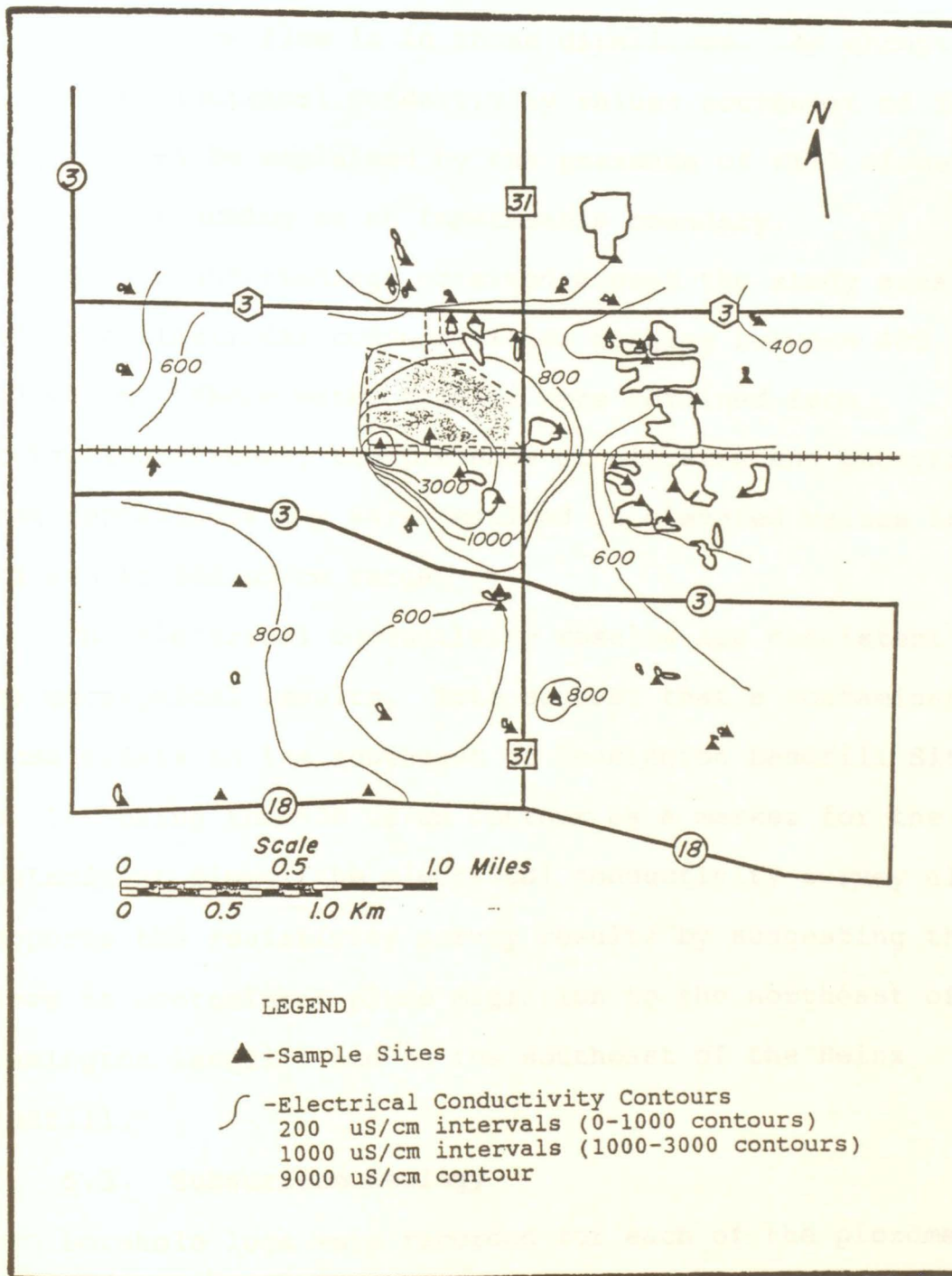


Figure 33. Electrical conductivity for surface water bodies.

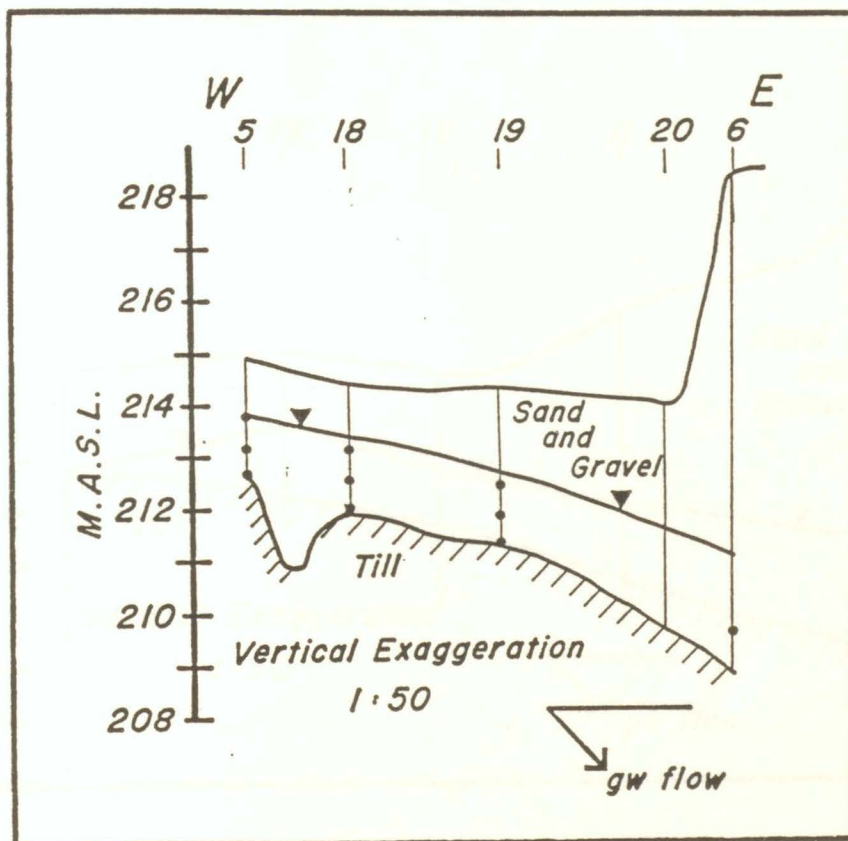
the groundwater flow is in those directions. An abrupt change in electrical conductivity values southwest of the landfill can be explained by the presence of till close to the surface acting as an impermeable boundary.

Background readings obtained around the study area indicate electrical conductivities ranging between 400 to 600 uS/cm. Where water samples were obtained from irrigation ditches, the presence of nitrates and phosphates from fertilizers may have resulted in elevated values in the mid 800 to 900 uS/cm range.

The electrical conductivity results are consistent with the geophysical results. Both suggest that a contaminant plume exists to the southeast of Leamington Landfill Site No. 2. Using the 800 uS/cm contour as a marker for the contaminant plume, the electrical conductivity survey also supports the resistivity survey results by suggesting that there is contaminant plume migration to the northeast of the Leamington landfill and to the southeast of the Heinz landfill.

5.3. Subsurface Geology

Borehole logs were recorded for each of the piezometer installations (Appendix I). All of the boreholes penetrate the unconfined sand and gravel aquifer and extend into the lower confining silty clay till unit as shown in the cross sections indicated in Figure 16 (Figures 34a,b,c,d).

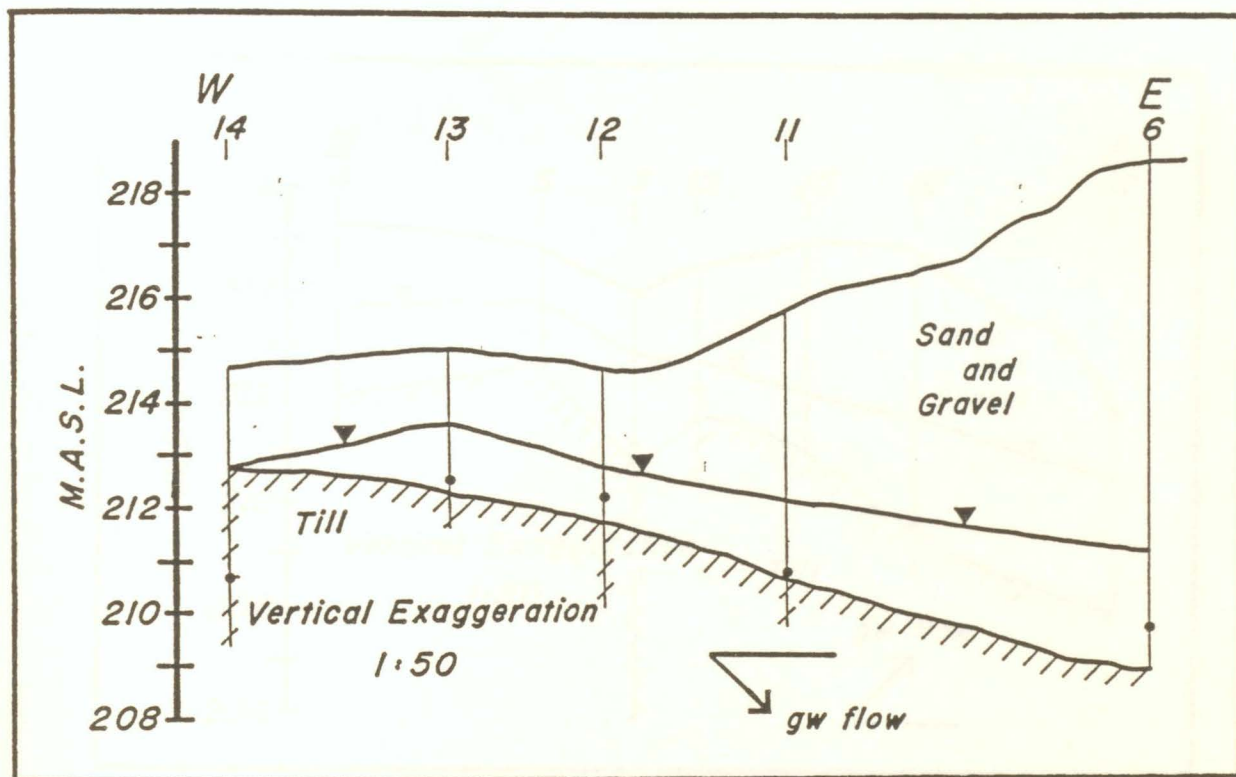


LEGEND

- -Location of Piezometer Screen
- | -Borehole Designation
- ▼ -Inferred Water Table (October 31, 1987)

Note* Geological contacts between boreholes are inferred.

Figure 34a. Subsurface profiles from A-A'.

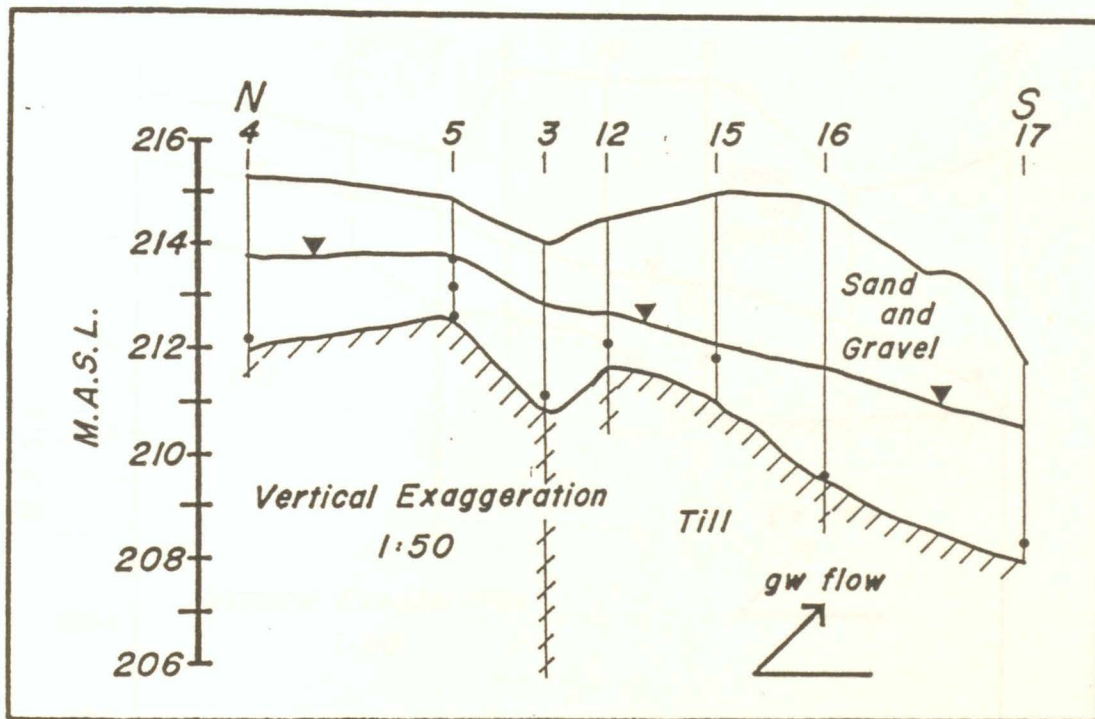


LEGEND

- -Location of Piezometer Screen
- | -Borehole Designation
- ▼ -Inferred Water Table (October 31, 1987)

Note* Geological contacts between boreholes are inferred.

Figure 34b. Subsurface profiles from B-B'.

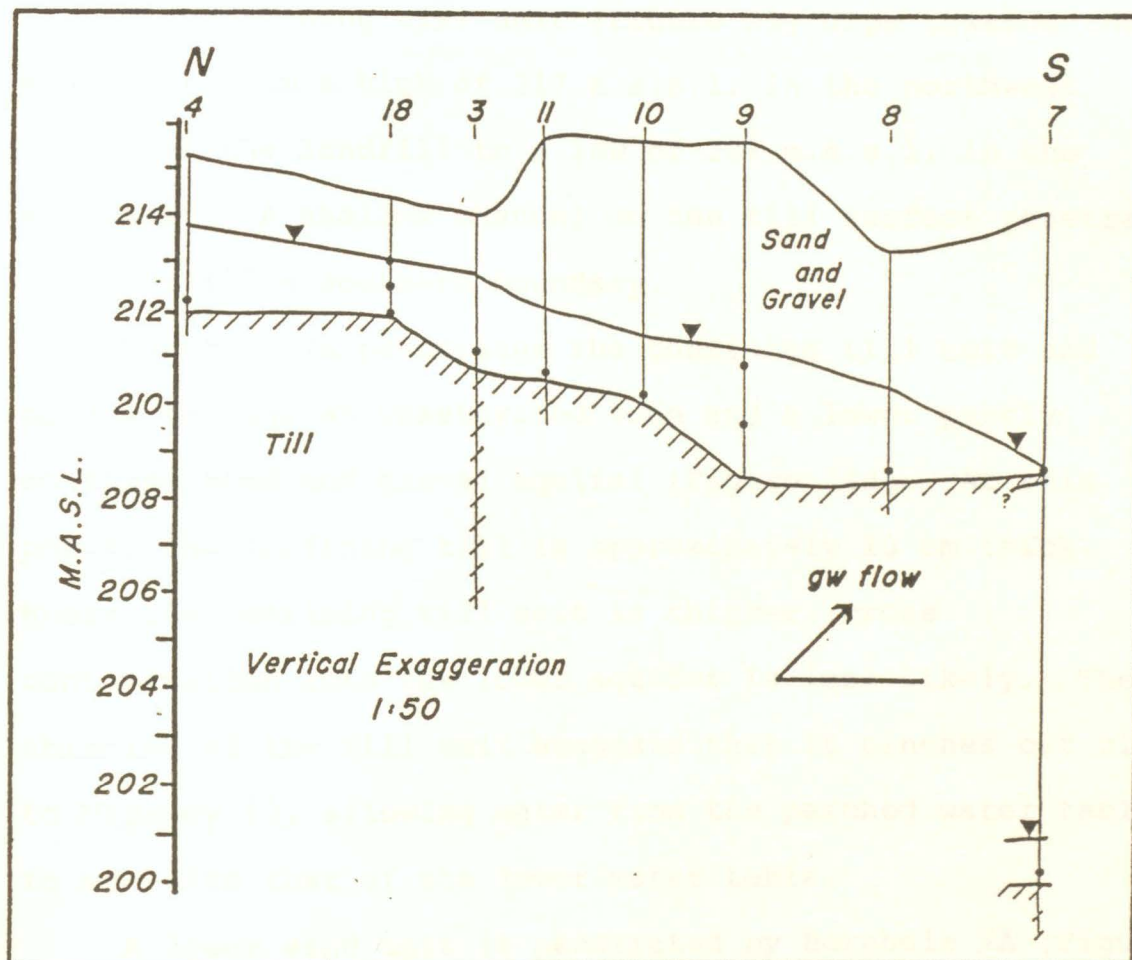


LEGEND

- -Location of Piezometer Screen
- | -Borehole Designation
- ▼ -Inferred Water Table (October 31, 1987)

Note* Geological contacts between boreholes are inferred.

Figure 34c. Subsurface profiles from C-C'.



LEGEND

- -Location of Piezometer Screen
- | -Borehole Designation
- ▼ -Inferred Water Table
(October 31, 1987)

Note* Geological contacts between boreholes are inferred.

Figure 34d. Subsurface profiles from D-D'.

The confining till unit (Figure 35) dips towards the southeast from a high of 217 m.a.s.l. in the northwest corner of the landfill to a low of 209 m.a.s.l. in the southeast. A shallow channel on the till surface penetrates the landfill's southern boundary.

Borehole 7A penetrates the confining till unit and passes through an unsaturated zone and a lower partly confined sand and gravel aquifer (Figure 34d). At this point, the confining till is approximately 10 cm thick. Where the confining till unit is thicker, cross contamination into the lower aquifer is less likely. The thinning of the till unit suggests that it pinches out close to Highway #3, allowing water from the perched water table to mix with that of the lower water table.

A lower sand unit is penetrated by Borehole 7A (Figure 34d). At this location the sand unit forms an unconfined aquifer approximately 10 m in thickness. Boreholes north of Borehole 7A penetrate the upper till unit by up to 4.5 m (Borehole 3) without intercepting this lower sand unit. This suggests that, if the lower sand unit passes below the landfill property, it is separated from the upper sand unit by at least 4.5 m of till.

5.4. Hydrogeological Analysis

5.4.1. Soil Identification

The till samples from the study area have a mean porosity of 28.5%, a mean bulk density of 2.14 g/cm^3 , a mean

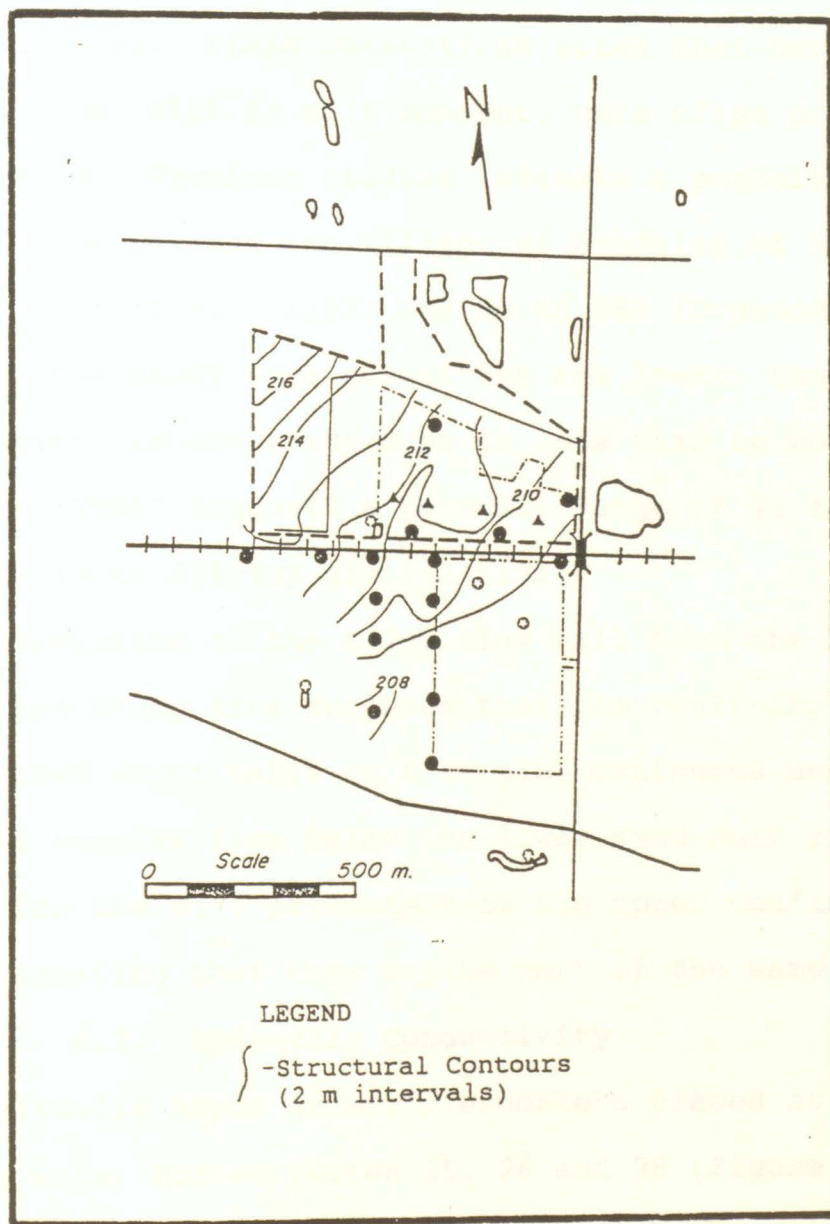


Figure 35. Topography of the till surface.

water content of 13.83%, and a mean degree of saturation of 0.92 (Table 6). Field observations noted that occasional till samples, high in silt content, were often unsaturated and friable. Previous studies indicate a porosity range for clayey deposits near the Village of Woodslee of 31 to 37% (Desaulniers *et al.*, 1981) and 33 to 38% (Orpwood, 1984). Although the study area porosities are lower, the silt and clay content in the study area is less than in Woodslee. Driscoll (1986) suggests a porosity range of 45 to 55% for clay and 10 to 25% for glacial till.

Correlation of the silty clay till from the boreholes within the study area suggests that the confining layer for the perched water table is a single continuous unit. Silt and till samples from below the lower sand unit show similar values for the soil parameters as the upper confining till unit suggesting that they may be part of the same till unit.

4.2. Hydraulic Conductivity

Hydraulic heads in minipiezometers placed at three surface water bodies (sites 25, 26 and 28 (Figure 16)) indicate discharge of groundwater through the northern banks and recharge through the southern banks. Vertical hydraulic gradients vary between 6.25×10^{-3} and 1.43×10^{-2} . Considering the field permeability and porosity values from Gartner Lee Associates Limited (1986), groundwater discharge velocities into the ponds range between 3.6×10^{-4} and 8.2×10^{-4} cm/s.

SAMPLE NUMBER	BULK DENSITY (g/cm ³)	WATER CONTENT (%)	POROSITY (%)	SATURATION
1-4	2.14	13.75	28.71	0.91
2-6	2.29	9.78	20.61	1.00
3-3a	2.16	14.08	28.06	0.96
3-3b	2.08	15.22	31.28	0.89
3-4	2.09	14.32	30.59	0.85
3-5	2.19	12.62	26.18	0.95
3-6	2.38	7.45	16.15	1.00
4-4	2.17	13.96	27.53	0.98
6-10b	2.17	12.70	26.98	0.91
7-2c	2.20	9.00	22.84	0.81
7-19a	2.29	8.60	19.79	0.92
7-19c	2.09	14.42	30.74	0.86
7-20b	2.33	8.25	18.48	0.97
7-20c	2.27	9.43	21.22	0.93
7-21	2.02	14.35	33.01	0.77
8-6	2.08	17.15	32.07	0.96
9-7b	2.21	14.99	27.21	1.00
10-5b	2.16	13.33	27.50	0.93
11-9b	2.15	13.58	28.06	0.92
11-10	2.12	13.95	29.26	0.90
12-3a	2.10	16.22	31.27	0.94
12-3c	2.06	14.71	31.59	0.86
12-4b	2.12	14.83	30.08	0.92
13-5b	2.09	14.80	30.96	0.88
14-3a	2.10	14.73	30.38	0.89
14-3c	2.13	15.47	30.16	0.96
14-4	2.06	17.47	33.59	0.92
15-4b	2.21	12.38	25.71	0.95
16-7	2.14	12.26	27.72	0.85
17-5b	2.08	15.31	31.49	0.89

Table 6. Values for parameters used in till identification.

Data from the slug and bail tests show the effects of gas bubbles and storage in the borehole annulus. These effects can be overcome by raising a line tangent to the steady state condition until it passes through the origin (Hvorslev, 1951) (Figure 36). Hydraulic time lag values for the slug and bail responses are similar in each piezometer (Table 7). Resulting hydraulic conductivities also mirror these similarities ranging between 6.54×10^{-4} to 1.17×10^{-2} cm/s. Since the Marafi geotextile filter wrap has a hydraulic conductivity of 10^{-2} cm/s, it has no effect on the response times of the slug and bail tests (Paul et al., 1988).

Percent passing values, obtained from 147 grain size analyses and 39 hydrometer analyses, were plotted against grain size (Appendix II). Hydraulic conductivities of the cored soil samples based on Hazen's formula range in magnitude from 10^{-3} to 10^{-2} cm/s (Table 8). Hydraulic conductivities ranging between 10^{-4} and 10^{-6} cm/s were found to be typical for the silts and tills, however silts and tills are not suitable for the Hazen's formula (Freeze and Cherry, 1979).

Comparison of the hydraulic conductivities from the slug and bail tests and from the grain size distributions indicate that laboratory determined values are almost an order of magnitude greater than field values (Table 9). Hydraulic conductivity differences are small considering the

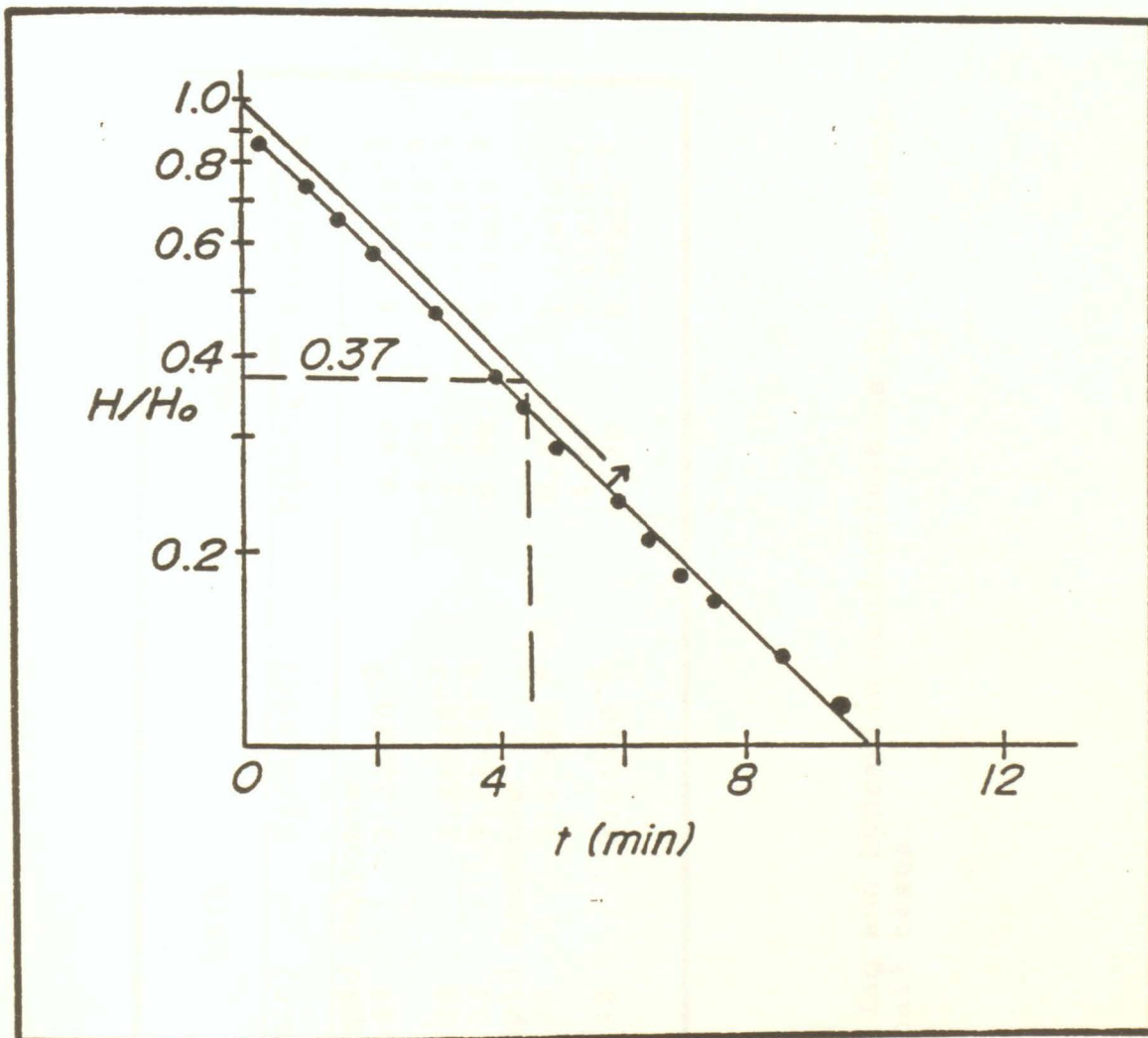


Figure 36. Example plot of the slug and bail test.

WELL #	BAIL		SLUG	
	T(min)	K(cm/sec)	T(min)	K(cm/sec)
1	Rapid Response			
2	0.44	7.20×10^{-3}	0.47	6.75×10^{-3}
3			4.85	6.54×10^{-4}
4	1.20	2.64×10^{-3}	1.20	2.64×10^{-3}
8	0.33	9.61×10^{-3}	0.38	8.34×10^{-3}
12	Rapid Response			
13	0.27	1.17×10^{-2}	0.27	1.17×10^{-2}
16			4.42	7.17×10^{-4}
17	1.20	2.64×10^{-3}	1.20	2.64×10^{-3}

Table 7. Time lag and hydraulic conductivities for the slug and bail tests.

SAMPLE	d10 (mm)	K (cm/sec) (10 ⁻⁴)	SAMPLE	d10 (mm)	K (cm/sec) (10 ⁻⁴)
1-1	0.160	2.560	9-1	0.168	2.822
1-2	0.170	2.890	9-2	0.380	14.440
1-3	0.185	3.423	9-3	0.215	4.623
1-4	0.005	0.002	9-4	0.152	2.310
2-1	0.120	1.440	9-5	0.170	2.890
2-2	0.095	0.903	9-6	0.175	3.063
2-3	0.170	2.890	9-7a	0.175	3.063
2-4	0.120	1.440	9-7b	0.013	0.016
2-5	0.180	3.240	10-1	0.150	2.250
2-6	0.005	0.003	10-2	0.150	2.250
3-1	0.150	2.250	10-3	0.140	1.960
3-2	0.185	3.423	10-4a	0.200	4.000
3-3b	0.006	0.003	10-4b	0.080	0.640
3-4	0.003	0.001	10-4c	0.115	1.323
3-5	0.003	0.001	10-5a	0.195	3.803
3-6	0.013	0.016	10-5b	0.005	0.003
4-1	0.170	2.890	11-1	0.130	1.690
4-2	0.150	2.250	11-2a	0.095	0.903
4-3	0.170	2.890	11-2b	0.008	0.006
4-4	0.009	0.008	11-3	0.142	2.016
6-1	0.160	2.560	11-4	0.152	2.310
6-2	0.205	4.203	11-5	0.179	3.204
6-3	0.280	7.840	11-6	0.170	2.890
6-4	0.125	1.563	11-7	0.180	3.240
6-5b	0.125	1.563	11-8	0.190	3.610
6-5c	0.008	0.006	11-9a	0.190	3.610
6-6a	0.140	1.960	11-9b	0.075	0.563
6-6b	0.175	3.063	12-1	0.145	2.103
6-7	0.008	0.006	12-2	0.190	3.610
6-8	0.160	2.560	12-3a	0.002	0.000
6-9	0.170	2.890	12-3b	0.145	2.103
6-10a	0.142	2.016	12-3c	0.005	0.002
6-10b	0.004	0.002	12-4a	0.120	1.440
A-1	0.200	4.000	12-4b	0.006	0.003
A-2	0.240	5.760	13-1a	0.090	0.810
A-3	0.185	3.423	13-1b	0.180	3.240
A-4	0.130	1.690	13-2	0.155	2.403
7-2a	0.130	1.690	13-3	0.170	2.890
7-2b	0.130	1.690	13-4	0.135	1.823
7-2c	0.008	0.006	13-5a	0.165	2.723
7-2d	0.130	1.690	13-5b	0.003	0.001
7-3	0.210	4.410	14-1	0.185	3.423
7-4	0.170	2.890	14-2a	0.004	0.001
7-5a	0.200	4.000	14-2b	0.002	0.000
7-5b	0.180	3.240	14-3a	0.003	0.001
7-6	0.150	2.250	14-3b	0.010	0.010
7-7	0.160	2.560	14-3c	0.014	0.019
7-8	0.175	3.063	14-4	0.011	0.012
7-9	0.130	1.690	15-1	0.155	2.403
7-10	0.130	1.690	15-2	0.270	7.290
7-11	0.160	2.560	15-3a	0.155	2.403
7-12	0.175	3.063	15-3b	0.155	2.403
7-13	0.135	1.823	15-4a	0.185	3.423
7-14	0.095	0.903	15-4b	0.005	0.003
7-15	0.095	0.903	16-1	0.205	4.203
7-16	0.095	0.903	16-2	0.100	1.000
7-18c	0.003	0.001	16-3a	0.182	3.312
7-19b	0.005	0.003	16-3b	0.162	2.624
7-19c	0.005	0.002	16-4	0.093	0.865
7-20a	0.010	0.010	16-5	0.142	2.016
7-20b	0.004	0.002	16-6	0.085	0.723
7-20c	0.005	0.002	16-7	0.013	0.017
7-21	0.001	0.000	17-1	0.150	2.250
8-1	0.130	1.690	17-2	0.162	2.624
8-2	0.155	2.403	17-3	0.110	1.210
8-3	0.175	3.063	17-4a	0.175	3.063
8-4	0.155	2.403	17-4b	0.098	0.960
8-5a	0.155	2.403	17-4c	0.140	1.960
8-5b	0.180	3.240	17-5a	0.098	0.960
8-6	0.008	0.006	17-5b	0.005	0.002

Table 8. Effective diameter and hydraulic conductivities using Hazen's formula.

WELL #	SLUG & BAIL	HAZEN
	K (cm/sec)	K (cm/sec)
2	6.98×10^{-3}	3.24×10^{-2}
3	6.54×10^{-4}	3.42×10^{-2}
4	2.64×10^{-3}	2.89×10^{-2}
8	8.98×10^{-3}	2.89×10^{-2}
13	1.17×10^{-2}	1.82×10^{-2}
16	7.17×10^{-4}	7.23×10^{-3}
17	2.64×10^{-3}	1.96×10^{-2}

Table 9. Hydraulic conductivities from Hazen's formula and the slug and bail tests.

difference in scale of the permeability tests. The Hvorslev method is an in situ test taking into account structures within the ground material around the piezometer. The values can also be affected by water movement through the annulus material and the presence of high partial pressures of gas in the contaminant plume.

Comparing the various hydraulic conductivities obtained for the site, values by Gartner Lee (10^{-2} cm/s) and by the Hazen formula (10^{-2} to 10^{-3} cm/s) are the highest hydraulic conductivity values. Hydraulic conductivity values obtained in the field at the surface water bodies (10^{-3} to 10^{-4} cm/s) and by the Hvorslev tests (10^{-3} - 10^{-4} cm/s) are slightly less. The variation in values may be a result of testing units of different composition or of different scales. Even a small percentage difference in clay or silt content in a sandy aquifer can have a large affect on hydraulic conductivity (Freeze and Cherry, 1979).

5.4.3. Water Table Levels

Water table levels were obtained for October 31, 1987 and March 19, 1988 (Table 10). Water table levels are highest for March suggesting that the groundwater sampled in early November, 1987 was obtained during low water table levels. Water table contours for both sets of data suggest that the flow pattern is related to the topography (Figure 37a,b). The water table contours are consistent with the results from the electrical resistivity mapping. Both sets

WELL	ELEVATION (m.a.s.l)	ELEVATION top of PVC (m.a.s.l)	WELL DEPTH (m.a.s.l)	W.T. LEVEL Oct. 31, 1987 (m.a.s.l)	W.T. LEVEL March 19, 1988 (m.a.s.l)
1	213.37	214.21	209.17	211.40	211.49
2	214.59	215.34	209.72	211.65	211.73
3	214.02	214.67	210.92	212.78	213.08
4	215.28	215.63	211.93	213.75	214.03
5A	214.88	215.78	212.53	213.73	214.16
5B	214.88	215.78	213.13	n.a.	n.a.
5C	214.88	215.78	213.73	n.a.	n.a.
6	218.55	219.50	209.40	211.02	211.13
7A	214.14	215.07	199.04	200.84	200.86
7B	214.18	214.93	209.36	209.39	209.42
8	213.29	213.97	208.45	210.46	210.52
9A	215.79	216.57	209.40	211.27	211.29
9B	215.73	216.47	210.64	211.31	211.30
10	215.61	217.01	209.99	211.55	212.23
11	215.78	216.49	210.42	212.11	212.19
12	214.57	216.69	211.92	212.73	214.55
13	215.00	215.71	212.25	213.62	215.07
14	214.67	215.47	210.65	212.69	213.68
15	215.00	215.88	211.63	212.14	212.28
16	214.82	215.73	209.24	211.70	211.80
17	211.73	212.58	208.18	210.53	210.57
18A	214.37	215.02	211.79	n.a.	213.59
18B	214.37	215.02	212.39	n.a.	n.a.
18C	214.37	215.02	212.99	n.a.	n.a.
19A	214.36	215.01	211.10	n.a.	212.81
19B	214.36	215.01	211.70	n.a.	n.a.
19C	214.36	215.01	212.30	n.a.	n.a.
20	213.93	n.a.	n.a.	n.a.	n.a.
G.L.1	214.00	214.95	209.12	n.a.	212.01
G.L.2	213.93	214.80	211.01	n.a.	212.27
G.L.4	214.57	214.93	211.37	n.a.	213.68
G.L.5	215.34	215.95	212.29	n.a.	214.65
G.L.6	214.68	214.68	211.02	n.a.	213.33

Table 10. Water table levels for October 31, 1987 and March 19, 1988.

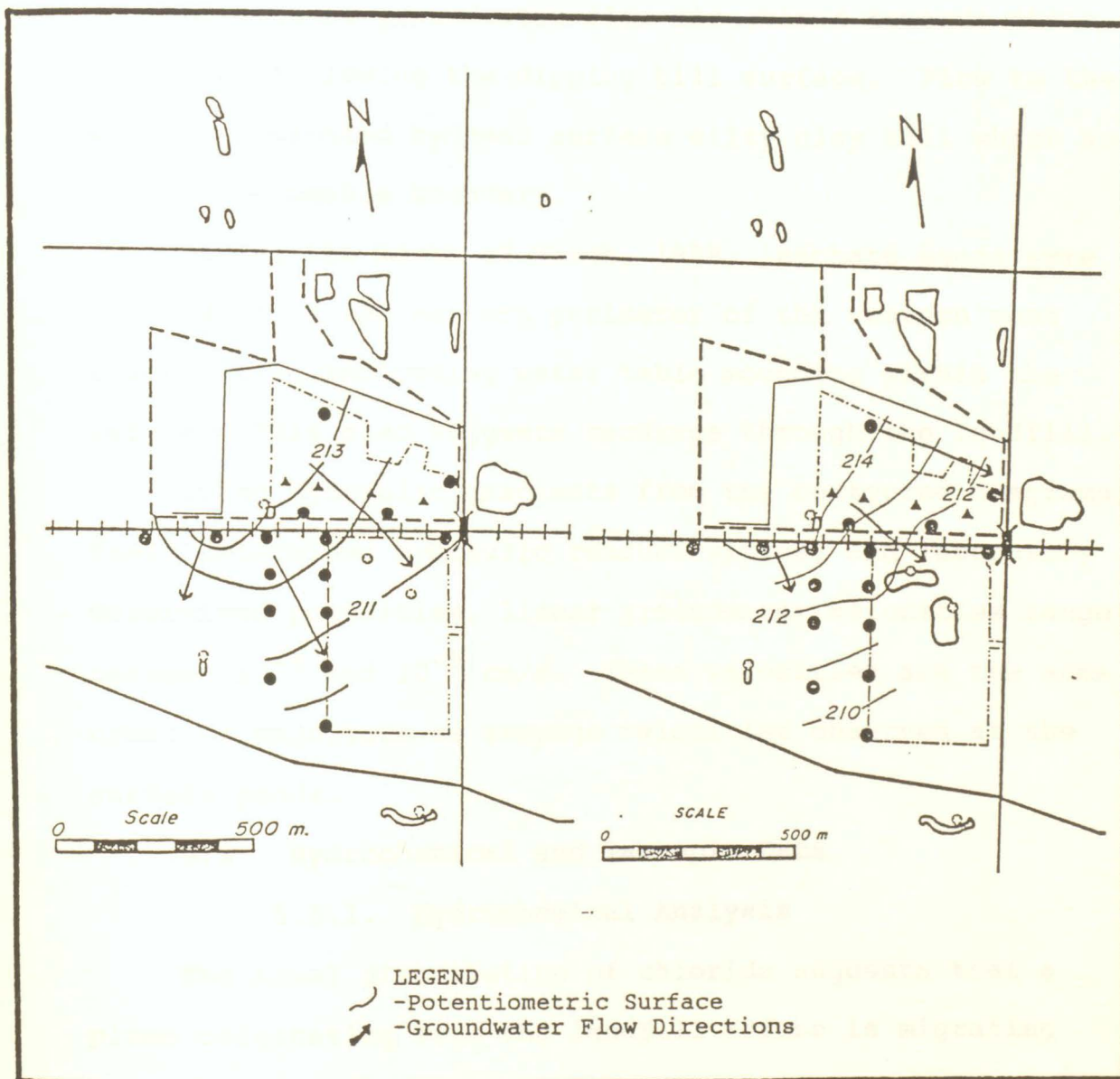


Figure 37. Water table and groundwater flow directions for (a) October 31, 1987 and for (b) March 19, 1988.

of data suggest groundwater flow directions towards the southeast following the dipping till surface. Flow to the west is prevented by near surface silty clay till which acts as an impermeable boundary.

During the month of March, 1988, leachate seeps were noticed along the eastern perimeter of the western most refuse cell, indicating water table mounding within the refuse. This also suggests recharge through the landfill.

Using hydraulic gradients from the contoured diagrams, field determined hydraulic conductivities, and laboratory determined porosities, linear groundwater velocities range between 10^{-4} and 10^{-5} cm/s. These velocities are the same order of magnitude as seepage velocities observed at the surface ponds.

5.5. Hydrochemical and Isotopic Data

5.5.1. Hydrochemical Analysis

The areal distribution of chloride suggests that a plume originating from the landfill refuse is migrating towards the southeast (Figure 38). Similar distributions exist with the other major ions. These trends are presented using stiff diagrams (Stiff, 1951) in Figure 39.

The more contaminated samples (highest concentrations of most major ions) are from monitoring sites located downgradient and closest to the landfill refuse (Table 11). They tend to show elevated concentrations of chloride, bicarbonate, sodium, potassium, and magnesium and high

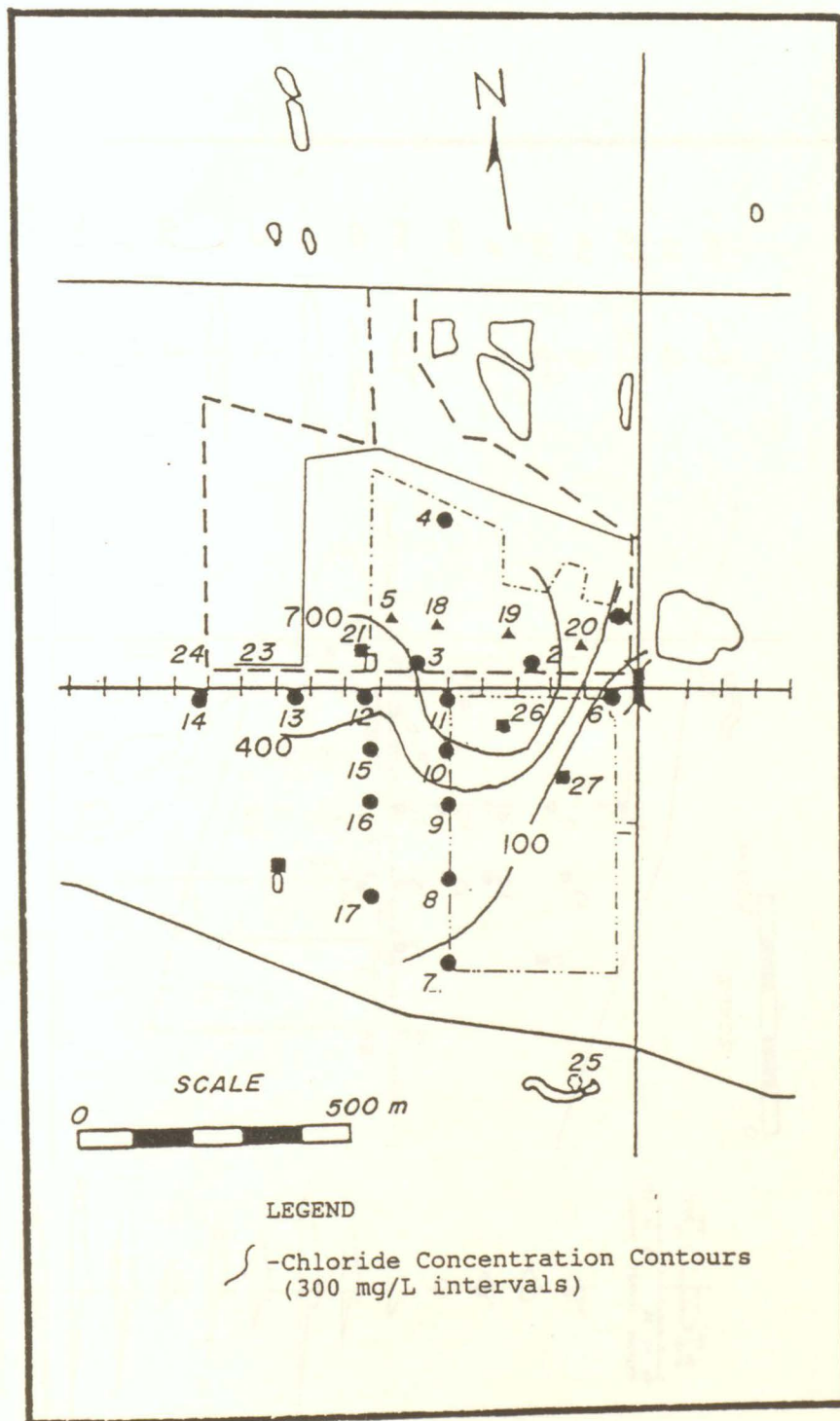


Figure 38. Areal distribution of chloride.

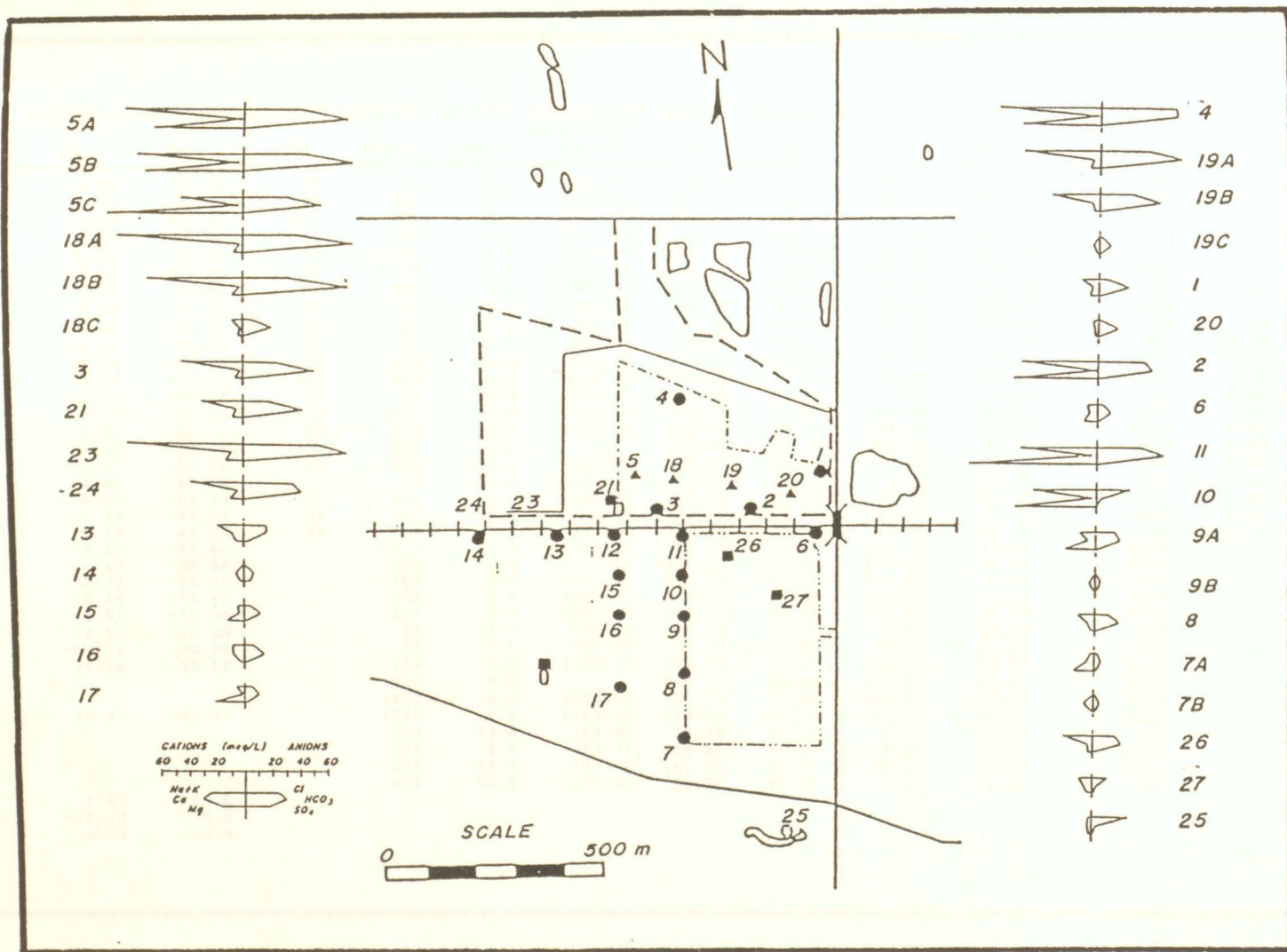


Figure 39. Areal distribution of the major ions.

SAMPLE	OXYGEN-18 (‰)	DEUTERIUM (‰)	TRITIUM (TU)	CHLORIDE (mg/L)	SULFATE (mg/L)	BICARBONATE ALKALINITY (mg/L)	SODIUM (mg/L)	CALCIUM (mg/L)	POTASSIUM (mg/L)	MAGNESIUM (mg/L)	ELECTRICAL CONDUCTANCE (uS/cm)	pH	HARDNESS as CaCO3 (meq/L)	Ca/Mg ratio (meq/L)
1	-9.34	-62.20	59	158	0.0	1108.60	150.49	63.28	168.27	63.37	2915	6.64	430.3	0.65
2	-8.69	-53.50	89	967	0.0	1972.18	957.15	68.04	203.73	618.70	5555	6.79	2585.2	0.02
3	-9.32	-54.80	677	692	0.0	2651.00	657.13	16.50	325.97	59.49	5567	6.95	306.4	0.25
4	-8.71	-58.80	43	1600	0.0	2761.86	1144.42	24.75	407.46	576.03	824	7.12	2400.0	0.01
5A	-8.70	-50.80	77	1250	0.0	3880.10	1352.49	12.62	458.39	650.70	8712	7.18	2723.5	0.02
5B	-9.11	-47.15	115	1310	0.0	4133.15	1102.80	19.22	590.82	704.04	9160	7.10	3010.3	0.04
5C	-9.49	-54.90	91	958	0.0	2884.77	624.23	46.27	387.09	960.05	626	6.84	4063.0	0.03
6	-8.96	-64.30	35	94	23.7	482.00	120.39	46.27	35.62	100.87	1288		640.6	0.54
7A	-8.49	-59.20	39	50	38.6	204.85	50.16	90.50	12.28	155.18	824	6.50	875.8	0.37
7B	-8.14	-58.80	41	36	30.1	200.03	10.88	95.26	1.63	11.76	657	6.98	364.1	6.53
8	-9.74	-66.10	115	250	35.0	855.55	218.21	126.56	66.33	27.16	2273	6.90	337.5	2.02
9A	-9.24	-61.40	132	384	33.6	855.55	178.08	90.50	98.26	219.84	2025	7.16	1141.6	0.26
9B	-8.08	-56.20	27	40	26.3	171.71	10.58	95.26	9.03	10.97	763	6.55	214.9	3.76
10	-8.93	-55.50	378	691	0.0	144.60	769.88	68.04	183.36	597.37	4763	7.12	2571.7	0.05
11	-8.71	-56.00	85	912	0.0	2422.05	915.53	46.27	244.48	938.72	5934	7.25	3987.2	0.03
12	-9.40	-58.00	72	526	0.0		338.60	51.03	295.41	56.90	4247	6.98	459.8	0.97
13	-8.17	-58.90	88	491	130.0	807.35	316.03	90.50	117.91	53.02	2766	6.98	557.5	1.56
14	-9.62	-69.00	7	15	165.0	367.53	13.00	136.08	4.44	25.08	934	6.62	340.8	2.30
15	-9.24	-66.50	27	141	33.0	596.48	65.21	95.26	52.81	129.32	1339	6.68	689.6	0.30
16	-9.63	-64.20	50	162	58.0	709.34	122.90	63.28	87.21	29.74	1812	6.88	461.8	2.78
17	-9.18	-66.30	37	156	65.0	512.13	112.87	136.08	8.44	232.78	1422	6.77	1015.1	0.06
18A	-8.50	-51.00		1170	1.4	4039.16	1452.95	23.24	412.65	76.59	8964		383.3	0.22
18B	-8.47	-50.90		998	0.0	4015.06	1013.24	27.39	492.01	88.03	8861		447.9	0.24
18C	-8.79	-60.00		166	0.0	1053.17	149.75	34.44	18.21	40.01	2479		251.5	0.53
19A	-8.94	-56.95		988	1.4	3053.47	860.30	34.86	341.23	76.59	7667		486.8	0.55
19B	-9.31	-59.00		689	0.0	2224.43	516.18	68.88	269.81	34.30	5911		330.1	1.34
19C	-9.60	-66.40		33	17.2	402.47	10.83	75.76	8.18	10.88	606		216.6	3.84
20	-10.19	-70.80		44	33.6	723.00	33.32	68.88	64.07	17.49	1393		161.0	1.24
21	-9.20	-58.00		517	0.0	2229.25	428.53	35.69	256.13	76.59	3501		486.8	0.55
22				437	0.0		308.72	68.88	216.73	66.30	2617		365.8	0.34
23				1630	0.0	3976.50	994.12	37.35	965.41	133.75	9389		893.6	0.62
24	-7.67	-49.90		1060	0.0	2193.10	573.53	137.75	295.53	96.03	6301		532.3	0.35
25				753	43.8	159.66	38.32	55.10	6.44	16.94	712		189.9	1.73
26				456	2.0	997.74	324.85	48.21	138.90	30.87	3053		247.2	0.95
27				330	25.8	149.42	165.88	48.21	26.12	15.57	1665		287.4	3.49
28				116	40.4	154.84	26.65	89.54	1.72	12.81	787		52.7	0.00
29	-8.84	-63.6												
30	-10.19	-70.5												
31	-8.72	-54.4												

Table 11. Chemical and isotopic concentrations of groundwater within the study area.

electrical conductivity and partial pressures of carbon dioxide. Concentrations of calcium and sulphate are lowest near the refuse, however, these increase downgradient. The pH of the groundwater within the study area varies between 6.5 and 7.5.

5.5.1.1. Carbon Dioxide

Partial pressures of carbon dioxide in the groundwater are almost three orders of magnitude above atmospheric (Table 12). The highest $p\text{CO}_2(\text{aq})$ is found to exist within the contaminant plume where biological activity is likely to be the greatest. The pressure decreases away from the landfill refuse, paralleling the increasing sulphate concentrations. Sample 14, obtained from a thin sand and gravel stringer has elevated $p\text{CO}_2$ relative to $p\text{CO}_2(\text{atm})$, suggesting that there is production of CO_2 during infiltration and migration. Samples obtained from areas in the contaminant plume where the topsoil has been removed generally do not show the lower $p\text{CO}_2$ expected from no contact with the soil root zone. This may be the result of high biological activity in the contaminant plume in those areas.

5.5.1.2. Chloride

Chloride concentrations range between 15 and 1630 mg/L with the highest concentrations near the landfill refuse. Samples 23 and 24 were obtained from the landfill site. Sample 24 was from the leachate collection system and 23 was

SAMPLE	S _{ical} .	S _{idol} .	LOG pCO ₂ (aq) (bars)
1	-0.03	0.25	-0.78
2	0.16	1.58	-0.62
3	-0.10	0.74	-0.70
4	0.18	1.85	-0.79
5A	0.07	2.09	-0.71
5B	0.27	2.53	-0.66
5C	0.16	1.75	-0.55
6	0.18	0.78	-1.91
8	0.45	0.44	-1.33
9A	0.52	1.65	-1.59
9B	-0.61	-2.00	-1.78
10	-0.50	0.16	-2.37
11	0.63	2.81	-1.23
13	0.35	0.64	-1.54
14	-0.11	-0.79	-1.52
15	0.05	0.42	-1.40
16	0.08	0.03	-1.43
17	0.02	0.45	-1.44

Table 12. Subsurface indices of calcite (SI_{cal}) and dolomite (SI_{dol}), and partial pressures of carbon dioxide.

from a drainage ditch on the southern perimeter of the landfill. Sample 23 has possibly undergone evaporation concentrating the chloride content, while Sample 24 may have been diluted by precipitation within the collection system. Samples 5A, 5B, 18A, and 18B may be good indicators of leachate because of their peak chloride concentrations and proximity to the refuse cells. High chloride concentrations for Sample 4 may be explained by the proximity of Piezometer 4 to earlier refuse cells located at the northeastern boundary of the landfill.

Calculated and measured groundwater velocities of 10^{-4} to 10^{-5} cm/s indicate a rate of migration great enough that diffusion effects of the contaminants should be negligible. Therefore, chloride should not migrate at a greater rate than the bulk water movement as suggested by Stewart (1980).

5.5.1.3. Alkalinity

The alkalinity present in the groundwater of the study area is a bicarbonate alkalinity. However, some variation in end point values during the alkalinity analysis for samples collected closest to the landfill refuse may be a result of the presence of organic acids (Baedecker and Back, 1979). Concentrations of 149 to 4133 mg/L (as CaCO_3) exist, with concentrations of the more contaminated samples exceeding 1500 mg/L. The bicarbonate concentrations are the highest of the contaminants (major ions) inferring that they

may be the controlling factor in maintaining groundwater pH near 7.

The elevated bicarbonate concentrations are associated with high levels of $p\text{CO}_2$ and undetectable levels of sulphate, suggesting that organic decomposition plays a significant role in bicarbonate production. However, the elevated bicarbonate concentrations cannot be explained solely by sulphate reduction, implying that carbonate dissociation helps maintain the elevated alkaline buffering capacity. The presence of calcite and dolomite supersaturated conditions are consistent with these trends.

Concentrations of bicarbonate decrease downgradient and in surface water bodies (sites 25,26,27,28 (Figure 16)). This can be explained by degassing of CO_2 , calcite precipitation, or methane production. The buildup of high methane pressures in the landfill have blown manhole covers and have resulted in methane migration into the basements of houses along County Road 31 (Jagger, personal communication).

The presence of reduced bicarbonate concentrations near the landfill refuse in the upper ports of the bundle piezometers (18C, 19C) suggests the existence of a zone of recently recharged water above the contaminated groundwater.

An excellent linear relationship exists between alkalinity and chloride concentrations (Figure 40). A progressive decrease in concentration away from the landfill

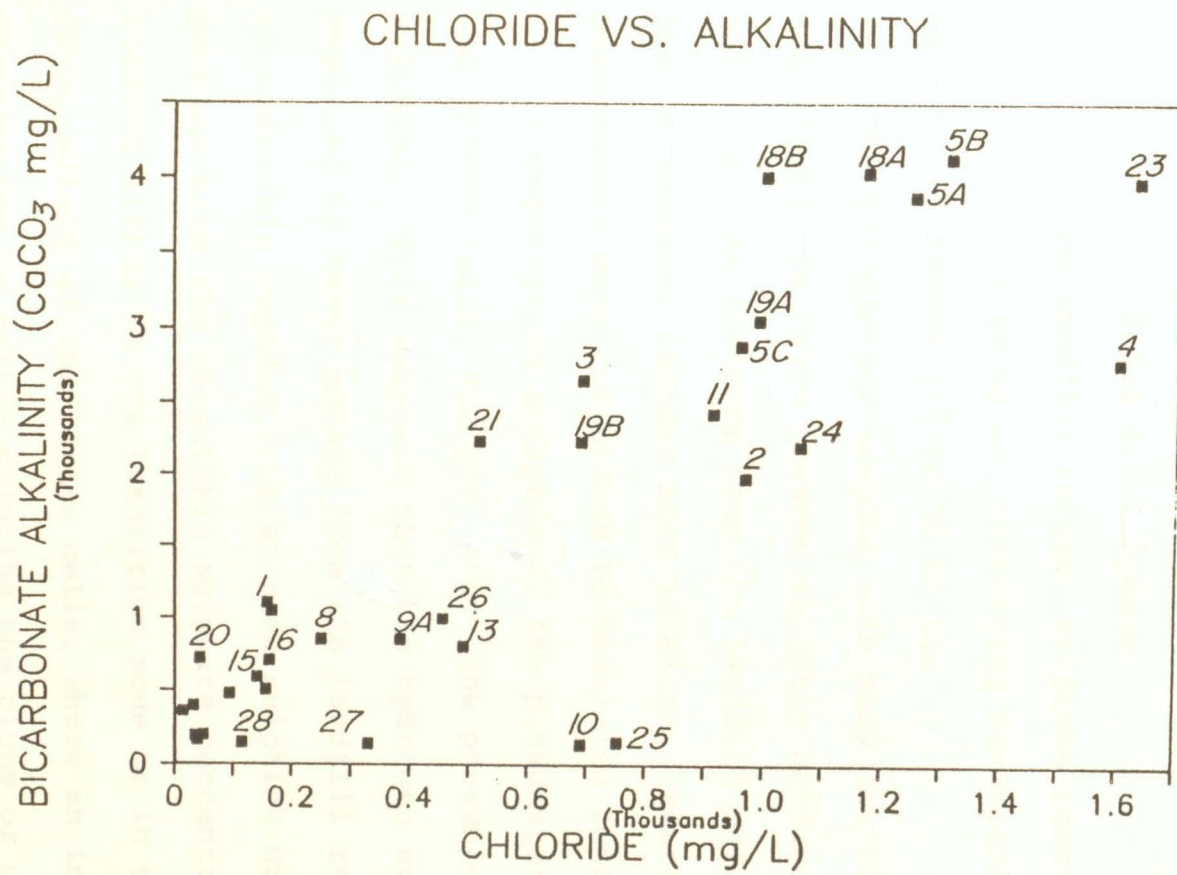


Figure 40. Chloride-alkalinity relationship.

is evident from the more contaminated samples to the least-contaminated samples. This suggests similar processes of attenuation for the chloride and bicarbonate contaminants.

5.5.1.4. Sulphate

Near the landfill refuse, sulphate concentrations are very low (0 to 10 mg/L), increasing downgradient towards background levels (10 to 70 mg/L).

The groundwater samples with very low sulphate concentrations range between slightly acidic and slightly alkaline. As distance from the landfill refuse increases, the groundwater becomes more alkaline, creating an environment more compatible to metal-ion adsorption.

A qualitative analysis of the piezometers closest to the refuse cells, did not detect the presence of hydrogen sulphide. This suggests that the hydrogen sulphide is captured by heavy metals from the landfill refuse, producing an insoluble residue such as zinc sulphide or iron sulphide. Samples with the detectable sulphate concentrations are located either in the transition zone or in the aerobic zone downgradient of the refuse cells, where an influx of local groundwater is either diluting the plume or oxidizing free sulphide ions, or gases, to sulphate.

5.5.1.5. Major Cations

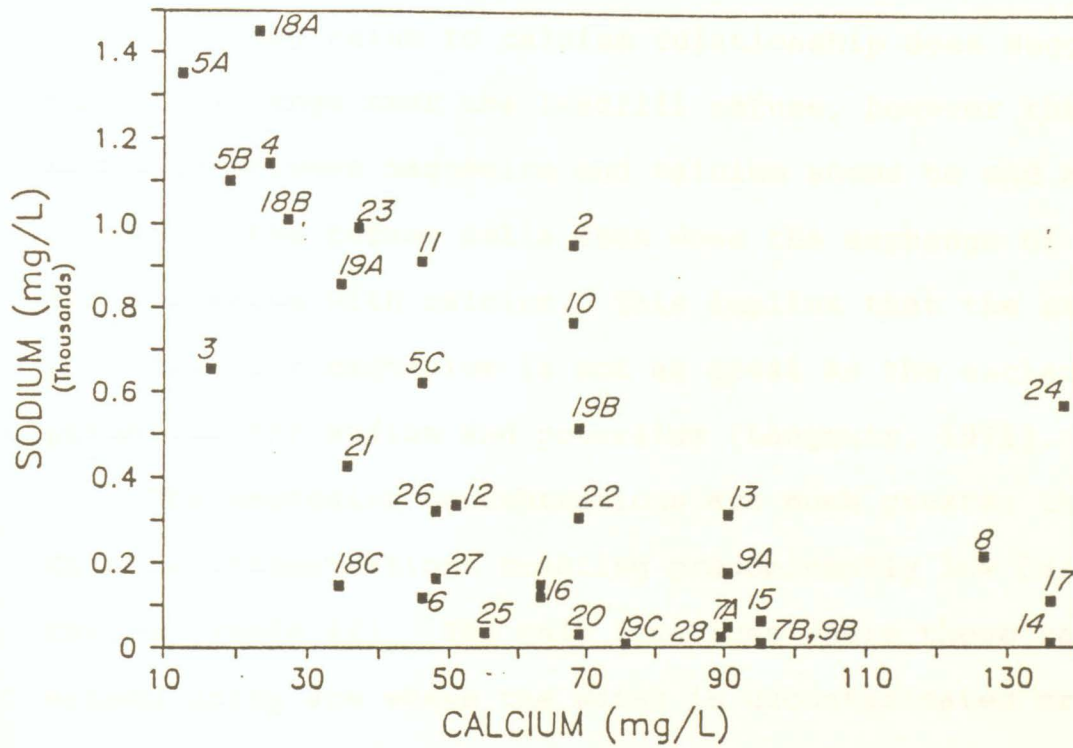
Concentrations of sodium and potassium range between 11 and 1453 mg/L and 2 and 965 mg/L, respectively. Both show decreased concentrations downgradient from the landfill

refuse. Calcium concentrations display the opposite trend, increasing away from the landfill refuse. Concentrations of calcium range between 13 and 138 mg/L. The calcium analyses may be low by 10% as a result of complexing with organics. A comparison of calcium concentrations with the bicarbonate concentrations indicate that there is not a 1:1 molal concentration ratio suggesting that other reactions, other than carbonate dissolution, are responsible for the bicarbonate and calcium concentrations listed in Table 11.

Contrasting concentrations of calcium to potassium and sodium suggest that a high degree of cation exchange is occurring near the landfill refuse as a result of the presence of organics, bacteria and/or high concentrations of exchangeable ions. The increasing calcium concentrations and the decreasing sodium and potassium concentrations away from the landfill refuse suggest that the cation exchange potential decreases downgradient. As the subsurface geological material shows little local variation, the decreased cation exchange potential may be a result of low organic concentrations due to decomposition, of decreased bacterial activity, or it may result from the dilution of the high concentrations of exchangeable ions by uncontaminated groundwater.

Magnesium concentrations range from 10 to 960 mg/L. The magnesium to calcium relationship is not as defined as the sodium and potassium to calcium relationships (Figure

CALCIUM VS. SODIUM



CALCIUM VS. POTASSIUM

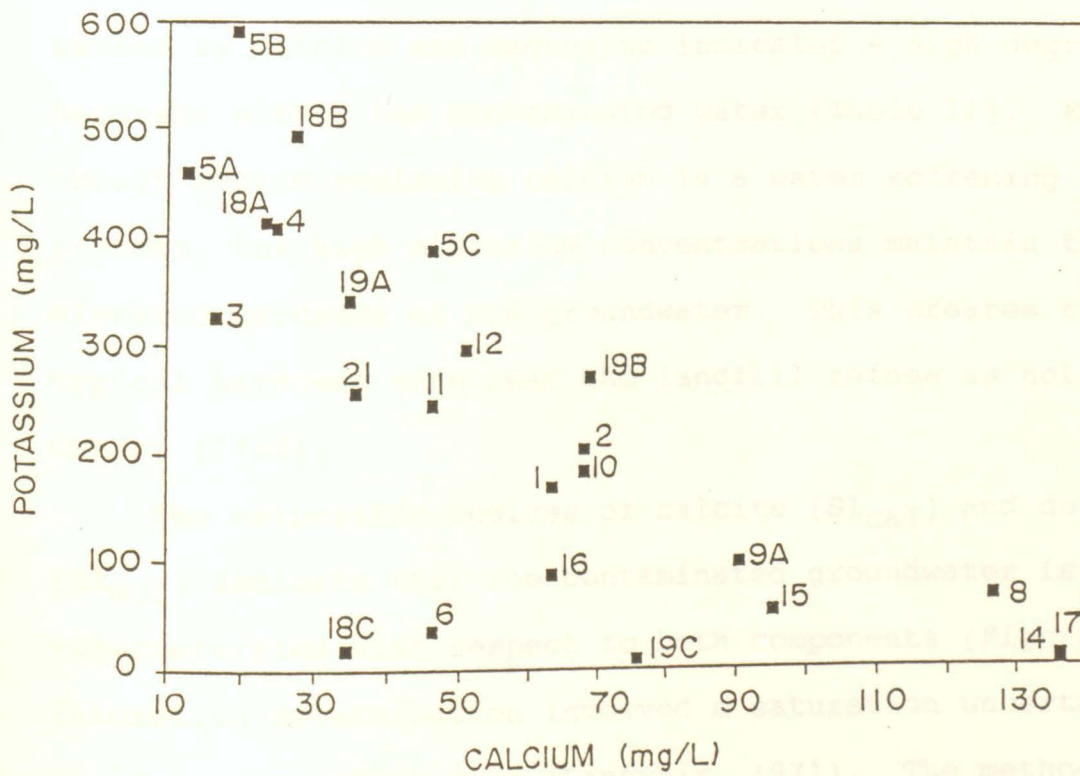


Figure 41. Calcium relationship with (a) sodium and (b) potassium.

42). The magnesium to calcium relationship does suggest cation exchange near the landfill refuse, however the exchange between magnesium and calcium seems to end much closer to the refuse cells than does the exchange of sodium and potassium with calcium. This implies that the exchange potential for magnesium is not as great as the exchange potential for sodium and potassium (Langmuir, 1971).

The magnesium concentrations are much greater than the calcium concentrations creating predominantly low Ca/Mg ratios (Table 11). The only locations where these ratios exceed unity are where the water is uncontaminated or where there is a high degree of mixing of contaminated and less contaminated water. Examination of hardness (as CaCO_3) caused by calcium and magnesium indicates a high degree of hardness within the contaminated water (Table 11). Even though sodium replacing calcium is a water softening process, the high magnesium concentrations maintain the elevated hardness of the groundwater. This creates the typical hardness zone near the landfill refuse as noted by Cherry (1983).

The saturation indices of calcite (SI_{cal}) and dolomite (SI_{dol}) indicate that the contaminated groundwater is supersaturated with respect to both components (Figure 43). Saturation determination involved a saturation uncertainty of ± 0.1 units about zero (Langmuir, 1971). The method of calculation was by Garrels and Christ (1965) using field pH

CALCIUM VS. MAGNESIUM

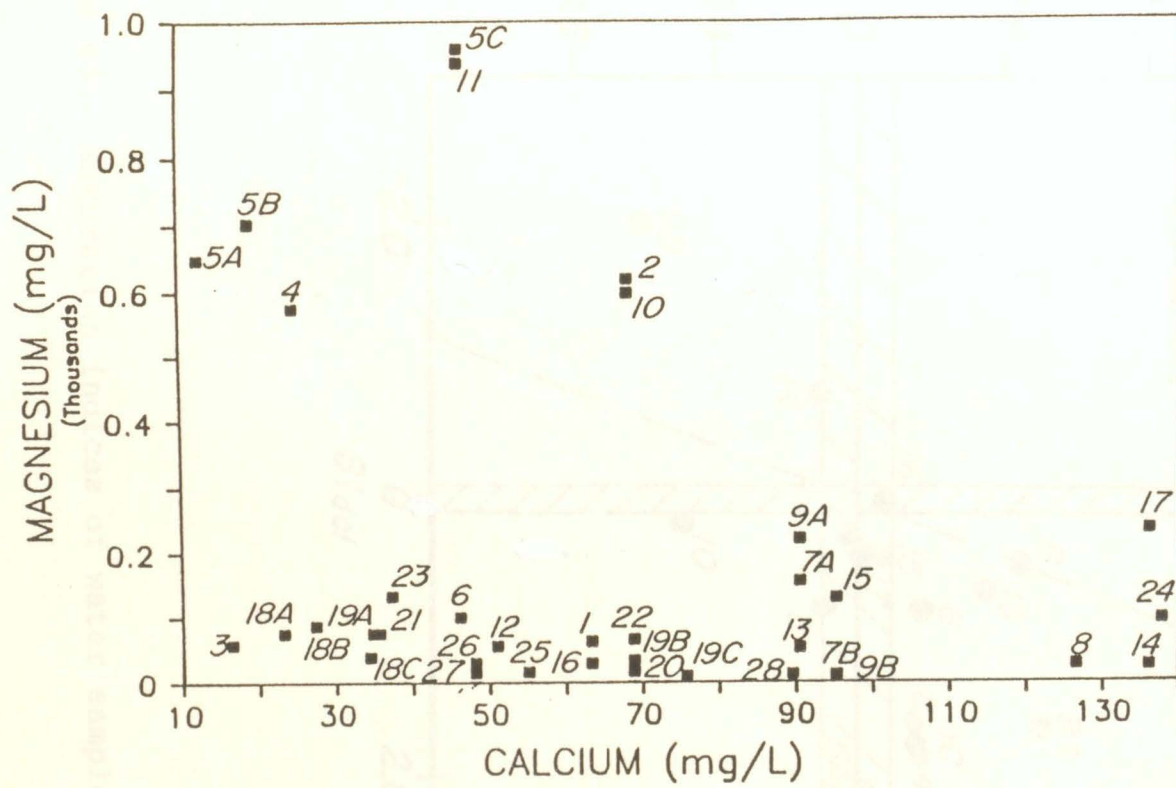


Figure 42. Calcium-magnesium relationship.

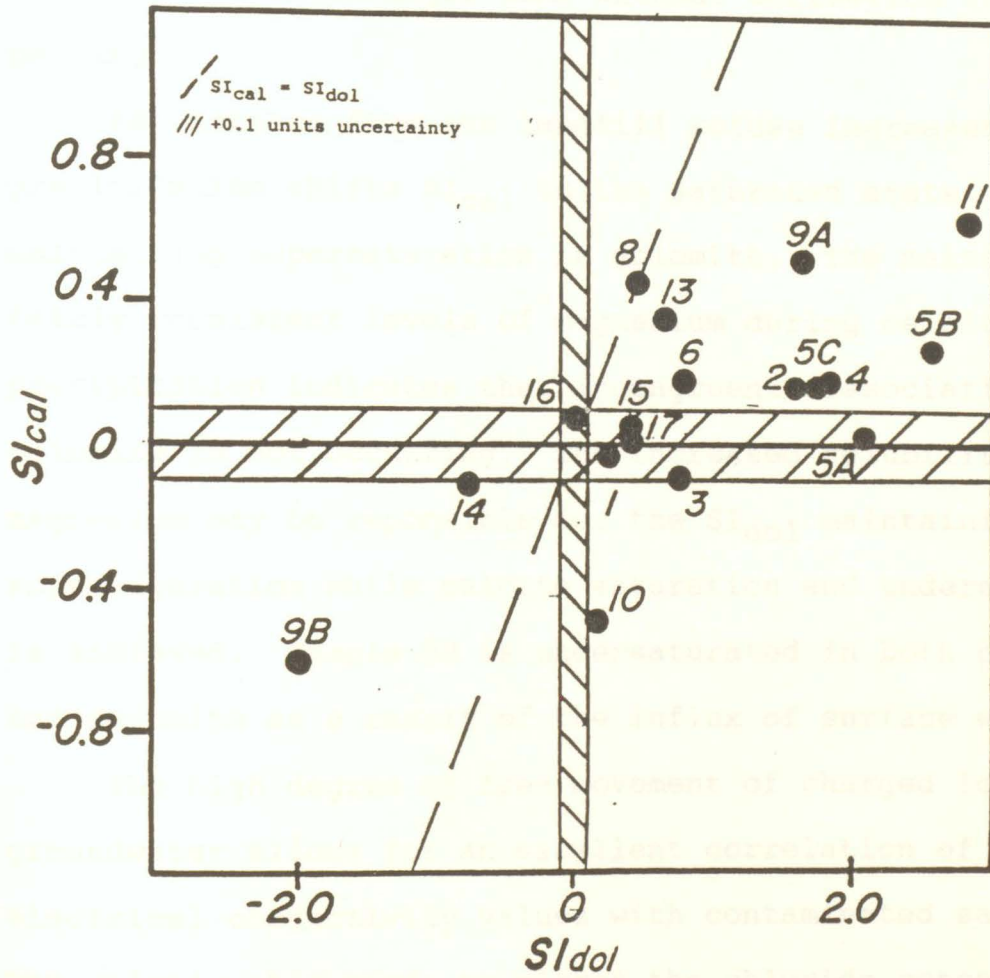


Figure 43. Saturation indices of water samples.

5.3.3. Isotopic Analysis

The areal distributions of ^{18}O , D and δ are all consistent with groundwater flow towards the southeast (Figure 43a,b,c). A regression analysis of the ^{18}O and D concentrations for the least-contaminated groundwater data indicate a linear relationship of:

and temperature values. Calculation of ionic strengths involved all seven major ions without correction for ion pairing.

As distance from the landfill refuse increases, calcite precipitation shifts SI_{cal} to the saturated state maintaining supersaturation in dolomite. The maintenance of fairly consistent levels of magnesium during calcite precipitation indicates that incongruent dissociation of dolomite is not occurring. The increased solubility of magnesium may be responsible for the SI_{dol} maintaining supersaturation while calcite saturation and undersaturation is achieved. Sample 9B is undersaturated in both calcite and dolomite as a result of the influx of surface water.

The high degree of free movement of charged ions in the groundwater allows for an excellent correlation of high electrical conductivity values with contaminated samples. The relationship tends to mirror the chloride concentrations very closely indicating the possibility of using electrical conductivity as an indicator of the chloride content in contaminated groundwater (Figure 44).

5.5.2. Isotopic Analysis

The areal distributions of ^{18}O , D and T are all consistent with groundwater flow towards the southeast (Figure 45a,b,c). A regression analysis of the ^{18}O and D concentrations for the least-contaminated groundwater data indicate a linear relationship of:

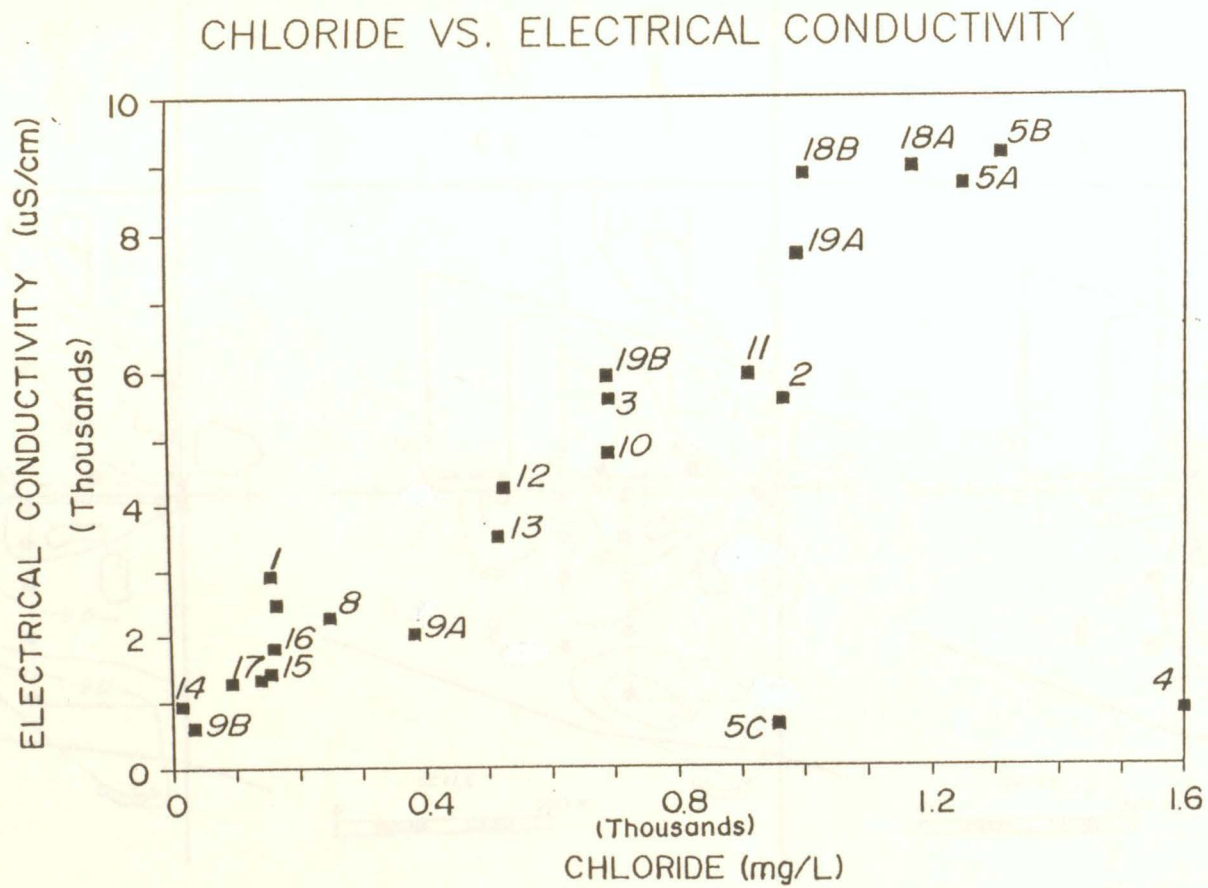


Figure 44. Electrical conductivity-chloride relationship.

Figure 45. Areal distribution of (a) ^{35}S and (b) ^{37}S in the (c) system.

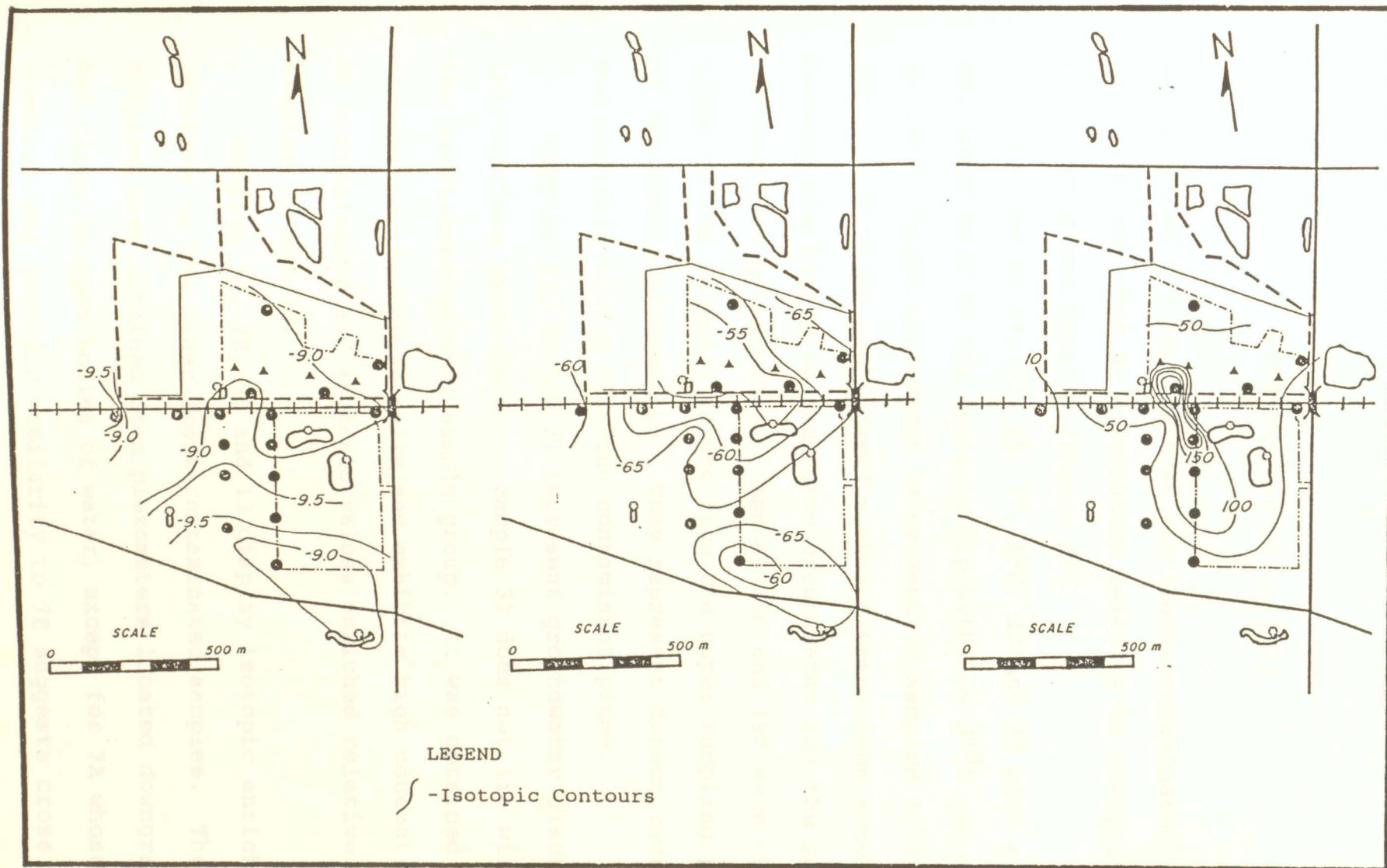


Figure 45. Areal distribution of (a) $\delta^{18}\text{O}$, (b) δD , and (c) tritium.

$$\delta D = 5.9 \delta^{18}O - 9.94. \quad (17)$$

The slope of 5.9 implies that the least-contaminated samples have been enriched by evaporation relative to precipitation in southwestern Ontario (Figure 46).

Samples 8, 14, 15, 16, 17, 19C, 20 and 30 plot along the lower half of the relationship with low $\delta^{18}O$ and δD values. Slight enrichment is evident in samples 1, 6, 9A, 18C and 29 which are located within a transition zone between the highly contaminated groundwater and the least-contaminated groundwater. Samples 18C and 19C were obtained close to the landfill refuse from the upper sampling ports of two bundle piezometers. They represent direct recharge and possible mixing with the contaminant plume.

Samples 29, 30 and 31 represent groundwater discharging into surface water bodies. Sample 31 does not lie within the least-contaminated sample group. It was obtained closest to the refuse cells and exhibits high concentrations of contaminants and isotopic values enriched relative to samples 29 and 30.

Samples 7A, 7B, 9B and 13 display isotopic enrichment relative to the other least-contaminated samples. These samples were obtained from piezometers located downgradient and close to open bodies of water, except for 7A whose chemical and isotopic similarity to 7B suggests cross

$\delta^{18}\text{O}$ VS. δD

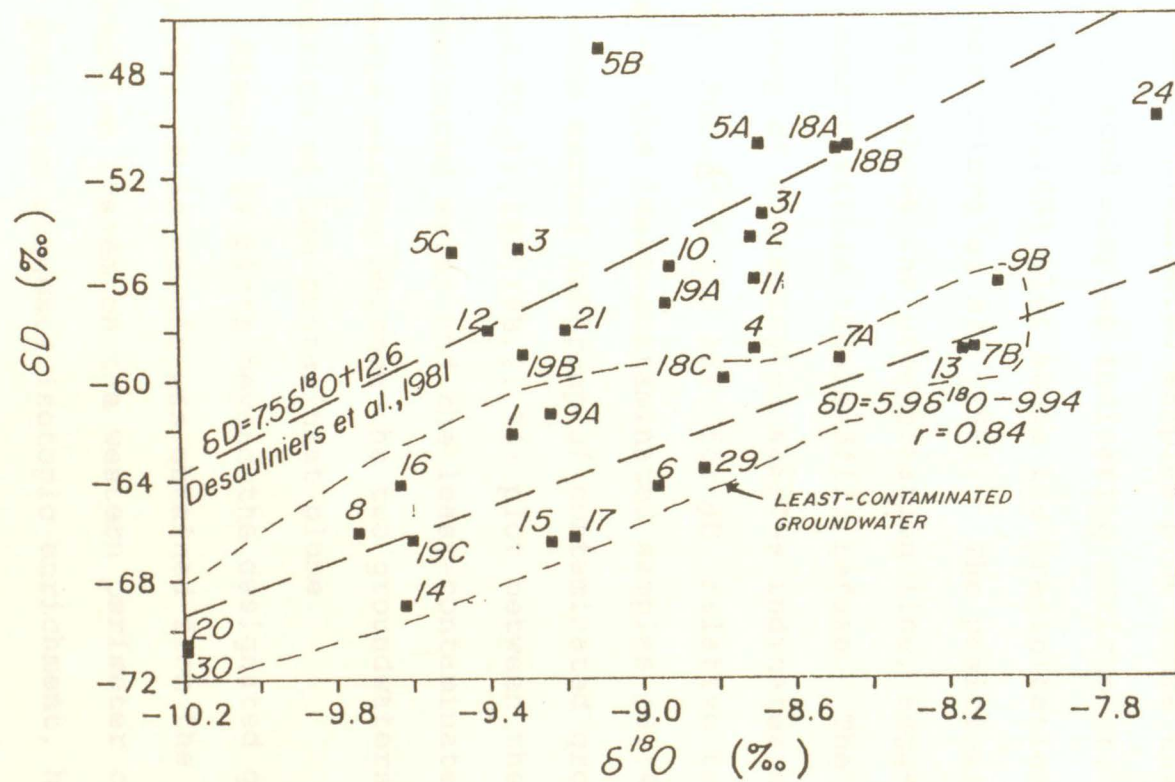


Figure 46. $\delta^{18}\text{O}$ - δD relationship for groundwater samples.

contamination. Therefore, recharge of evaporated surface water would explain their placement in the $\delta^{18}\text{O}$ - δD relationship.

The contaminated samples plot above the least-contaminated samples indicating enrichment. One subgroup (5A,5B,18A,18B) plot above the precipitation line developed by Desaulniers *et al.* (1981). The positioning of this subgroup above the precipitation line, suggests isotopic enrichment within the landfill refuse. The mean of this subgroup of contaminated samples indicates enrichment of 0.78% for $\delta^{18}\text{O}$ and 16% for δD , relative to the mean of some of the least-contaminated samples (8,14,15,16,17).

The second subgroup of contaminated groundwater samples (2,3,4,5C,11,19A,19B,21,24) plot between the highly contaminated water and the least-contaminated water. This suggests mixing between the two groundwaters during migration of the contaminant plume.

Sample 24 plots beyond the designated groupings of samples. This sample was obtained from the leachate collection system on the western perimeter of the landfill. Its position suggests isotopic enrichment, however, dilution by precipitation and uncontaminated groundwater may have minimized enrichment.

Some extremely high T values are found to exist within the study area. Samples 3 (677 TU) and 10 (378 TU) exceed the peak background value of 201 ± 50 from the sand aquifer

north of Leamington (Gillham *et al.* 1978). Their presence suggests the possibility of a T source within the landfill. Although a relationship is not evident between $\delta^{18}\text{O}$ and T, there appears to be two $\delta\text{D-T}$ relationships (Figure 47a,b).

Movement from the tritiated high of sample 3 (677 TU) through samples 10 (378 TU), 9A (132 TU), and 8 (115 TU) indicate a possible flow direction of the groundwater to the southeast. This is substantiated by water table configurations and flow directions (Figure 45c).

There is a second relationship of the remaining data where higher T values correlate with the enriched deuterium data. This implies that the refuse cells are the site of isotopic enrichment (of ^{18}O and D) and of recharge into the unconfined aquifer.

5.5.3. Chemical and Isotopic Relationships

A cluster analysis was performed on the chemical and isotopic data using SAS (1982). The cluster analysis created groupings of the sample points based on similarities in concentrations of the contaminants (major ions) and the isotopes D and ^{18}O . Two distinct groupings are revealed: (1) contaminated groundwater and (2) least-contaminated groundwater (Figure 48). The contaminated samples were further subdivided into two subgroupings ($r^2=0.85$).

Lines of best fit for the sample data (Table 13) represent lines of mixing between the contaminated and least-contaminated groundwater. Five samples

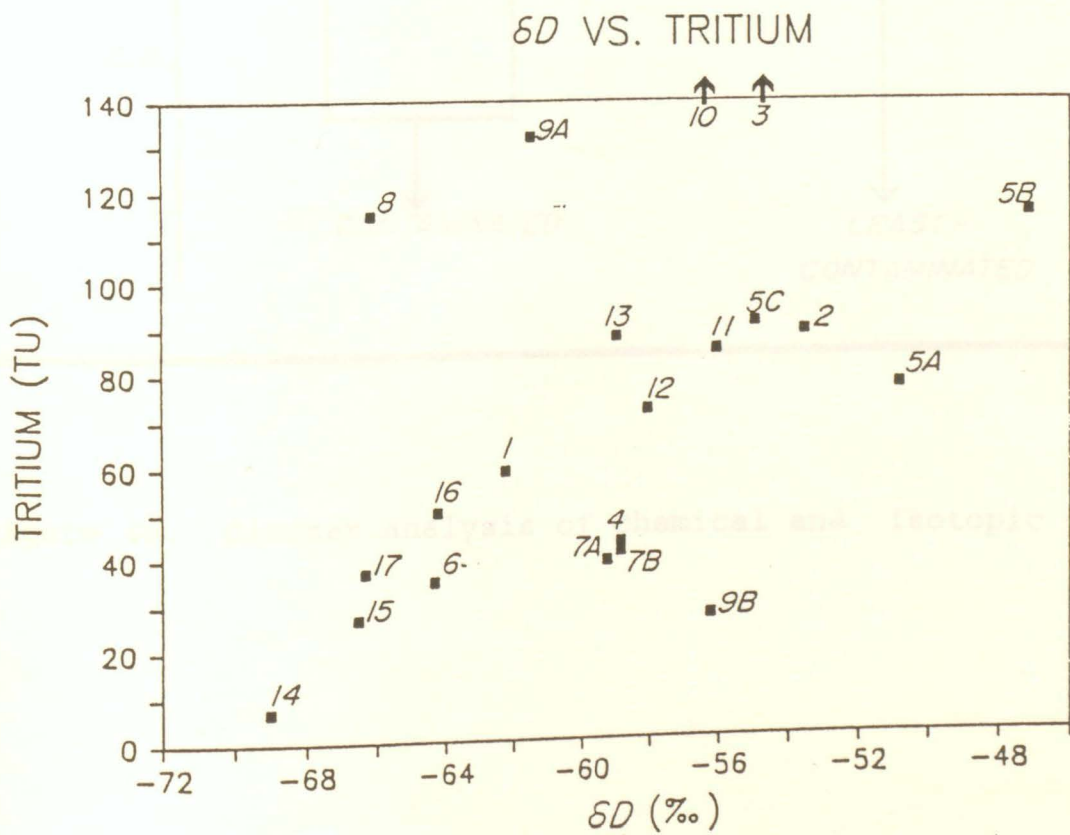
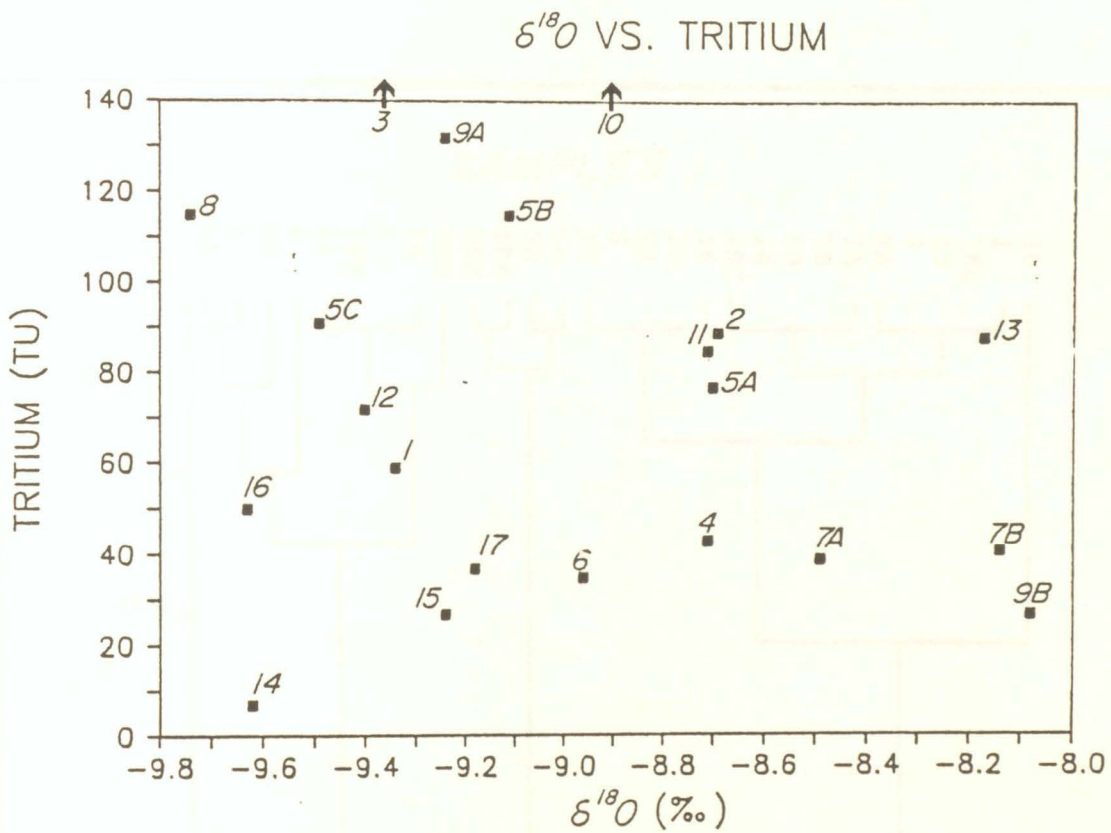


Figure 47. Relationship between tritium and (a) $\delta^{18}O$ and (b) δD .

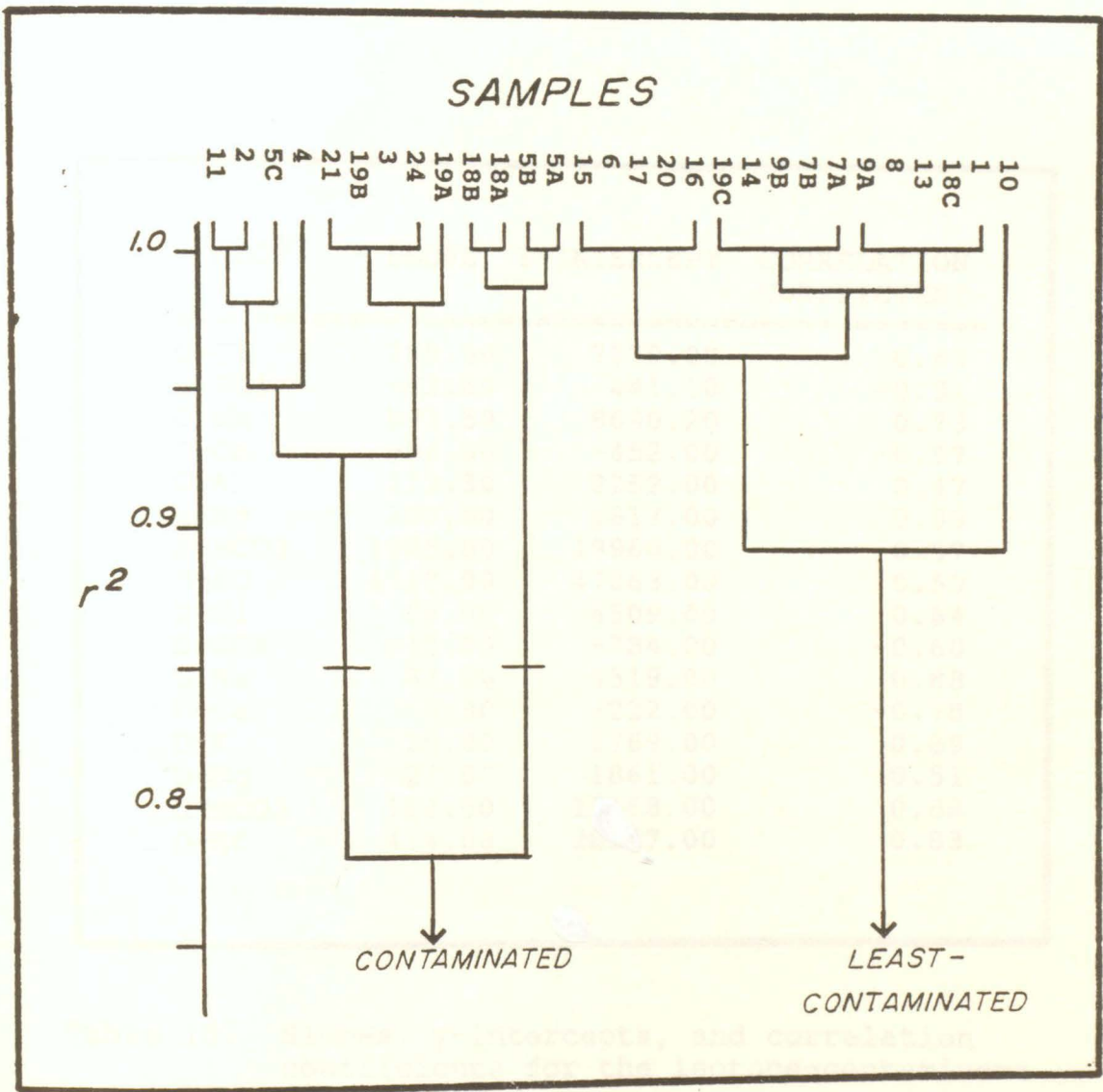


Figure 48. Cluster analysis of chemical and isotopic data.

PLOT	SLOPE	Y-INTERCEPT	CORRELATION COEFFICIENT
O-Cl	785.40	7779.00	0.63
O-SO ₄	-52.60	-441.10	-0.31
O-Na	892.50	8690.20	0.73
O-Ca	-56.00	-452.00	-0.57
O-K	222.30	2252.00	0.47
O-Mg	280.00	2817.00	0.33
O-HCO ₃	1985.00	19960.00	0.57
O-EC	4717.00	47063.00	0.59
D-Cl	66.00	4509.00	0.84
D-SO ₄	-12.80	-784.00	-0.60
D-Na	67.00	4519.00	0.88
D-Ca	-4.80	-222.00	-0.78
D-K	26.00	1769.00	0.89
D-Mg	27.00	1861.00	0.51
D-HCO ₃	192.00	13168.00	0.88
D-EC	414.00	28387.00	0.83

Table 13. Slopes, y-intercepts, and correlation coefficients for the isotope-contaminant relationships.

(7A, 7B, 9B, 13, 24) were omitted from the linear regression since they have been diluted by the influx of evaporated water. Sample 20 was not used because of excessive disruption of the subsurface during piezometer installation.

A correlation coefficient of 0.84 for δD -chloride indicates that a very good linear relationship exists between the two (Figure 49b). Two groupings of data, highest-contaminated (upper right hand corner) and least-contaminated (lower left hand corner) groundwater, are bisected by the line of mixing. Sample data plotting between highest-contaminated and least-contaminated groundwater are in the transition zone. These relationships suggest that samples lying along the line of mixing show decreasing contamination away from the landfill refuse. In the case of chloride contamination, it also suggests that the refuse is the source of chloride and that attenuation is a result of dilution. If chloride was attenuated by processes other than dilution, samples would not plot along the line of mixing, resulting in a poorer correlation coefficient.

The $\delta^{18}O$ -chloride relationship shows more scatter of data points, resulting in a lower correlation coefficient of 0.63 (Figure 49b). This suggests that the ^{18}O enrichment is a result of different reactions than those which cause D enrichment. Sample 4 plots above the line of mixing indicating that it is influenced either by an extraneous

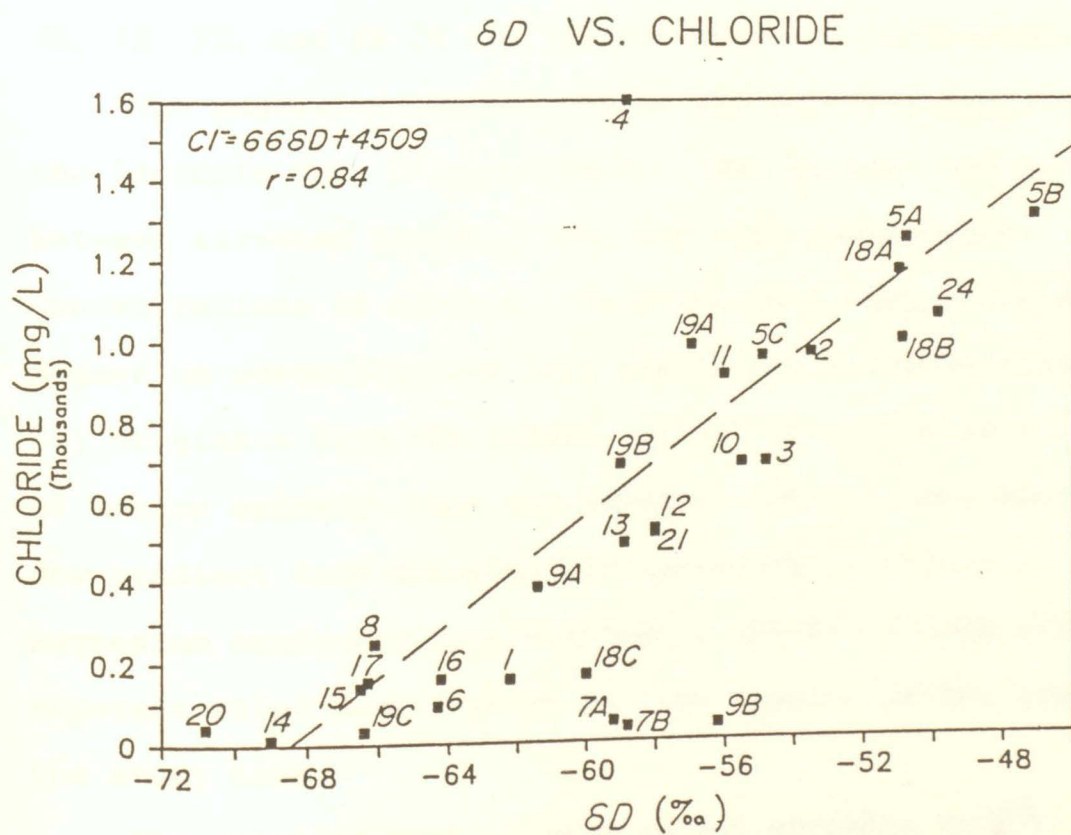
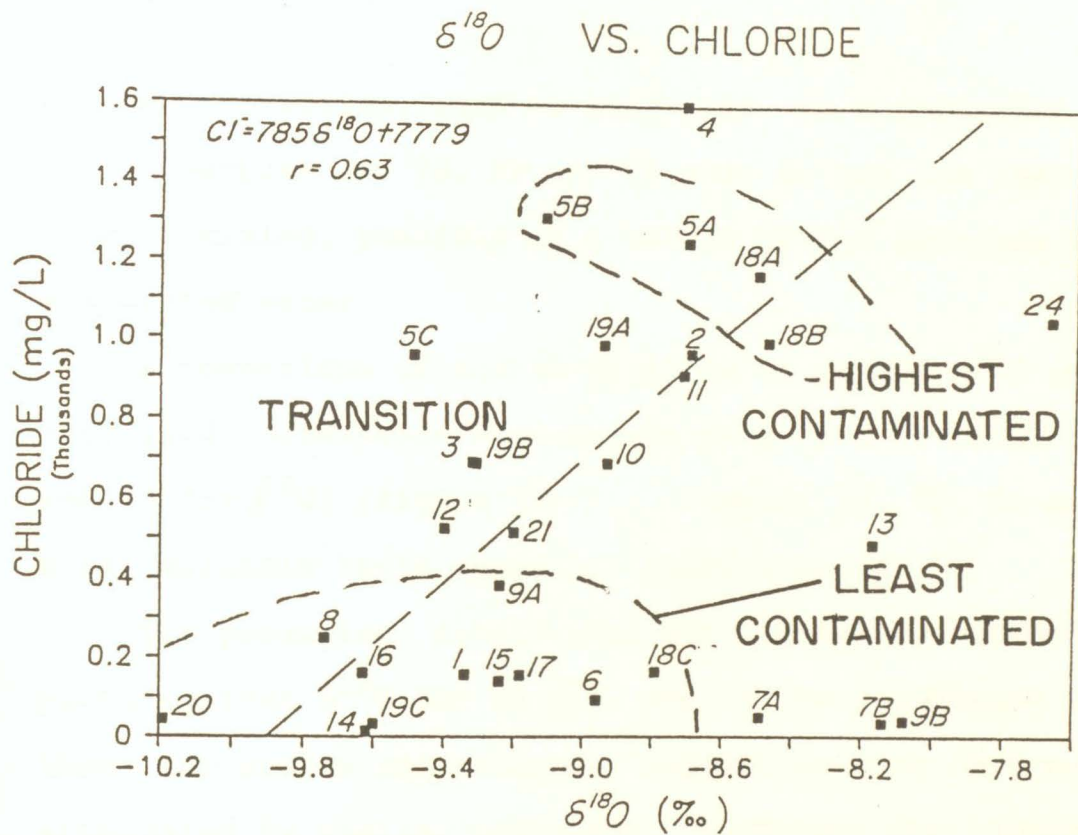


Figure 49. Relationship between chloride and (a) $\delta^{18}O$ and (b) δD .

source of chloride, such as road salt, or a different refuse cell. Samples 7A, 7B, 9B and 20 also do not lie near the line of mixing, possibly as a result of the recharge of evaporated water.

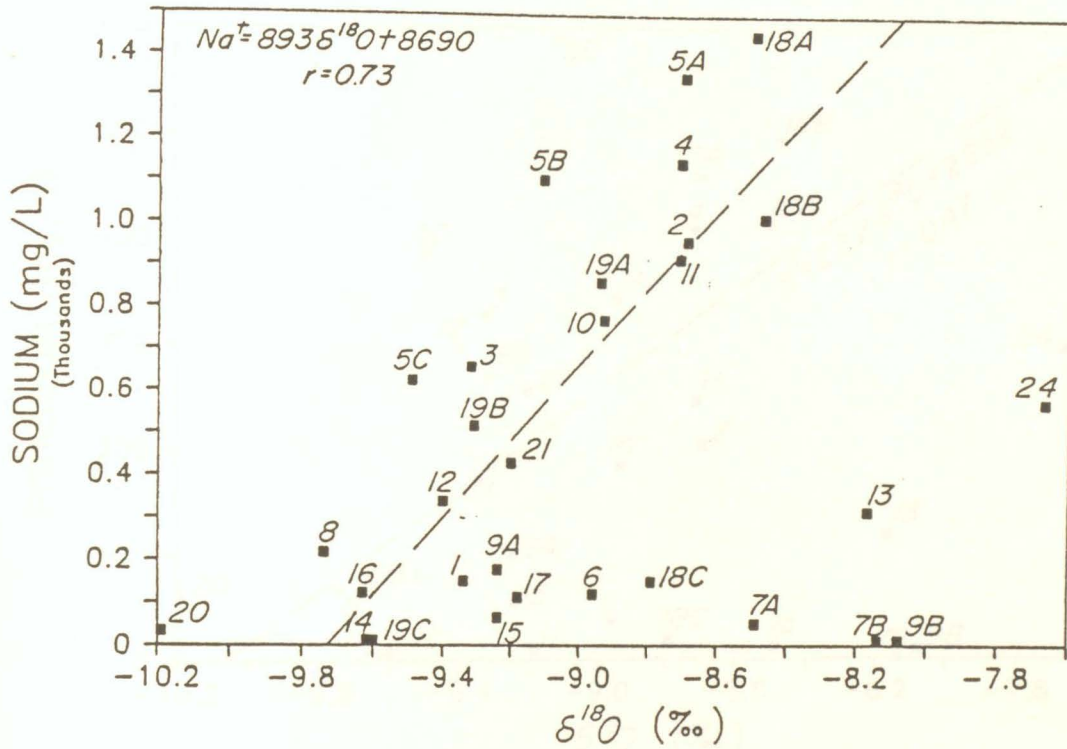
A comparison of sodium relative to δD and $\delta^{18}O$ shows a very good correlation between the data ($r=0.88$ for δD and $r=0.73$ for $\delta^{18}O$) (Figure 50a,b). Samples 7A, 7B, 9B and 20 still maintain their anomalous relationships.

The potassium, alkalinity, and electrical conductivity plots against $\delta^{18}O$ and δD show similar relationships to those for sodium and chloride, suggesting that they are attenuated by similar processes. Anomalous positioning of 7A, 7B, 9B, and 20 in the relationships is maintained.

The magnesium concentrations are poorly correlated with the isotopic data (Figure 54a,b). The typical connection between elevated isotopic data and high contaminant concentrations is subdued. This suggests that elevated magnesium concentrations near the landfill refuse either: (1) originate from the refuse, or (2) originate as a result of cation exchange near the landfill refuse, then decrease downgradient from dolomite precipitation or dilution. The magnesium concentrations eventually achieve a more stable supersaturated level, which is then maintained throughout the study area.

The relationships of calcium and sulphate to $\delta^{18}O$ and δD are very different from those of the other parameters

$\delta^{18}O$ VS. SODIUM



δD V.S. SODIUM

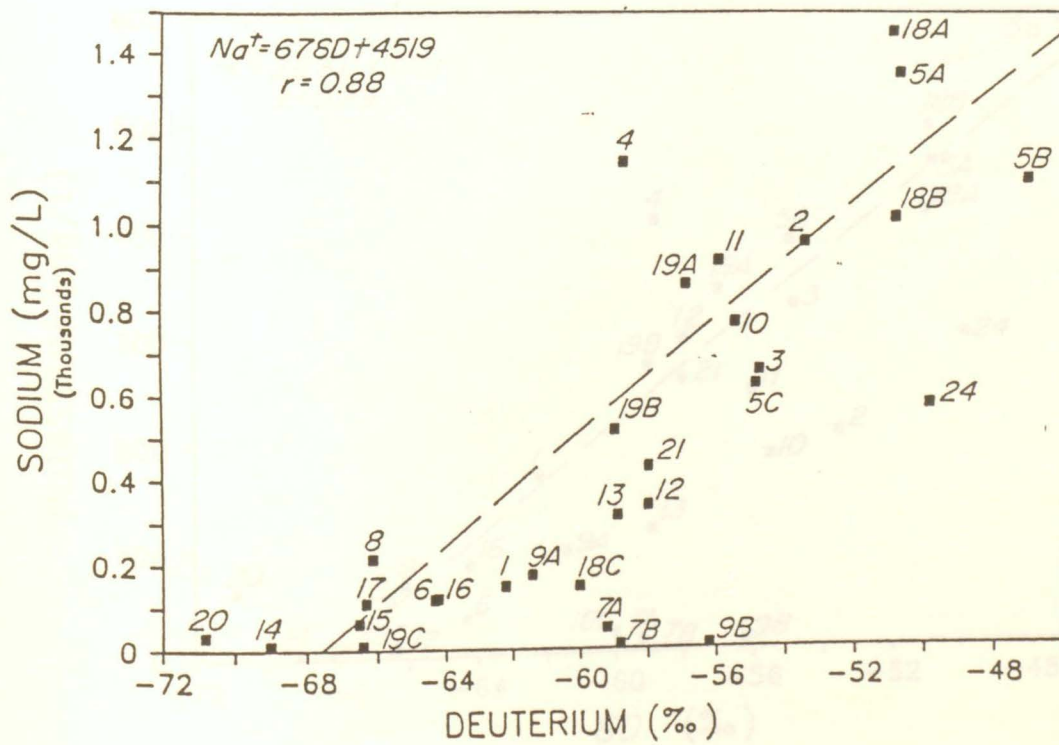
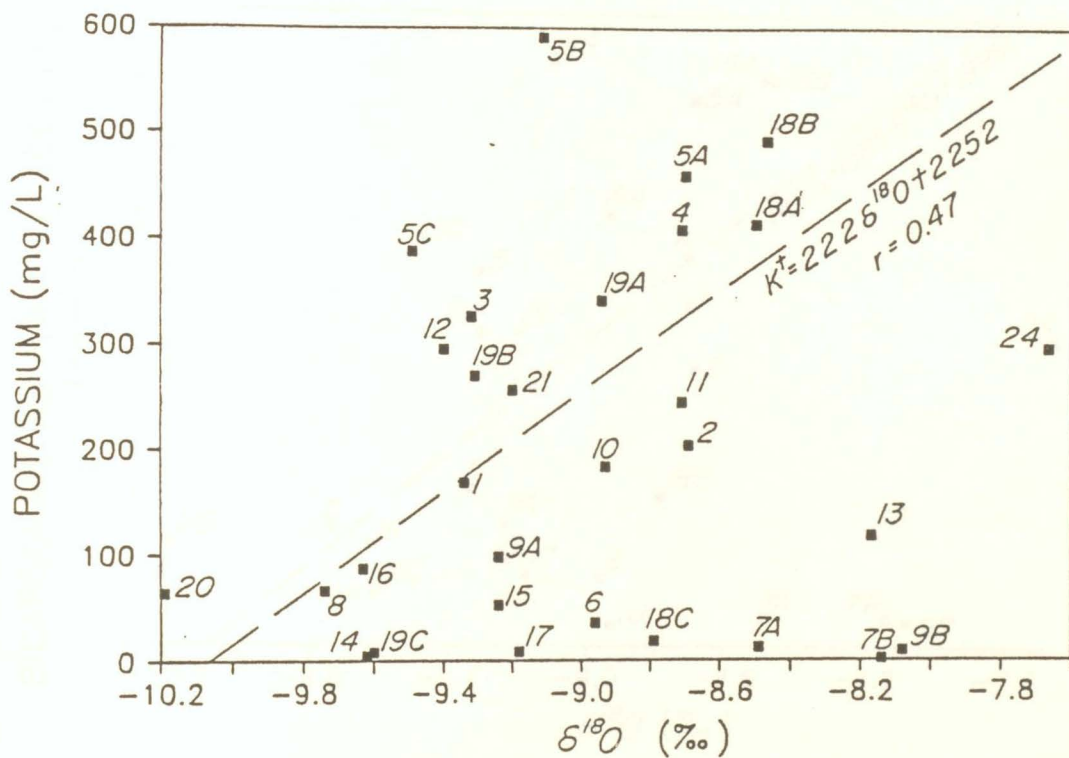


Figure 50. Relationship between sodium and (a) $\delta^{18}O$ and (b) δD .

$\delta^{18}O$ VS. POTASSIUM



δD VS. POTASSIUM

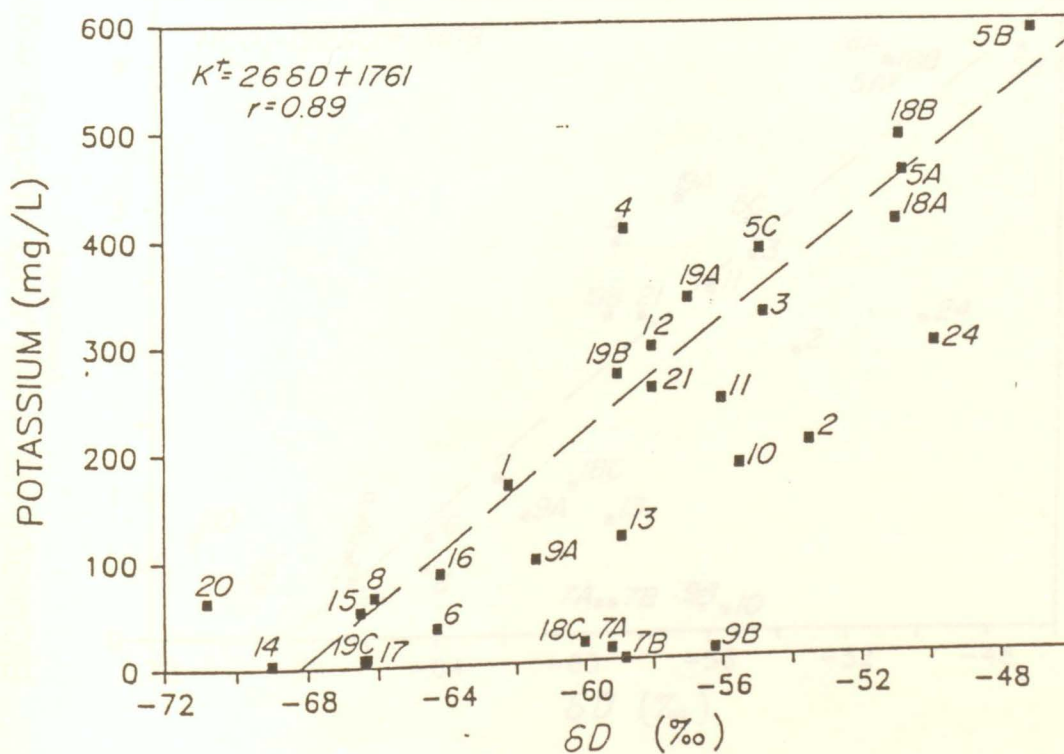


Figure 51. Relationship between potassium and (a) $\delta^{18}O$ and (b) δD .

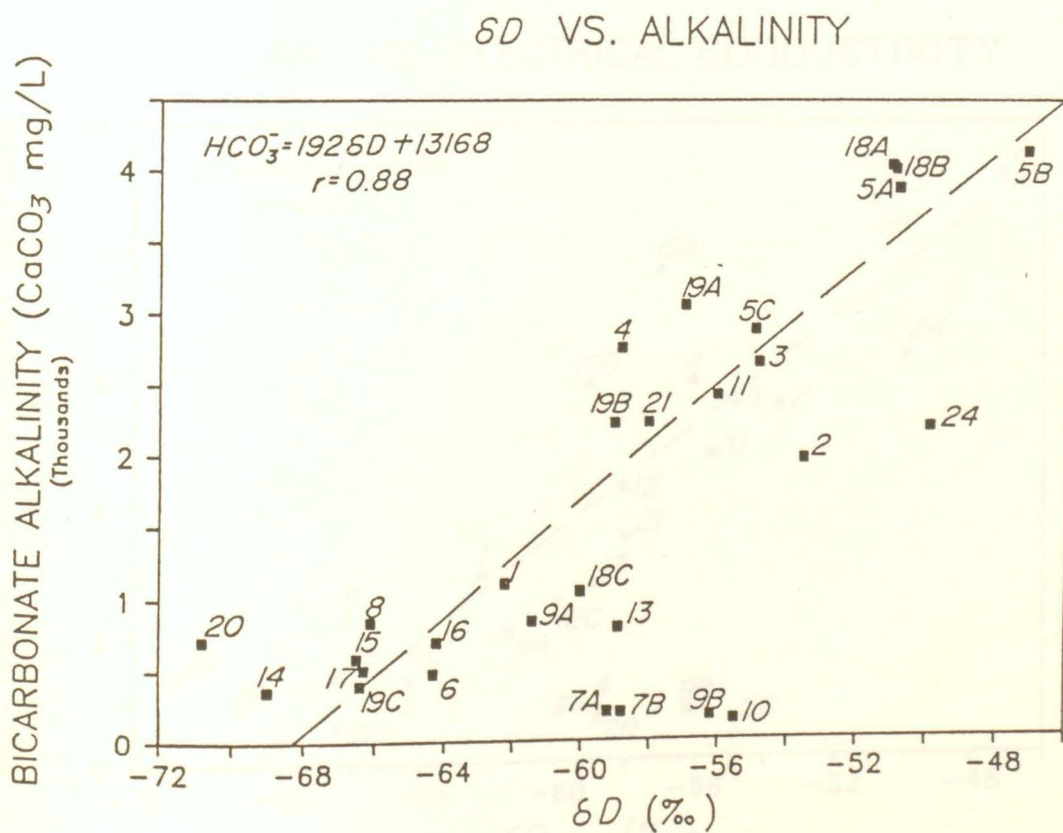
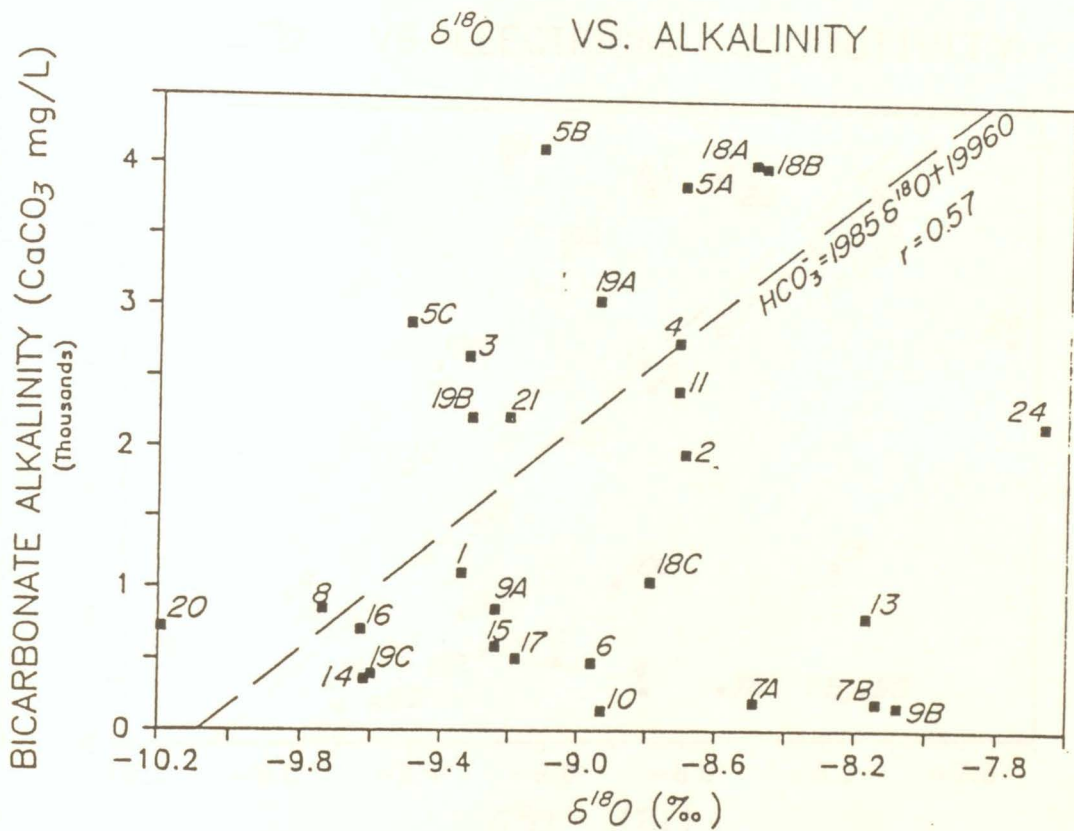
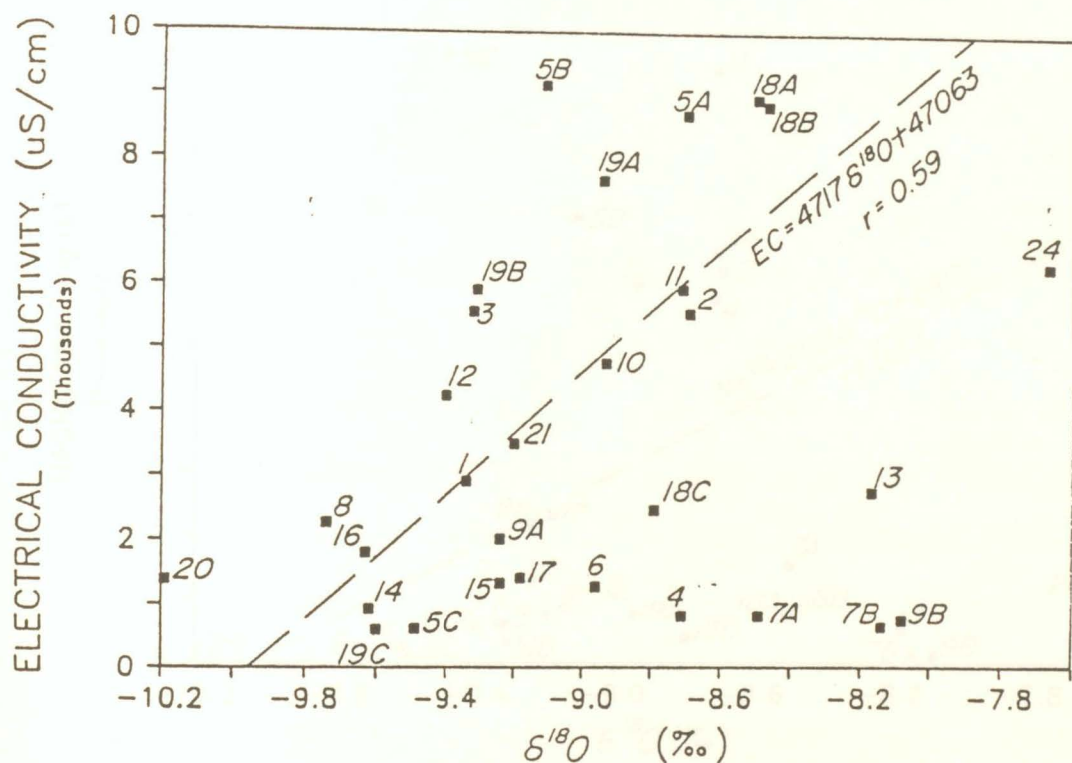


Figure 52. Relationship between alkalinity and (a) $\delta^{18}O$ and (b) δD .

$\delta^{18}O$ VS. ELECTRICAL CONDUCTIVITY



δD VS. ELECTRICAL CONDUCTIVITY

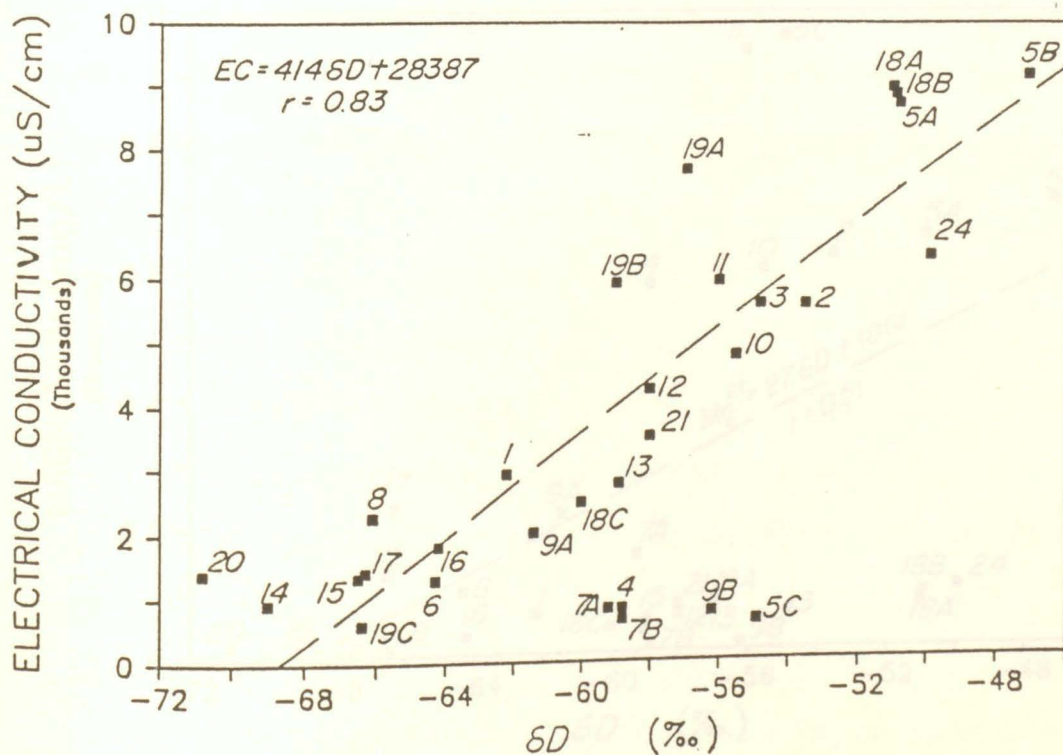
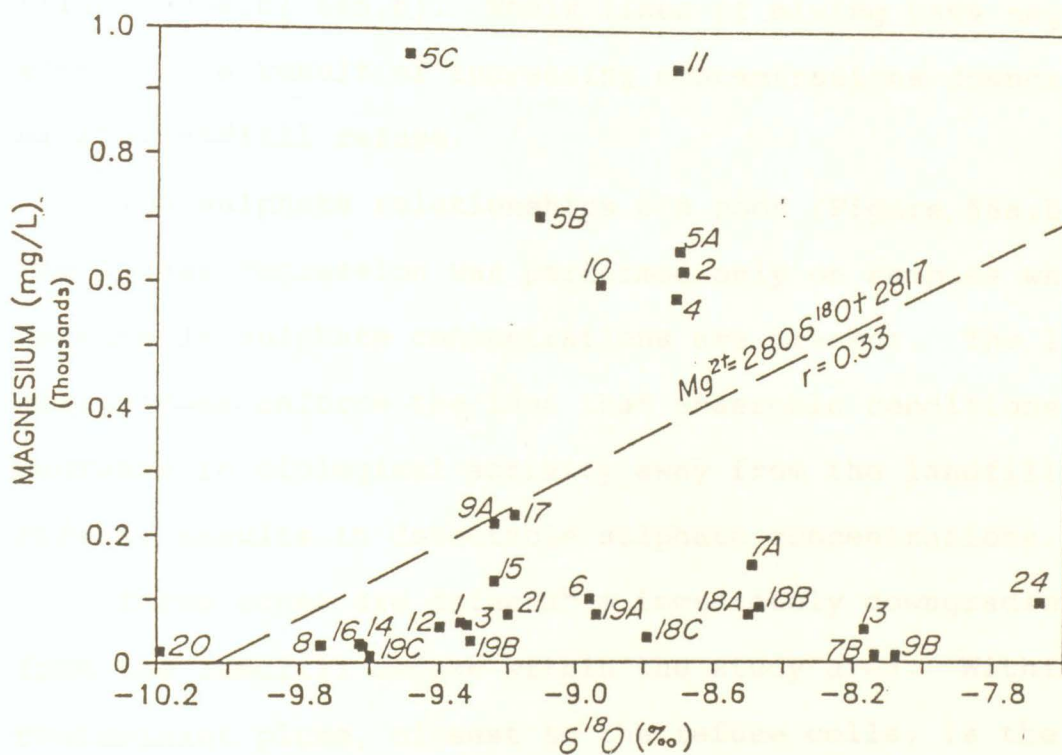


Figure 53. Relationship between electrical conductivity and (a) $\delta^{18}O$ and (b) δD .

$\delta^{18}O$ VS. MAGNESIUM



δD VS. MAGNESIUM

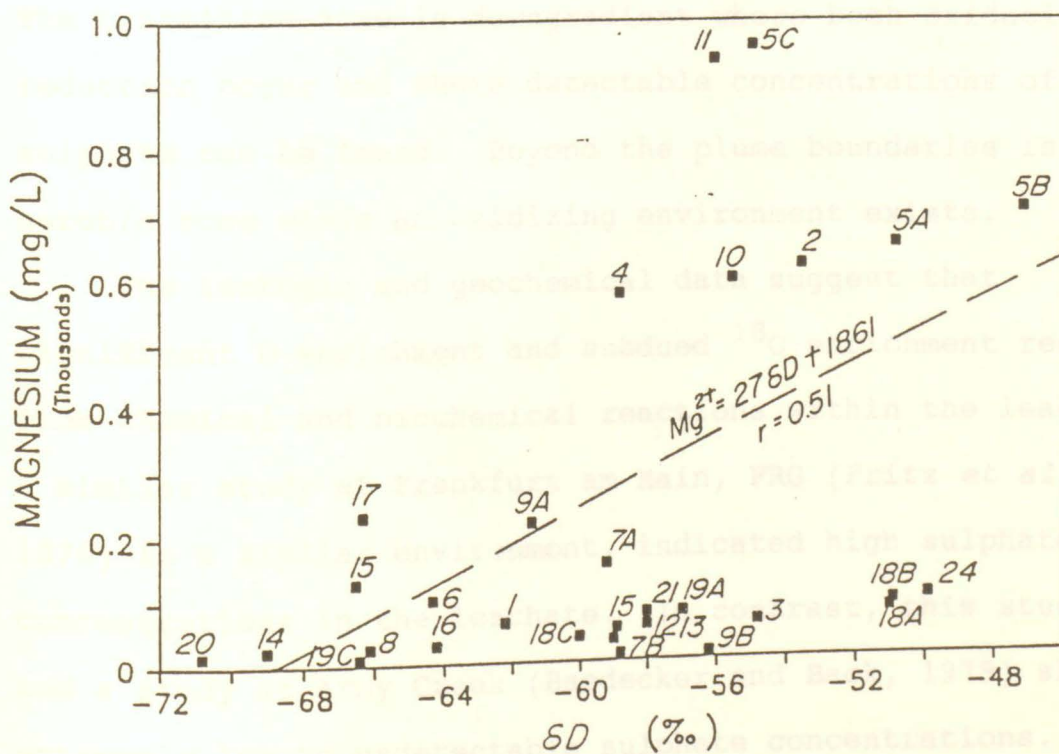


Figure 54. Relationship between magnesium and (a) $\delta^{18}O$ and (b) δD .

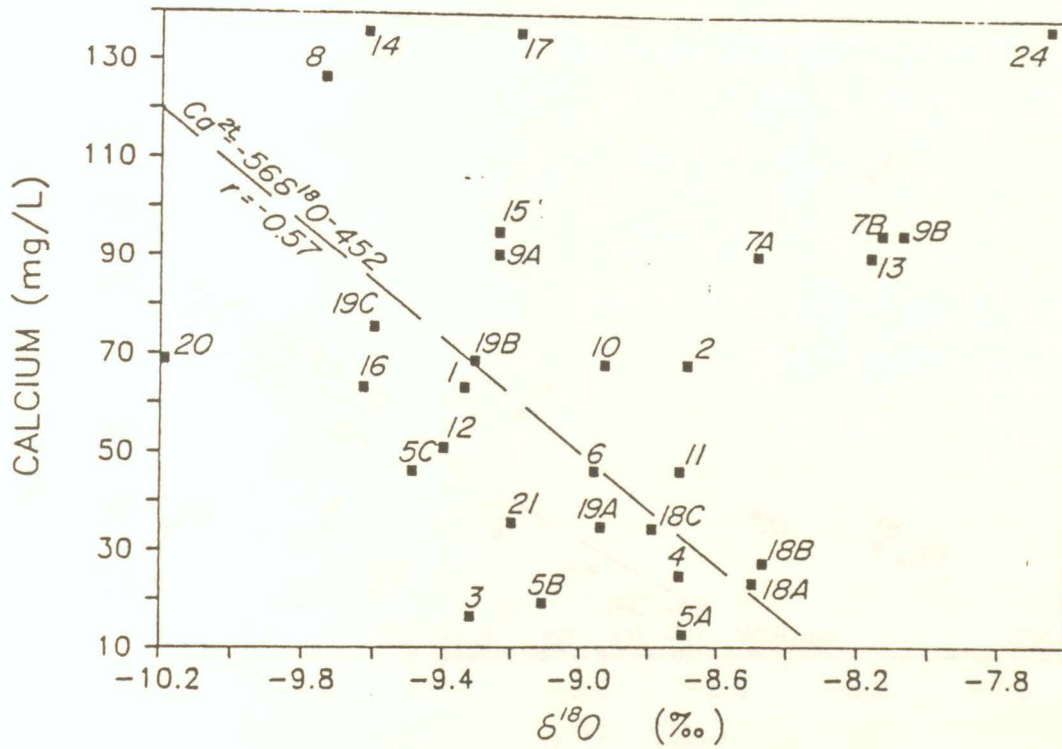
(Figure 55a,b; 56a,b). Their lines of mixing have negative slopes as a result of increasing concentrations downgradient of the landfill refuse.

The sulphate relationships are poor (Figure 56a,b). The linear regression was performed only on samples where detectable sulphate concentrations are present. The line of mixing does enforce the idea that anaerobic conditions and a decrease in biological activity away from the landfill refuse, results in detectable sulphate concentrations.

Three zones are detectable immediately downgradient from the landfill refuse within the study area. Within the contaminant plume, closest to the refuse cells, is the anaerobic zone where a reducing environment is maintained. The transition zone is downgradient where both oxidation and reduction occur and where detectable concentrations of sulphate can be found. Beyond the plume boundaries is an aerobic zone where an oxidizing environment exists.

The isotopic and geochemical data suggest that significant D enrichment and subdued ^{18}O enrichment result from chemical and biochemical reactions within the leachate. A similar study at Frankfurt am Main, FRG (Fritz *et al.*, 1976) in a similar environment, indicated high sulphate concentrations in the leachate. In contrast, this study, and a study at Army Creek (Baedecker and Back, 1979) show extremely low to undetectable sulphate concentrations. This suggests that ^{18}O enrichment is dependent on the amount, and

$\delta^{18}O$ VS. CALCIUM



δD VS. CALCIUM

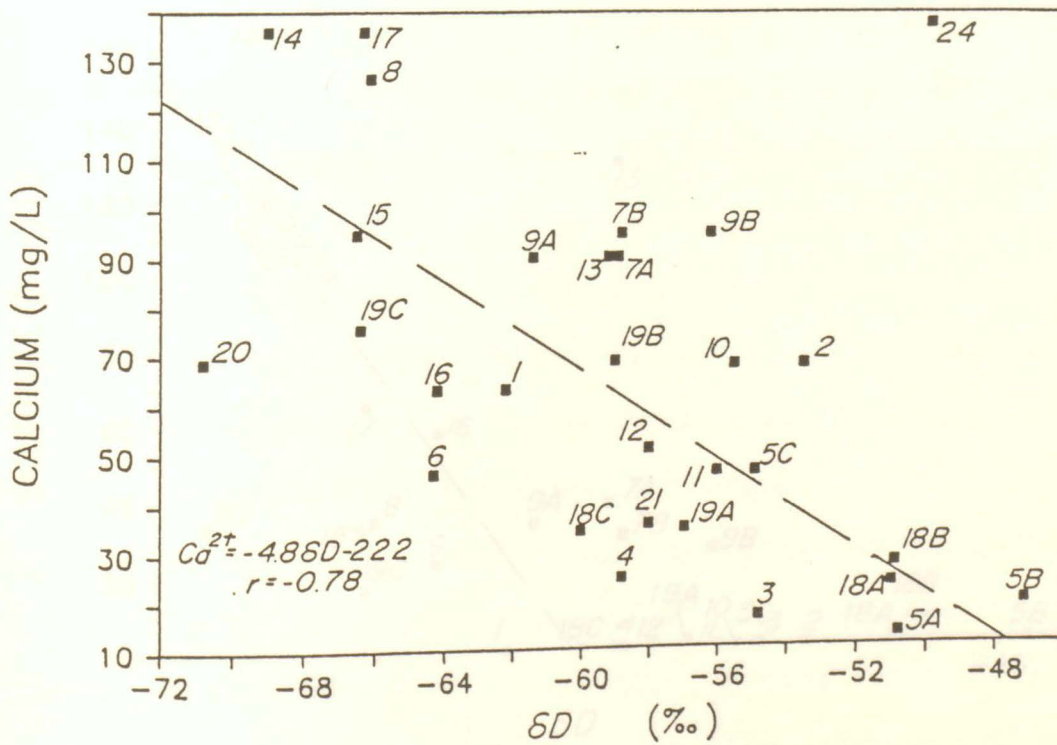


Figure 55. Relationship between calcium and (a) $\delta^{18}O$ and (b) δD .

$\delta^{18}\text{O}$ VS. SULPHATE

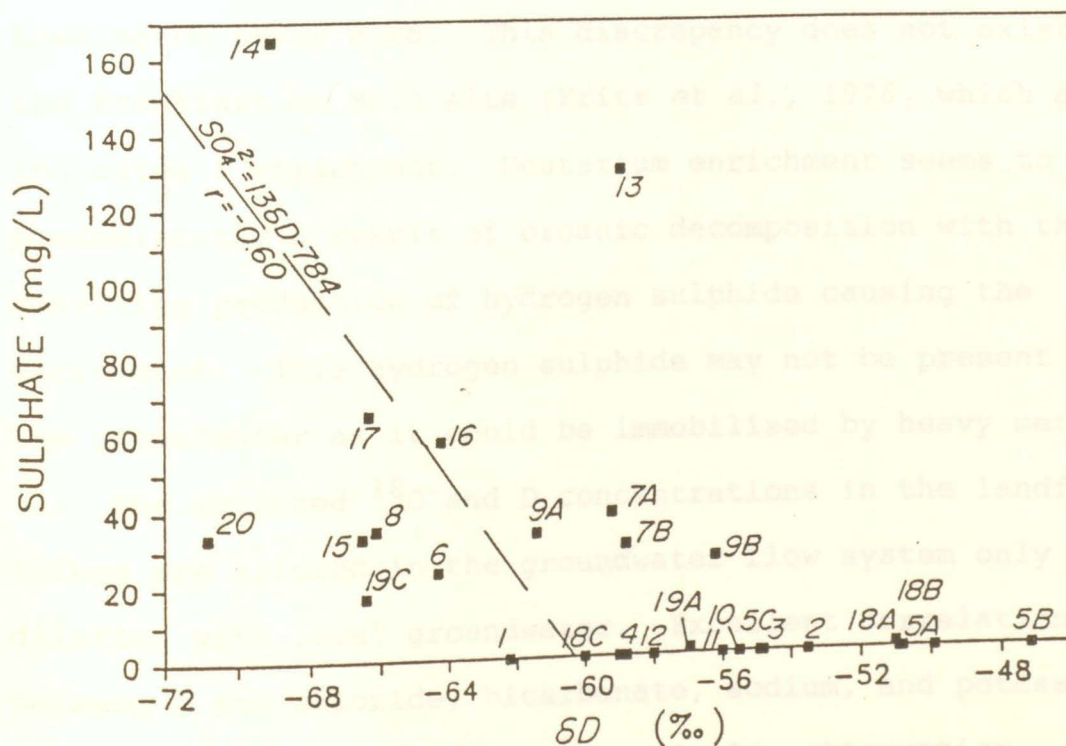
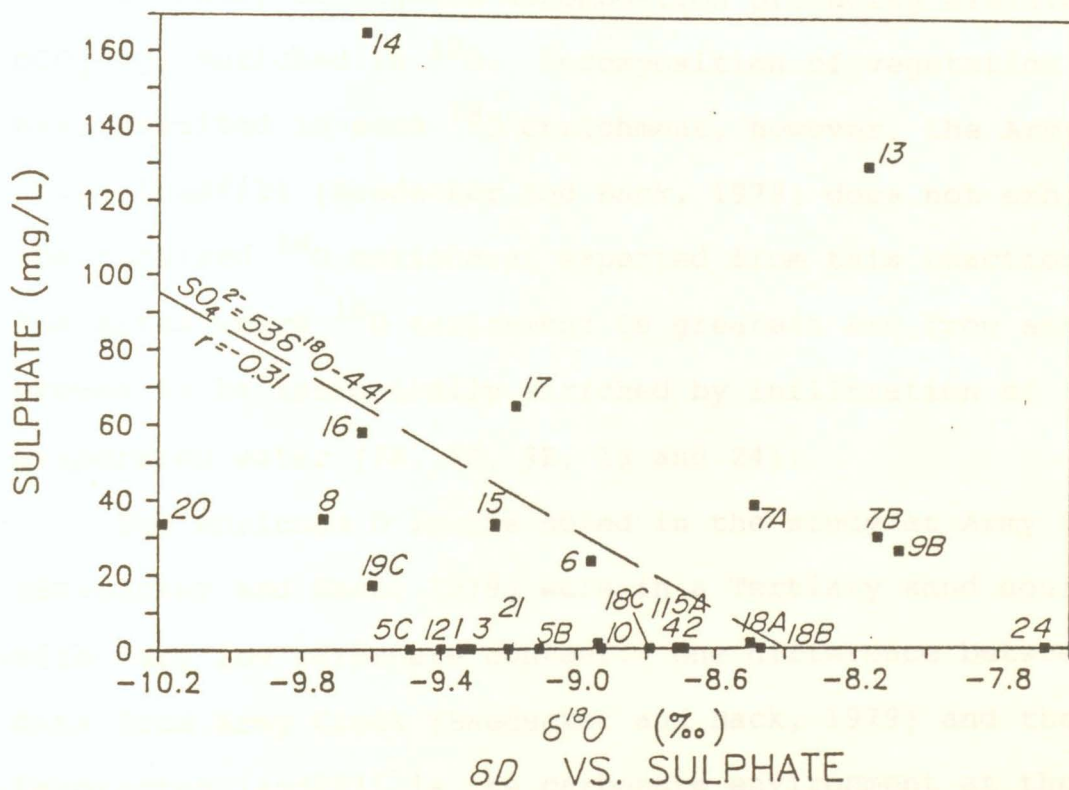


Figure 56. Relationship between sulphate and (a) $\delta^{18}\text{O}$ and (b) δD .

perhaps rate, of organic decomposition producing elevated $p\text{CO}_2(\text{aq})$ enriched in ^{18}O . Decomposition of vegetation may have resulted in some ^{18}O enrichment, however, the Army Creek landfill (Baedecker and Back, 1979) does not exhibit the required ^{18}O enrichment expected from this reaction. The sites where ^{18}O enrichment is greatest are from samples proven to be isotopically enriched by infiltration of evaporated water (7A, 7B, 9B, 13 and 24).

The enriched D levels noted in the study at Army Creek (Baedecker and Back, 1979) were in a Tertiary sand aquifer with very low carbonate content. One difference between the data from Army Creek (Baedecker and Back, 1979) and the Leamington landfill is the carbonate environment at the Leamington study area. This discrepancy does not exist with the Frankfurt am Main site (Fritz *et al.*, 1976) which also indicates D enrichment. Deuterium enrichment seems to be predominantly a result of organic decomposition with the resulting production of hydrogen sulphide causing the enrichment. This hydrogen sulphide may not be present in the groundwater as it could be immobilized by heavy metals.

The enriched ^{18}O and D concentrations in the landfill refuse are altered in the groundwater flow system only from dilution with local groundwater. Excellent correlation between D and chloride, bicarbonate, sodium, and potassium suggest that they are undergoing similar attenuation processes. Since the contaminants react differently to

adsorption, precipitation, coprecipitation, and biological degradation, the excellent correlations suggest that dilution is the dominant attenuating factor of the contaminant plume.

Sulphate displays a poor correlation with ^{18}O and D as dissimilatory reduction is the dominant attenuating process of sulphate. This poor sulphate correlation emphasizes what the relationships of chloride, bicarbonate, sodium, and potassium with ^{18}O and D would resemble if the other attenuating processes predominated in place of dilution.

Samples 18C and 19C which were obtained near the surface are slightly contaminated and plot on the line of mixing. This indicates that contaminant dilution also involves vertical hydrodynamic dispersion.

6.0. CONCLUSIONS AND RECOMMENDATIONS

6.1. Conclusions

A substantial list of conclusions arise from this study at the Essex County Sanitary Landfill Site No. 2. These conclusions are:

1. The resistivity survey obtained a depth of current penetration of 0.5 to 0.66 of an 'a' spacing. Statistical analyses of the resistivity readings did not detect a consistent group of anomalous values to delineate a plume, but did allow identification of areas of probable contamination.
2. Hammer seismic velocities correlated with known subsurface lithologies, however there was very poor correlation between seismic determined geological contacts and borehole identified geological contacts. Poor depth correlation was probably a result of subsurface heterogeneity and a thin saturated zone.
3. The electrical conductivity survey of surface water bodies was consistent with geophysical results, suggesting contaminant plumes to the southeast and northeast of the Leamington landfill and to the southeast of the Heinz landfill.
4. Landfill leachate is migrating through a near surface unconfined sand aquifer. This sand aquifer thickens towards the south and east. A till unit located below the sand aquifer creates a perched condition. At least 4.5 m thick

below the landfill, this till unit dips towards the southeast where it eventually pinches out. Below the till unit is a deeper unconfined sand aquifer. This deeper sand aquifer is penetrated by only one borehole (7A), where it is 10 m thick at that point. A lower confining till unit is also penetrated by borehole 7A.

5. The upper till unit may be one continuous layer below the landfill, and may be part of the lower confining till unit.

6. Surface ponds southeast of the landfill show groundwater discharge through their north banks and recharge through their south banks. This supports the idea of a southeastern groundwater flow direction.

7. Field and laboratory hydraulic conductivities of the upper sand unit vary by one order of magnitude. Field hydraulic conductivities range between 10^{-3} and 10^{-4} cm/s.

8. Water table elevations indicate that the groundwater flow pattern follows the topography with some flow towards the southeast.

9. In March, 1988, seeps on the eastern side of the eastern refuse cell were discovered suggesting mounding within, and recharge through, the landfill refuse.

10. Examination of the distribution of contaminants (major ions) supports the idea that groundwater flow is towards the southeast.

11. Monitors near the refuse cells show the highest concentrations of chloride, bicarbonate, sodium, potassium and magnesium. Concentrations of calcium and sulphate are very low.
12. The pH within the entire study area is maintained between 6.5 and 7.5 by carbon dioxide production and carbonate dissociation.
13. Partial pressures of carbon dioxide near the refuse cells are three orders of magnitude greater than atmospheric partial pressures of carbon dioxide. This suggests that there is a high degree of biological activity near the landfill refuse.
14. Elevated bicarbonate concentrations are a result of sulphate reduction and carbonate dissociation. Reduced bicarbonate concentrations in monitors 18C and 19C suggest vertical zoning within the contaminant plume.
15. Sulphate concentrations are undetectable near the refuse cells as a result of bacterial dissimilatory reduction. Hydrogen sulphide is undetectable suggesting formation of compounds with heavy metals, and adsorption to the subsurface material. Sulphate becomes detectable in the transition zone, and reaches background concentrations in the aerobic zone.
16. Sodium, potassium and magnesium show similar trends against calcium. That is, high concentrations of sodium, potassium and magnesium with low calcium concentrations, and

viceversa. The trends of magnesium concentrations are more subdued than those for sodium and potassium.

17. The cation exchange capacity of the subsurface material is constant. The presence of high cation concentrations in leachate near the landfill refuse permit a high degree of exchange. Downgradient from the landfill refuse, leachate contaminant concentrations decrease, as does the degree of cation exchange.

18. There is a low calcium to magnesium ratio in the contaminant plume. The high magnesium concentrations result in a zone of hardness close to the landfill refuse cells.

19. The groundwater is supersaturated with respect to calcium and dolomite near the refuse cells. Downgradient the groundwater becomes unsaturated to saturated in calcium, but maintains its supersaturation in dolomite. This seems to be a result of the higher solubility of dolomite.

20. Electrical conductivity measurements are proportional to chloride concentrations.

21. Distribution of oxygen-18, deuterium, and tritium support flow towards the southeast.

22. The least-contaminated samples show an isotopic relationship of:

$$\delta D = 5.9 \delta^{18}O - 9.94$$

This suggests that the least-contaminated groundwater has undergone evaporation.

23. Contaminated groundwaters plot above the ^{18}O -D relationship for the least-contaminated groundwater, suggesting enrichment. Enrichment for $\delta^{18}\text{O}$ ranges between 0.5 to 1.0‰ and between 10 to 20‰ for δD .
24. Between the contaminated and least-contaminated samples are samples in the transition zone. These are samples of groundwater undergoing attenuation.
25. Very high tritium values (677 TU) were detected near the landfill refuse. Compared to tritium values north of the study area in a similar geological environment (201 ± 50 TU), these values suggest a tritium source within the landfill refuse. The tritium concentrations decrease towards the southeast.
26. Tritium and deuterium correlate very well suggesting that the refuse cells are the site of isotopic enrichment and of groundwater recharge.
27. The excellent correlations of the chloride, bicarbonate, sodium, potassium, and calcium with deuterium, suggest that dilution is the dominant attenuation process within the near surface sand aquifer.
28. Both enrichment processes are mainly a result of organic decomposition. The oxygen-18 enrichment is from the oxygen-18 in carbon dioxide, enriched during bacterial activity, equilibrating with the oxygen-18 in the contaminated groundwater. Thus, the groundwater enrichment occurs where bacterial activity is greatest. Deuterium

enrichment occurs as a result of the production of hydrogen sulphide which may not be detectable in the groundwater. Within the contaminant plume, oxygen-18 and deuterium cannot be classified as conservative tracers because of this enrichment. However, beyond the limits of the contaminant plume, the isotopic tracers are conservative.

In general, there are three advantages of using isotopic tracers instead of contaminant tracers. They are as follows:

1. Isotopic tracers can be used where extraneous point sources of contaminants are present. For example chloride tracers may be affected by road salt, brine ponds or intense fertilization.
2. Isotopic tracers would be useful in environments detrimental to some contaminant tracers. This would be the case when chloride is used as a tracer in a coastal environment.
3. A correlation of contaminant tracers and isotopic tracers would allow the identification of the location and impact of outside sources of water, or contaminants, on the contaminant plume.

Two limiting factors for isotopic tracer use could be:

1. Using isotopes as tracers may be limited to sand and gravel environments since the presence of clay can retard the isotopes. Contaminants such as chloride can also be retarded in clays.

2. Where surface water is abundant or where the water table is very close to the surface, evaporation may not only cause isotopic enrichment, but it may alter contaminant concentrations preventing their use for cross-checking sources of contamination.

6.2. Recommendations

To enhance the understanding of the isotopic enrichment at the Leamington Sanitary landfill Site No. 2 it is recommended that:

1. Two sets of groundwater samples be analysed over a significant time period. This would allow an examination of variations in isotopic enrichment with time, which would hopefully parallel changing contaminant concentrations, supporting the study's conclusions.
2. An analysis of any detectable sulphate for: a) sulphur isotopes to determine sulphate sources and to examine bacterial activity, and b) for oxygen-18 enrichment, would better define the effects of organic decomposition on oxygen-18 and deuterium enrichment.

Although chemical reactions are occurring within the subsurface at the Leamington landfill, the decreased contaminant concentrations are mainly the result of dilution. Therefore, the dilution potential of the subsurface will be maintained only as long as the background groundwater quality is substantially better than the

contaminant plume quality. In time, there is the possibility of an expanding plume.

Since self-purification of local groundwater is minimal, installation of a spray irrigation system for treatment of leachate could possibly result in further groundwater contamination and a reduction in the groundwater dilution potential.

The present leachate collection system prevents mounding and contaminant migration only to the west and southwest of the landfill. An extension of this collection system around the total perimeter is not feasible. The inverts must remain in the till, requiring excavation of large quantities of sand in an area where a near surface water table causes quicksand conditions. Leachate collected in this system would be diluted by groundwater, requiring treatment of immense volumes of contaminated water.

Since the best method of treating the leachate is by shipping it to the Leamington Sewage Treatment Plant, it would be most economical to collect the leachate in its most concentrated state. This could be achieved by installing a collection system as close to the present refuse cells as economically feasible. Also, lining and draining of future refuse cells would allow removal of the leachate before dilution by the local groundwater.

REFERENCES

- Airey, P.L., Calf, G.E., Hartley, P.E., Roman, D., and Spragg, W.T., 1975. Use of environmental isotopes and artificial tracers to study recharge to groundwater in the Burdekin Delta, Queensland. *Isotope Techniques in Groundwater Hydrology 1974* (Proc. Symp. Vienna, 1974) 1, IAEA, Vienna, 115-126.
- Ali, J., 1984. Geophysical surveys of groundwater contamination at three sanitary landfills in Essex County, Ontario. Unpubl. MSc. Thesis.
- Allison, G.B., Gat, J.R., and Leaney, F.W.J., 1985. The relationship between deuterium and oxygen-18 delta values in leaf water. *Chemical Geology (Isotope Geoscience Section)*. 58, 145-156.
- Baedecker, M.J., and Back, W., 1979. Hydrogeological processes and chemical reactions at a landfill. *Ground Water*, 17, No. 5, 429-437.
- Barcelona, M.J., Gibb, J.P., and Miller, R.A., 1983. A guide to the selection of materials for monitoring well construction and ground-water sampling. Illinois State Water Survey, ISWS Contract Report 327, 78p.
- Basharmal, M., 1985. Isotopic composition of aqueous sulphur at landfill sites. Unpubl. MSc. Thesis. University of Waterloo.
- Benson, R.C., Glaccum, R.A., and Noel, M.R., 1982. Geophysical techniques for sensing buried wastes and waste migration. Environmental Monitoring Systems Laboratory, Office of Research and Development, U.S. EPA, 236 p.
- Canter, L.W., Knox, R.C., and Fairchild, D.M., 1987. Ground water quality protection. Lewis Publishers, Inc., U.S.A., 562p.
- Cherry, J.A., 1983. Occurrence and migration of contaminants in groundwater at municipal landfills on sand aquifers. *The Environment and Solid Wastes*, Oak Ridge Life Sciences Series, Ann Arbour Press, 127-138.
- Chapman, L.J., and Putnam, D.F., 1973. The physiography of southern Ontario. Ontario Research Foundation, Toronto, 386 p.
- Costa, J.E., and Baker, V.C., 1981. Surficial geology. Building with the earth. John Wiley & Sons, Inc., Canada, 498p.

- Craig, H., 1961a. Isotopic variations in meteoric waters. *Science*, 133, 1702-1703.
- Craig, H., 1961b. Standards for reporting concentrations of deuterium and oxygen-18 in natural waters. *Science*, 133, 1833-1834.
- Dansgaard, W., 1964. Stable isotopes in precipitation. *Tellus*, 16, 436-468.
- Desaulniers, D.E., Cherry, J.A., and Fritz, P., 1981. Origin, age and movement of pore water in argillaceous Quaternary deposits at four sites in southwestern Ontario. *Journal of Hydrology*, 50, 231-257.
- Drever, J., 1982. The geochemistry of natural waters. Prentice Hall Inc., New Jersey, 388p.
- Driscoll, F.G., 1986. Groundwater and wells. Johnson Division, St. Paul, Minnesota, 1089p.
- Egboka, B.C.E., Cherry, J.A., Farvolden, R.N., and Frind, E.O., 1983. Migration of contaminants at a landfill: a case study. 3. Tritium as an indicator of dispersion and recharge. *Journal of Hydrology*, 63, 51-80.
- Essop, S., and Brown, D., 1980. Well contamination investigations in Gosfield South and Mersea Townships near Essex County Landfill No. 2. Draft. MOE Southwestern Region.
- Experimental Farms Service, 1947. Soil map of Essex County, Ontario. Soil Survey Report No. 11, Ottawa, Scale 1:63,360.
- Freeze, R.A., and Cherry, J.A., 1979. Groundwater. Prentice-Hall, Inc., New Jersey, 604p.
- Fritz, P., and Fontes, J.C., 1980. Handbook of environmental isotope geochemistry. Volume 1: the terrestrial environment. Elsevier Scientific Publishing Company, Amsterdam, Oxford, 1-179.
- Fritz, P., Matthes, G., and Brown, R.M., 1976. Deuterium and oxygen-18 as indicators of leachwater movement from a sanitary landfill. Interpretation of Environmental Isotope and Hydrochemical Data in Groundwater Hydrology, IAEA, Vienna, 131-142.

- Fritz, P., Drimmie, R.J., and Render, F.W., 1975. Stable isotope contents of a major prairie aquifer in central Manitoba, Canada. *Isotope Techniques in Groundwater Hydrology 1974* (Proc. Symp. Vienna, 1974) 1, IAEA, 379-397.
- Garrels, R.M., and Christ, C.L., 1965. *Solutions, minerals and equilibria*. Harper and Row, New York, 450p.
- Gartner Lee Associates Limited, 1986. *Leachate management aspects*. Final report. Hydrogeological/geotechnical component. Essex County Landfill Site No. 2.
- Gilkeson, R.H., and Cartwright, K., 1983. The application of surface electrical and shallow geothermic methods in monitoring network design. *Groundwater Monitoring Review*, 3, No. 3, 30-41.
- Gillham, R.W., Hendry, M.J., Cherry, J.A., Frind, E.O., and Pucovsky, G.M., 1978. Studies of the agricultural contribution to nitrate enrichment of groundwater and the subsequent nitrate loading to surface waters. Part 1. Field investigations of the processes controlling the transport of nitrate in groundwater. University of Waterloo Research Institute, Project No. 41122, 203p.
- Hem, J.D., 1970. Study and interpretation of the chemical characteristics of natural water. Geological Survey Water-supply Paper 1473, Washington, 363p.
- Hoefs, J., 1973. *Stable isotope geochemistry*. Springer Valley, New York, 140p.
- Hvorslev, M.J., 1951. Time lag and soil permeability in ground-water observations. Waterway Experiment Station, Corps of Engineers, U.S. Army, Bulletin No. 36, 50p.
- I.A.E.A., 1979. Environmental isotope data. World summary of isotope concentrations in precipitation (1953-1975). I.A.E.A. Technical Report Series 96, 117, 129, 147, 165, 192.
- Kunkle, G.R., and Shade, J.W., 1976. Monitoring ground-water quality near a sanitary landfill. *Ground Water*, 14, No. 1, 11-20.
- Lambe, T.W., 1951. *Soil testing for engineers*. Series in soil engineering. John Wiley and Sons, New York, 165p.

- Langmuir, D., 1971. The geochemistry of some carbonate ground waters in central Pennsylvania. *Geochimica et Cosmochimica Acta*, 35, 1023-1045.
- Lee, R.D., and Cherry, J.A., 1978. A field exercise on groundwater flow using seepage meters and minipiezometers. *Journal of Geological Education*, 27, 6-10.
- MacFarlane, D.J., Cherry, J.A., Gillham, R.W., and Sudicky, E.A., 1983. Migration of contaminants in groundwater at a landfill: a case study. 1. Groundwater flow and plume delineation. *Journal of Hydrology*, 63, 1-29.
- McKeague, J.A., 1978. Manual on soil sampling and methods of analysis. 2nd ed. Canadian Society of Soil Science, Canada, 212p.
- Ministry of the Environment 1984. Water well records for Ontario - Essex County 1946-1984. Bulletin 2-19, Groundwater Series, Toronto.
- Orpwood, T.G., 1984. An evaluation of methods used to measure groundwater flow and transport characteristics in clayey deposits at two sites in Essex County, Ontario. Unpubl. MASc thesis.
- Paul, D.G., Palmer, C.D., and Cherkauer, D.S., 1988. The effect of construction, and development on the turbidity of water in monitoring wells in fine-grained glacial till. *Ground Water Monitoring Review*, 8, No. 1, 73-82.
- Postgate, J.R., 1979. The sulphate-reducing bacteria. Cambridge University Press, Cambridge, 151p.
- Proctor and Redfern Limited 1985. Pre-design report. Leachate management alternatives. Board of Management. Essex County Landfill Site No. 2.
- Rand, M.C., and Greenberg, A.E., Taras, M.J., 1975. Standard methods for the examination of water and wastewater. 14th ed. APHA-AWWA-WPCF, U.S.A., 1193p.
- Reardon, E.J., Dance, J.T., and Lolcama, J.L., 1983. Field determination of cation exchange properties for calcareous sand. *Ground Water*, 4, No 4, 421-428.
- Sanderson, M., 1980. The climate of the Essex region, Canada's southland. University of Windsor, 105 p.
- Sanford, B.V., 1969. Geology Toronto-Windsor area Ontario. Geol. Surv. Canada, Map 1236A, Scale 1:250,000.

- SAS, 1982. SAS user's guide: statistics. SAS Institute Inc., Cary, North Carolina, 584p.
- Saxena, R.K., 1987. Oxygen-18 fractionation in nature and estimation of groundwater recharge. Uppsala University, Report Series A, No. 4, 152p.
- Snoeyink, V.L., and Jenkins, D., 1980. Water chemistry. John Wiley and Sons, Inc., U.S.A., 463p.
- Sklash, M.G., 1983. The feasibility of using environmental isotopes for streamflow hydrograph separations in the Apios calibrated watersheds. Industrial Research Institute of the University of Windsor, IRI 16-15, 74p.
- Sklash, M.G., Mason, S., and Scott, S., 1986. An investigation of the quantity, quality and sources of groundwater seepage into the St. Clair River near Sarnia, Ontario, Canada. Water Pollution Research Journal of Canada, 21, No. 3, 351-367.
- Stewart, G.L., 1967. Fractionation of tritium and deuterium in soil water. Isotope Techniques in the Hydrologic Cycle, Geophysical Monograph No. 11, 159-168.
- Stewart, G.L., 1980. The behaviour of tritium in the soil. Tritium, Tritium Symposium 1971, 462-470.
- Stiff, H.A., Jr., 1951. The interpretation of chemical water analysis by means of patterns. Jour. Petroleum Technology, 4, 273-289.
- Stumm, W., and Morgan, J.J., 1970. Aquatic chemistry. An introduction emphasizing chemical equilibria in natural waters. John Wiley and Sons, U.S.A., 583p.
- Surveys and Mapping Branch, 1970. Kingsville Essex County, Ontario. Dept. of Energy, Mines and Resources, Scale 1:25,000.
- Surveys and Mapping Branch, 1970. Leamington Essex County-Mersea Township, Ontario. Dept. of Energy, Mines and Resources, Scale 1:25,000.
- Telford, W.M., Geldart, L.P., Sheriff, R.E., and Keys, D.A. 1976. Applied geophysics. Cambridge University Press, Cambridge, 859 p.
- Vagners, U.J. 1972. Quaternary geology of the Windsor-Essex area (eastern part) southern Ontario. Ontario Dept. Mines and Northern Affairs, Prelim. Map P750, Geol. Ser., Scale 1:50,000.

- Vagners, U.J., 1972. Granular potential of the Windsor -Essex area (eastern part) southern Ontario. Ontario Div. Mines, Prelim. Map P578, Scale 1:50,000.
- Vagners, U.J., Sado, E.V., and Yundt, S.E., 1973. Drift thickness of the Windsor-Essex area (eastern part) southern Ontario. Ontario Div. Mines, Prelim. Map P815, Drift Thickness Ser., Scale 1:50,000.
- Van Duijvenbooden, W., 1985. Effects of local sources of pollution on ground water quality in the Netherlands. Ground Water Quality, John Wiley and Sons, Inc., U.S.A., 68-93.
- Yazicigil, H., and Sendlein, V.A., 1982. Surface geophysical techniques in groundwater monitoring part II. Groundwater Monitoring Review, 2, No. 1, 56-61.

APPENDIX I

BOREHOLE LOGS

FOR

SUNNY CREEK SANITARY LANDFILL SITE NO. 2

APPENDIX I
BOREHOLE LOGS

The following information was obtained from the borehole logs and descriptions used in the borehole logs.

The location of the piezometer is shown above the log and was surveyed in using the surveyed points. The water level piezometer is shown as follows:

The ground surface of geological

APPENDIX I
BOREHOLE LOGS
FOR
ESSEX COUNTY SANITARY LANDFILL SITE NO. 2

The following symbols denote representative symbols denoting material in the piezometer screen, natural backfill and

The following symbols denote the identification of the material in the piezometer screen, natural backfill and

The piezometer was surveyed using a split spoon (ss) sampler.

The following symbols denote a determination of hydraulic conductivity, porosity, and bulk density. These parameters were commonly determined on the samples.

EXPLANATION OF THE FORM OF THE BOREHOLE LOGS

This explanatory section provides the user with background to the headings and descriptions used in the borehole logs.

SUBSURFACE PROFILE

Elevation:

Elevation is the location of the piezometer in metres above sea level. Elevations were surveyed in using the surveyed elevations of Gartner Lee Limited piezometers as bench marks.

Depth:

Depth is the distance below ground surface of geological contacts.

Description:

This column gives a description of subsurface material based on visual interpretation of soil samples and auger cuttings.

Piezometer Description:

Piezometer description gives representative symbols denoting locations of the piezometer screen, natural backfill and bentonite seal.

SAMPLES

Number:

The sample number is a numerical identification of the borehole location and the location where each sample was obtained in the borehole.








Type:

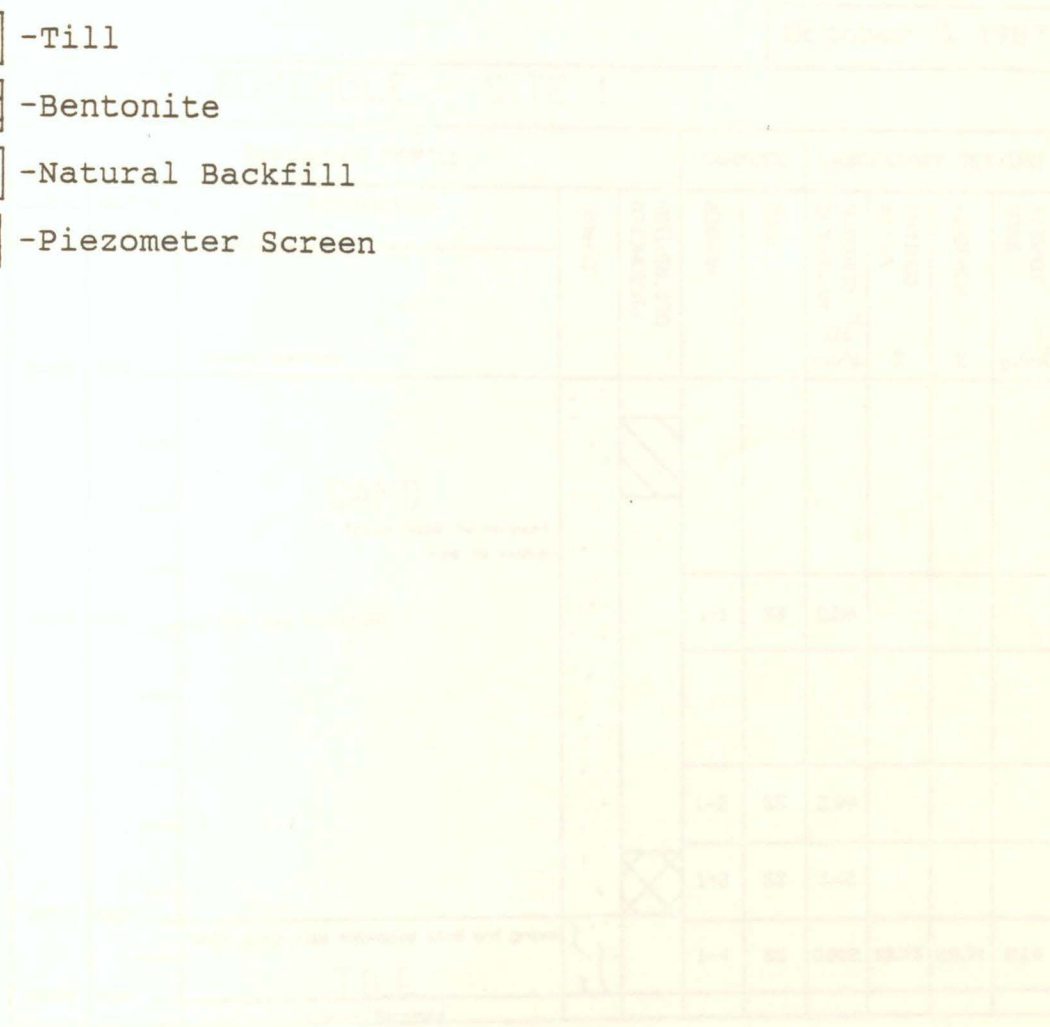
All samples were obtained using a split spoon (ss) sampler.

LABORATORY TESTING

Laboratory testing involved a determination of hydraulic conductivity, water content, porosity, and bulk density where possible. All four parameters were commonly determined for the cohesive samples.

MONITOR LEGEND

-  -Topsoil
-  -Sand
-  -Silt
-  -Till
-  -Bentonite
-  -Natural Backfill
-  -Piezometer Screen



October 5, 1987

LOG OF BOREHOLE - SITE 1											
SUBSURFACE PROFILE					SAMPLES		LABORATORY TESTING				
ELEV. m	DEPTH m	DESCRIPTION	SYMBOL	PIEZOMETER DESCRIPTION	NUMBER	TYPE	HYDRAULIC CONDUCT. $\times 10^{-2}$ cm/s	WATER CONTENT %	POROSITY %	BULK DENSITY g/cm ³	
213.37	0.00	Ground Surface									
		<p style="text-align: center;">SAND</p> <p style="text-align: center;">Brown loose to compact Fine to medium</p> <p>Thin clay lamination</p>									
211.40	1.98				1-1	SS	2.56				
					1-2	SS	2.89				
					1-3	SS	3.42				
209.10	4.27				Soft grey clay embedded sand and gravel			1-4	SS	0.002	13.75
203.00	4.88	TILL									
		End of Borehole									

October 7, 1987

LOG OF BOREHOLE - SITE 2										
SUBSURFACE PROFILE					SAMPLES		LABORATORY TESTING			
ELEV. m	DEPTH m	DESCRIPTION	SYMBOL	PIEZOMETER DESCRIPTION	NUMBER	TYPE	HYDRAULIC CONDUCT. $\times 10^{-2}$ cm/s	WATER CONTENT %	POROSITY %	BULK DENSITY g/cm ³
214.59	0.00	Ground Surface								
		Grey medium Gravelly	▨		2-1	SS	1.44			
		SAND	·							
		Light brown fine to medium	·		2-2	SS	0.90			
		Fine	·		2-3	SS	2.89			
	3.80	Coarse gravel	·		2-4	SS	1.44			
	4.11		·							
		Dark grey coarse	▩		2-5	SS	3.24			
	4.82	Soft silty clay Embedded sand and gravel	·		2-6	SS	0.003	9.78	20.61	2.29
209.10	5.49	TILL	·							
		End of Borehole								

October 8, 1987

LOG OF BOREHOLE - SITE 3										
SUBSURFACE PROFILE					SAMPLES		LABORATORY TESTING			
ELEV. m	DEPTH m	DESCRIPTION	SYMBOL	PIEZOMETER DESCRIPTION	NUMBER	TYPE	HYDRAULIC CONDUCT. $\times 10^{-4}$ cm/s	WATER CONTENT %	POROSITY %	BULK DENSITY g/cm ³
214.02	0.00	Ground Surface								
		Brown Fine to medium SAND	· · · · ·		3-1	SS	2.25			
					3-2	SS	3.42			
		Clayey	· · · · ·							
210.67	3.35				3-3a	SS	0.003	14.08	28.06	2.16
					3-3b	SS	0.003	15.22	31.28	2.08
		Grey silty clay Embedded sand and gravel	· · · · ·							
		TILL	· · · · ·		3-4	SS	0.001	14.32	30.59	2.09
					3-5	SS	0.001	12.62	26.18	2.19
	7.92									
		SILT Grey clayey	· · · · ·		3-6	SS	0.016	7.45	16.15	2.38
5.79	8.23	End of Borehole								

October 8, 1987

LOG OF BOREHOLE - SITE 4

SUBSURFACE PROFILE			SAMPLES		LABORATORY TESTING						
ELEV. n	DEPTH n	DESCRIPTION	SYMBOL	PIEZOMETER DESCRIPTION	NUMBER	TYPE	HYDRAULIC CONDUCT. x10 cm/s	WATER CONTENT %	POROSITY %	BULK DENSITY g/cm	
215.28	0.00	Ground Surface									
		SAND Brown Fine to medium	.	/ /							
					4-1	SS	2.89				
					4-2	SS	2.23				
					4-3	SS	2.89				
211.96	3.32	Grey coarse Gravel	◇								
		Soft grey silty clay. Embedded sand and gravel	?		4-4	SS	0.008	13.96	27.53	2.17	
211.32	3.96	TILL End of Borehole	?								

October 7, 1987

LOG OF BOREHOLE - SITE 6

SUBSURFACE PROFILE				SAMPLES		LABORATORY TESTING				
ELEV. ft	DEPTH ft	DESCRIPTION	SYMBOL	PIEZOMETER DESCRIPTION	NUMBER	TYPE	HYDRAULIC CONDUCT. $\times 10^{-2}$ cm/sec	WATER CONTENT %	POROSITY %	BULK DENSITY g/cm ³
218.55	0.00	Ground Surface								
	0.30	TOPSOIL								
		Reddish brown coarse to medium Gravel			6-1	SS	2.56			
		Brown			6-2	SS	4.20			
		SAND			6-3	SS	7.84			
		Grey fine to medium			6-4	SS	1.56			
		Gravel			6-5a					
212.00	6.53	SILT Grey clayey			6-5b	SS	1.56			
	6.86	Medium to coarse Gravel			6-5c		0.006			
		Brown Fine to medium			6-6a		0.006			
		SAND			6-6b	SS	3.06			
					6-7	SS	1.96			
					6-8	SS	2.56			
					6-9	SS	2.89			
208.80	9.75	Grey silty clay			6-10a	SS	2.02			
208.49	10.06	TILL Embedded sand and gravel End of borehole			6-10b	SS	0.002	12.70	26.98	2.17

October 5, 1987

LOG OF BOREHOLE - SITE 7A,7B

SUBSURFACE PROFILE					SAMPLES		LABORATORY TESTING			
ELEV. m	DEPTH m	DESCRIPTION	SYMBOL	PIEZOMETER DESCRIPTION	NUMBER	TYPE	HYDRAULIC CONDUCT. x10 cm/s	WATER CONTENT %	POROSITY %	BULK DENSITY g/cm
214.16	0.00	Ground Surface								
	0.30	TOPSOIL	~		A-1	SS	4.00			
		Reddish brown Medium to coarse	▨							
		Brown Gravel	▧		A-2	SS	3.76			
		SAND	•••							
		Light brown Fine to medium	•••		A-3	SS	3.42			
	5.06		▨		A-4	SS	1.69			
	5.33	Reddish brown fine	•••		7-2a		1.69			
	5.49	Gravel	▧		7-2b	SS	1.69			
208.63		TILL	▨		7-2c		0.006	9.00	22.84	2.20
		Grey silty clay stones Dry grey Coarse to medium	▨		7-2d		1.69			
		Medium	•••		7-3	SS	4.41			
			▨		7-4	SS	2.89			
	7.32	Brown fine	•••		7-5a	SS	4.00			
		Grey medium	•••		7-5b		3.24			
		Brown medium	•••		7-6	SS	2.25			

Depth (m)	Soil Description	Soil Type	Moisture (%)	W _p (%)	W _L (%)	W _u (%)
7-7		SS	2.56			
7-8		SS	3.06			
7-9		SS	1.69			
7-10		SS	1.69			
7-11		SS	2.56			
7-12		SS	3.06			
7-13		SS	1.82			
7-14		SS	0.90			
7-15		SS	0.90			
7-16		SS	0.90			
7-17		SS				
7-18a						
7-18b		SS				
7-18c			0.001			
7-19a				8.60	19.79	2.29
7-19b		SS	0.003			
7-19c			0.002	14.42	30.74	2.09
7-20a			0.01			
7-20b		SS	0.002	8.25	18.48	2.33
7-20c			0.002	9.43	21.22	2.27
7-21		SS	10	14.35	33.01	2.02
14.20	Reddish brown					
15.12	Grey dense silt					
15.42	Grey silty clay stones					
15.54	Grey fine sand and gravel					
15.85	Grey silty clay stones					
16.15	Grey dense silty fine sand					
16.30	Grey coarse sand and gravel					
16.46	Grey dense silt					
	Grey silty clay					
	Embedded sand and gravel					
17.07	TILL					
17.37	Grey dense silt					
196.79	End of Borehole					

October 5, 1987

LOG OF BOREHOLE - SITE 8										
SUBSURFACE PROFILE					SAMPLES		LABORATORY TESTING			
ELEV. m	DEPTH m	DESCRIPTION	SYMBOL	PIEZOMETER DESCRIPTION	NUMBER	TYPE	HYDRAULIC CONDUCT. $\times 10^{-2}$ cm/s	WATER CONTENT %	POROSITY %	BULK DENSITY g/cm ³
213.29	0.00	Ground Surface								
	0.30	TOPSOIL	~							
		Reddish brown Medium to coarse	· · ·		8-1	SS	1.69			
	2.01	Gravel	—		8-2	SS	2.40			
		SAND	· · ·							
		Brown Fine to medium	· · ·		8-3	SS	3.06			
			· · ·		8-4	SS	2.40			
	4.72	Rust red coarse	· · ·	X	8-5a	SS	2.40			
208.41	4.88	Grey coarse	· · ·	X	8-5b	SS	3.24			
		Grey silty clay	· · ·							
		Embedded sand and gravel	· · ·		8-6	SS	0.006	17.15	32.07	2.08
207.80	5.49	TILL	· · ·							
		End of Borehole								

October 5, 1987

LOG OF BOREHOLE - SITE 9A, 9B											
SUBSURFACE PROFILE					SAMPLES		LABORATORY TESTING				
ELEV. m	DEPTH m	DESCRIPTION	SYMBOL	PIEZOMETER DESCRIPTION	NUMBER	TYPE	HYDRAULIC CONDUCT. $\times 10^{-2}$ cm/s	WATER CONTENT %	POROSITY %	BULK DENSITY g/cm ³	
215.75	0.00	Ground Surface									
	0.20	TOPSOIL									
		Reddish brown Fine			9-1	SS	2.82				
		SAND									
						9-2	SS	14.44			
						9-3	SS	4.62			
						9-4	SS	2.31			
						9-5	SS	2.89			
	5.67		Dense fine								
					9-6	SS	3.06				
		Boulder									
					9-7a	SS	3.06				
208.47	7.32	Grey silty clay			9-7b		0.016	14.99	27.21	2.21	
208.13	7.62	TILL Embedded sand and gravel									
		End of Borehole									

October 7, 1987

LOG OF BOREHOLE - SITE 10

SUBSURFACE PROFILE					SAMPLES		LABORATORY TESTING			
ELEV. m	DEPTH m	DESCRIPTION	SYMBOL	PIEZOMETER DESCRIPTION	NUMBER	TYPE	HYDRAULIC CONDUCT. $\times 10^{-4}$ cm/s	WATER CONTENT %	POROSITY %	BULK DENSITY g/cm ³
215.61	0.00	Ground Surface								
	0.30	TOPSOIL	~		10-1	SS	2.25			
		Reddish brown Fine to medium Gravel	•••							
		Light brown Fine to medium	•••		10-2	SS	2.25			
		SAND	•••							
		Fine	•••		10-3	SS	1.96			
	4.88		•••		10-4a		4.00			
	5.03	Rust red fine to medium	•••		10-4b	SS	0.64			
	5.18	Gravel Grey medium to coarse	•••		10-4c		1.32			
		Brown fine to medium	•••		10-5a	SS	3.80			
210.12	5.49	Grey silty clay	~	?	10-5b		0.003	13.33	27.50	2.16
209.82	5.79	TILL Embedded sand and gravel End of borehole	~							

October 11, 1987

LOG OF BOREHOLE - SITE 11										
SUBSURFACE PROFILE					SAMPLES		LABORATORY TESTING			
ELEV. m	DEPTH m	DESCRIPTION	SYMBOL	PIEZOMETER DESCRIPTION	NUMBER	TYPE	HYDRAULIC CONDUCT. $\times 10^{-2}$ cm/s	WATER CONTENT %	POROSITY %	BULK DENSITY g/cm ³
215.78	0.00	Ground Surface								
	0.30	TOPSOIL	~							
		Reddish brown Fine to medium	.		11-1	SS	1.69			
			.		11-2a		0.90			
	1.00	Clayey	.		11-2b	SS	0.006			
			.		11-3	SS	2.02			
			.		11-4	SS	2.31			
			.		11-5	SS	3.20			
			.		11-6	SS	2.99			
			.		11-7	SS	3.24			
			.		11-8	SS	3.61			
	4.70	Dense light brown fine	.							
		Brown fine	.		11-9a	SS	3.61			
210.60	5.18	Grey silty clay Embedded sand and gravel	~		11-9b		0.56	13.58	28.06	2.15
		TILL	~		11-10	SS		13.95	29.26	2.12
209.68	6.10	End of Borehole								

October 6, 1987

LOG OF BOREHOLE - SITE 12

SUBSURFACE PROFILE					SAMPLES		LABORATORY TESTING			
ELEV. m	DEPTH m	DESCRIPTION	SYMBOL	PIEZOMETER DESCRIPTION	NUMBER	TYPE	HYDRAULIC CONDUCT. $\times 10^2$ cm/s	WATER CONTENT %	POROSITY %	BULK DENSITY g/cm ³
214.57	0.00	Ground Surface								
	0.30	TOPSOIL	~		12-1	SS	2.10			
		Reddish brown Fine to medium	•••••							
		SAND	•••••		12-2	SS	3.61			
		Brown	•••••							
211.52	3.05	TILL	•••••		12-3a	SS	<10 ⁻³	16.22	31.27	2.10
	3.20	Grey silty clay	•••••		12-3b	SS	2.10			
	3.40	Grey fine sand	•••••		12-3c	SS	0.002	14.71	31.59	2.06
	3.66	TILL	•••••		12-4a	SS	1.44			
	3.81	Grey silty clay	•••••		12-4b	SS	0.003	14.83	30.08	2.12
210.10	4.27	TILL	•••••							
		Embedded sand and gravel	•••••							
		End of Borehole								

October 7, 1987

LOG OF BOREHOLE - SITE 13

SUBSURFACE PROFILE					SAMPLES		LABORATORY TESTING			
ELEV. m	DEPTH m	DESCRIPTION	SYMBOL	PIEZOMETER DESCRIPTION	NUMBER	TYPE	HYDRAULIC CONDUCT. $\times 10^{-2}$ cm/s	WATER CONTENT %	POROSITY %	BULK DENSITY g/cm ³
215.06	0.00	Ground Surface								
	0.17	TOPSOIL								
		Brown fine to medium Organics and gravel			13-1a	SS	0.81			
		Gravel Brown clayey fine Coarse to medium			13-1b	SS	3.24			
	0.70	Dark brown Coarse to medium Gravel			13-2	SS	2.40			
		SAND								
		Fine			13-3	SS	2.89			
					13-4	SS	1.82			
212.17	2.83	Grey silty clay Embedded sand and gravel			13-5a	SS	2.72			
211.65	3.35	TILL			13-5b	SS	0.001	14.80	30.96	2.09
		End of Borehole								

October 7, 1987

LOG OF BOREHOLE - SITE 14

SUBSURFACE PROFILE				SAMPLES		LABORATORY TESTING				
ELEV. m	DEPTH m	DESCRIPTION	SYMBOL	PIEZOMETER DESCRIPTION	NUMBER	TYPE	HYDRAULIC CONDUCT. $\times 10^{-2}$ cm/s	WATER CONTENT %	POROSITY %	BULK DENSITY g/cm ³
214.67	0.00	Ground Surface								
	0.20	TOPSOIL	~							
		Reddish brown Medium to coarse Sand	· · ·		14-1	SS	3.42			
		Dry dense friable Silty clay	· · ·		14-2a 14-2b	SS	0.001 <10 ⁻³			
	1.98	Grey silty clay Embedded sand and gravel	} · ·							
		TILL	} · ·							
211.32	3.35	Grey clayey gravel	· · ·		14-3a 14-3b 14-3c	SS	0.001 0.01 0.02	14.73 15.47	30.38 30.16	2.10 2.13
	3.51	Grey silty clay Embedded sand and gravel	} · ·							
		TILL	} · ·							
209.49	5.18	End of Borehole	· · ·		14-4	SS	0.01	17.47	33.59	2.06

October 8, 1987

LOG OF BOREHOLE - SITE 15										
SUBSURFACE PROFILE					SAMPLES		LABORATORY TESTING			
ELEV. m	DEPTH m	DESCRIPTION	SYMBOL	PIEZOMETER DESCRIPTION	NUMBER	TYPE	HYDRAULIC CONDUCT. $\times 10^{-4}$ cm/s	WATER CONTENT %	POROSITY %	BULK DENSITY g/cm ³
215.00	0.00	Ground Surface								
	0.30	TOPSOIL			15-1	SS	2.40			
		Reddish brown Medium Gravel								
		SAND								
		Dark brown Medium			15-2	SS	7.29			
		Fine to medium			15-3a	SS	2.40			
	3.54	Fine			15-3b		2.40			
					15-4a	SS	3.42			
210.98	4.02	Grey silty clay			15-4b		0.003	12.38	25.71	2.21
210.73	4.27	Embedded sand and gravel End of Borehole		2.2						

October 6, 1987

LOG OF BOREHOLE - SITE 16

SUBSURFACE PROFILE				SAMPLES		LABORATORY TESTING				
ELEV. m	DEPTH m	DESCRIPTION	SYMBOL	PIEZOMETER DESCRIPTION	NUMBER	TYPE	HYDRAULIC CONDUCT. $\times 10^{-2}$ cm/s	WATER CONTENT %	POROSITY %	BULK DENSITY g/cm ³
214.82	0.00	Ground Surface								
	0.30	Reddish brown Coarse to medium Gravel	{ }		16-1	SS	4.20			
		Brown Fine to medium Fine black laminations	{ }		16-2	SS	1.00			
	3.05	SAND Black Coarse to medium Brown Fine to medium	{ }		16-3a	SS	3.31			
		Gravel	{ }		16-3b	SS	2.62			
			{ }		16-4	SS	1.69			
			{ }		16-5	SS	2.02			
		Dark brown	{ }		16-6	SS	0.72			
209.33	5.49	Grey silty clay Embedded sand and gravel	{ }		16-7	SS	0.017	12.26	27.72	2.14
208.15	6.10	TILL	{ }							
		End of Borehole								

October 6, 1987

LOG OF BOREHOLE - SITE 17										
SUBSURFACE PROFILE					SAMPLES		LABORATORY TESTING			
ELEV. m	DEPTH m	DESCRIPTION	SYMBOL	PIEZOMETER DESCRIPTION	NUMBER	TYPE	HYDRAULIC CONDUCT. $\times 10^{-2}$ cm/s	WATER CONTENT %	POROSITY %	BULK DENSITY g/cm ³
211.73	0.00	Ground Surface								
	0.30	TOPSOIL	⋄							
		Reddish brown Fine to medium	⋄		17-1	SS	225			
		SAND	⋯							
		Grey fine to medium	⋯		17-2	SS	262			
		Brown	⋯		17-3	SS	121			
	2.74	Brown-red medium to coarse	⋯		17-4a		3.06			
	3.05	Grey-red laminated fine to medium	⋯		17-4b	SS	0.96			
	3.25	Gravel Grey medium	⋄		17-4c		1.96			
		Fine	⋯		17-5a	SS	0.96			
207.92	3.81	TILL Grey silty clay stones	⋄		17-5b		0.002	15.31	31.49	2.08
207.77	3.96	End of Borehole								

APPENDIX II

GRAIN SIZE DISTRIBUTION CURVES
(M.I.T. Classification System)

GRAVEL		2.0 - 50.0 mm
	Coarse	0.6 - 2.0 mm
SAND	Medium	0.2 - 0.6 mm
	Fine	0.05 - 0.2 mm
	Coarse	0.02 - 0.05 mm
SILT	Medium	0.006 - 0.02 mm
	Fine	0.0002 - 0.006 mm
CLAY		< 0.0002 mm

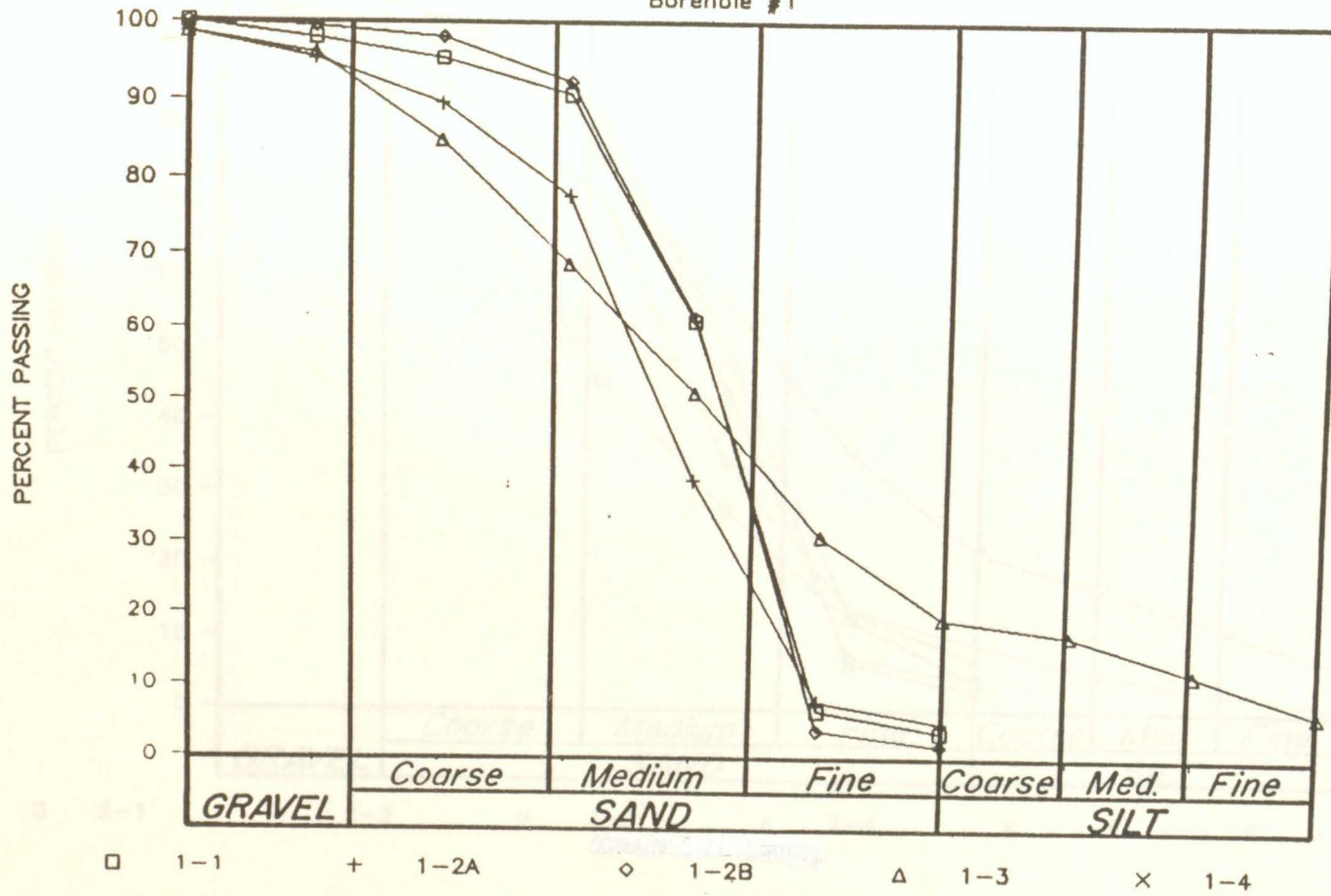
SAMPLE	SIEVE SIZE ANALYSIS						
	4 PASSING (%)	8 PASSING (%)	16 PASSING (%)	30 PASSING (%)	50 PASSING (%)	100 PASSING (%)	200 PASSING (%)
1-1	99.70	98.83	96.05	87.71	43.16	13.45	6.66
1-2A	93.72	91.36	88.43	80.90	50.12	18.34	7.55
1-2B	100.00	99.92	98.64	86.58	62.32	38.13	21.65
1-3	98.19	96.92	92.23	69.85	28.29	11.83	6.58
1-4	98.75	97.10	93.99	89.27	46.16	10.17	5.47
1-5	99.22	98.87	96.31	81.91	29.55	6.03	3.01
1-6	99.33	98.10	95.84	88.62	50.91	7.47	3.70
1-7	96.18	93.34	88.18	72.37	30.05	6.30	3.88
1-8	90.68	88.60	84.52	74.70	39.39	5.04	2.53
1-9A	99.55	98.75	96.55	89.20	48.15	4.95	2.67
1-9B	98.71	96.75	89.82	79.85	65.69	38.92	9.84
2-1	98.23	96.96	94.77	86.57	42.53	8.58	3.89
2-2	94.06	84.55	52.24	18.99	5.25	2.33	1.18
2-3	99.67	99.29	97.85	85.66	23.55	3.35	1.65
2-4	99.74	99.20	97.63	92.52	48.37	10.16	5.89
2-5	98.36	97.97	96.63	90.58	50.72	7.81	3.32
2-6	99.90	99.12	97.50	91.41	58.98	6.16	2.79
2-7A	98.21	96.50	93.89	87.50	58.93	7.81	3.52
2-7B	98.90	97.14	91.32	81.09	64.14	36.87	14.34
3-1	70.65	68.74	64.30	52.39	26.84	11.66	6.79
3-2	83.19	77.84	71.49	60.46	30.00	9.11	5.13
3-3	99.75	99.39	98.02	91.36	47.40	6.62	3.54
3-4	96.79	95.70	93.97	85.94	50.54	9.70	4.80
3-5A	98.72	98.35	97.67	95.32	66.09	9.95	3.14
3-5B	91.22	83.32	72.01	61.75	33.41	6.02	2.51
3-6	99.18	97.09	88.77	75.19	59.35	37.54	15.11
4-1	96.36	89.97	76.73	48.53	18.57	6.06	3.02
4-2	80.85	72.37	60.10	39.02	13.72	6.49	3.96
4-3	99.89	99.80	99.42	92.36	36.73	5.18	2.75
4-4	99.72	99.38	98.87	97.03	68.68	11.86	4.79
5-1	99.05	96.92	92.59	82.09	33.82	8.15	4.88
5-2A	98.59	94.90	89.87	83.36	48.98	12.97	6.04
5-2B	58.06	43.36	35.10	28.45	19.83	11.40	7.68
5-2C	88.44	84.51	77.93	66.99	51.02	33.53	20.48
5-2D	88.66	73.42	52.91	34.79	20.13	12.35	7.64
5-3	88.15	72.41	49.05	28.13	14.48	7.10	4.30
5-4	96.38	92.61	73.41	38.61	18.23	10.56	6.94
5-5A	100.00	100.00	99.13	94.63	54.87	6.47	2.96
5-5B	99.24	96.57	79.52	40.23	16.93	8.99	6.11
5-6	98.76	96.68	85.25	51.07	21.52	10.58	6.58
5-7	99.54	98.22	91.20	57.92	20.90	9.95	6.57
5-8	99.74	98.96	92.83	55.12	18.79	8.88	5.91
5-9	99.57	98.36	89.81	60.30	22.97	9.71	5.50
5-10	99.05	97.91	87.45	53.87	21.81	11.20	6.87
5-11	99.60	97.60	84.95	48.05	20.18	10.46	6.32
5-12	91.79	81.59	64.05	38.13	17.70	9.97	6.27
5-13	90.31	78.98	64.93	44.96	22.19	11.24	6.68
5-14	100.00	99.97	99.82	98.69	72.85	19.34	7.31
5-15	100.00	100.00	99.92	99.64	84.38	19.03	6.11
5-16	100.00	100.00	99.93	99.75	90.16	22.17	5.22
5-17	100.00	100.00	99.91	99.81	99.56	80.72	24.42
5-18A	100.00	99.98	99.68	99.27	96.82	76.06	29.40
5-18B	100.00	100.00	100.00	99.86	99.67	98.49	41.34

SAMPLE	SIEVE SIZE ANALYSIS						
	4 PASSING (%)	8 PASSING (%)	16 PASSING (%)	30 PASSING (%)	50 PASSING (%)	100 PASSING (%)	200 PASSING (%)
11-3	72.86	52.43	33.71	19.21	10.48	6.17	3.72
11-4	98.63	95.97	89.43	71.46	44.30	13.41	4.96
11-5A	93.74	89.89	86.35	83.28	80.79	75.60	54.82
11-5B	95.34	94.78	90.17	78.39	48.81	11.77	8.81
11-5C	98.94	87.77	56.44	38.11	28.85	19.52	10.68
11-6A	95.19	91.78	87.25	81.80	75.29	64.14	41.10
11-6B	84.10	66.56	50.19	33.10	18.02	11.07	7.23
11-7	99.44	98.96	98.11	94.45	59.66	6.33	2.89
11-8	98.92	98.55	97.64	93.39	60.02	8.82	3.49
11-9	99.84	99.57	99.14	98.09	76.73	7.18	3.03
11-10A	99.87	99.69	99.18	97.78	78.22	9.97	4.82
11-10B	96.61	95.06	86.43	69.96	51.85	32.68	20.03
12-1	94.23	89.54	83.71	59.54	30.84	9.31	5.34
12-2	98.89	96.69	82.80	46.81	11.08	4.13	2.06
12-3A	96.91	93.66	87.15	73.02	38.98	8.74	4.98
12-3B	96.33	95.99	95.11	91.96	62.08	8.92	4.90
12-4A	96.59	94.90	92.40	85.99	50.97	4.56	2.15
12-4B	97.55	96.93	94.55	81.21	61.75	39.46	22.22
13-1	88.71	86.96	82.22	68.14	33.32	10.93	6.07
13-2	95.60	89.85	81.90	61.53	23.57	10.82	7.48
13-3	99.62	99.55	98.89	92.86	44.35	5.88	2.96
13-4A	99.58	98.74	96.27	87.69	42.17	3.69	2.02
13-4B	99.85	99.00	94.84	72.06	30.80	16.22	9.38
13-4C	84.61	77.69	69.64	57.88	35.22	14.67	5.85
13-5A	99.52	98.49	94.21	84.22	36.75	4.32	2.45
13-5B	98.74	97.30	87.79	71.45	52.54	33.89	21.16
14-1	97.00	89.64	71.83	45.71	27.44	12.53	4.22
14-2	96.57	91.89	82.45	70.21	33.92	14.07	9.13
14-3	97.94	96.60	92.65	81.48	43.99	7.46	4.16
14-4	96.43	93.21	89.14	80.48	48.66	13.51	7.19
14-5	96.43	93.40	88.32	79.22	51.17	6.39	2.61
14-6	98.79	97.84	91.11	75.36	56.50	35.10	21.58
15-1	99.09	97.83	94.27	78.88	45.44	11.32	3.62
15-2	99.66	97.99	94.86	83.21	43.53	5.43	3.19
15-3B	99.52	97.05	90.54	81.19	67.59	44.02	18.42
15-4	98.98	97.45	88.56	73.46	55.36	35.93	23.84
15-5	98.26	96.32	88.34	70.86	51.24	31.84	20.05
15-6	90.64	85.84	79.12	70.11	56.82	31.44	15.34
16-1	99.98	99.88	99.46	96.84	59.34	6.64	3.08
16-2	98.58	97.51	95.42	87.17	68.85	10.46	4.70
16-3	98.01	96.49	93.43	86.74	63.86	6.42	3.07
16-4	99.28	96.33	88.75	75.98	60.63	35.51	14.22
17-1	100.00	98.11	95.44	90.80	60.72	6.39	3.52
17-2	98.64	95.54	89.67	77.66	38.36	7.79	4.83
17-3	99.93	99.48	98.18	92.43	61.25	3.73	1.69
17-4	98.68	96.13	84.97	68.59	50.67	30.53	19.10

SAMPLE	SIEVE SIZE ANALYSIS						
	4 PASSING (%)	8 PASSING (%)	16 PASSING (%)	30 PASSING (%)	50 PASSING (%)	100 PASSING (%)	200 PASSING (%)
5-18C	95.71	91.85	85.51	75.43	66.17	56.93	47.55
5-19A	88.44	82.43	72.69	61.37	51.6	15.37	1.2
5-19B	100.00	100.55	100.42	96.19	88.87	83.31	60.86
5-19C	100.00	99.83	99.06	94.50	86.81	77.67	56.94
5-20A	97.24	94.82	88.05	72.77	57.44	45.16	35.16
5-20B	96.12	91.88	84.26	70.23	50.86	35.24	22.54
5-20C	93.46	90.47	84.08	70.82	52.94	36.48	23.85
5-21C	100.00	98.68	93.33	82.66	71.85	63.22	45.06
6-1	98.21	96.59	93.87	82.61	44.72	13.21	5.43
6-2	99.72	99.60	97.44	85.31	36.97	5.17	2.80
6-3A	98.85	97.47	89.66	75.53	58.20	39.33	24.34
6-3B	81.34	85.96	76.45	65.66	45.56	10.81	3.55
6-3C	98.65	97.58	93.05	81.87	66.87	48.16	32.31
6-4A	94.98	88.09	77.15	63.81	40.88	13.56	6.51
6-4B	95.77	94.34	84.56	69.21	51.44	31.58	19.99
7-1	94.68	90.56	84.70	68.06	19.68	5.67	3.97
7-2	100.00	100.00	99.81	98.72	90.71	25.05	3.04
7-3A	87.90	83.63	72.04	57.25	21.88	6.20	3.59
7-3B	99.87	99.80	99.15	96.03	70.83	7.10	2.86
7-4	99.71	99.07	97.16	92.92	75.44	12.84	3.98
7-5	99.49	98.60	97.03	91.86	66.80	11.09	4.49
7-6	99.96	99.85	99.24	96.93	84.76	29.07	5.30
7-8	99.32	97.67	92.19	83.81	67.42	41.36	14.47
8-1	99.72	98.98	96.89	82.09	32.87	10.25	5.57
8-2	100.00	99.52	98.47	91.53	51.91	7.64	3.48
8-3	99.88	99.80	99.46	98.10	74.62	14.43	7.29
8-4A	71.94	61.04	47.92	38.73	27.75	7.20	3.22
8-4B	98.81	97.62	95.74	93.40	89.74	29.94	3.72
8-4C	79.33	65.68	51.33	38.66	25.24	10.94	3.34
8-5A	91.71	88.47	84.09	79.89	69.10	23.53	4.78
8-5B	97.84	96.72	91.35	74.12	54.79	36.25	22.66
9-1	84.03	79.99	65.46	49.93	24.45	6.66	2.83
9-2A	99.67	98.32	90.13	73.21	54.58	36.22	22.33
9-2B	99.14	98.48	93.31	77.28	57.91	38.34	24.24
9-3A	96.31	92.29	89.28	79.88	63.87	23.90	18.52
9-3B	82.06	78.99	68.75	52.26	36.40	21.66	12.22
9-3C	96.65	95.08	85.95	69.88	50.32	30.86	12.61
9-4	97.51	93.08	76.90	58.70	40.82	24.78	12.72
S.P.	97.29	93.54	84.34	72.05	36.67	12.51	5.28
10-1A	93.32	89.32	82.26	64.62	37.63	16.39	8.63
10-1B	65.57	55.15	46.64	35.73	21.18	7.87	3.40
10-2	66.08	61.02	53.63	42.81	28.19	10.13	4.38
10-3	100.00	99.93	99.36	95.57	51.13	7.12	3.41
10-4	99.38	98.79	97.37	92.33	63.81	11.45	5.91
10-5A	100.00	99.35	98.67	93.22	58.27	7.21	3.18
10-5B	96.66	96.06	88.71	72.14	53.95	35.57	21.28
11-1	89.29	78.55	60.27	37.24	20.19	8.46	4.76
11-2	87.57	68.70	44.77	24.44	12.88	7.62	4.52

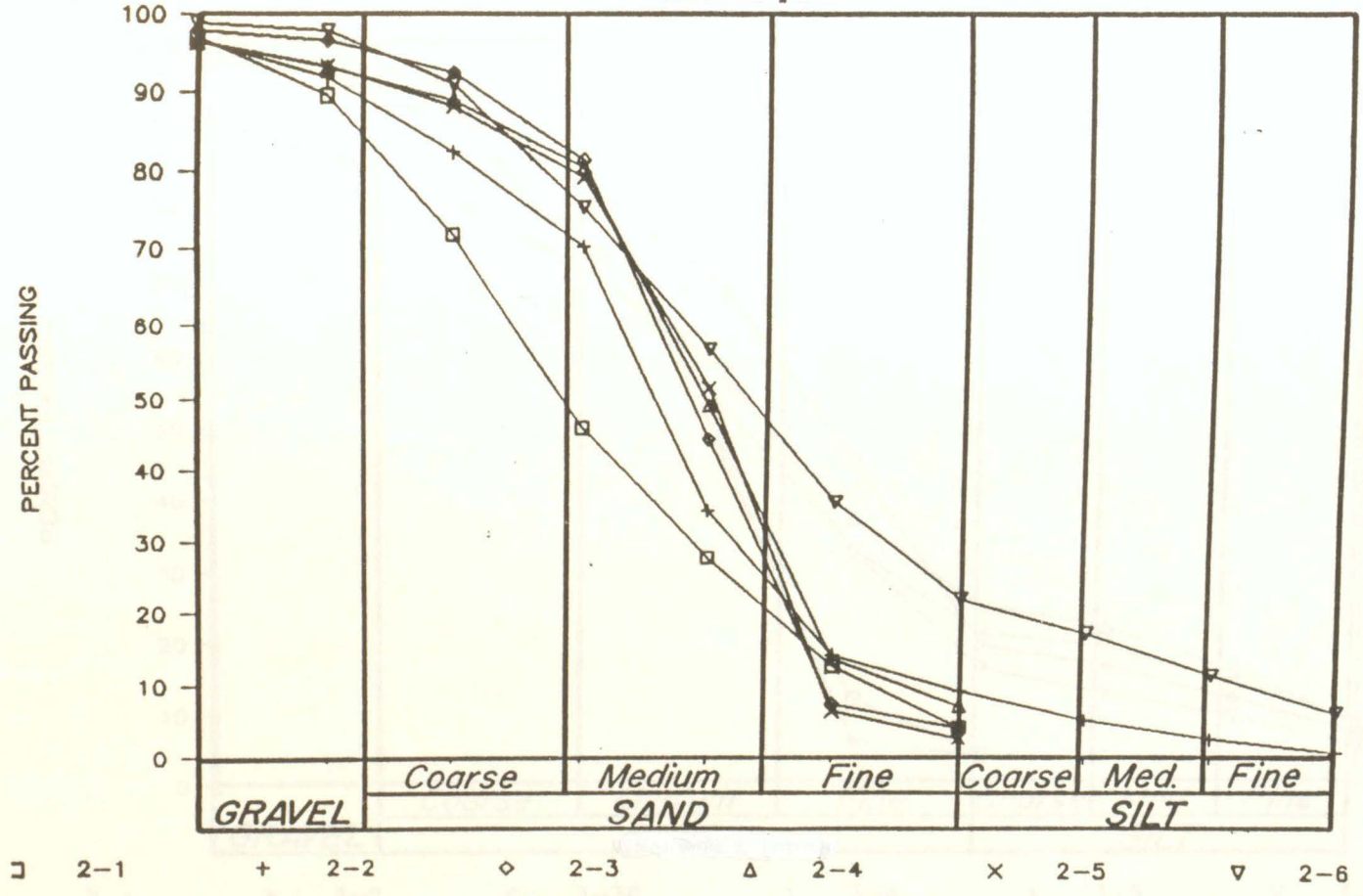
GRADATION ANALYSIS

Borehole #1



GRADATION ANALYSIS

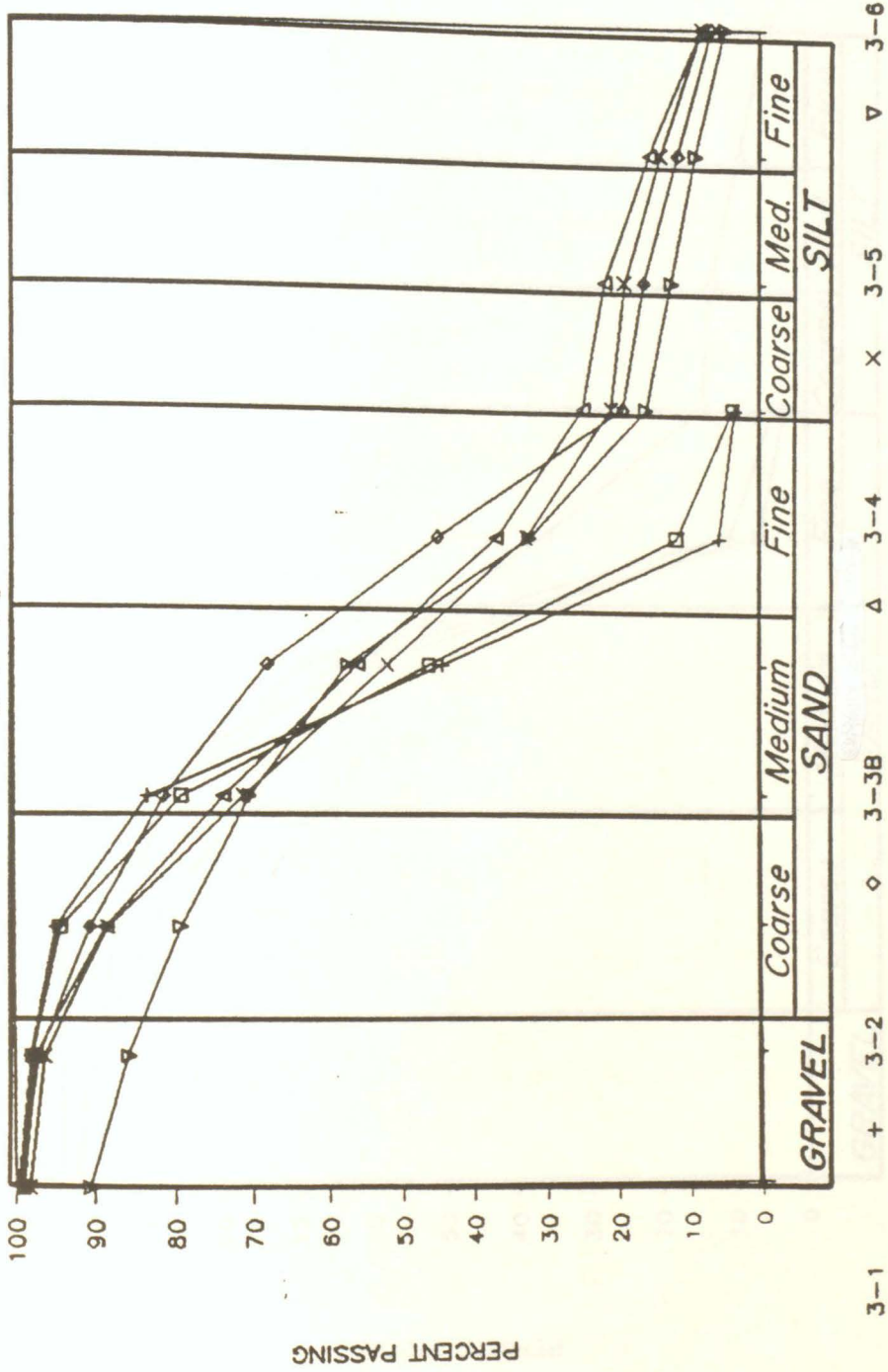
Borehole #2



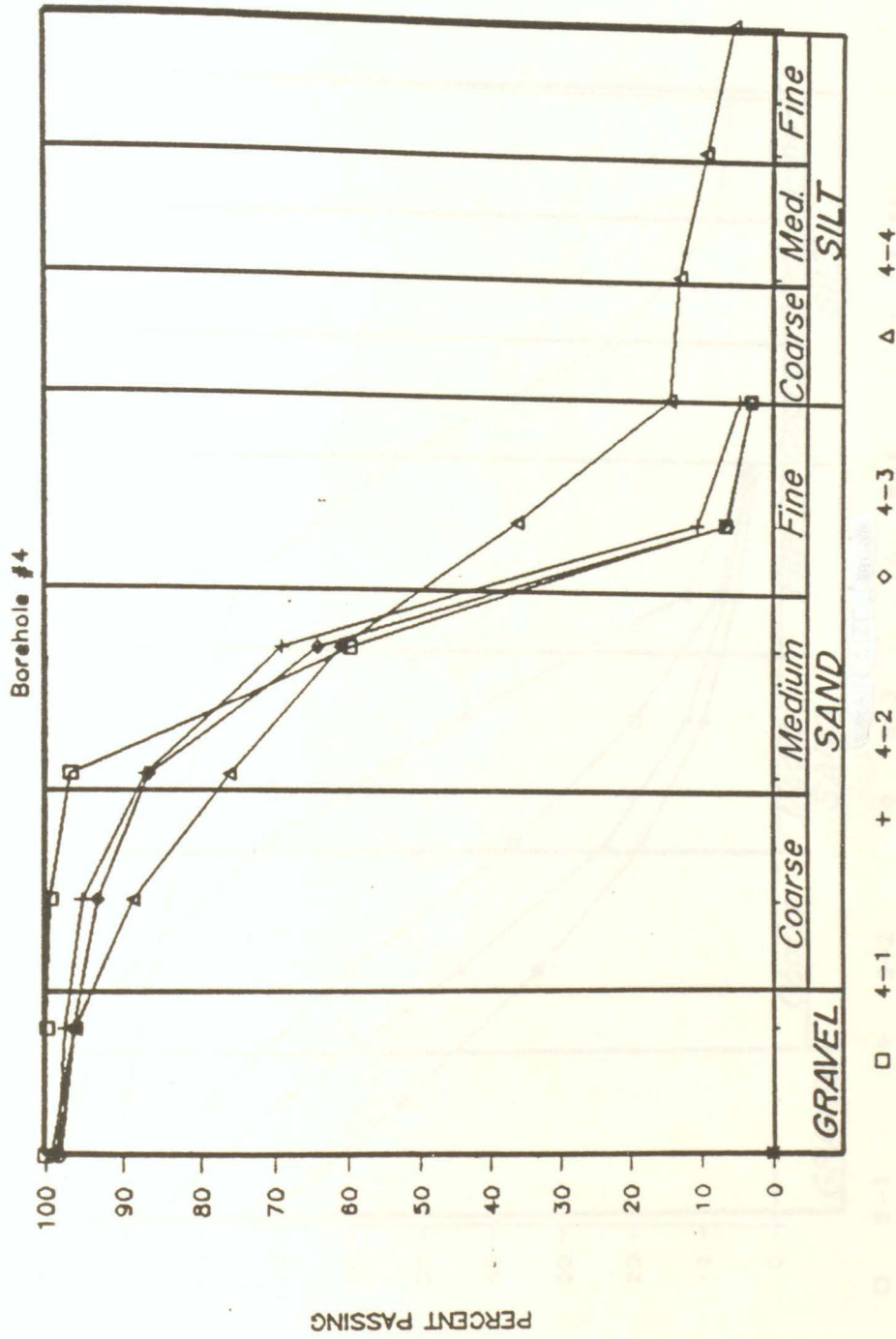
□ 2-1 + 2-2 ◇ 2-3 Δ 2-4 × 2-5 ▽ 2-6

GRADATION ANALYSIS

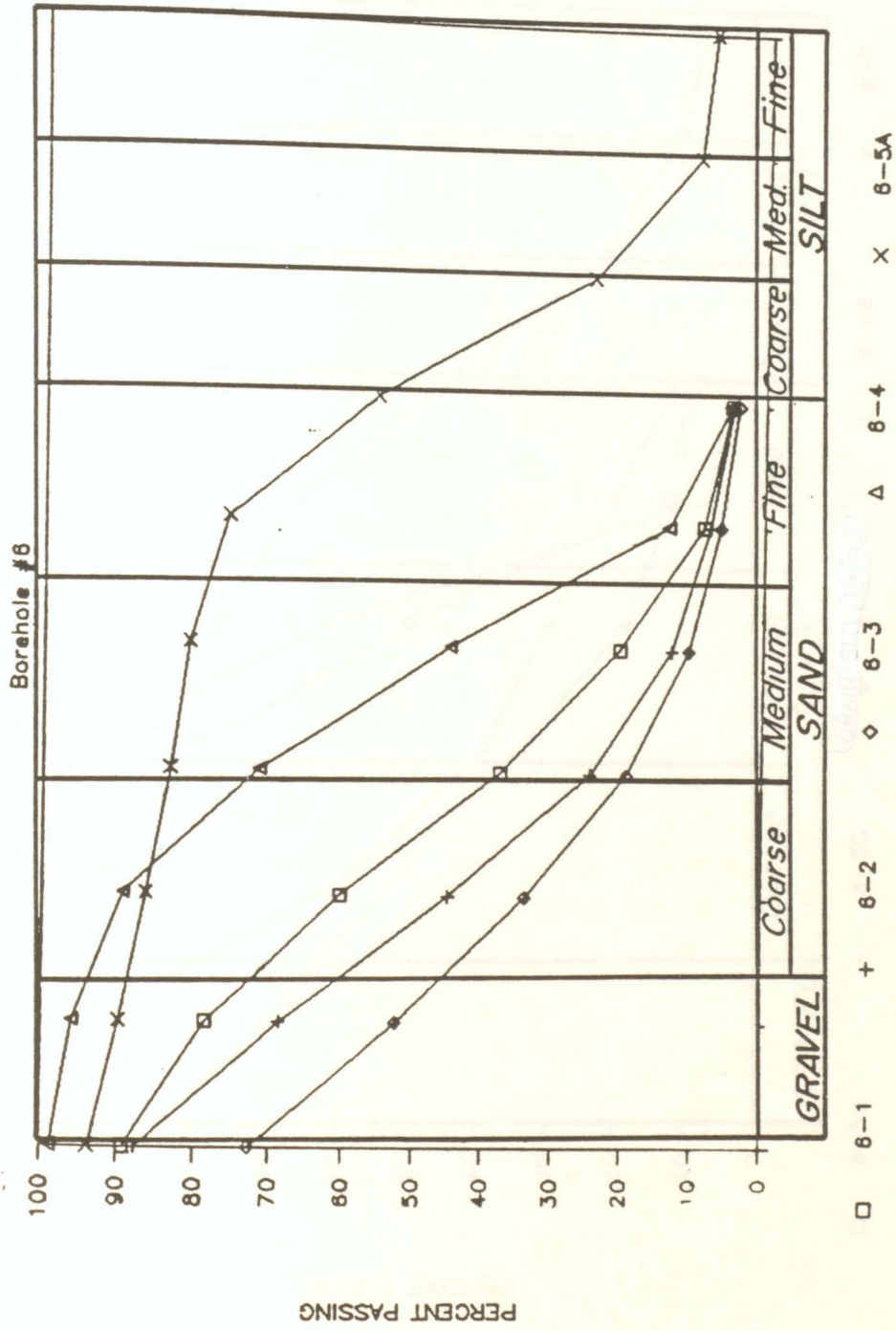
Borehole #3



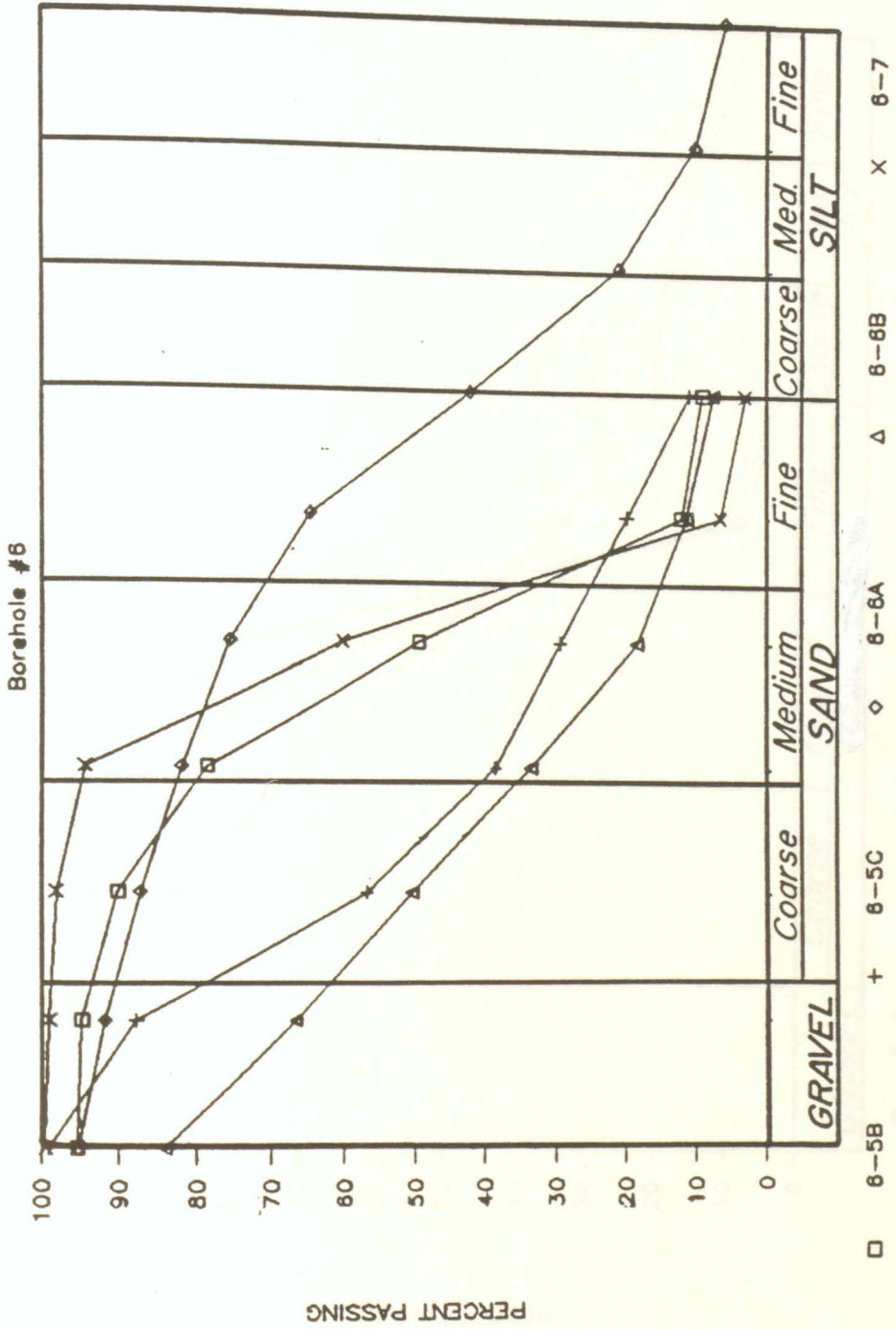
GRADATION ANALYSIS



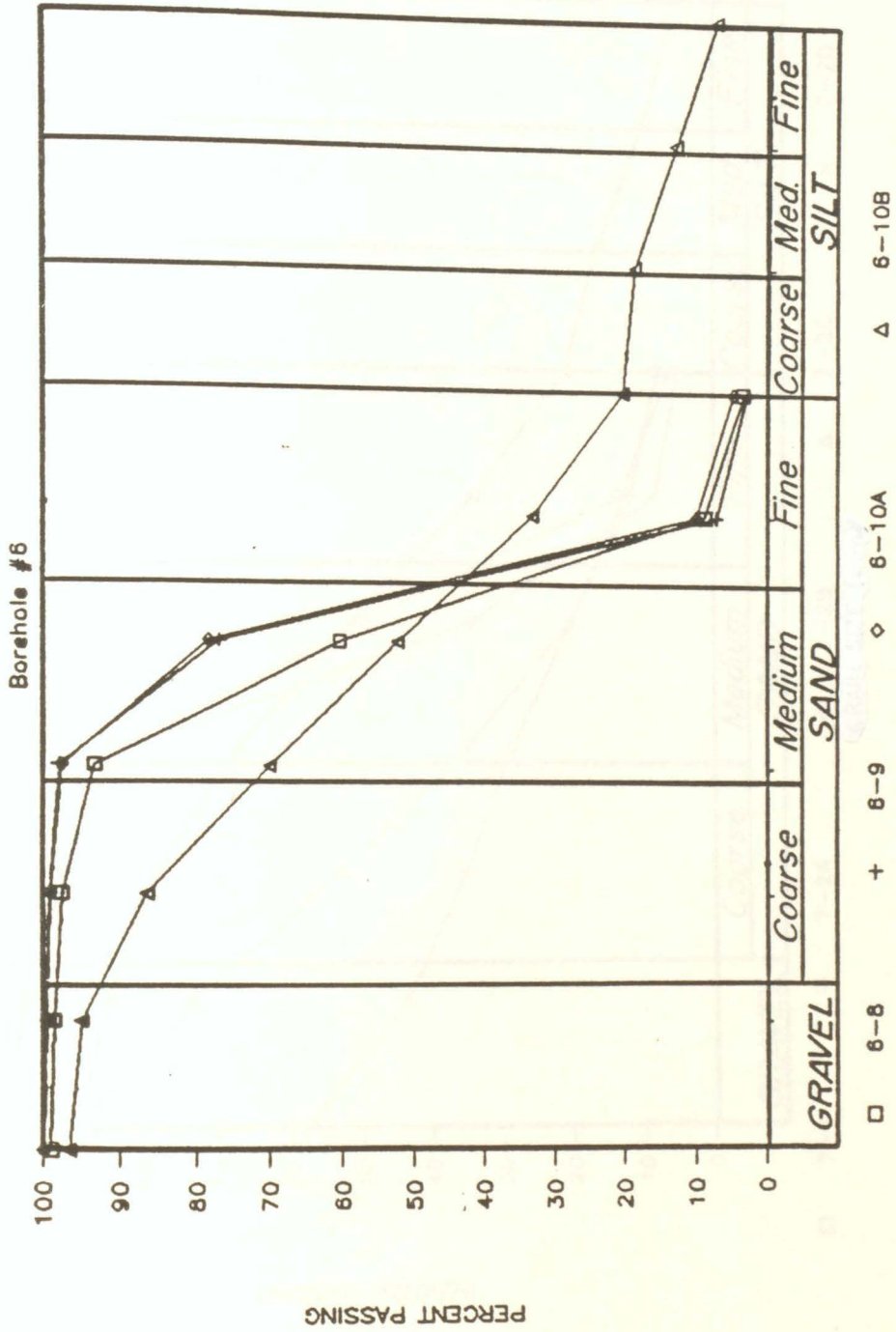
GRADATION ANALYSIS



GRADATION ANALYSIS

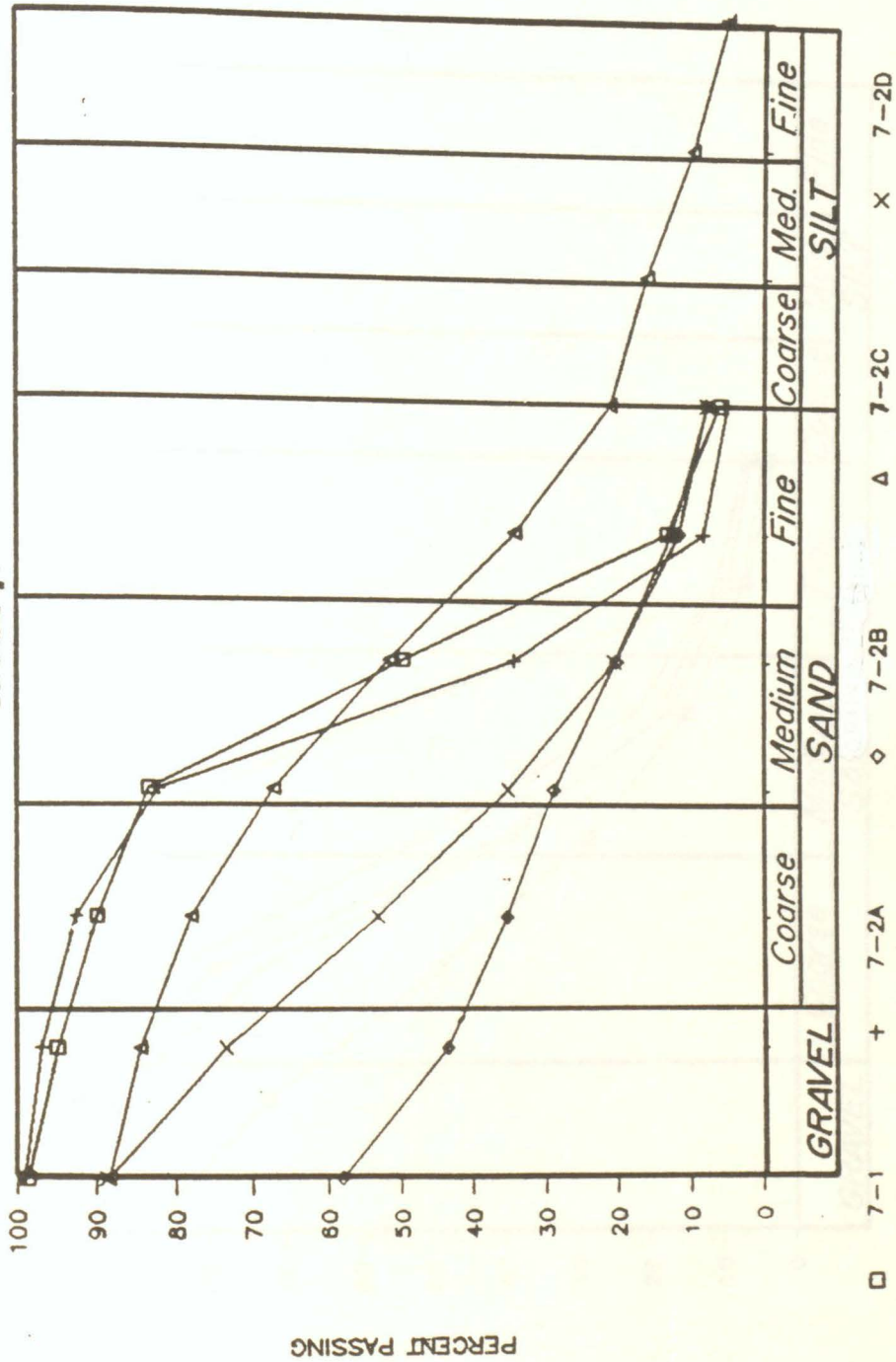


GRADATION ANALYSIS

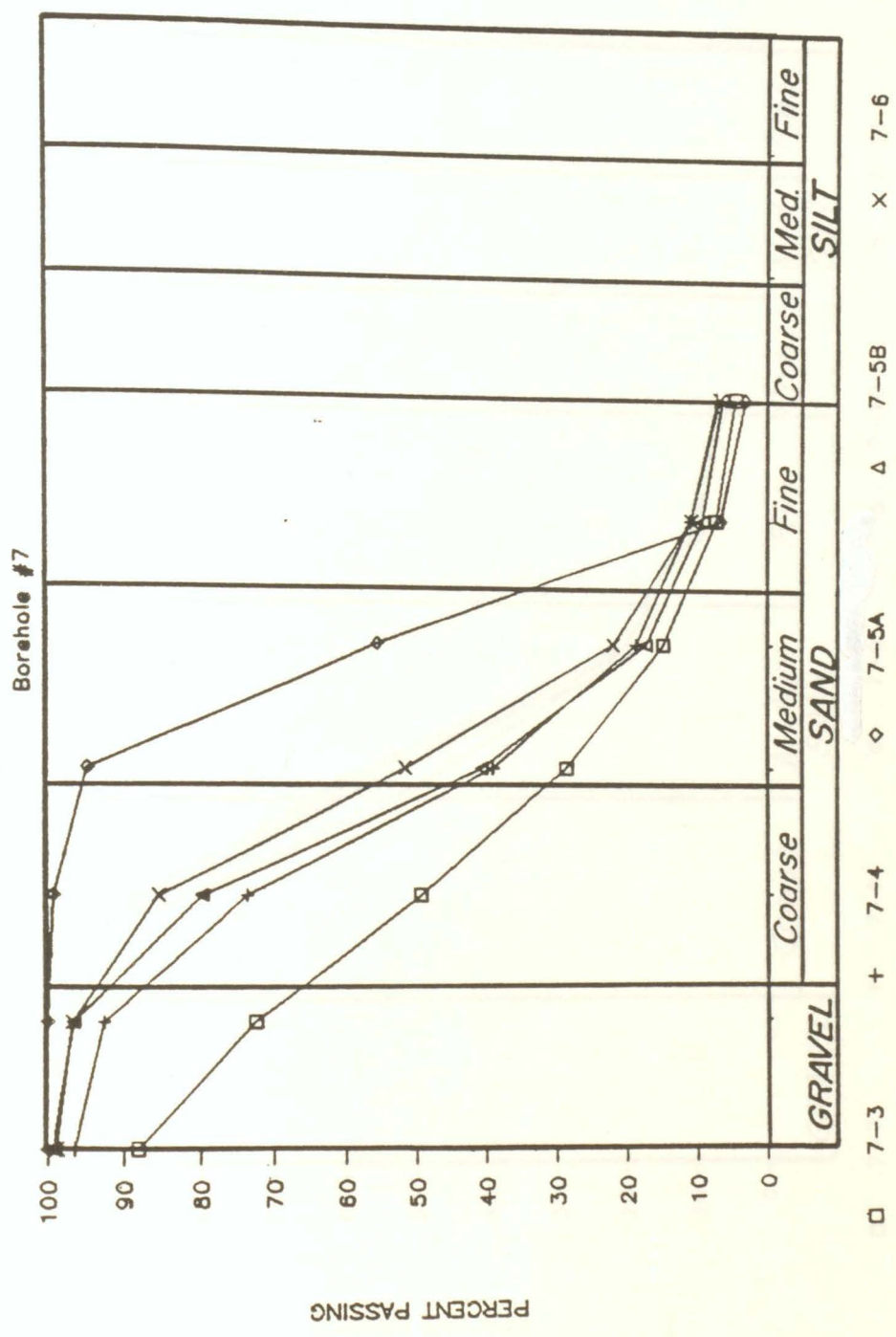


GRADATION ANALYSIS

Borehole #7

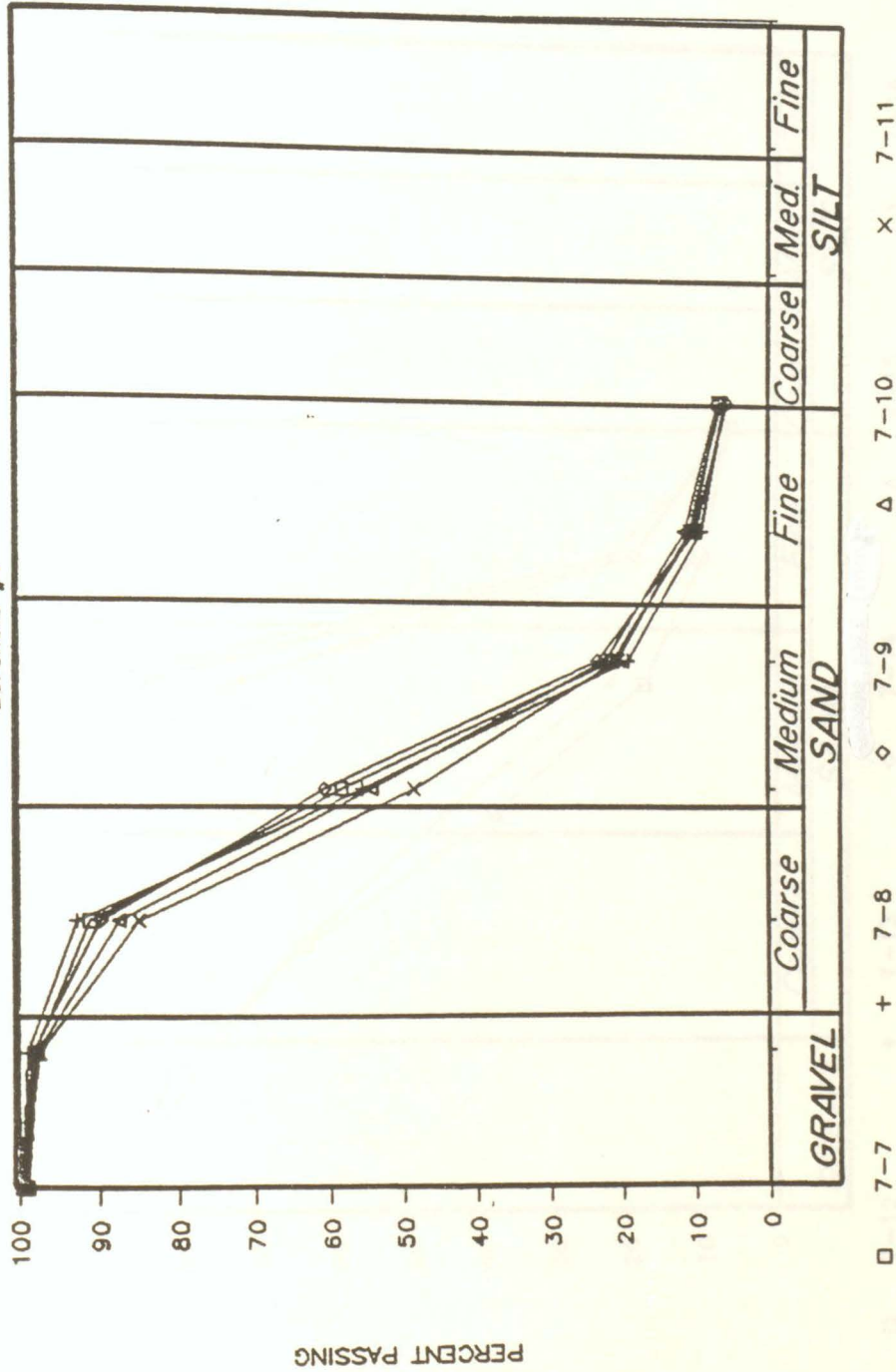


GRADATION ANALYSIS

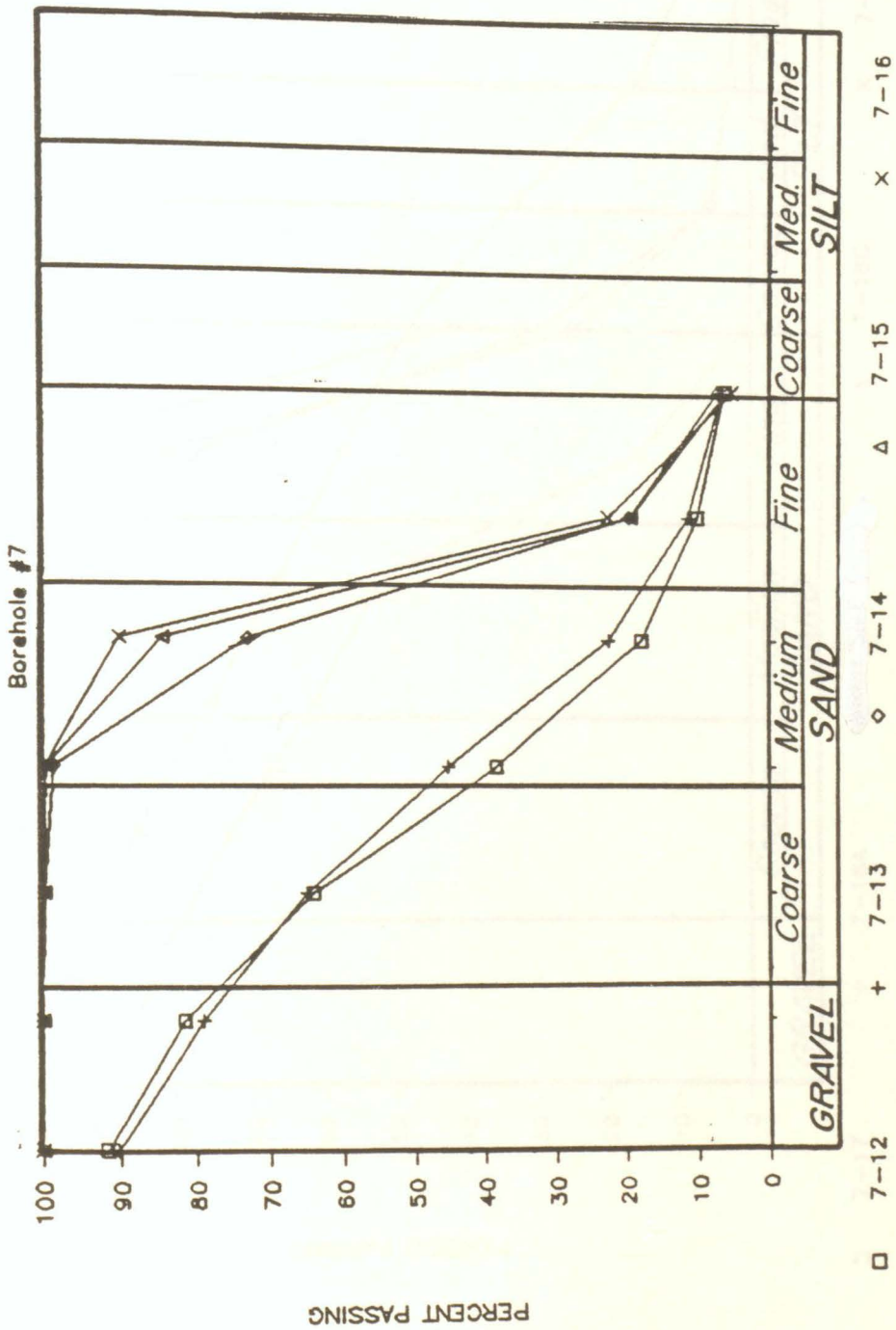


GRADATION ANALYSIS

Borehole #7

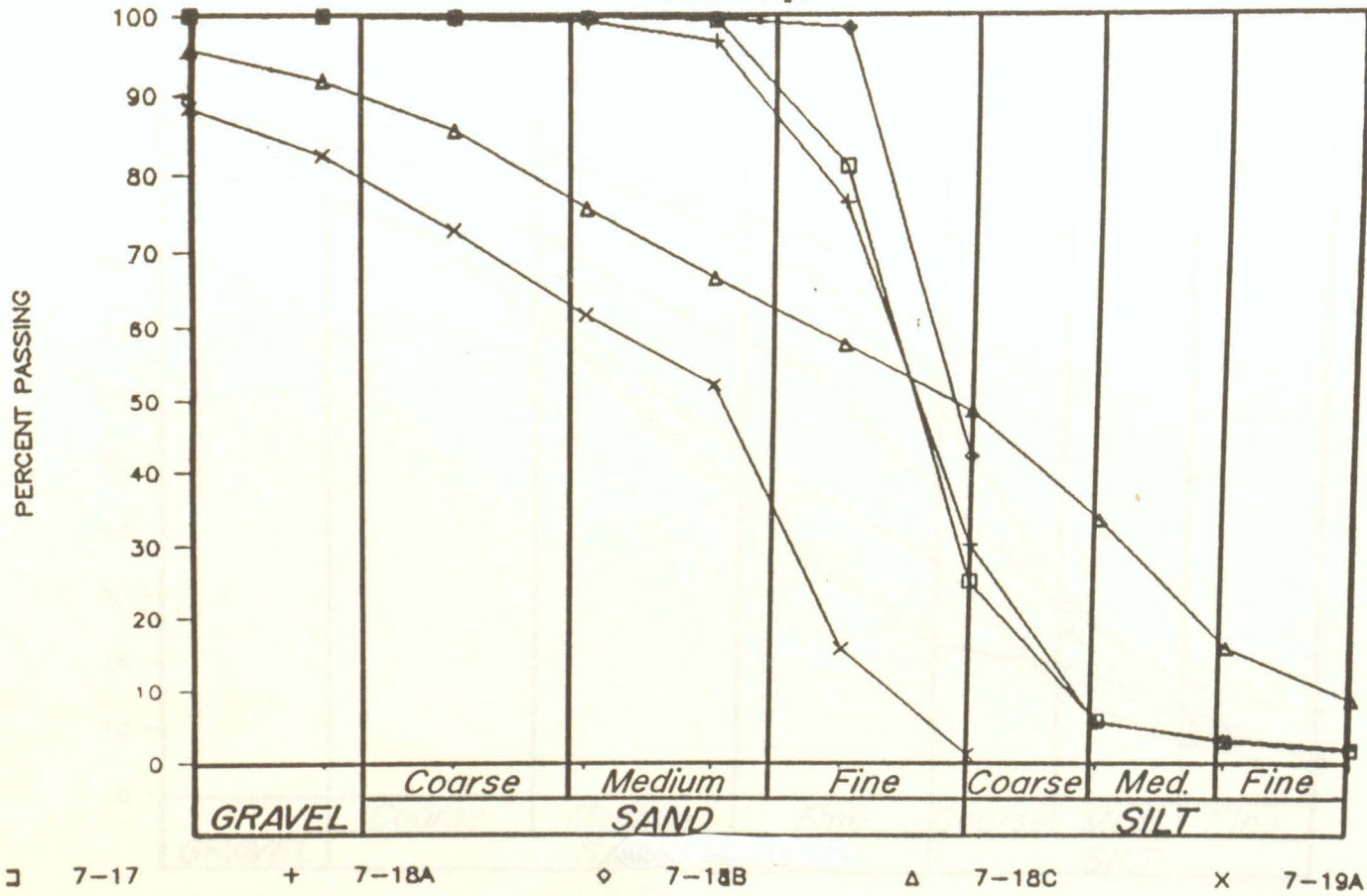


GRADATION ANALYSIS



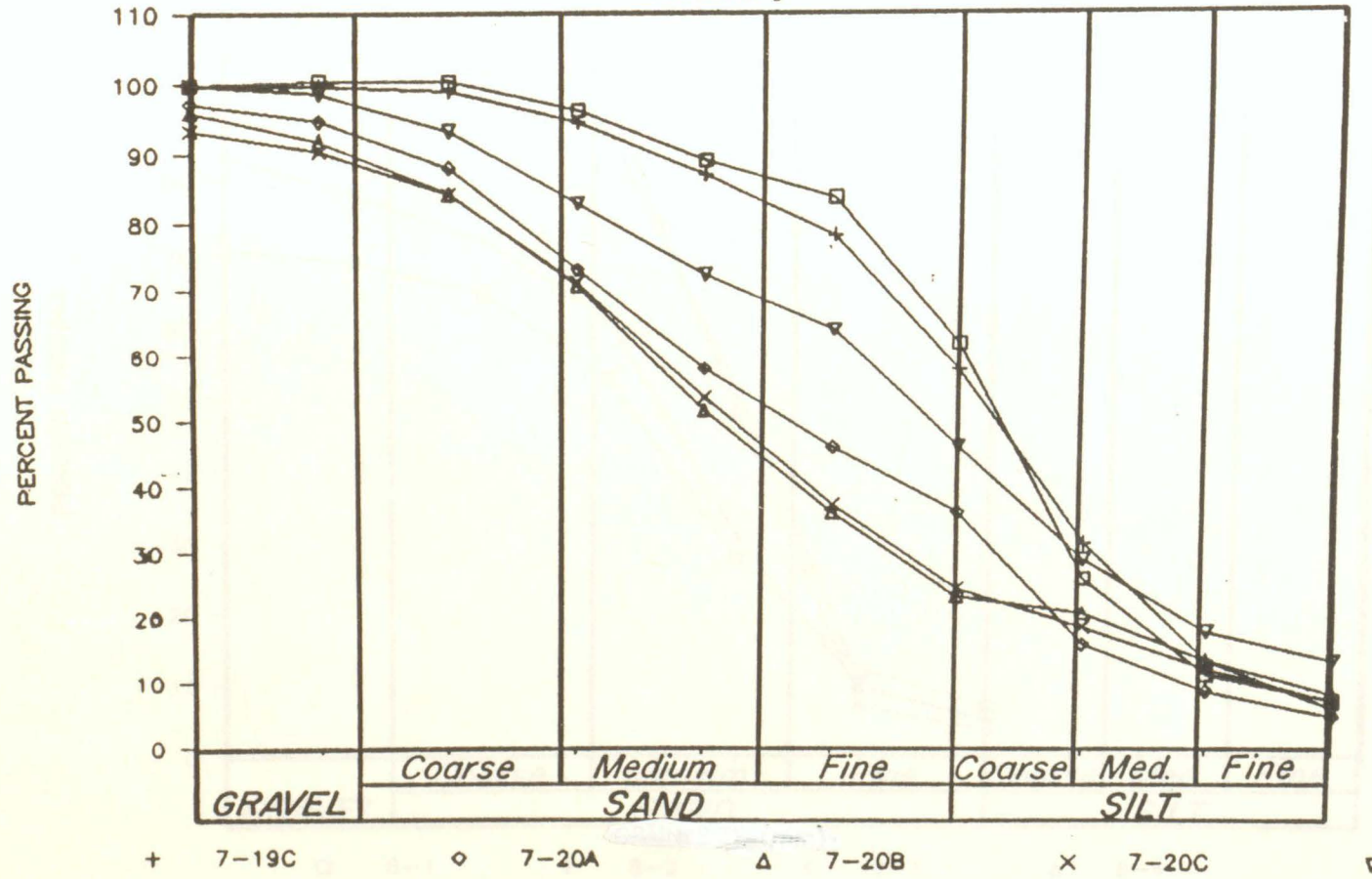
GRADATION ANALYSIS

Borehole #7

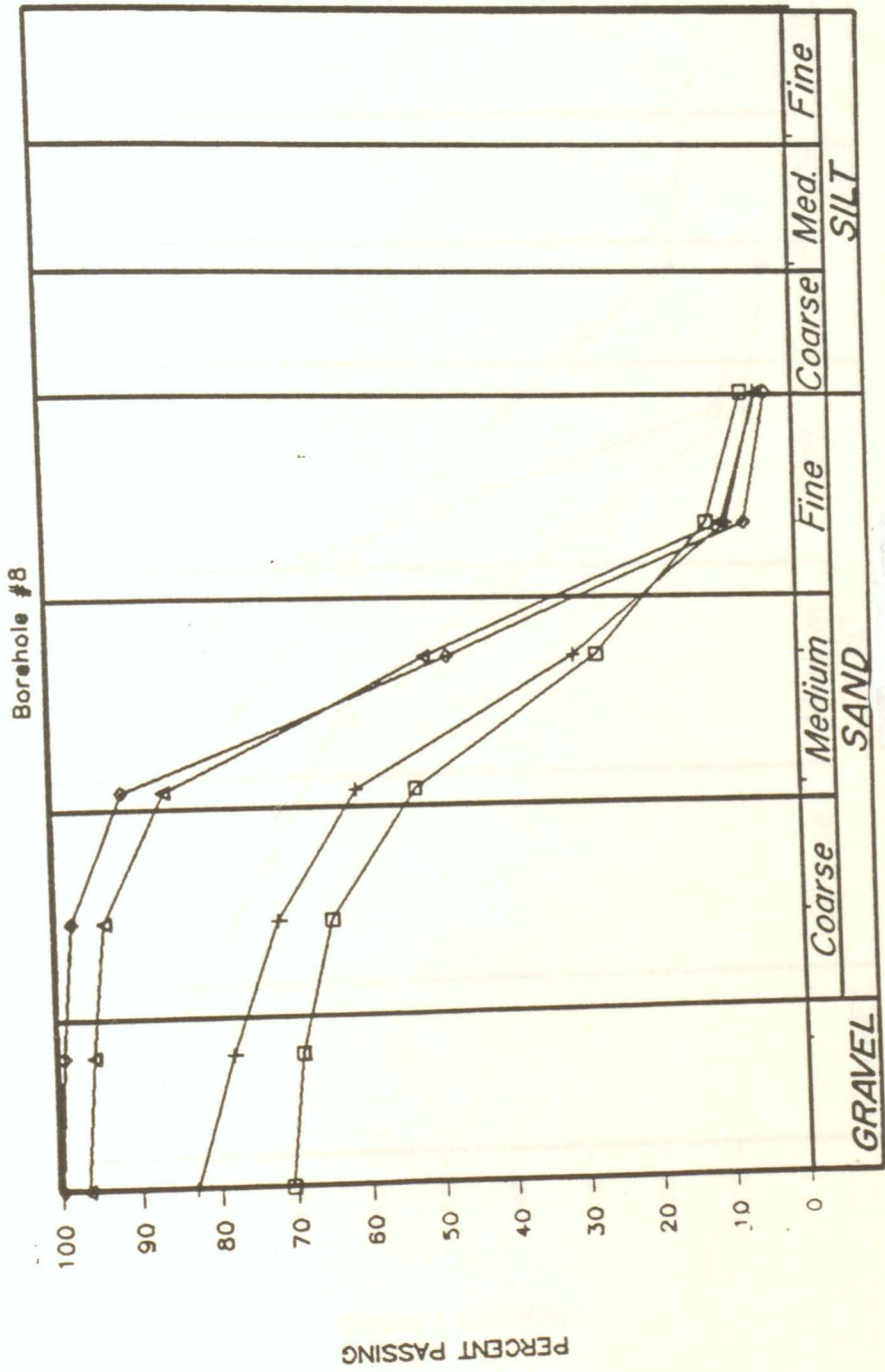


GRADATION ANALYSIS

Borehole #7

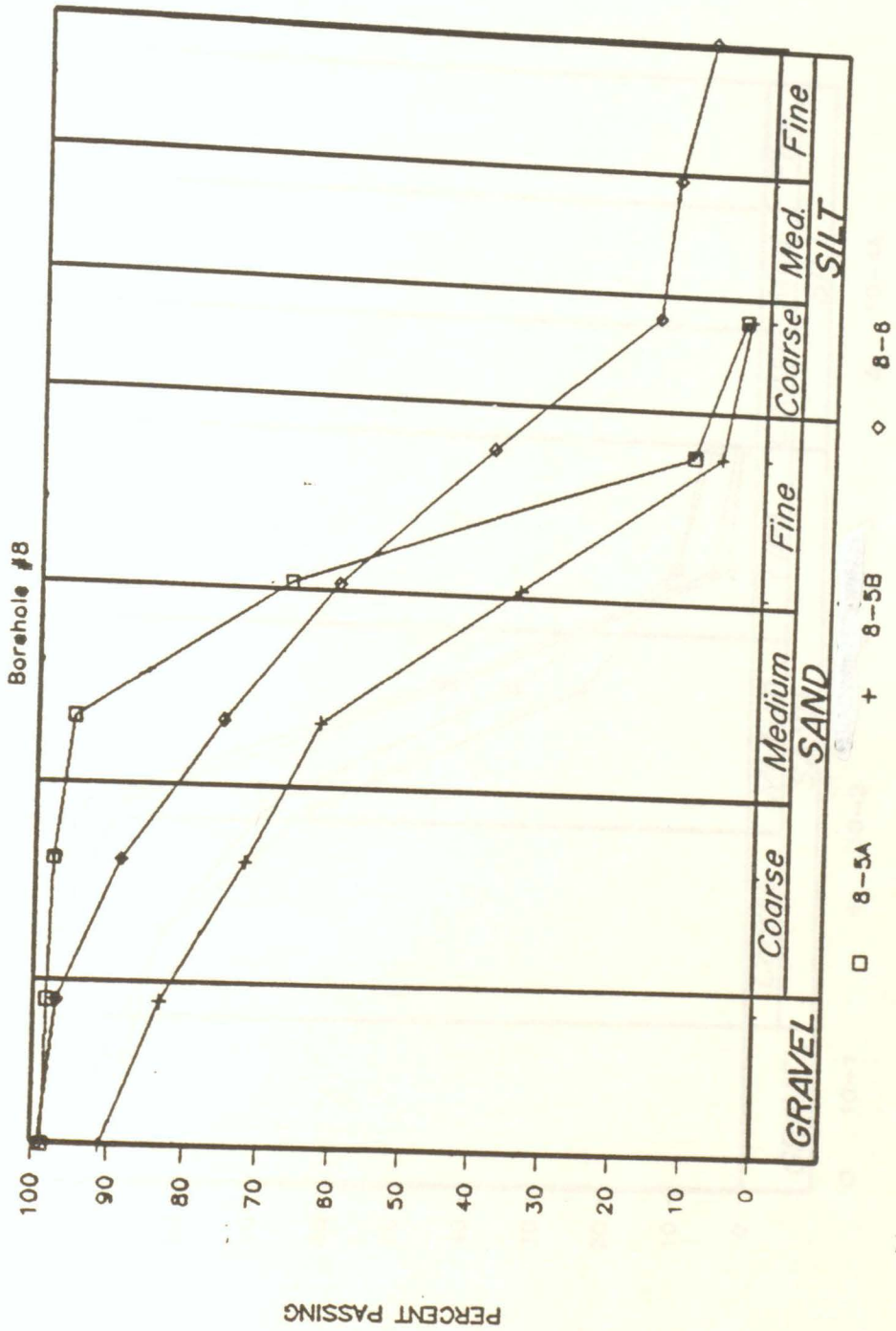


GRADATION ANALYSIS

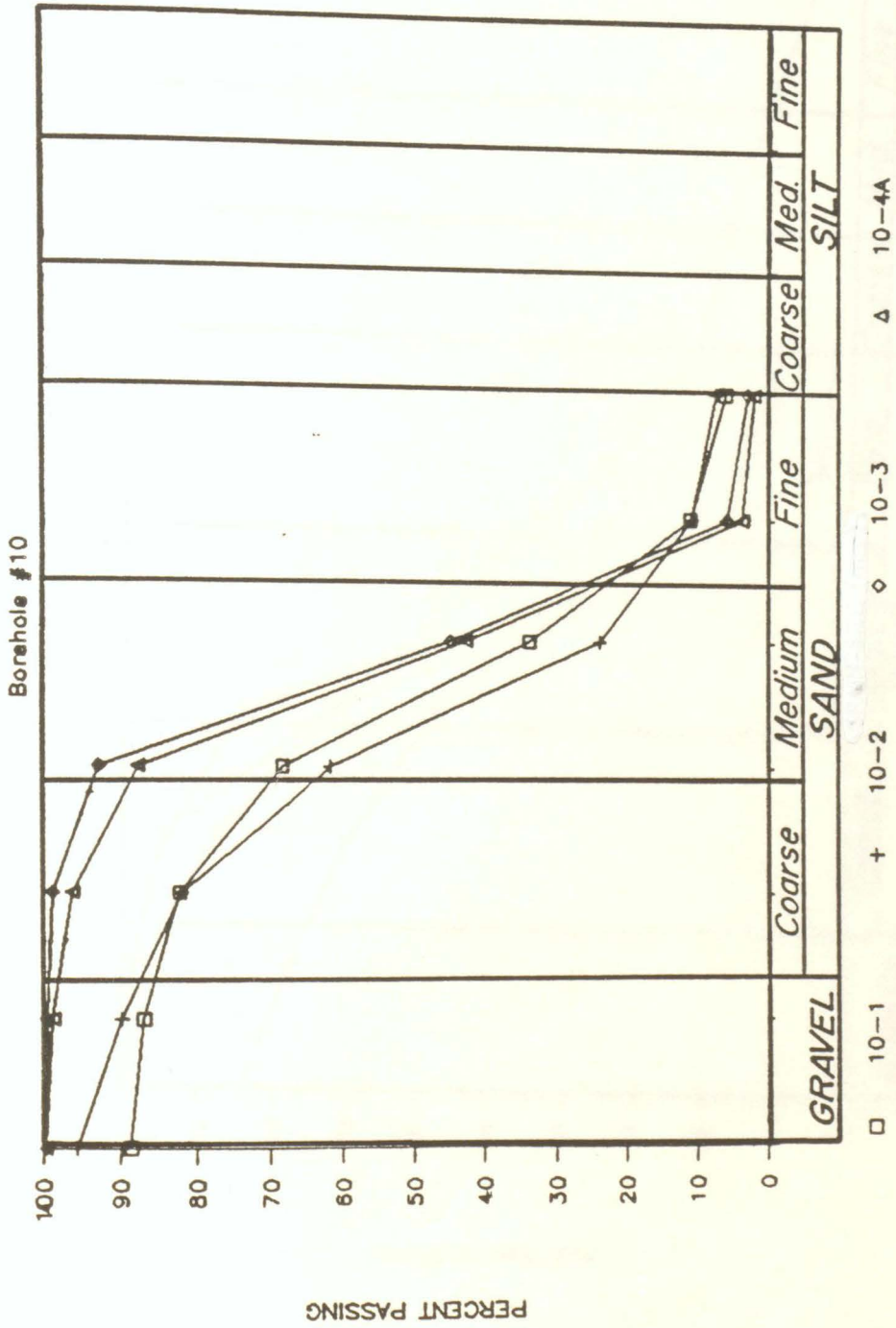


□ 8-1 + 8-2 ◇ 8-3 △ 8-4

GRADATION ANALYSIS

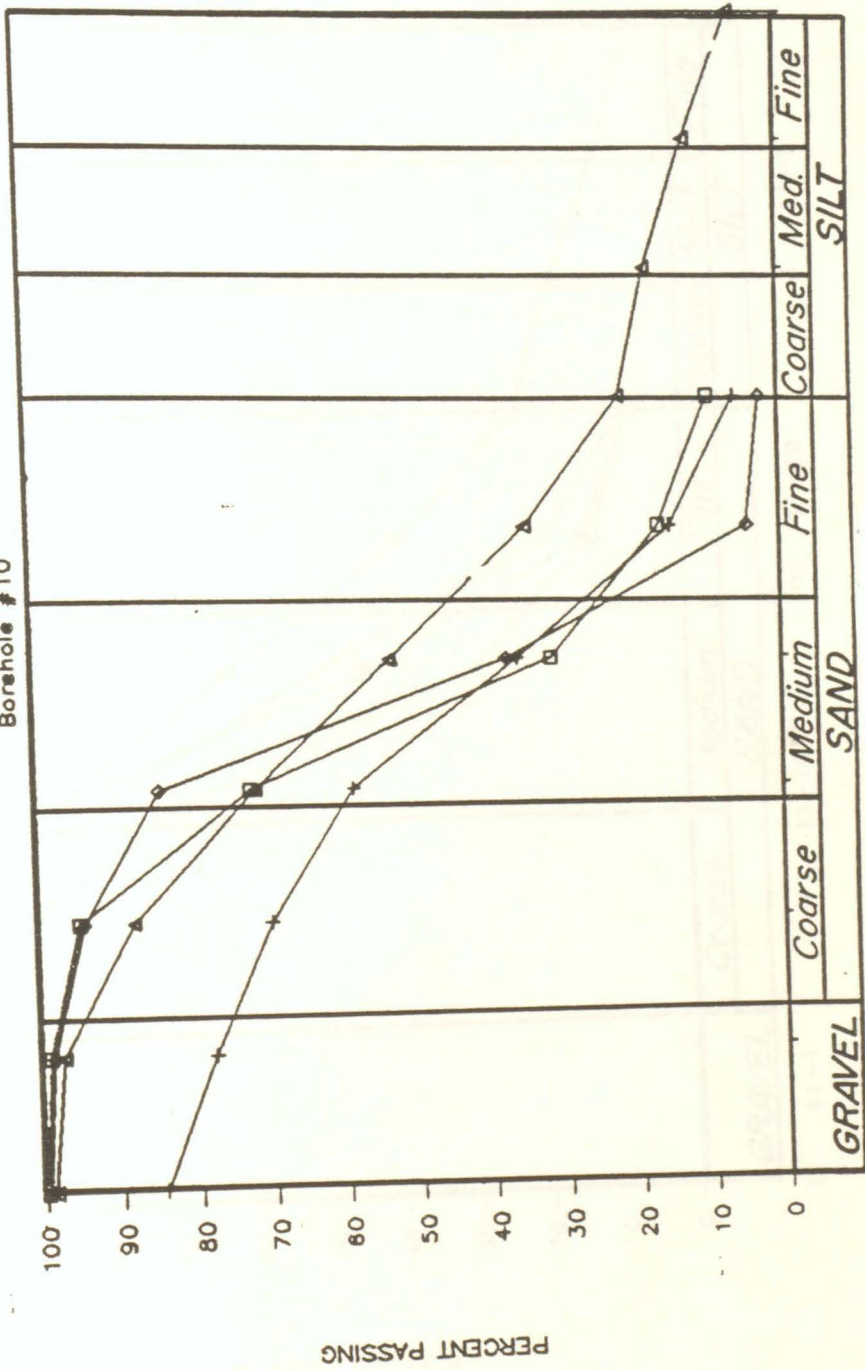


GRADATION ANALYSIS



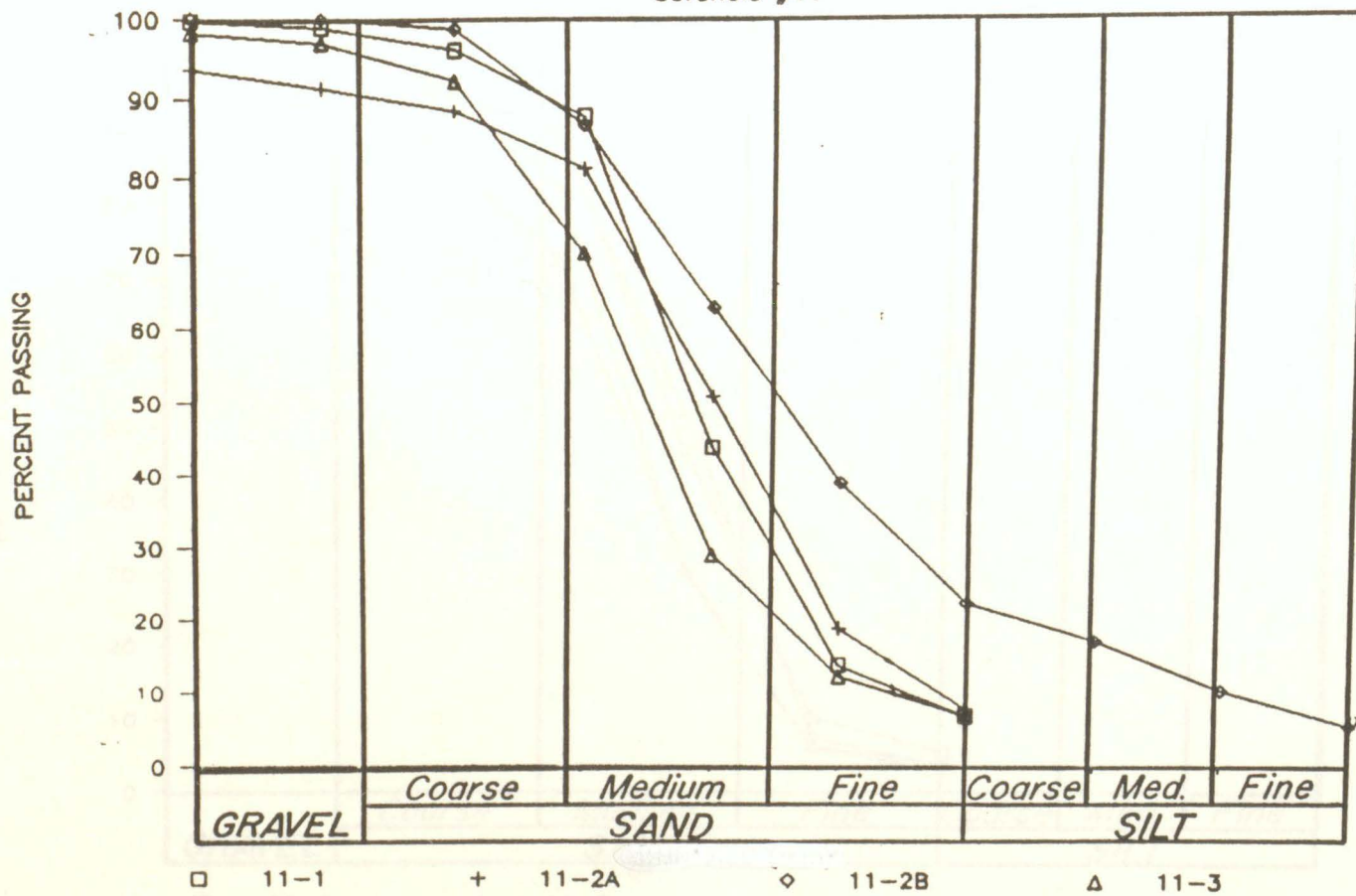
GRADATION ANALYSIS

Borehole #10



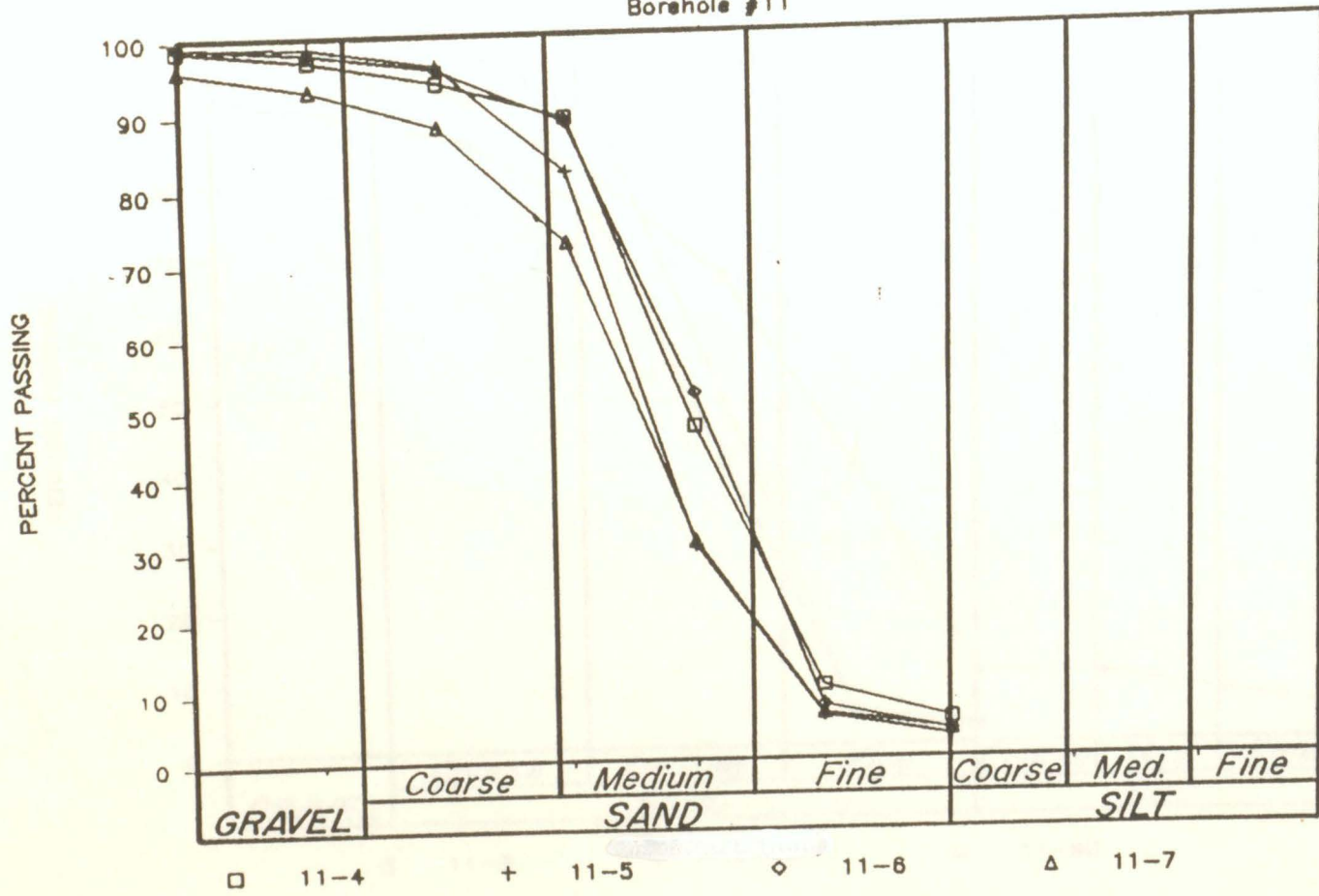
GRADATION ANALYSIS

Borehole #11



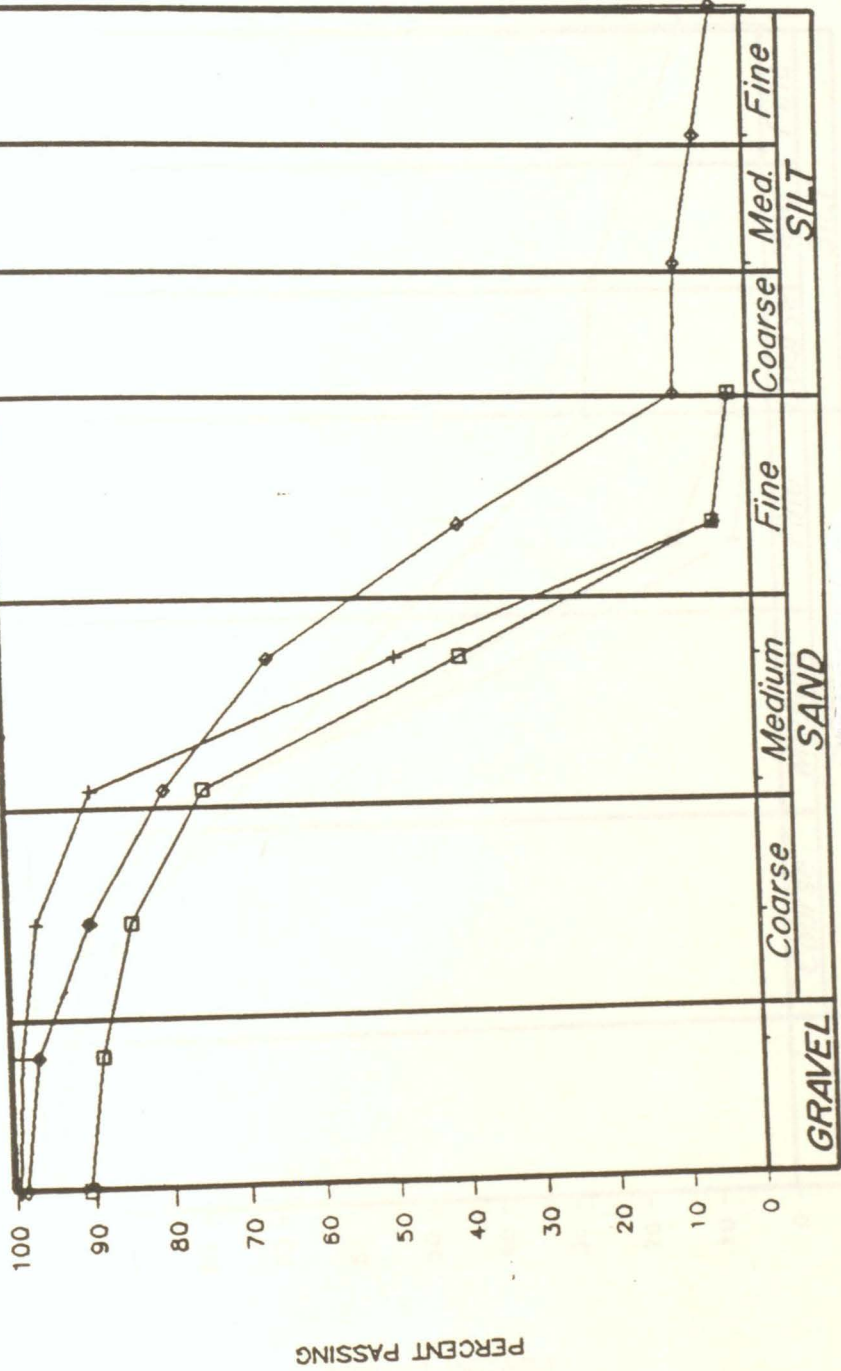
GRADATION ANALYSIS

Borehole #11



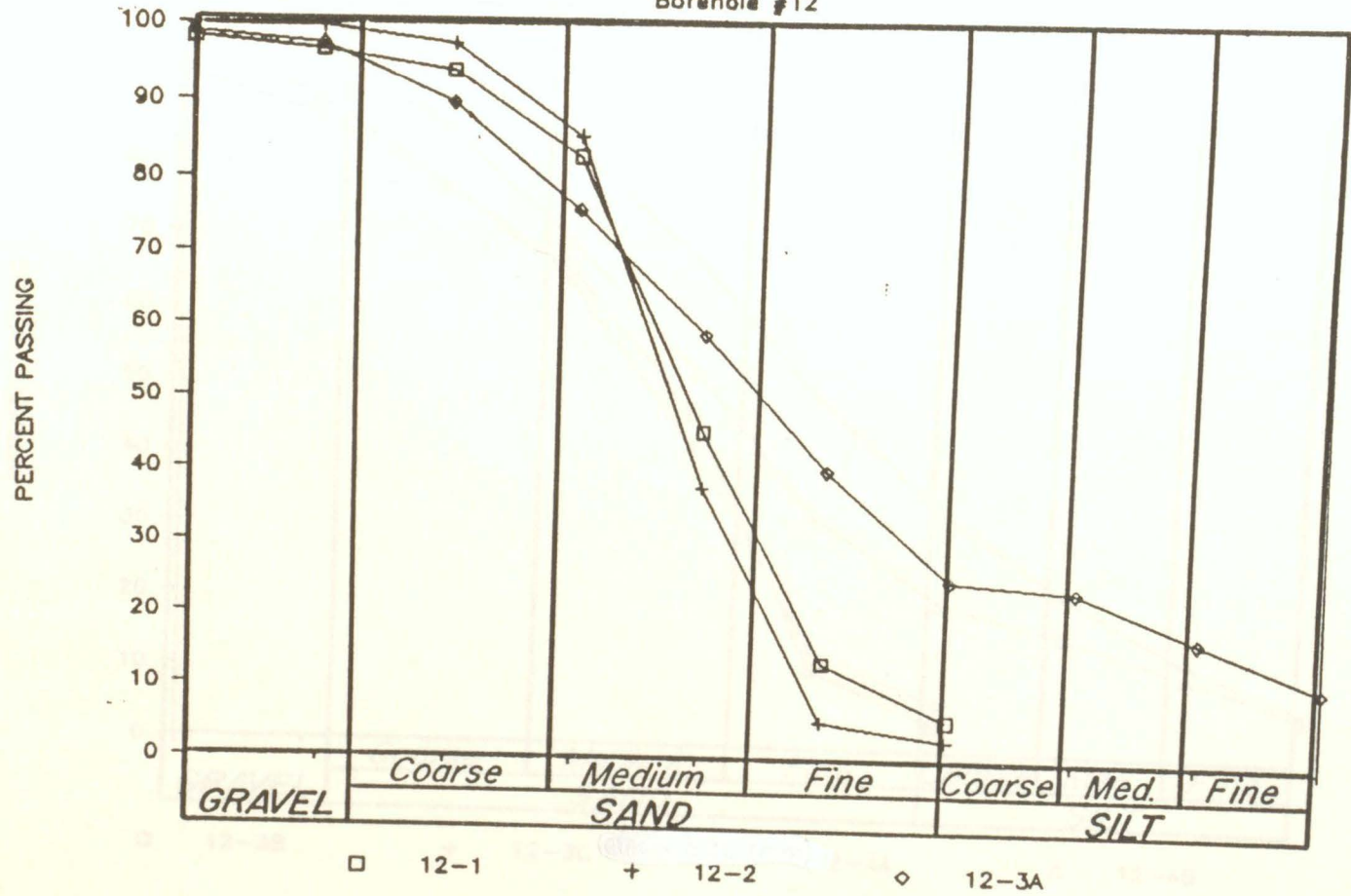
GRADATION ANALYSIS

Borehole #11



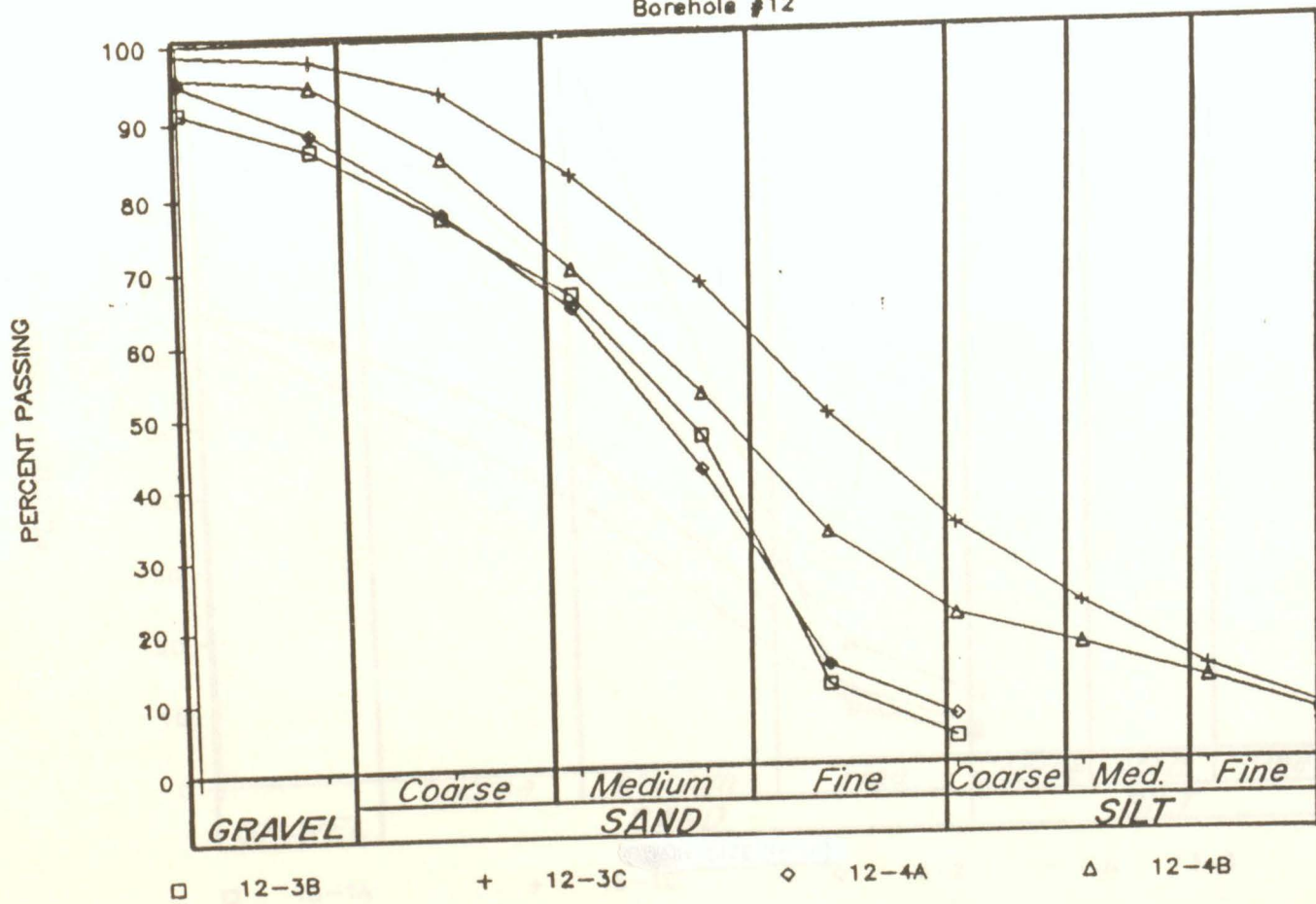
GRADATION ANALYSIS

Borehole #12



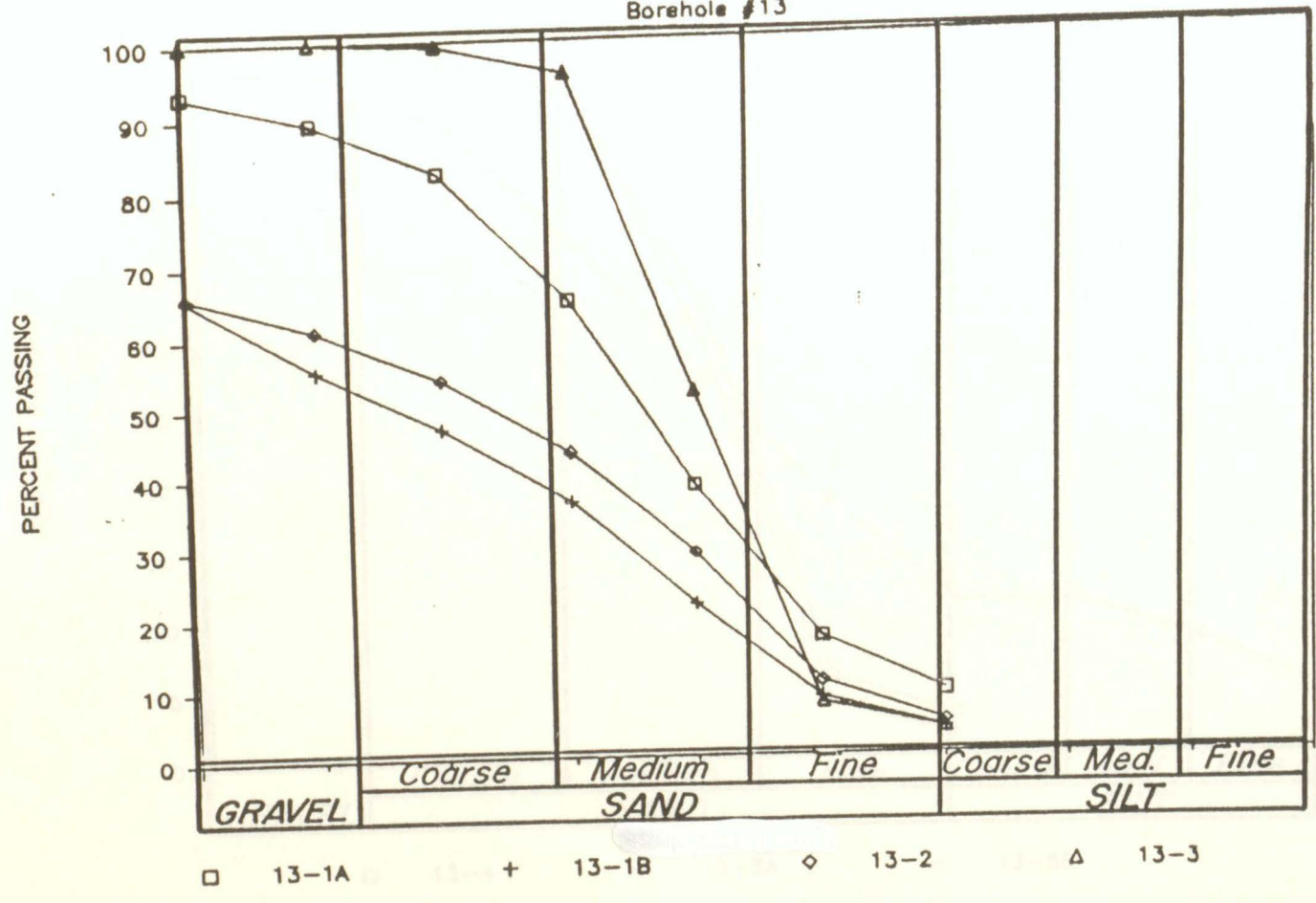
GRADATION ANALYSIS

Borehole #12



GRADATION ANALYSIS

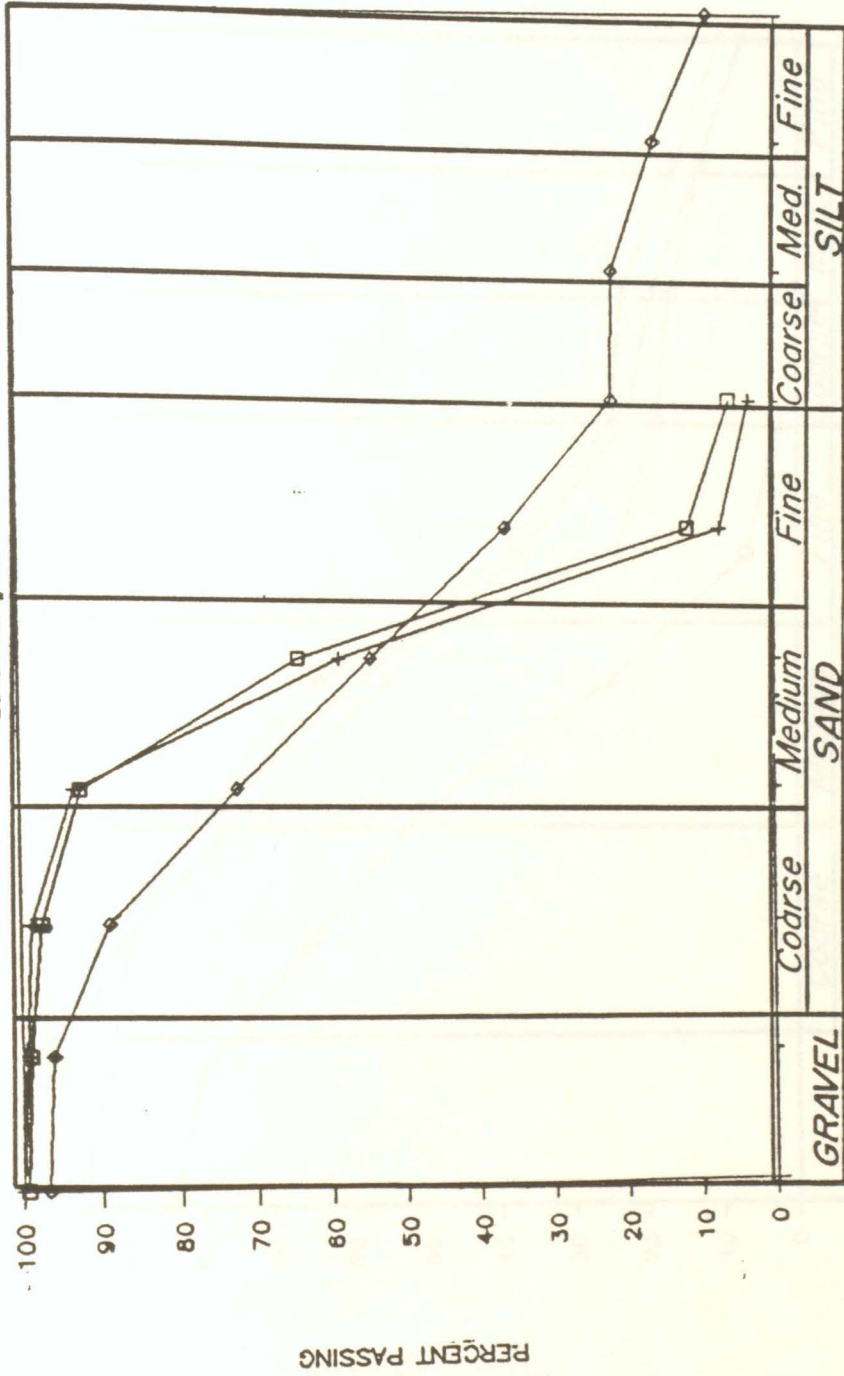
Borehole #13



220

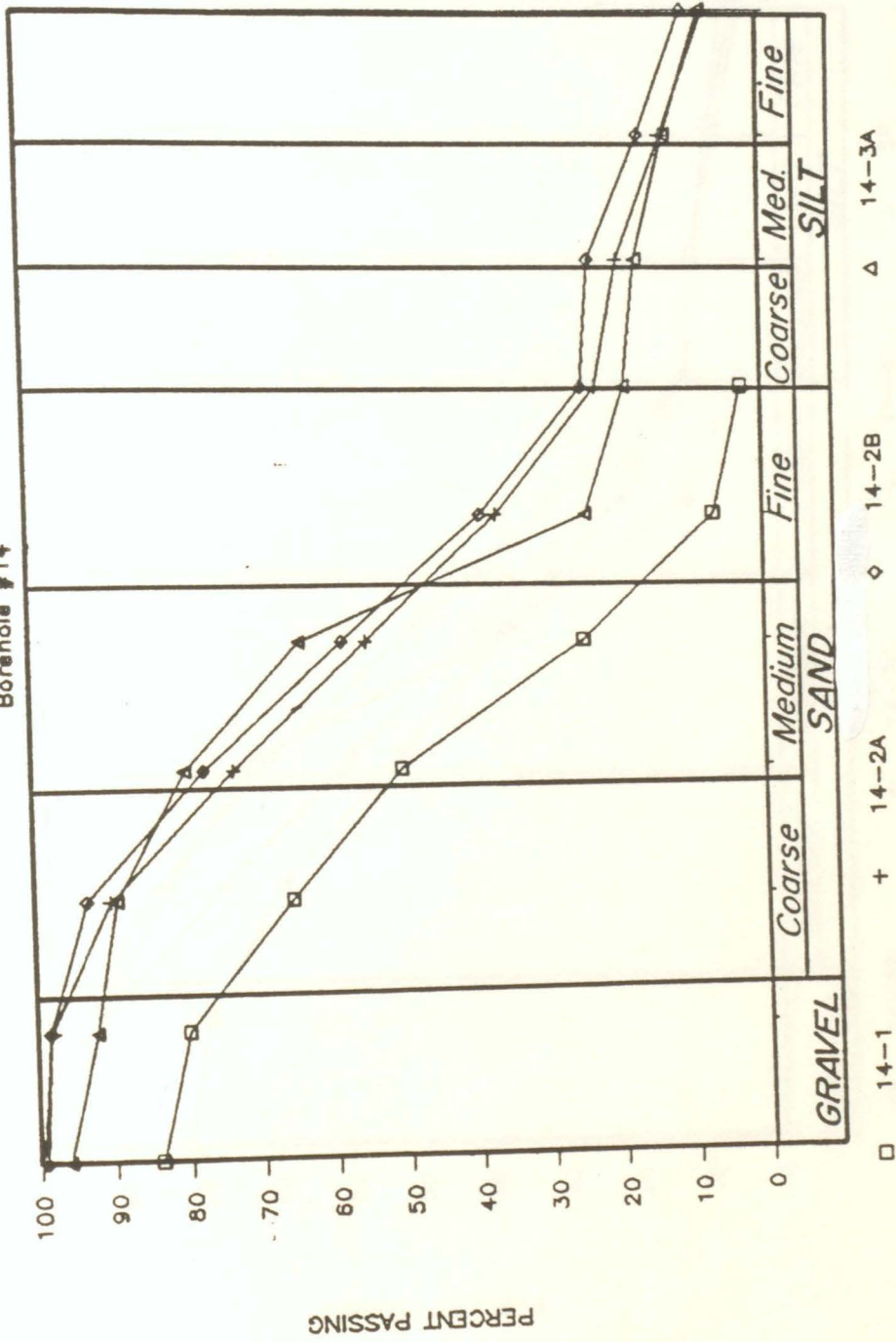
GRADATION ANALYSIS

Borehole #13



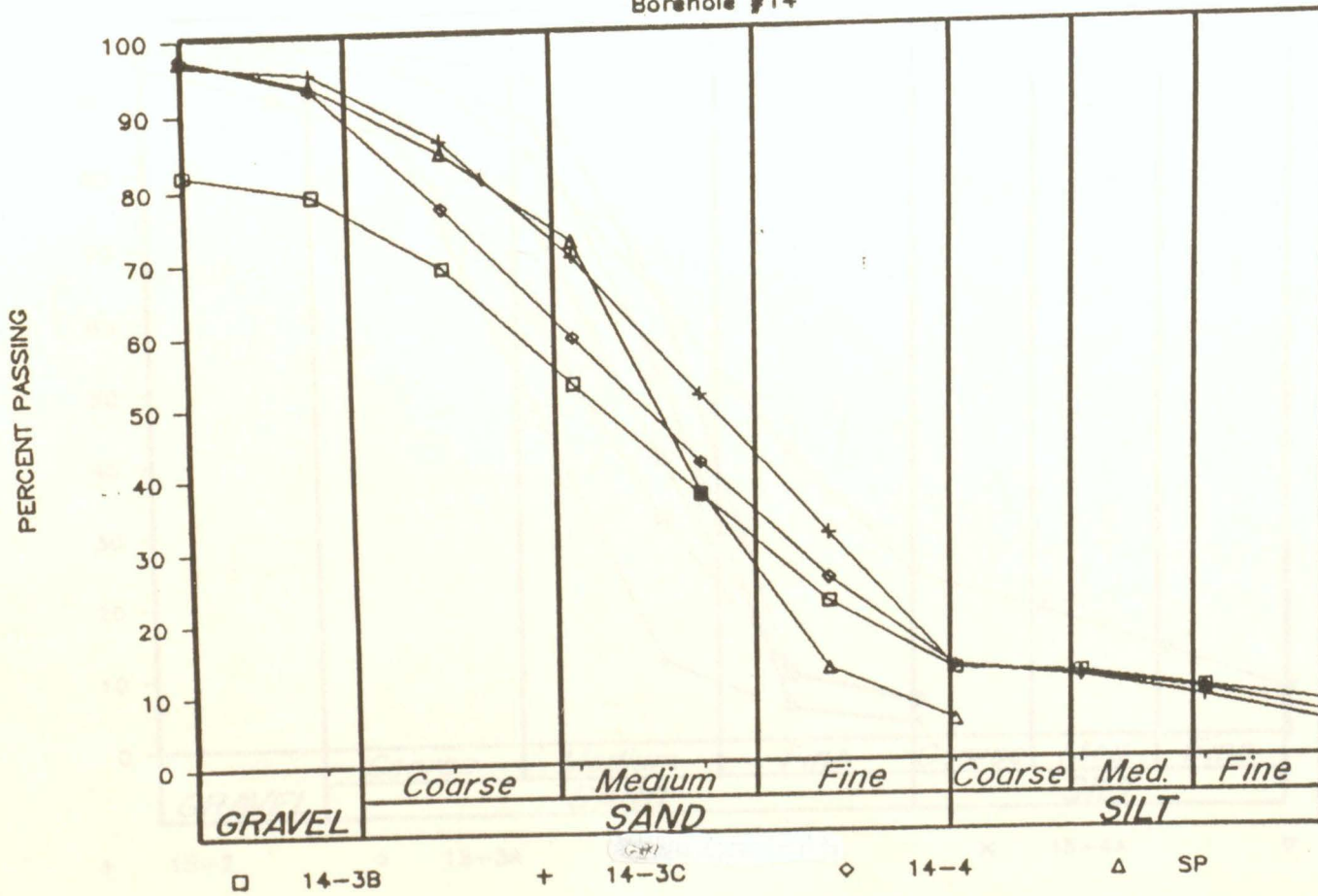
GRADATION ANALYSIS

Borehole #14



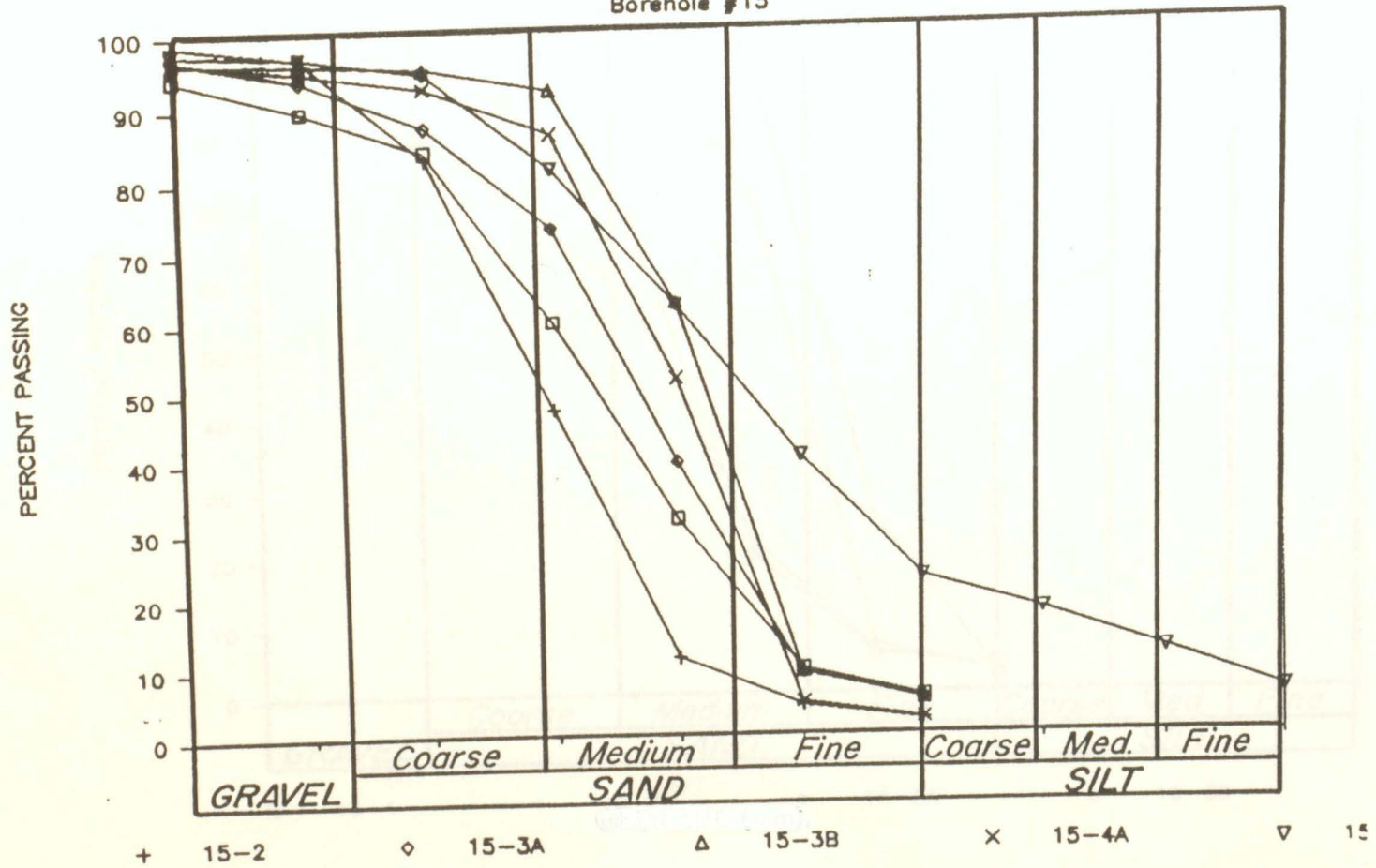
GRADATION ANALYSIS

Borehole #14



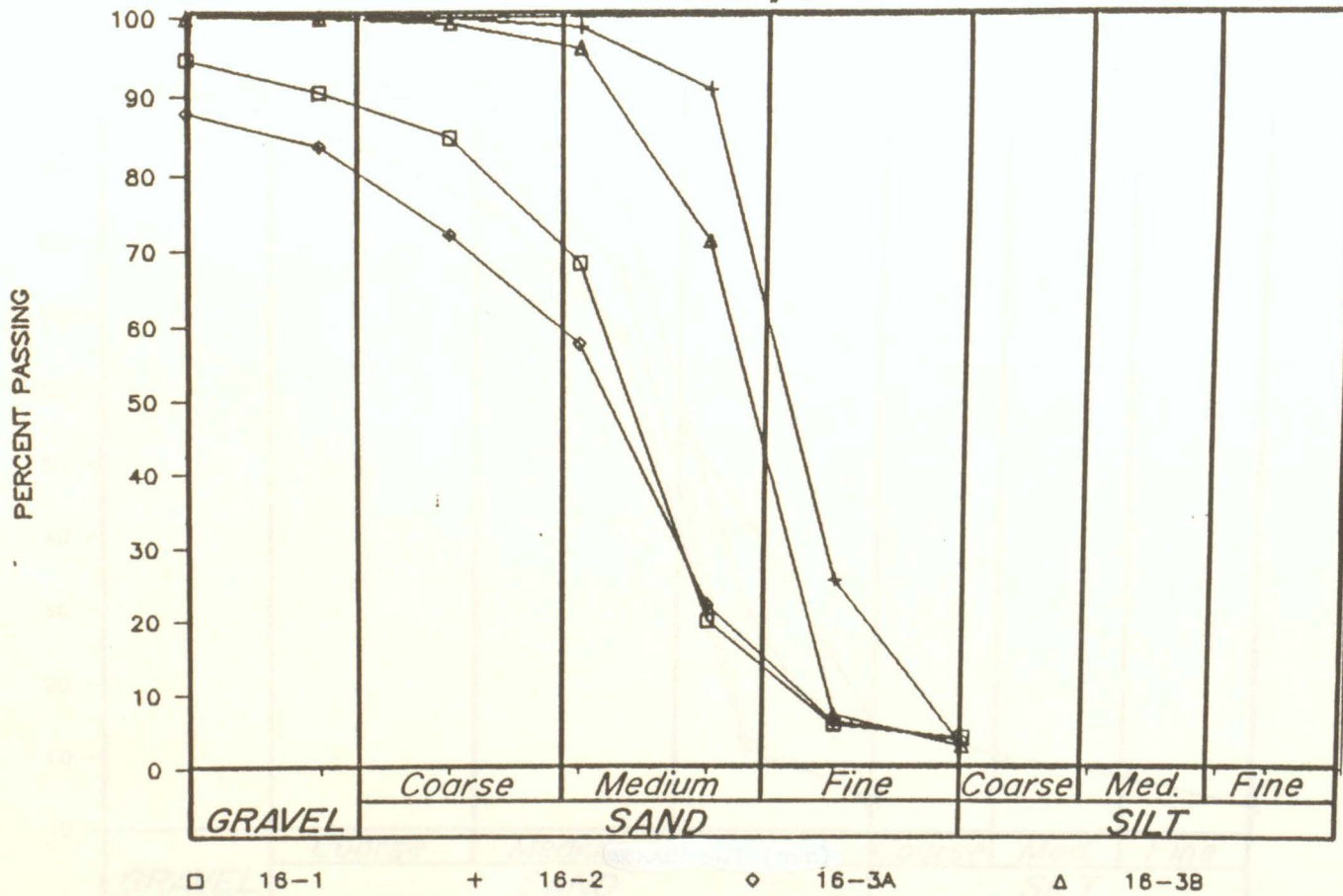
GRADATION ANALYSIS

Borehole #15

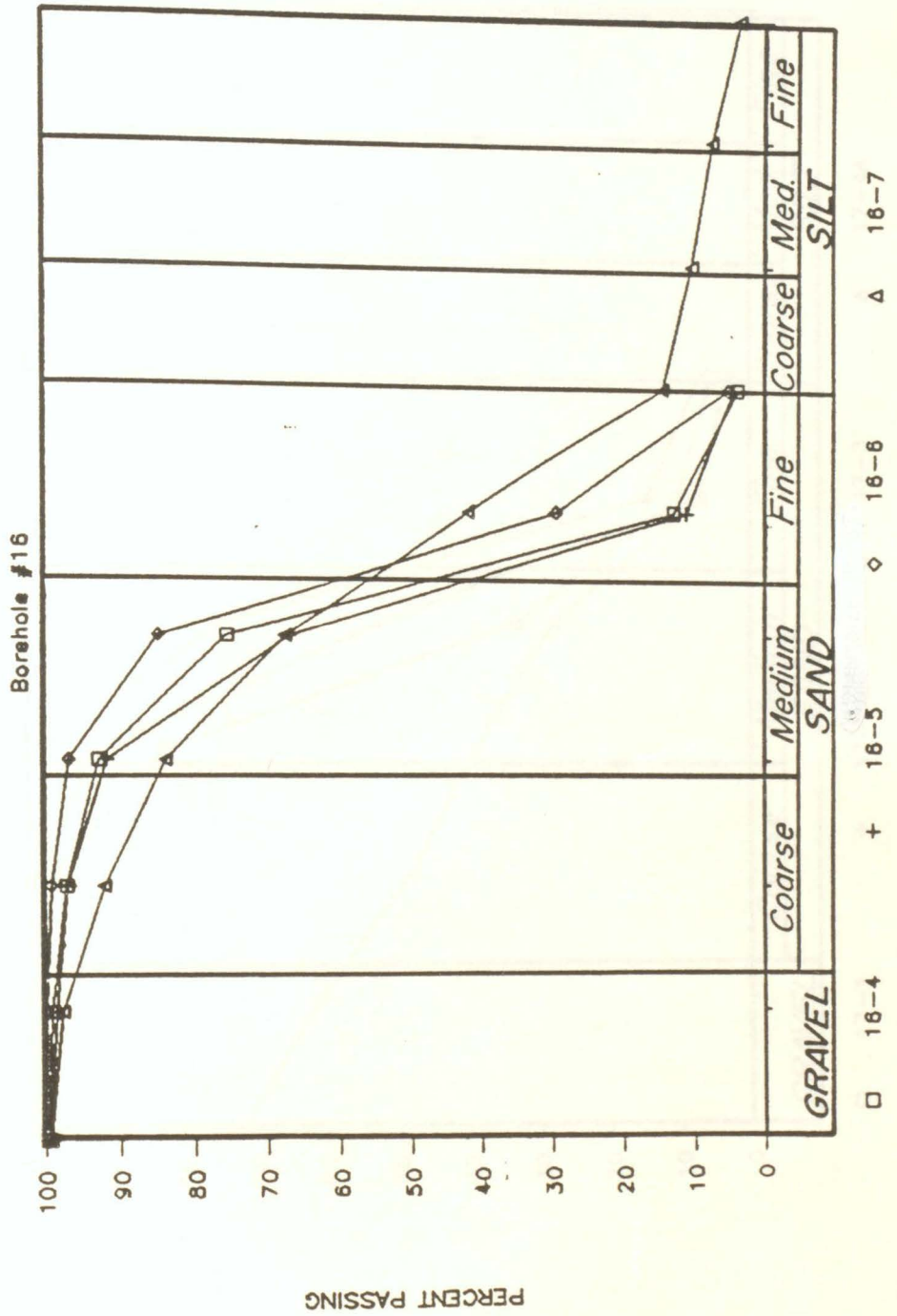


GRADATION ANALYSIS

Borehole #16

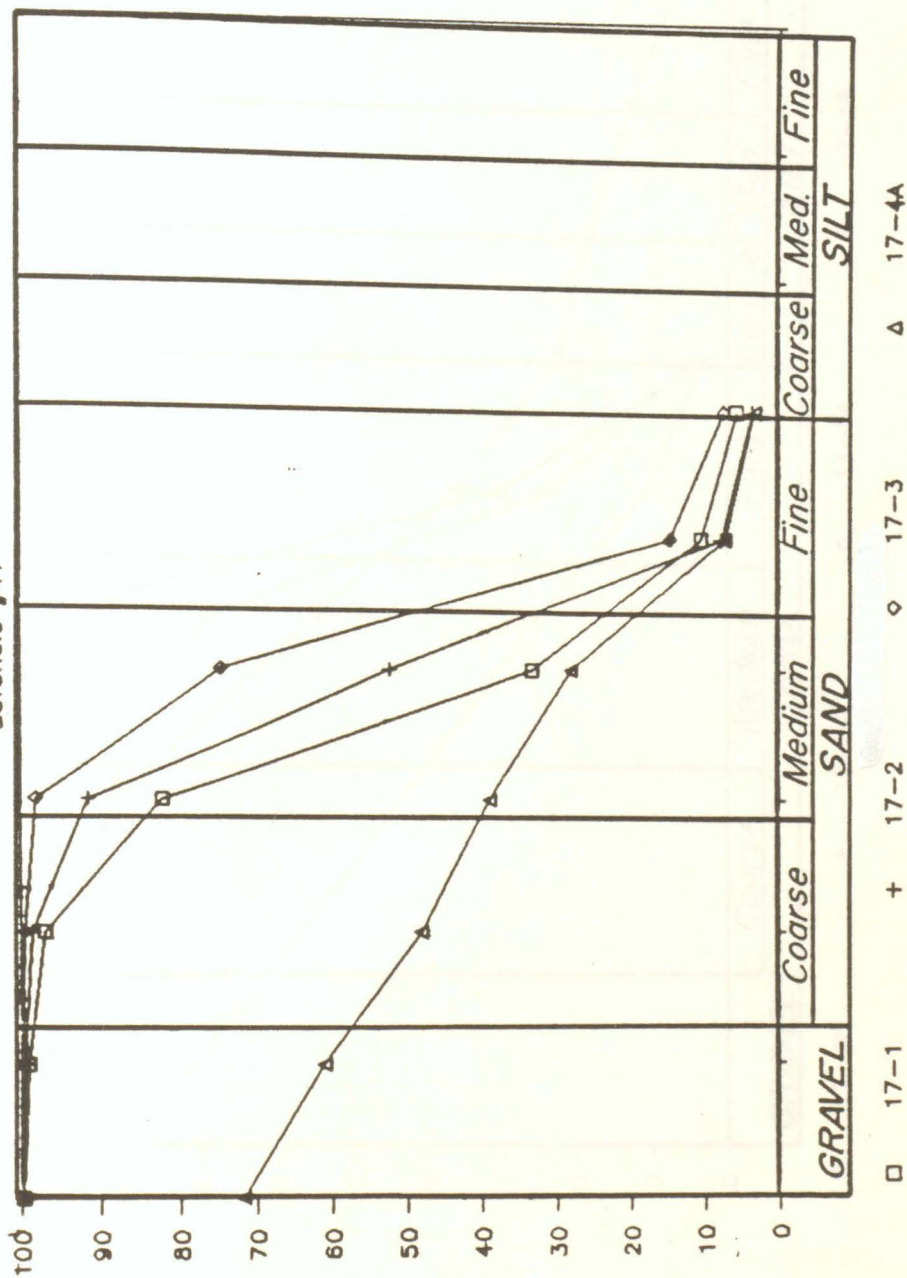


GRADATION ANALYSIS



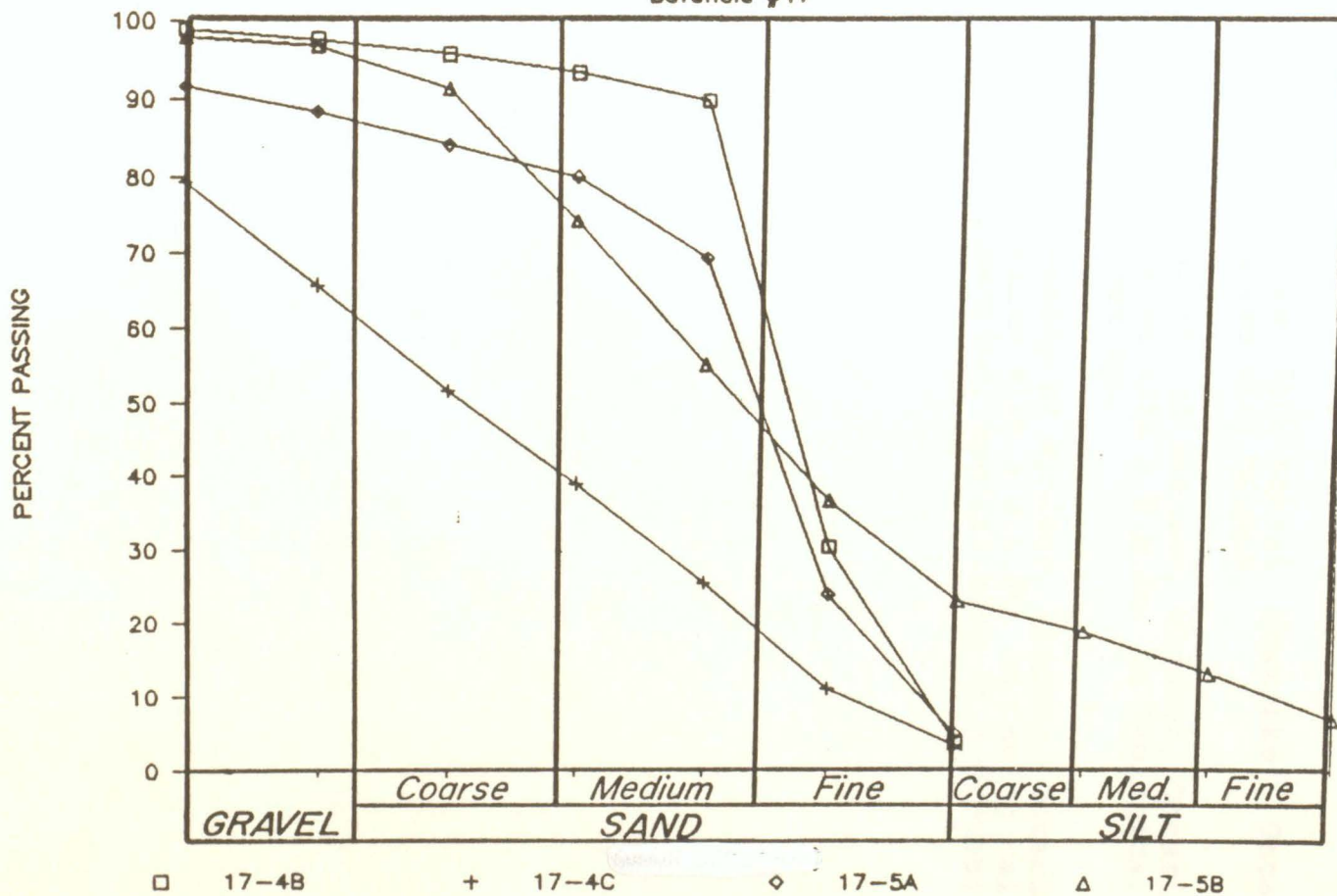
GRADATION ANALYSIS

Borehole #17



GRADATION ANALYSIS

Borehole #17



S002SA1

VITA AUCTORIS

JASON THOMAS BALSDON

Born June 7, 1963 in Fergus, Ontario, Canada.

EDUCATION

1977-1982 Newmarket High School, Newmarket, Ontario.
Graduated with OSSHGD.

1982-1986 University of Windsor, Windsor, Ontario.
Graduated with a B.A.Sc. in Geological
Engineering.

1986-1988 University of Windsor, Windsor, Ontario.
Graduated with a M.A.Sc. in Geological
Engineering, specializing in Hydrogeology.